CONTRIBUTORS TO THIS VOLUME

W. A. BINGEL
C. H. CARLISLE
G. DAS
R. DAUDEL
M. J. FEINBERG
D. J. KLEIN
WŁODZIMIERZ KOŁOS
W. KUTZELNIGG
PER-OLOV LÖWDIN
F. A. MATSEN
ERNEST L. MEHLER
E. E. NIKITIN
KLAUS RUEDENBERG
ARNOLD C. WAHL

ADVANCES IN
QUANTUM CHEMISTRY

EDITED BY

PER-OLOV LÖWDIN

DEPARTMENT OF QUANTUM CHEMISTRY
UPPSALA UNIVERSITY
UPPSALA, SWEDEN
AND
QUANTUM THEORY PROJECT
UNIVERSITY OF FLORIDA
GAINESVILLE, FLORIDA

VOLUME 5—1970

ACADEMIC PRESS New York · London

ACADEMIC PRESS, INC.
111 Fifth Avenue, New York, New York 10003

United Kingdom Edition published by
ACADEMIC PRESS, INC. (LONDON) LTD.
Berkeley Square House, London W1X 6BA

LIBRARY OF CONGRESS CATALOG CARD NUMBER: 64-8029

PRINTED IN THE UNITED STATES OF AMERICA

LIST OF CONTRIBUTORS

Numbers in parentheses indicate the pages on which the authors' contributions begin.

W. A. BINGEL, Theoretical Chemistry Group, University of Göttingen Göttingen, Germany (201)

C. H. CARLISLE, Molecular Physics Group, Department of Chemistry, The University of Texas, Austin, Texas (219)

G. DAS, Argonne National Laboratory, Argonne, Illinois (261)

R. DAUDEL, Sorbonne and Centre de Mécanique, Ondulatoire Appliquée, Paris, France (1)

M. J. FEINBERG, Department of Chemistry, Tufts University, Medford, Massachusetts (27)

D. J. KLEIN[1], Molecular Physics Group, Department of Chemistry, The University of Texas, Austin, Texas (219)

WŁODZIMIERZ KOŁOS, Department of Theoretical Chemistry, University of Warsaw, Warsaw, Poland (99)

W. KUTZELNIGG, Theoretical Chemistry Group, University of Göttingen, Göttingen, Germany (201)

PER-OLOV LÖWDIN, Department of Quantum Chemistry, Uppsala University, Uppsala, Sweden and Quantum Theory Project, University of Florida, Gainesville, Florida (185)

F. A. MATSEN, Molecular Physics Group, Department of Chemistry, The University of Texas, Austin, Texas (219)

ERNEST L. MEHLER, Institute of Atomic Research, Department of Chemistry, Department of Physics, Iowa State University, Ames, Iowa (27)

E. E. NIKITIN, Institute of Chemical Physics, Academy of Sciences, Moscow (135)

KLAUS RUEDENBERG, Institute of Atomic Research, Department of Chemistry, Department of Physics, Iowa State University, Ames, Iowa (27)

ARNOLD C. WAHL, Argonne National Laboratory, Argonne, Illinois (261)

[1] *Present address:* Department of Chemistry, Princeton University, Princeton, New Jersey 08540.

PREFACE

In investigating the highly different phenomena in nature, scientists have always tried to find some fundamental principles that can explain the variety from a basic unity. Today they have not only shown that all the various kinds of matter are built up from a rather limited number of atoms, but also that these atoms are constituted of a few basic elements of building blocks. It seems possible to understand the innermost structure of matter and its behavior in terms of a few elementary particles: electrons, protons, neutrons, photons, etc., and their interactions. Since these particles obey not the laws of classical physics but the rules of modern quantum theory of wave mechanics established in 1925, there has developed a new field of "quantum science" which deals with the explanation of nature on this ground.

Quantum chemistry deals particularly with the electronic structure of atoms, molecules, and crystalline matter and describes it in terms of electronic wave patterns. It uses physical and chemical insight, sophisticated mathematics, and high-speed computers to solve the wave equations and achieve its results. Its goals are great, but perhaps the new field can better boast of its conceptual framework than of its numerical accomplishments. It provides a unification of the natural sciences that was previously inconceivable, and the modern development of cellular biology shows that the life sciences are now, in turn, using the same basis. "Quantum biology" is a new field which describes the life processes and the functioning of the cell on a molecular and submolecular level.

Quantum chemistry is hence a rapidly developing field which falls between the historically established areas of mathematics, physics, chemistry, and biology. As a result there is a wide diversity of backgrounds among those interested in quantum chemistry. Since the results of the research are reported in periodicals of many different types, it has become increasingly difficult both for the expert and the nonexpert to follow the rapid development in this new borderline area.

The purpose of this serial publication is to try to present a survey of the current development of quantum chemistry as it is seen by a number of the internationally leading reasearch workers in various countries. The authors have been invited to give their personal points of view of the subject freely and without severe space limitations. No attempts have been made to avoid overlap—on the contrary, it has seemed desirable to have certain important research areas reviewed from different points of view. The response from the authors has been so encouraging that a sixth volume is now being prepared.

The editor would like to thank the authors for their contributions which give an interesting picture of the current status of selected parts of quantum chemistry. The topics covered in this volume range from the treatment of symmetry properties in quantum mechanics, over studies of the fundamental concepts in valence theory to reaction kinetics. Some of the papers emphasize the use and aid given by large-scale electronic computers.

It is our hope that the collection of surveys of various parts of quantum chemistry and its advances presented here will prove to be valuable and stimulating, not only to the active research workers but also to the scientist in neighboring fields of physics, chemistry, and biology, who are turning to the elementary particles and their behavior to explain the details and innermost structure of their experimental phenomena.

Some Aspects of the Quantum Theory of Photochemical Reactivity of Organic Molecules*

R. DAUDEL

Sorbonne and Centre de Mécanique
Ondulatoire Appliquée
Paris, France

I. General Introduction

The main methods which can be used to interpret the chemical reactivity of organic molecules during the classical thermoreactions have already been summarized (Daudel, 1967). This paper is concerned with photochemical reactions. It is mainly concerned with pointing out the differences and the analogies between thermo and photoreaction in order to indicate what are the methods which can be applied in both cases and what special

---

* This paper is based on my courses of lectures delivered during the last NATO Summer Institute in Menton (July, 1968).

procedures can be, or must be, used in studying photochemical processes.

Sections II and III are devoted to equilibrium constants, Sections IV and V to rate constants.

II. Brief Summary Concerning the Calculations of Equilibrium Constants for Molecules in Their Ground State

Let us consider the equilibrium

$$\mathrm{A} + \mathrm{B} \underset{K}{\rightleftharpoons} \mathrm{C} + \mathrm{D} + \cdots. \tag{1}$$

It is well known that (see, for example, Daudel, 1967)

$$K = \frac{f_{\mathrm{C}} f_{\mathrm{B}} \cdots}{f_{\mathrm{A}} f_{\mathrm{B}}} e^{-\Delta\varepsilon/kT}, \tag{2}$$

in which the f denotes the partition functions describing the distribution of the various molecules among the energy levels and

$$\Delta\varepsilon = \varepsilon_{0\mathrm{C}} + \varepsilon_{0\mathrm{D}} + \cdots - \varepsilon_{0\mathrm{A}} - \varepsilon_{0\mathrm{B}}, \tag{3}$$

the ε_0 representing the ground state energies.

For an equilibrium reaction taking place in a solvent between conjugated molecules Eq. (2) becomes

$$K = \frac{f_{\mathrm{C}}^s f_{\mathrm{D}}^s}{f_{\mathrm{A}}^s f_{\mathrm{B}}^s} \exp\left(- \frac{\Delta\varepsilon_v + \Delta\varepsilon_l + \Delta\varepsilon_d + \Delta\varepsilon_{nb} + \Delta\varepsilon_s(T)}{kT} \right), \tag{4}$$

where

$\Delta\varepsilon_v$ represents the null point vibrational energy change,
$\Delta\varepsilon_l$ represents the localized bond energy change,
$\Delta\varepsilon_d$ represents the delocalized bond energy change,
$\Delta\varepsilon_{nb}$ represents the nonbonded atoms energy change, and
$\Delta\varepsilon_s(T)$ represents the solvation energy change.

It is usually impossible to calculate all the terms which appear in this equation, so it is not possible to compute K. It is easier to determine the ratio K'/K of two equilibrium constants related to similar reactions. In such a case, with obvious notations,

$$\frac{K'}{K} = \frac{f'}{f} \exp\left(- \frac{\Delta\Delta\varepsilon_v + \Delta\Delta\varepsilon_l + \Delta\Delta\varepsilon_d + \Delta\Delta\varepsilon_{nb} + \Delta\Delta\varepsilon_s(T)}{kT} \right). \tag{5}$$

Very often f'/f is not very different from unity, and of all the $\Delta\Delta\varepsilon$ one or two appears to be greater than the others. In that case it is only necessary to compute this term or these two terms to calculate the relative rate. It has been seen, for example (see Daudel, 1967), that the calculation of $\Delta\Delta\varepsilon_d$ leads to a clear understanding of the behavior of the magnetic susceptibility in a family of quinodimethanes. It has also been shown that $\Delta\varepsilon_d$ and $\Delta\varepsilon_s(T)$ are the main factors which determine the variation of the base strength in a family of amino derivatives of heteromolecules.

III. Base Strength of Conjugated Molecules in Their Electronic Excited States

A. Introduction

Coulson and Jacobs (1949) studied, theoretically, charge migration in aniline under the effects of irradiation. They observed that the electronic charge on nitrogen is smaller in the first singlet excited state than in the ground state; that is, the excited state should be less basic. Forster (1949) effectively observed that if a base, such as 3-aminopyrene (which must have a similar behavior), is irradiated by normal light, the excited molecules have acidic properties. To interpret this result, Sandorfy (1951) calculated the distribution of the electronic charges in an aromatic amine by the molecular-orbital method, taking account of both the σ and the π orbitals. He found that the nitrogen which is negative in the ground state becomes positive in the first excited electronic state, which explains why the molecule becomes an acid. We shall discuss this phenomenon further, as it provides an example of the study of equilibrium constants for molecules in excited states. Many questions arise when such a problem is under discussion.

We know that, as yet, it is difficult to obtain good wave functions for molecules in their ground state. Very often for conjugated molecules only π orbitals are considered. Clementi (1967), however, recently calculated an all-electron SCF wave function for the ground state of pyridine and was led to the surprising conclusion that the π orbitals have negligible contributions to the electronic charges on the various carbon atoms in this molecule. For the excited states the situation is worse. Conjugated molecules are usually assumed to have well-separated bands of π and σ orbitals. The representation of the first excited states is assumed to retain the same σ orbitals as the ground state. In fact this separation is known not to be true, even for ethylene (Robin *et al.*, 1966). However, as we shall see, many satisfactory results have been obtained by using the usual π approximation.

Another difficult point is to know if the reaction studied corresponds to a thermodynamic equilibrium. Forster (1949, 1950) and Weller (1952, 1957, 1958, 1961) developed a method of measuring the pK which provides an answer to this question. In this method the fluorescence spectrum of a solution of the molecule is analyzed at various pH values. In this way, for example, it is possible to determine the concentration of a basic molecule and also the concentration of the corresponding positive ion. We can be sure that an equilibrium exists between these two species since the lifetime of an excited state is usually of the order of 10^{-8} sec and the necessary time to obtain thermal equilibrium and reorganization of the molecules in the solvent is of the order of 10^{-11} sec (Hercules and Rogers, 1960). Another procedure for measuring the pK of a molecule in an excited state is based on the determination of the absorption spectra of this molecule and that of the corresponding ion. Let us consider the acid–base equilibrium for the ground state.

$$\mathrm{B} + \mathrm{H}^+ \underset{K}{\rightleftharpoons} \mathrm{BH}^+ \tag{6}$$

and the corresponding equilibrium for an excited state

$$\mathrm{B}^* + \mathrm{H}^+ \underset{K^*}{\rightleftharpoons} \mathrm{BH}^{*+}. \tag{7}$$

We can write

$$K = \frac{f_{\mathrm{BH}^+}}{f_{\mathrm{B}}\, f_{\mathrm{H}^+}}\, e^{-\Delta\varepsilon/kT} \tag{8}$$

$$K^* = \frac{f_{\mathrm{BH}^{*+}}}{f_{\mathrm{B}^*}\, f_{\mathrm{H}^+}}\, e^{-\Delta\varepsilon^*/kT}. \tag{9}$$

If we assume that the ratio of the partition functions is about the same for the two state we obtain

$$M(\mathrm{p}K^* - \mathrm{p}K) = \frac{1}{kT}(\Delta\varepsilon^* - \Delta\varepsilon), \tag{10}$$

where M denotes the modulus which converts the decimal logarithm to neperian ones. Figure 1 clearly shows that

$$\Delta\varepsilon^* - \Delta\varepsilon = h\nu_{\mathrm{BH}^+} - h\nu_{\mathrm{B}} \tag{11}$$

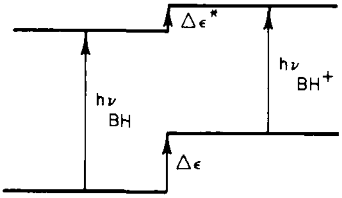

Fig. 1

where the $h\nu$ denotes the transition energies between the ground and the excited states for the O → O bands. It is therefore possible to determine pK^* if pK is known by studying the absorption spectra of B and BH^+ in solution in a given solvent. We must be careful, however, because the absorption spectra gives the Franck–Condon energies and we need the transition energies corresponding to the O → O bands. A suitable correction must be effected. Furthermore during the absorption process the molecules of the solvent do not have the time to reorganize, necessitating another correction.

B. Base Strength of Alternant Hydrocarbons and Derivatives

Various authors have studied the pK of alternant hydrocarbons and their derivatives on the first excited states (Colpa *et al.* 1963: Flurry, in press). Let us consider the equilibrium

$$ArH^* + H^+ \overset{K^*}{\rightleftharpoons} ArH_2^{*+}. \tag{12}$$

As an example, consider anthracene. It is probable that the positive ion will have the following structure:

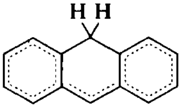

Therefore, the contribution $\Delta\varepsilon_d^*$ of the delocalized system to $\Delta\varepsilon^*$ will be the corresponding localization energy. As $\Delta\varepsilon_d^*$ is in such a case the leading term in $\Delta\varepsilon^*$ we can anticipate a linear relationship between pK and the lowest localization energy of the excited state concerned.

Flurry (in press) has calculated the various localization energies for the polymethyl benzenes using the Pariser–Parr–Pople approximation with interaction of all singly excited configuration. Flurry compared the excited state localization energies with the spectroscopically determined experimental excited state basicities and obtained a good linear fit.

C. Qualitative Discussion about the Strength of Heteromolecules and Substituted Compounds

This section will be devoted to the study of the base strength of molecules like pyridine, quinoline, phenols, and aromatic amines in their first excited states. We shall try to understand in a qualitative manner why the pK of the excited states differ from the ones of the ground states.

As in the case of the ground state, it is tempting to see if there is a correlation between the pK and the charge of the atom on which the fixation of a proton occurs for a given family of analogous molecules.

More precisely, Itoh (1957, 1958, 1959) suggested the existence of a linear relation between the pK and the charge on the basic atom of a given molecule in various electronic states. Jaffé *et al.* (1964) observed effectively a rather fair relation between the difference of pK of two excited states of azobenzene and the difference of charge on the nitrogen atoms for these states.

Therefore, if we are able to predict the change which occurs in the charge of an atom of a conjugated molecule under irradiation we must be able to predict the variation of the pK under the same effect, at least in a qualitative manner. Bertran (1968) used various methods to predict this change. The simplest one is based on Mulliken's charge transfer theory. Let us consider a molecule like β-naphtylamine. The NH_2 group can be considered as an electron donor D and the naphthalene system as an acceptor A. Let Ψ_{A-D} be the wave function corresponding to no charge transfer and $\Psi_{A^+-D^-}$ the wave function corresponding to a transfer of one electron. The actual wave function can be written as

$$\Psi = a\Psi_{A-D} + b\Psi_{A^+-D^-}. \tag{13}$$

Assuming that in the ground state the charge transfer is small, we must have

$$|b| \ll |a|. \tag{14}$$

We shall associate with the first excited state

$$\Psi^* = a^*\Psi_{A-D} + b^*\Psi_{A^+-D^-}. \tag{15}$$

Neglecting the overlap the orthogonality relation leads to

$$aa^* + bb^* = 0; \tag{16}$$

that is,

$$|a/b| = |b^*/a^*|. \tag{17}$$

Therefore,

$$|b^*| \gg |a^*|. \tag{18}$$

The final conclusion is that *if a group is a weak donor in the ground state it becomes a strong donor in the first excited state.* In the present case we must anticipate that the molecule becomes less basic when it is excited. Effectively the pK of the naphthylamine is 4.1 for the ground state and -2 for the first excited singlet state. Following in an analogous way it can be anticipated that an acceptor will become a stronger acceptor in the first excited state. This is why acridine, which has a pK of 5.5 in its ground state, becomes more basic with a p*K* of 10 in its first excited singlet state. It can, however, be seen that the charge of the leading atom is not the only factor which determines the p*K* of an excited state. Table I shows some values of p*K* measured by Jackson and Porter (1961). It is seen that the p*K* of the triplet states look similar to the p*K* of the ground state. On the contrary the p*K* of the first excited singlet are completely different. Therefore the first triplet and the first excited singlet differ very much in their basicities. But Bertran (1968) has developed arguments showing that the electronic charge of the leading atom is about the same in the molecule under consideration for the first triplet state and for the first singlet excited state. This is why Bertran suggests that identical atomic charges do not have an equivalent effect on p*K* if they do not correspond to the same distribution of spin density.

TABLE I

SOME p*K* VALUES

	Ground state	First triplet	First excited singlet
α-Naphthol	9.46	8.1	2.8
β-Naphthylamine	4.1	3.3	−2
Acridine	5.5	5.6	10.6

D. The Quantitative Calculation of p*K* of Conjugated Molecules

The equation already established,

$$M(\mathrm{p}K^* - \mathrm{p}K) = \frac{1}{kT}(\Delta\varepsilon^* - \Delta\varepsilon), \tag{19}$$

shows that the calculation of

$$\Delta\mathrm{p}K = \mathrm{p}K^* - \mathrm{p}K \tag{20}$$

only needs the calculation of $\Delta\varepsilon$ and $\Delta\varepsilon^*$. The calculations of $\Delta\varepsilon$ and $\Delta\varepsilon^*$ can be performed by using methods which permit the determinations of the energy levels of conjugated molecules; Cetina *et al.* (1967) have done such calculations in the case of acridine and quinoline using an electrostatic model to represent the effect of the proton in the positive ions of the molecules concerned. They used the Pariser–Parr approximation with a large configuration interaction. Table II shows their results. The agreement

TABLE II

OBSERVED AND CALCULATED VALUES OF pK

	Ground state	First triplet state		First singlet state	
	Obs.	Obs.	Calc.	Obs.	Calc.
Quinoline	5.1	6.0	6.2		10.8
Acridine	5.6	5.6	3.6	10.6	10.7

between theory and experiment is satisfactory. In particular, theory and experiment both suggest very different values of pK for the first triplet and the first excited singlet state.

IV. Brief Summary Concerning the Calculation of Rate Constants for Molecules in Their Ground State

Let us consider a bimolecular step of a chemical reaction

$$\mathrm{A} + \mathrm{B} \xrightarrow[k]{} \mathrm{C} + \mathrm{D} + \cdots. \tag{21}$$

The only theory which has been applied in the field of organic chemistry to estimate k is the transition state theory. According to this theory, it is assumed that there is a certain state $M^{\ddagger}$ of the intermediate complex formed during the collision which is in thermodynamical equilibrium with the reagent:

$$\mathrm{A} + \mathrm{B} \underset{K^{\ddagger}}{\rightleftharpoons} \mathrm{M}^{\ddagger} \xrightarrow[k^{\ddagger}]{} \mathrm{C} + \mathrm{D} + \cdots. \tag{22}$$

Therefore, it is possible to write

$$k = k^{\ddagger} \frac{[M^{\ddagger}]}{[\mathrm{A}][\mathrm{B}]}, \tag{23}$$

where $k^{\ddagger}$ denotes the rate constant of decomposition of this transition state $M^{\ddagger}$. The rate constant $k^{\ddagger}$ may be written as

$$k^{\ddagger} = \frac{kT}{h} (1 + t)\eta. \tag{24}$$

Using a formula analogous to (4) to express the term $[M^{\ddagger}]/[A][B]$ we are led to the final expression

$$k = \frac{kT}{h} (1 + t)\eta f \exp\left(- \frac{\Delta\varepsilon_{v}{}^{\ddagger} + \Delta\varepsilon_{l}{}^{\ddagger} + \Delta\varepsilon_{d}{}^{\ddagger} + \Delta\varepsilon_{nb}^{\ddagger} + \Delta\varepsilon_{s}{}^{\ddagger}(T)}{kT} \right), \tag{25}$$

which shows that the chemical reactivity for such a bimolecular process depends on eight factors, namely:

(a) $(1 + t)$ associated with the tunnel effect above the potential barrier,
(b) η the transmission coefficient,
(c) f the ratio of the partition functions,
(d) the contribution of vibrational energy $\Delta\varepsilon_v^\ddagger$ to the potential barrier,
(e) the corresponding contribution of the localized bonds $\Delta\varepsilon_l^\ddagger$,
(f) the corresponding contribution of the delocalized bonds $\Delta\varepsilon_d^\ddagger$,
(g) the contribution of nonbonded atom interaction $\Delta\varepsilon_{nb}^\ddagger$ to the potential barrier, and
(h) the corresponding contribution $\Delta\varepsilon_s^\ddagger(T)$ due to the solvent effect (see, for example, for more details, Daudel, 1967).

As it was for equilibrium constants, cases where it is possible to compute all these factors are exceptional. But if the relative rates of a family of analogous molecules are investigated for a given kind of reaction one or two of the eight factors dominate. In such cases the calculation of only these terms permits us to interpret or predict the behavior of the reaction for that family of compounds. In the case of substitution reactions on aromatic alternant hydrocarbons the factor which appears to be the most important is $\Delta\varepsilon_d^\ddagger$. This term is usually calculated by assuming that in the transition state the perturbated carbon atom becomes a saturated one which is excluded from the delocalized bond:

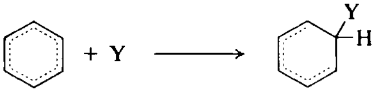

This is the Wheland model. The $\Delta\varepsilon_d^\ddagger$ calculated in this way is called the localization energy. For addition reactions analogous terms called *para* and *ortho* localization energies can be calculated. In many cases there are linear relations between these localization energies and the measured rate constants. Such localization energies are called *dynamic indices* because they take account of the assumed structure of the intermediate state; that is, the path of the reaction. For alternant hydrocarbons it is possible to establish relations between the localization energies and the free valence numbers or the bond orders associated with the structure of the reacting hydrocarbons.

Free valence numbers and bond orders are usually called *static indices* because they only depend on the structure of the hydrocarbon and not on the reaction path.

The relations existing between dynamic indices and static indices furnish a theoretical background for the use of the latter one for predicting the reactivity of alternant hydrocarbons.

For heteromolecules and substituted conjugated molecules the situation becomes less simple. For example, there is no clear-cut relation between the localization energies associated with nucleophilic reactions and the electronic charges of the substituted atoms.

Brown and Harcourt (1959) have shown that in some cases the charges can be more useful to predict the position of the reactive centers than are the localization energies. This happens with reagents leading to fast reactions like R^-, OH^-. On the contrary when smooth reagents like CN^- are considered, the dynamic indices have better predictive power.

In order to explain this surprising fact Brown and Harcourt remark that when the reaction is fast the potential barrier is small. They assume that in such a case the Wheland structure of the intermediate complex is not reached, which explains why the localization energies are not good indices. The transition state would have a structure similar to the structure of the initial molecule, suggesting the use of static indices. If, for example, it is assumed that the approach of an atom of electronic charge q to the reagent affects the coulombic integral α associated with this atom by $d\alpha$, the corresponding change in the energy associated with the delocalized system can be written as

$$d\varepsilon = q\, d\alpha, \tag{26}$$

if simple Huckel theory is used. This very simple expression helps us to understand why $\Delta\varepsilon_a^\ddagger$ would be related to the static index q.

V. Rate of Photochemical Reaction

A. Introduction

Let us consider the simple photochemical reaction

$$\mathrm{AH} + h\nu \rightarrow \mathrm{AH}^* \tag{27}$$

$$\mathrm{AH}^* + \mathrm{B} \xrightarrow{k_R} \mathrm{AB} + \mathrm{H}. \tag{28}$$

The rate constant k_R is the true measure of the reactivity of the AH^* molecule. Unfortunately it is difficult to determine this constant experimentally. Usually the measured quantity is the quantum yield. It is easy to see that this quantum yield γ can only be related to k_R when a number of other rate processes have been measured.

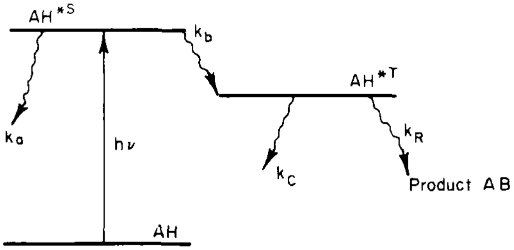

Fig. 2

Figure 2 shows the various processes which usually occur in such a reaction. The term k_a denotes the sum of the various specific rates of deactivation of the excited molecule AH^{*S}. It is assumed that this excited state is a singlet state. The term k_b represents the rate of crossing from this state to a triplet state AH^{*T} which is assumed to be the reactive state. The term k_c is the sum of specific rates of deactivation of this triplet state.

If such a mechanism occurs it is easy to show (Porter, 1967) that

$$\gamma = \frac{k_R k_b}{(k_a + k_b)(k_c + k_R)}$$
$$= k_R k_0 \tau_{AH^{*S}} \tau_{AH^{*T}}, \qquad (29)$$

where τ_n refers to the lifetime of a state n. Therefore in a given set of reactions the quantum yield is proportional to the reactivities k_R only if $k_0 \tau_{AH^{*S}} \tau_{AH^{*T}}$ remains a constant.

Finally, it is clear that the experimental determination of the rate constant of a photochemical reaction is much more difficult than the measurement of the rate constant of a reaction taking place between non-excited molecules.

Furthermore, the theoretical calculation of k_R is also much more difficult. The use of the transition state theory for excited states is open to criticism (Laidler, 1955). Obviously the hypothesis of a transition state in thermodynamic equilibrium with the medium is not convenient. It is possible to show that more restricted hypothesis can be sufficient.

From the experimental viewpoint, however, the temperature coefficients appear to be very small (and negative in some cases) (Havinga *et al.*, 1956; Letsinger *et al.*, 1965). Therefore, if they exist, the potential barriers are probably small.

This is the reason why many photochemists believe that excited state molecules do not climb energy mountain tops, especially when low-energy routes are available (Zimmerman, 1966). But even in this last case it is not clear whether the lowest-energy route is followed. The case with which an excited state species having a certain geometry can form its unexcited ground state counterpart may be an important factor (Hammond, 1964; Malrieu, 1966). In some cases the loss of electronic excitation is possible without gross molecular change, generating a molecule with excess vibrational energy. A molecular rearrangement of this vibrationally excited but electronically unexcited species can follow. Solvent deactivation strongly competes with this rearrangement (Zimmerman and Wilson, 1964).

Figure 3 makes it possible to compare the beginning of two possible photochemical pathways with a usual pathway.

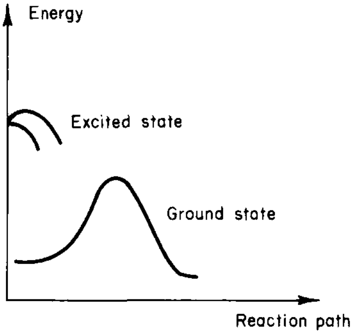

Fig. 3

B. Static and Dynamic Indices in Photochemistry

We saw that the justification of the use of static indices for unexcited molecules is mainly based on the existence of relationships between static and dynamic indices (Daudel *et al.*, 1950; Roux, 1950; Burkitt *et al.*, 1951). However, we also saw that in some cases (for very reactive reagents) the static indices can furnish better results than dynamic indices (Brown and Harcourt, 1959). A possible explanation of this fact has been given.

Historically the first uses of static indices in photochemistry were mainly based on chemical intuition. Pullman and Daudel (1946) calculated the bond orders and the free valence numbers for the ground state and the first excited state of butadiene using the valence bond method. They found that in the ground state the two bonds 1–2 and 3–4 have the higher bond orders. The free valence numbers in 1 and 4 are still important; they become very large in the first excited state in which the central bond 2–3 becomes similar to a double bond. Correspondingly, the bond orders in 1–2 and 3–4 become very small in the first excited state. The same results can be described in other words. The wave function Ψ describing butadiene can be written as

$$\Psi = a\Psi_{\mathrm{I}} + b\Psi_{\mathrm{II}}, \qquad (30)$$

in which $\Psi_{\rm I}$ represents the function associated with the Kekulé formula (I) and $\Psi_{\rm II}$ the function associated with the Dewar formula (II):

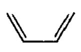
(I)


(II)

In the ground state *a* is found to be large and *b* small. In the excited state the reverse is true. Therefore, the ground state is conveniently represented by the Kekulé formula and the excited state by the Dewar formula. It could be anticipated that under the effect of light, butadiene could be transformed into cyclobutene. In 1946, there was no experimental evidence for such a phenomenon, but recently Srinivasan (1963) has found that when butadiene is irradiated in dilute ether solution, cyclobutene (III) is formed.

In 1951, Fernandez-Alonso calculated the distribution of the electronic charges for various electronic states of nitrobenzene. He found that for the ground state the *ortho* and *para* positions are the most positive, but that for one of the first excited states which could be reached under usual photochemical conditions the *meta* positions become the most positive. Therefore the author anticipated that light could change the orientating effect of the nitro group.

Analogous calculations have been performed by Fernandez-Alonso and Domingo (1955) for nitroanilines. Again the *ortho* and *para* positions are calculated to be the most positive in the ground state. In the first excited states the nitro group withdraws electrons mainly from the *meta* positions.

Somewhat later, Havinga *et al.* (1956) studied the photochemical hydrolysis of the isomeric nitrophenyl dihydrogen phosphates and also the bisulfate esters. They observed that this process is most efficient for the *meta* isomers, suggesting the nitro group is able to withdraw electrons from the phenolic-phosphate oxygen atom in the excited state of these molecules, thus facilitating heterolytic fission.

Zimmerman (1963) studied the photochemical behavior of the trityl ethers of *m*-nitrophenol and *p*-nitrophenol in aqueous dioxane. They observed that the *meta* compound is stable in the dark at 25°, whereas the *para* is slowly hydrolyzed. Under the effect of light, on the contrary, the quantum yield is much greater for the *meta* compound than for the *para* derivative. Again an interpretation is possible if we admit that in some excited states of these molecules the nitrogroup withdraws electrons from the *meta* position.

As nitrophenols and nitroanilines are π-isoelectronic and must have the same qualitative behavior, these facts may be considered as supporting the predictions of Fernadez-Alonso.

Many other studies of photochemical reactivities are based on static indices. The study of the photodimerization of acenaphthylene by Crawford and Coulson (1948) is another example. In a similar way Buu-Hoï *et al.* (1951) have shown that the bond order of the central bond of stilbene in its first excited state is smaller than that of the ground state. This latter could be an explanation of the *trans-cis* photoisomerization of stilbene. Following the same procedure, Masse (1954) and Bloch-Chaudé and Masse (1955) try to explain the photochromic properties of some derivative of pyranospirane.

The symmetry properties of molecular orbitals used by Woodward and Hoffmann (1965) to predict the conformation of molecules produced during photocyclization are also, in a sense, a static index.

It is clear that the use of static indices in photochemistry has been successful. We must now try to understand why.

Various works have been performed to see if the reason lies in the existence of a relation between static and classical dynamic indices. Trsic *et al.* (1966) tried to see if the fair relation which exists for the ground state of alternant hydrocarbons between free valence numbers and localization energies remains significant in the case of the first excited states. They found this *not* to be so. Also, Bessis *et al.* (1967) found that there is no longer a relationship between atom–atom autopolarizabilities and localization energies. It is, therefore, tempting to find out what are, from the pragmatic viewpoint, the best indices.

Such a study has been done by de Bie and Havinga (1965) who studied the photodeuteration of nitrobenzene, anisol, and nitro anisols. In this reaction, the reagent is considered to be an electrophilic one. Table III makes it possible to compare the experimental rate of photodeuteration with the electronic charges and the localization energies in the case of nitrobenzene.

TABLE III

PHOTODEUTERATION OF NITROBENZENE

Position	Rate (% in 4 hr)	Electronic charge	Localization energies (in β unit)
Ortho	1	0.91	0.180
Meta	0.5	0.89	0.161
Para	8.6	0.99	0.213

It appears that the rates run parallel to the charge but there is no satisfactory relationship between these rates and the localization energies. Therefore these classical dynamic indices are not convenient. Feler has discussed in the same way the case of nitroanisols and was led to analogous conclusions. These results are not very surprising if we bear in mind the discussion of Brown and Harcourt (1959). They suggest that if the potential barrier of a photochemical reaction exists, it must be small. In a sense such a reaction is thus similar to a reaction between a conjugated molecule in the ground state and a strong reagent.

Daudel and Chalvet (1967), however, try to explain the success of static indices in photochemistry with the help of another argument. These authors assume that the rate-determining step of the reaction goes through an intermediate complex (I) in which the delocalized bond of the conjugated molecule is extended over the deuterium of the reagent D–V. We shall denote the stabilization energy which comes from that extension of the delocalized bond as $\Delta\varepsilon_d^{\ddagger}$. Let X be the function which represents the electronic distribution of an electron added to D. This function depends on the position of the reagent D–V with respect to the conjugated molecule and on the various molecules of solvent. The integral

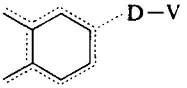

$$\alpha_D = \int X^* h^{SCF} X \, dv \qquad (31)$$

will depend, in particular, on the extension of the D–V bond during the deuterium transfer. A conjugated molecule in its first excited state is usually represented in the MO approximation by determinants containing the lowest unoccupied orbital of the ground state. It is well known that $\Delta\varepsilon_d^{\ddagger}$ will become significant when the energy α_D becomes equal to the energy associated with this orbital (resonance criteria). The corresponding value of $\Delta\varepsilon_d^{\ddagger}$ can be considered to be a dynamic index. It is not necessarily associated with a potential barrier, but, on the contrary, can give an idea of the negative slope of the energy surface at the beginning of the reaction path. To estimate the value of $\Delta\varepsilon_d^{\ddagger}$ we can use the perturbation method described by Dewar (1952). In that case the following equation is found:

$$\Delta\varepsilon_d^{\ddagger} = |c|\,\beta', \qquad (32)$$

where β' denotes the resonance integral between D and the conjugated molecule and C represents the coefficient of the carbon atom bonded with

D in the LCAO expansion of the molecular orbital under consideration. Daudel and Chalvet observed that for a given molecule like phenol, *p*-nitrophenol, and *m*-nitrophenol, the $\Delta\varepsilon_d{}^{\ddagger}$ values increase with the electronic charge of the carbon atom considered. Therefore, there is a satisfactory relation between the charge and a dynamic index. This relation gives an interpretation of the validity of the static index. Mayer (1965) has suggested another approach, which is related to the collision theory. Let us consider two carbon atoms which are negatively charged, the charge of the atom A being higher than the charge of the atom B. The greater attractive potential A will create a larger cross section for electrophilic reaction. It would certainly be interesting to develop this idea in a quantitative way.

C. Mechanism of Photooxidation

The pioneering work of Dufraisse and his school (see, for example, the reviews by Dufraisse, 1955, and Etienne, 1949) has established that a 1,4 photoaddition of molecular oxygen can occur with a cyclic delocalized system which has retained enough dienic reactivity. The photoaddition of oxygen on rubrene is a typical example:

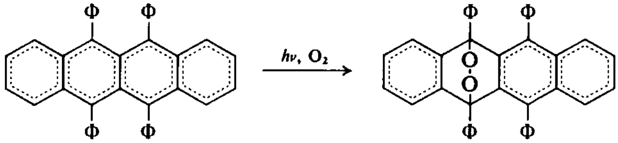

(33)

A number of sophisticated experiments (Arbuzov 1965; Bowen, 1963; Foote and Wexler, 1964; McKeown and Waters, 1966; Corey and Taylor, 1964) led to the assumption that the process of photooxidation can be represented by the following set of equations:

$$^1A \xrightarrow{h\nu} {}^1A^* \rightarrow {}^3A^* \tag{34}$$

$$^3A^* + {}^3O_2 \rightarrow {}^1A + {}^1O_2^* \tag{35}$$

$$^1A + {}^1O_2^* \rightarrow AO_2 \tag{36}$$

Absorbing a photon the conjugated hydrocarbon A goes from its ground state to the first excited state which is usually a singlet. A radiationless transition leads to the first triplet state $^3A^*$. The second step of the reaction should be a collision between $^3A^*$ and a nonexcited triplet oxygen molecule. This collision could lead to the formation of an excited singlet oxygen molecule $^1O_2^*$.

The last step would be a collision betweenth is excited oxygen molecule and another molecule of the hydrocarbon A leading to the formation of the photooxide AO_2.

Chalvet *et al.* (1968) have made quantum mechanical calculations in order to verify the mechanism of this last step. Their discussion is based on recent experimental results showing the effect of substituents on the site of photooxidation (Dufraisse *et al.*, 1965; Rigaudy *et al.*, 1967; and unpublished results).

For anthracene derivatives it has been found that, depending on the nature and position of substituents, 1, 4 or 9, 10 photooxide is obtained (or both). Table IV summarizes the main results.

TABLE IV

PERCENTAGE OF PHOTO-OXIDES FORMED IN PHOTOOXIDATIONS

Compound	1, 4 substituents	9, 10 substituents	1, 4 photooxide V	9, 10 photooxide IV
I_a	$Z=Z'=H$	$R=H$	0	100
I_b	$Z=Z'=H$	$R=C_6H_5$	0	100
III_f	$Z=Z'=OCH_3$	$R=H$	100	0
III_e	$Z=Z'=OCH_3$	$R=C_6H_5$	100	0
III_h	$Z=Z'=CH_3$	$R=H$	65	35
III_g	$Z=Z'=CH_3$	$R=C_6H_5$	75	27
III_j	$Z=OCH_3$, $Z'=H$	$R=C_6H_5$	50	50

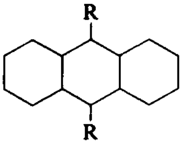

(I)

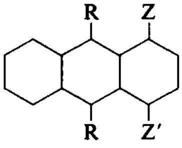

(III)

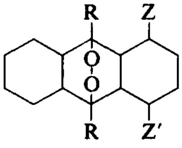

(IV)

a, $R=H$
b, $R=C_6H_5$

e, $R=C_6H_5$, $Z=Z'=OCH_3$
f, $R=H$, $Z=Z'=OCH_3$
g, $R=C_6H_5$, $Z=Z'=CH_3$
h, $R=H$, $Z=Z'=CH_3$
j, $R=C_6H_5$, $Z=OCH_3$, $Z'=H$

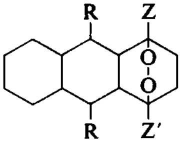

(V)

It appears that in the 1,4 substituted anthracene series the electron-donor substituents are able to deviate the oxygen addition from the 9, 10 to the ordinarily less reactive 1, 4 positions.

Various authors have pointed out the analogy between the last step of photooxidation and the diene-synthesis; Chalvet *et al.* (loc. cit.) used in their calculations an intermediate complex similar to those introduced by Brown (1949) for diene-synthesis. This Wheland-type intermediate complex can be written as follows:

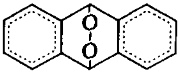

In this case the corresponding contribution to the potential barrier $\Delta\varepsilon_d^\ddagger$ is known as the *para*-localization energy. It is usually considered to be the main factor which determines the rate of the reaction. Table V contains the values of the *para*-localization energies obtained by using the Huckel method with convenient parameters.

TABLE V

PARA-LOCALIZATION ENERGIES $\Delta\varepsilon_d^\ddagger$ (IN β UNITS)

Positions	Anthracene	1, 4-Dimethoxyanthracene
1, 4	−3.63	−4.38
9, 10	−3.31	−3.34
5, 8	−3.63	−3.63

From this table it would be predicted that the effect of the substituent strongly decreases the possibility of reaction at the 1, 4 positions as β is a negative unit. This prediction is exactly opposite to the experimental result given in Table IV.

This is why Chalvet *et al.* tried another type of intermediate complex. They introduced an intermediate complex containing an extension of the delocalized bond on the oxygen molecule. The following diagram symbolizes this complex:

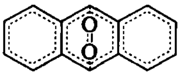

which has a certain analogy with the one used to interpret the photodeuteration of aromatic compounds. Table VI shows the values of the $\Delta\varepsilon_d\ddagger$ obtained with such an intermediate complex.

TABLE VI

Values of $\Delta\varepsilon_d^{\ddagger}$ (in β Units)

Compound	1, 4 Photooxide	9, 10 Photooxide
I_a	0.76	0.84
I_b	0.80	0.86
III_f	1.13	1.01
III_e	1.14	1.10
III_h	1.07	1.03
III_g	0.98	0.98
III_j	0.91	0.93

We must recall that β is a negative unit. Therefore $\Delta\varepsilon_d^{\ddagger}$ now appears to be a stabilizing energy. It is seen that for compound III_f and III_e this energy is higher in 1, 4 than in 9, 10. This result is in agreement with the fact that the introduction in 1, 4 of the methoxy group deviates the addition of the oxygen molecule from the 9, 10 to the 1, 4 positions.

The fact that in the case of compounds III_g and III_j both isomers are produced (Table IV) is also accounted for.

D. Photocyclization

The irradiation of various conjugated molecules may produce cyclizations. The simplest example has been discussed: It is the case of butadiene leading to cyclobutene. Many other reactions of this kind are known and quantum mechanical calculations have been done to predict the site of the cyclization. The most usual approach is based on the use of static indices. More precisely it is observed that the bond appears during the cyclization corresponds to a site for which the bond order increases during the process of excitation (Simon, 1964; Malrieu, 1966; Zimmerman, 1966; Feler, 1968). This observation may be understood when it is recalled that during the approach of two atoms the stabilizing energy is proportional to the bond order (Coulson and Longuet-Higgins, 1947).

To give a typical example of the application of this rule let us study the photocyclization of muconic anhydride (Chapman *et al.*, 1962). This reaction leads to *cis*-3-cyclobutene-1, 2-dicarboxylic anhydride:

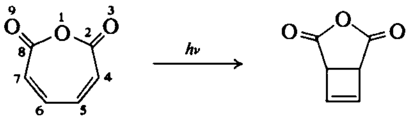

(37)

Table VII clearly shows that the photocyclization occurs along the bond which corresponds to the highest variation of bond order during the absorption of light.

TABLE VII

VARIATION IN BOND ORDERS DURING EXCITATION OF MUCONIC ACID

Bonds	Variation in bond orders
2–4	−0.066
4–5	−0.199
5–6	+0.136
4–7	+0.291

Feler (1968) established simple rules which permit one to predict qualitatively the variation in bond orders during photoexcitation without performing any calculations. For example, it is shown that in a linear polyene represented by a Kekulé formula the bond orders between atoms separated by an even number of simple bonds decrease when the molecule goes from the ground state to the first electronic excited state. On the other hand the bond orders of bonds separated by an odd number of simple bonds increase.

Another aspect of photocyclization can be studied with the help of quantum chemical calculations. Let us consider the cyclization of I,I′-bicyclohexenyl:

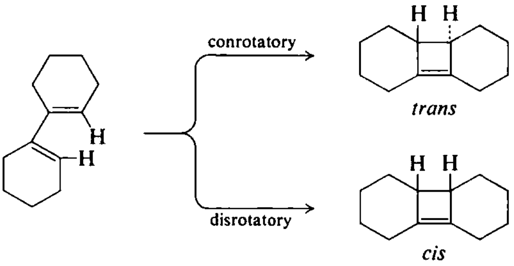

(38)

A priori, we can predict the possible formation of two different products: a *trans* and a *cis* derivative. Woodward and Hoffmann (1965) suggested that the steric course of such a reaction is determined by the symmetry of the highest occupied molecular orbital of the initial molecule and should therefore differ for different electronic states. If the first excited state is considered it is known that the orbital is symmetric with respect to a plane perpendicular to the central bond and passing through its center. Woodward and Hoffmann assumed that rotations around the bonds are such that positive (or negative) parts of π atomic orbitals overlap during the formation of the new σ bond. Figure 4 shows clearly that in the present case this rule leads to a disrotatory process and therefore to a *cis*-product in complete agreement with experiment (for more details see Dauben, 1967).

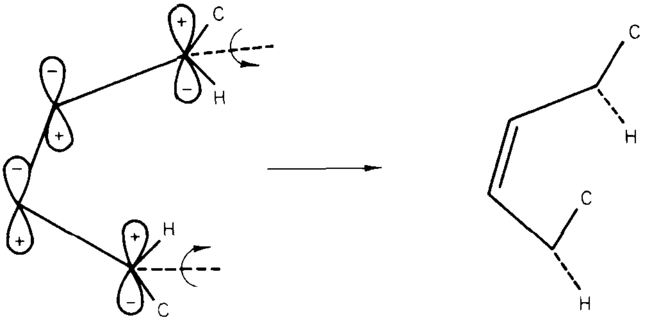

Fig. 4

E. Photochemical Cycloadditions

Various photocycloadditions occur between conjugated molecules. Photodimerizations are examples of this kind of reaction. Salem (1968) assumed that the interaction between such molecules is well described in terms of the π orbitals of the separate systems. He derived expressions for the interaction energy of two conjugated molecules when both are in their ground state, or when one is in an excited state, in terms of overlap $S_{rr'}$ between pairs of atoms r, r' and an interaction integral $\eta_{rr'}$. His expression permits one to obtain a "reaction surface" which suggests reaction paths. Both conjugated molecules are assumed to have well-separated bands of π and σ orbitals. Therefore the major interactions will arise from the less tightly bound π electron manifold. The total Hamiltonian is written as

$$H = \sum_i h(i), \qquad h = t + v + v', \tag{39}$$

where t is the kinetic energy operator, v an effective potential operator for the first molecule, and v' an effective potential operator for the second molecule. The matrix elements between molecular orbitals on the same molecule are

$$\int \psi_j h \psi_k \, dv = \delta_{jk} E_j, \qquad \int \psi_{j'} h \psi_{k'} \, dv = \delta_{j'k'} E_{j'}. \tag{40}$$

The corresponding terms for orbitals on two different molecules can be written as

$$\int \psi_j h \psi_{j'} \, dv = \tfrac{1}{2} E_j S_{jj'} + \tfrac{1}{2} E_{j'} S_{jj'} + I_{jj'} \tag{41}$$

if

$$S_{jj'} = \int \psi_j \psi_{j'} \, dv \qquad \text{and} \qquad I_{jj'} = \frac{1}{2} \int \psi_j (v + v') \psi_{j'} \, dv. \tag{42}$$

If molecular orbitals are now expanded in the usual LCAO form, the calculation of the preceding matrix elements introduces the following terms:

$$S_{rr'} = \int \phi_r \phi_{r'} \, dv \tag{43}$$

$$\eta_{rr'} = \frac{1}{2} \int \phi_r (v + v') \phi_{r'} \, dv, \tag{44}$$

where the ϕ_r are the atomic orbitals. Salem observed that in the significant range of ditances (2.5–3.5 Å) where the core repulsive wall is small the overlap is usually smaller than 0.2. Let us suppose that the interacting molecules are identical, and that one molecule is in the excited state corresponding to the one-electron (nondegenerate) excitation $\psi_j \rightarrow \psi_{k'}$. Figure 5 shows the two possible orbital diagrams depending on the sign of

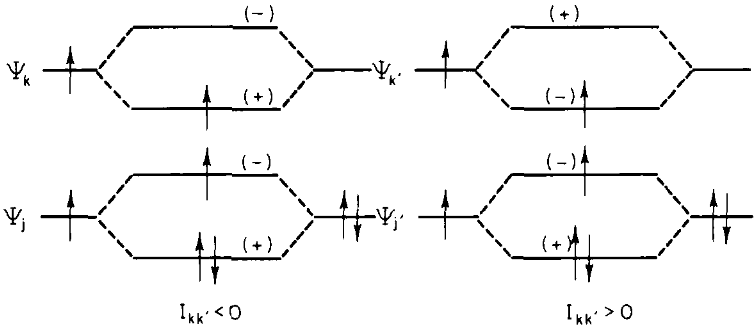

Fig. 5

$I_{kk'}$. It is easy to show that the interaction energy in this case can be written as

$$\Delta E_{\text{int}}^{j\to k} = -(|I_{kk'}| + |I_{jj'}|) + (I_{jj'}S_{jj'} - I_{kk'}S_{kk'}) \tag{45}$$

If now the molecular orbitals are expanded as

$$\psi_j = \sum_r c_{jr}\phi_r \tag{46}$$

the following equation is obtained:

$$\begin{aligned}\Delta E_{\text{int}}^{j\to k} = {} & -\left(\left|\sum_{rr'} c_{jr}c_{j'r'}\eta_{rr'}\right| + \left|\sum_{rr'} c_{kr}c_{k'r'}\eta_{rr'}\right|\right) \\ & + \sum_{rr'} (c_{jr}^2 - c_{kr}^2)\eta_{rr'}S_{rr'} \\ & + \sum_{\substack{\text{all } j' \\ (\neq j)}} \frac{(\sum_{rr'} c_{jr}c_{j'r'}\eta_{rr'})^2}{E_{j'} - E_j} - \sum_{\substack{\text{all } j' \\ (\neq k)}} \frac{(\sum_{rr'} c_{kr}c_{j'r'}\eta_{rr'})^2}{E_{j'} - E_k} + \cdots.\end{aligned} \tag{47}$$

It is interesting to notice that in this formula the first two terms, which are the more important, are directly proportional to the C_{jr}, which may be considered as static indices. This equation shows, once more, *the possibility of using static indices in studying photochemical reactions.* If the molecules are different, an analogous term may appear if there is an accidental degeneracy between ψ_j or ψ_k and any $\psi_{j'}$. If not, the linear term in η_{rr} disappears. As it is obviously an important one, we are led to the conclusion that such a resonance can be a source of reactivity. Let us recall that Daudel and Chalvet (1967) used such a resonance phenomenon to interpret the success of static indices in photochemistry.

In the same paper, formulas have been established which make it possible to calculate the interaction energy between doubly occupied orbitals and, therefore, between two molecules in their ground states.

Salem used these formulas to discuss various topics including photodimerization of butadiene, discussion of Hoffmann and Woodward rules, and the photodimerization of tropone.

Hoffmann and Woodward (1965) established that the one-step condensation of two conjugated systems, one with m π-electrons and the other with n π-electrons, should occur thermally if $m + n = 4q + 2$ and photochemically if $m + n = 4q$ (q, an integer). The corresponding expression for $\Delta E^{(j\to k)}$ permits one easily to give a justification of this rule in the case of a photochemical reaction. In $\Delta E^{(j\to k)}$ the first term,, is the most important. In linear polyenes atomic orbital coefficients at the end atoms are either equal or opposite. Starting from this remark it is easy to show that the first term in ΔE will be particularly large if

$$n + m = 4q. \tag{48}$$

Therefore when $n + m = 4q$ photocycloaddition will be favored.

In this manner Salem is led to the following final conclusions, which are more precise than those of Woodward and Hoffmann[1]:

(a) Thermal reactions between neutral molecules are strongly favored and occur in one step if the total number of π-electrons or atoms is $4q + 2$ and forbidden if it is $4q$. Thermal reactions between a neutral and an ionic component are weakly permitted whatever the (even) total number of electrons.

(b) Photochemical reactions between neutral molecules are strongly favored and occur in one step if the total number of π-electrons or atoms is $4q$ and forbidden if it is $4q + 2$. Photochemical reactions between a neutral and an ionic component are weakly permitted whatever the total number of π-electrons.

VI. General Conclusions

The main theoretical problem which was discussed during the last "Conseil Solvay" seems now to be at least partially solved. We have begun to understand the success of the molecular diagram method; that is, the use of static indices to predict photochemical reactivity. The main reason seems to be that, as in the case of the ground state, there exists relationships between these static indices and dynamic indices. But these dynamic indices are not the same as they are for the thermochemical reaction because the Wheland structure of the transition state is not reached. On the contrary we are led to assume that the reaction path corresponds to complexes in which an *extension* of the delocalized system is suggested.

REFERENCES

ARBUZOV, Y. A. (1965). *Russian Chem. Rev.* (*English Transl.*) **34**, 8, 558.
BERTRAN, J. (1968). Thèses, Paris, Sciences.
BESSIS, G., CHALVET, O. et, POLYDOROPOULOS, C. (1967). *Compt. Rend.* **264**, 1368.
BLOCH-CHAUDÉ, O., and MASSE, J. L. (1955). *Bull. Soc. Chim. France.*, 625.
BOWEN, E. J. (1963). *Advan. Photochem.* **1**, 23.

---

[1] Strictly valid only for alternant hydrocarbons.

Brown, R. D., (1949). *Australian J. Sci.* **2A**, 564.

Brown, R. D. and Harcourt, R. D. (1959). *J. Chem. Soc.*, 3451.

Burkitt, F. H., Coulson, C. A., and Longuet-Higgins, H. C. (1951). *Trans. Faraday Soc.* **47**, 553.

Buu-Hoï, N. P., Daudel, P., Daudel, R., Jacquignon, P., Morin, G., Muxart, R., and Sandorfy, C. (1951). *Bull. Soc. Chim. France* **18**, 132.

Cetina, R., Jain, D. V. S., Peradejordi, F., Chalvet, O., and Daudel, R. (1967). *Compt. Rend.* **264**, 874.

Chalvet, O., Daudel, R., Ponce, C., and Rigaudy, J. (1968). *Intern. J. Quantum Chem.* **2**, 521.

Chapman, O. L., Pasto, D. J., Borden, G. W., and Groswold, A. A. (1962). *J. Am. Chem. Soc.* **84**, 36.

Clementi, E. (1967). *J. Chem. Phys.* **46**, 4731.

Colpa, J. P., McLean, C., and Mackor, E. L. (1963). *Tetrahedron* **19**, 65.

Corey, E. J., and Taylor, W. C. (1964). *J. Am. Chem. Soc.* **86**, 3881.

Coulson, C. A., and Longuet-Higgins, H. C. (1947). *Proc. Roy. Soc.* **A191**, 39; **A192**, 16.

Coulson, C. A., and Jacobs, J. (1949). *J. Chem. Soc.*, 1983.

Crawford, V. A., and Coulson, C. A. (1948). *J. Chem. Soc.*, 1990.

Dauben, W. G. (1967). *in* "Reactivity of the Photoexcited Organic Molecule," p. 171. Wiley (Interscience), New York.

Daudel, R. (1967). *Adv. in Quantum Chem.* **3**, 161.

Daudel, R. (1967). "Theorié Quantique de la Réactivité Chimique." Gauthier Villars Paris.

Daudel, R., and Chalvet O. (1967). *Compt. Rend.* **264**, 1267.

Daudel, R., Sandorfy, C., Vroelant, C., Yvan, D., and Chalvet, O. (1950). *Bull. Soc. Chim. France.* **17**, 66.

de Bie, D. A., and Havinga, E. (1965). *Tetrahedron*, **21**, 2359.

Dewar, M. J. S. (1952). *J. Am. Chem. Soc.* **74**, 3341.

Dufraisse, C. (1955). *Exp. Supple.* **II**, 57.

Dufraisse, C., Rigaudy, J., Basselier, J. J., and Nguyen Kim Cuong (1965). *Compt. Rend.* **260**, 5031.

Etienne, A. (1949). *in* "Traité de Chimie Organique de V. Grignard," **II**, p. 1299. Masson publ. XVII.

Feler, G. (1968). *Theoretica Chim. Acta.* **10**, 33.

Fernandez-Alonso, J. I. (1951). *Compt. Rend.* **233**, 2403.

Fernandez-Alonso, J. I., and R. Domingo (1955). *Anales Real Soc. Esp. Fis. Quim.* (*Madrid*) **51**, 321.

Foote, C. S., and Wesler, S. (1964). *J. Am. Chem. Soc.* **86**, 3879.

Förster, Th. (1949). *Naturwiss.* **36**, 186.

Förster, Th. (1950). *Z. Elektrochem.* **54**, 42, 531.

Hammond, G. S. (1964). *Photochem. Symp. IUPAC Disc.* Strasbourg, France.

Havinga, E. de Jongh, R. O., and Dorst, W. (1956). *Recueil Trav. Chim. Pays-Bas* **75**, 378.

Hercules, R., and Rogers, J., (1965). *J. Phys. Chem.* **64**, 397.

Hoffman, R., and Woodward, R. B. (1965). *J. Am. Chem. Soc.* **87**, 2046.

Itoh, R. (1957). *J. Phys. Soc. Japan* **12**, 644, 809.

Itoh, R. (1958). *J. Phys. Soc.* **13**, 389.

ITOH, R. (1959). *J. Phys. Soc. Japan* **14**, 1224.

JACKSON, G., and PORTER, G. (1961). *Proc. Roy. Soc.* **260**, 13.

LAIDLER, K. J. (1955). "The Chemical Kinetics of Excited States," p. 41. Oxford Univ. Press, London and New York.

LETSINGER, R. L., TAMSAY, O. B., and DE CAIN, J. H. (1965). *J. Am. Chem. Soc.* **87**, 2945.

MALRIEU, J. P. (1966). *Photochem. Photobiol.* **5**, 291.

MASSE, J. L. (1954). *Compt. Rend.* **258**, 1320.

MAYER, J. E. (1965). *in* "Reactivity of the Photoexcited Organic Molecules," p. 73. Wiley, New York.

PORTER, G. (1967). *in* "Reactivity of the Photoexcited Organic Molecules," p. 82, Wiley (Interscience), New York.

PULLMAN, A. and DAUDEL, R. (1946). *Compt. Rend.* **222**, 288.

RIGAUDY, J., COHEN, N. C., and NGUYEN KIM CUONG (1967). *Compt. Rend.* **264C**, 1851.

ROBIN, M. B., HART, R. R., and KUEBLER, N. A. (1966). *J. Chem. Phys.* **44**, 2664.

ROUX, M. (1950). *Bull. Soc. Chim. France.* **17**, 861.

SALEM, L. (1968).

SIMON, Z. (1964). *Zh. Fiz. Khim.* **38**, 1609.

SRINIVASAN, R. (1963). *J. Am. Chem. Soc.* **85**, 4045.

TRSIC, M., BESSIS, G., CHALVET, O., and DAUDEL, R. (1966). *Compt. Rend.* **263**, 386.

WELLER, A. (1952). *Z. Elektrochem.* **56**, 662.

WELLER, A. (1957). *Z. Elektrochem.* **61**, 956.

WELLER, A. (1958). *Z. Physik. Chem.* **17**, 224; **18**, 163.

WELLER, A. (1961). "Progress in Reaction Kinetics." Pergamon Press, Oxford.

WOODWARD, R. B., and HOFFMAN, R. (1965). *J. Am. Chem. Soc.* **87**, 395.

ZIMMERMAN, H. E. (1963). *Tetrahedron* **19**, Suppl. 2, 397.

ZIMMERMAN, H. E. (1966). *Science* **153**, 837.

ZIMMERMAN, H. E. (1966). *J. Am. Chem. Soc.* **88**, 1564.

ZIMMERMAN, H. E., and WILSON, J. W. (1964). *J. Am. Chem. Soc.* **86**, 4063.

The Origin of Binding and Antibinding in the Hydrogen Molecule-Ion

M. J. FEINBERG*
Department of Chemistry
Tufts University
Medford, Massachusetts
and
KLAUS RUEDENBERG
and ERNEST L. MEHLER†
Institute of Atomic Research
Dept. of Chemistry, Dept. of Physics
Iowa State University
Ames, Iowa

---

* Contribution No. 355 from the Department of Chemistry, Tufts University.

† Work was performed in part in the Ames Laboratory of the U. S. Atomic Energy Commission, Contribution No. 2233.

I. Introduction

Current progress towards better quantum chemical calculations is leading to increasingly complex wave functions, making it more and more difficult to relate them to qualitative ideas about chemical binding. Thus a need arises for conceptual interpretations which are appropriate for such wavefunctions and at the same time allow for the development of a corresponding physical and chemical intuition.

A general interpretative scheme was recently developed by Ruedenberg (1962) and subsequently applied to a number of homonuclear and heteronuclear diatomics as well as to the water molecule (Rue and Ruedenberg, 1964; Layton, Jr., and Ruedenberg, 1964; and Edmiston and Ruedenberg, 1964). Applications to nitriles were made by Popkie and Moffat (1968). Although these analyses yielded interesting results, it became apparent that detailed investigations of simple prototype molecules would be desirable in order to clarify many aspects essential for the understanding of larger systems.

For this reason, a careful analysis of the simplest case, namely the hydrogen molecule-ion, is carried through in the present investigation. It is hoped that possible uncertainties and ambiguities have been examined with sufficient attention to detail so that answers are found to many questions likely to be raised with respect to the origin of binding in this molecule.

II. Premises

Although it has been more than thirty years since the first successful calculations were made on the hydrogen molecule and molecule-ion, discussion persists with regard to an appropriate physical interpretation even for these simple systems. Closer examination shows that various types of reasoning put forth as explanations of the origin of binding usually differ because different *initial premises* are selected as bases for the argumentation. It is therefore essential that we clarify at the outset various concepts and premises which underlie the present approach. They include the objective of physical pictures, the use of the variation principle as basis for a physical interpretation, in particular as regards the binding energy, and the role of the virial theorem in characterizing solutions to the variational problem.

A. Physical Pictures, Variation Principle, Binding Energy

1. Objective of Physical Pictures

In the present investigation, we regard a physical picture as a set of conceptual constructs and analogies with the help of which one can *qualitatively but correctly* anticipate results which one would obtain *quantitatively* by executing the quantum mechanical calculation. In other words, we insist that a physical picture represents a *bona-fide facsimile* of the mathematical workings of the Schrödinger equation. *Only such pictures can form the basis for an intuition in harmony with quantum mechanics.*

The ability to serve well in achieving the aim just described is, in our view, ample justification for the value of such pictures, *regardless of whether or not they represent directly observable quantities.* Using non-observable pictorial concepts to gain insight into characteristic features of wave functions in no way interferes with those concepts which are necessary to describe relations between wave functions and measurement. The two kinds of constructs serve different purposes and no conflict is possible as long as this separation of usage is clearly maintained.[1]

2. Variation Principle as Basis for Physical Pictures

We choose the variation principle as basis for understanding wave functions. The operation of the variation principle is visualized as the process which selects the solution of the Schrödinger equation by seeking that wave function which has the lowest energy expectation value. Thus, the characteristics of this solution can be understood by analyzing the terms which contribute to the energy integral and, hence, are responsible for singling out the *actual* solution from all *virtual* wave functions germane to the problem.

In this context, we introduce physical pictures whose purpose is to make possible a meaningful estimate of the terms just referred to without

---

[1] For further comments on this subject see the introduction of Ruedenberg (1962).

having to resort to detailed numerical calculations. In order to achieve this end we shall partition the energy expectation value into fragments which satisfy the following desiderata, as well as possible:

(a) with each fragment, a physical picture can be associated;
(b) using the concepts embodied in these pictures, one can assess the energies of the various fragments;
(c) when the wave function is varied, the energies of the fragments exhibit variations explainable in terms of these physical pictures;
(d) putting together the estimates deduced in this fashion, one can then understand why certain wave functions minimize the energy integral.

3. *Binding Energies and Variation Principle*

Binding energies and energies of reactions are differences between *eigenstates*, in particular ground state energies of various atoms and molecules. A physical picture which is to account for the phenomenon of binding must therefore be closely related to those pictures which offer an explanation for the magnitudes of the energies of such states.

The variation principle is particularly suited to give insight into the energy differences occurring in a chemical reaction because, in contrast to the Schrödinger equation itself, it allows for the comparison of energy expectation values, $\langle \Phi | \mathscr{H} | \Phi \rangle$, of various virtual wave functions, which are not actual solutions.

Consider the case where the product system has a lower energy than the reactant system. By virtue of the variation principle there must then exist comparison functions $\tilde{\Phi}_P$ for the product system which have energy expectation values $\langle \tilde{\Phi}_P | \mathscr{H}_P | \tilde{\Phi}_P \rangle$ equal to the energy of the reactants. Suppose now that by exploiting certain resemblances to the reactant systems, it is possible to construct such a function $\tilde{\Phi}_P$. Suppose also that the aforementioned physical pictures for the energy fragments enable one to explain why the energy integral $\langle \tilde{\Phi}_P | \mathscr{H}_P | \tilde{\Phi}_P \rangle$ is:

(a) approximately equal to the energy of the reactants;
(b) higher than the energy integral $\langle \Phi_P | \mathscr{H}_P | \Phi_P \rangle$, where Φ_P is the true product wave function.

Then, the energy lowering in the reaction can be understood by the following argument: There are comparison functions of the product system whose energy expectation values can be shown to be approximately equal to the energy of the reactants, and there are other wave functions of the product system which can be shown to give a lower energy expectation value. By virtue of the variation principle, the true solution for the product has therefore necessarily a lower energy than that for the reactants.

Frequently a more general argument is convenient, in which four wave functions are considered; namely, Φ_P and Φ_R, the true solutions of the product and reactant systems, respectively, as well as $\tilde{\Phi}_P$ and $\tilde{\Phi}_R$, virtual comparison functions for the systems indicated by the subscripts. Because of the variation principle, the inequalities

$$\langle\tilde{\Phi}_P|\mathscr{H}_P|\tilde{\Phi}_P\rangle > \langle\Phi_P|\mathscr{H}_P|\Phi_P\rangle$$

$$\langle\tilde{\Phi}_R|\mathscr{H}_R|\tilde{\Phi}_R\rangle > \langle\Phi_R|\mathscr{H}_R|\Phi_R\rangle$$

are known to hold. Moreover, $\tilde{\Phi}_R$ and $\tilde{\Phi}_P$ are chosen in such a manner that, with the help of suitable physical pictures, it is possible to understand these inequalities as well as the quantitative value of the energy difference

$$\langle\tilde{\Phi}_P|\mathscr{H}_P|\tilde{\Phi}_P\rangle - \langle\tilde{\Phi}_R|\mathscr{H}_R|\tilde{\Phi}_R\rangle.$$

In this way, *physical pictures which make possible a comparison of energy integrals*, in conjunction with the *variation principle, which provides a criterion to distinguish true solutions from virtual comparison functions*, furnish an interpretative scheme for understanding reaction energies.

It is crucial that a way exists to make a quantitative comparison between *some* product energy integral $\langle\tilde{\Phi}_P|\mathscr{H}_P|\tilde{\Phi}_P\rangle$ and *some* reactant energy integral $\langle\tilde{\Phi}_R|\mathscr{H}_R|\tilde{\Phi}_R\rangle$. Unless one can develop physical pictures, which furnish the means for doing *this*, it would appear difficult indeed to formulate a logically coherent interpretation of reaction energies. This requirement also puts certain limitations on the possible choices of $\tilde{\Phi}_R$ and $\tilde{\Phi}_P$ which, frequently, will have to be virtual intermediate states.

4. *Relation to Previous Approaches*

The point of view outlined in the previous section is not new in quantum chemistry, although it never seems to have been formulated as explicitely.

A classical example is the understanding of the aromatic stability of benzene. The reactants are three ethylene molecules; the "intermediate" state, $\tilde{\Phi}_P$, corresponds to a single Kekulé structure; the benzene molecule itself is the reaction product. The energy difference between the reactants and the Kekulé structure is predicted from the concepts of aliphatic chemistry. It is now observed that, because of degeneracy, a superposition of two Kekulé structures can be expected to give a lower energy integral than one Kekulé structure. *By virtue of the variation principle, it is then concluded that the actual ground state wave function for benzene is closer to* *this superposition and that it therefore possesses an additional stability beyond that predicted from aliphatic bond energies.*

Another example is the "kinetic explanation" of chemical binding which goes as follows. Two separate atoms are considered as two separate boxes with free electrons. The "intermediate state," $\tilde{\Phi}_P$, corresponds to the situation where the two boxes are moved side by side so as to have one wall in common. It is assumed that this juxtaposition does not change the energy appreciably because the interatomic coulombic interactions cancel each other. Now the central wall is removed. The electronic wave function for the new box, Φ_P, has a larger wavelength and hence, a lower kinetic energy than $\tilde{\Phi}_P$. Implying that changes in the potential energy can be neglected, the variation principle is applied to the kinetic energy alone and it is concluded that the molecule can be considered to be the box which results by removal of the central wall. These arguments yield a kinetic origin of chemical binding.

There is an opposite point of view which regards changes in the kinetic energy as negligible and applies the variation principle to the potential energy in the following way. Two atoms are juxtaposed without electron sharing to form an "intermediate" state, $\tilde{\Phi}_P$. Interatomic coulombic interactions are again assumed to cancel. Then electron sharing is considered and found to generate a characterisic overlap between atomic orbitals resulting in an accumulation of charge in the bond. This latter is now presumed to lower the potential energy, and hence the total energy, because the attraction of both nuclei is said to be effective in the bond. By virtue of the variation principle, it is then concluded that the true molecular wave function exhibits electron sharing and thereby leads to chemical binding. Thus, one arrives at a purely "potential explanation" of chemical binding.

5. *Remarks*

(1) It may be noted that, in the last two examples, arguments originating from the variation principle are applied to either the kinetic or the potential energy *alone* instead of to the *total* energy. We will see below that, in fact, the variation of neither quantity can be neglected.

(2) It should also be stressed that the kind of "variational thinking" developed in the preceding sections must be applied to the energy integral in its original form. That is to say, *it is no longer valid after the energy integral has been transformed by substitutions which are based on relationships satisfied only by the actual solution of the Schrödinger equation.* Such relationships are, for example, the virial theorem and the Hellmann–Feynman theorem.

(3) Finally, it should be emphasized that the phenomenon of the eigen state is intimately related to the fact that molecules are subject to the laws of quantum mechanics; there are no ground states in classical mechanics or electrostatics. Consequently, *a physical picture seeking to describe chemical binding must necessarily incorporate features which distinguish quantum mechanics from classical mechanics and electrostatics.* Using the energy variation principle does indeed meet this criterion since the classical equations of motion cannot be obtained by minimizing the classical energy. It may be added that the existence of a ground state is intrinsically connected with the fact that the variation integral contains *both kinetic and potential energy*, as will be amplified in the subsequent section. Omission of one or the other from consideration cannot, therefore, lead to a full interpretation of binding.

B. Competition between Virtual Kinetic and Potential Energies, Virial Theorem

1. *Competition Between Virtual Kinetic and Potential Energies*

Characteristic properties of molecular wave functions derive from the fact that the integral which is to be minimized, i.e., the energy, consists of two parts with opposite sign, namely the positive kinetic energy integral and the negative potential energy integral. The minimization process therefore seeks wave functions which will either lower the absolute value of the kinetic energy integral or increase the absolute value of the potential energy integral, or do both. In the case of bound states the total energy is negative, i.e., the potential energy is greater in absolute value than the kinetic energy.

An essential point is now that the negative value of the potential energy arises solely from the coulombic attraction of the electrons by the nuclei. Only by confining the electronic wave function to the vicinity of the nuclear positions is it possible to obtain large negative potential energies. Such contraction of the wave function will, however, lead to a strong increase in the kinetic energy which arises from an increase in the gradient of the wave function and can be related to the uncertainty principle. The minimization of the total energy has therefore the character of a competition between the kinetic energy and the potential energy integrals which can be formulated as follows: The *nuclear suction* tends to concentrate the variational trial functions near the nuclear centers whereas the *kinetic energy pressure* tends to expand these functions as much as possible. *The actual solution can be said to establish the optimal compromise in the competition between nuclear suction and kinetic energy pressure.*

2. An Example: The H Atom. As an example, let us understand the hydrogen atom ground state by applying the variation principle to the trial functions

$$\Phi_H(\alpha) = (\pi\alpha^3)^{-1/2} \exp(-r/\alpha). \tag{1}$$

The variation parameter α represents a measure of the extension of the electronic cloud. Here and in the sequel atomic units are used, i.e.,

$$\begin{aligned}\text{unit of length} &= a = \hbar^2/me^2 = 1 \quad \text{bohr}\\ \text{unit of energy} &= e^2/a = \hbar^2/ma^2 = 1 \quad \text{hartree.}\end{aligned}$$

The kinetic, potential, and total energies are given by

$$T_H(\alpha) = \tfrac{1}{2}\int d\tau[\nabla\Phi_H(\alpha)]^2 = 1/2\alpha^2 = \tfrac{1}{2}\zeta^2 \tag{2}$$

$$V_H(\alpha) = -\int d\tau\Phi_H{}^2(\alpha)/r = -1/\alpha = -\zeta \tag{3}$$

$$E_H(\alpha) = \tfrac{1}{2}\zeta^2 - \zeta, \tag{4}$$

where

$$\zeta = \alpha^{-1}. \tag{5}$$

The graphical representation of these quantities as functions of α, given in Fig. 1, clearly exhibits the competition between T and V leading to the optimal compromise at $\alpha = 1$ where E has its minimum. The wave function $\Phi_H(\alpha = 1)$ will be denoted by Φ_H.

Whereas the variation of V corresponds to that of an electrostatic space charge, the increase of T with the decrease of α clearly arises from the fact that the gradient of $\Phi_H(\alpha)$ gets larger and larger as the wave function is localized. This behavior can be related to the uncertainty principle in the following way. Consider the electron as traveling on a circle of radius α and the uncertainty principle in the form

$$\Delta p_x \,\Delta x = \hbar. \tag{6}$$

For this circular motion, one has

$$\Delta p_x = p, \qquad \Delta x = \alpha, \tag{7}$$

where p is the absolute value of the *total* momentum, and one finds therefore

$$p^2/2m = \tfrac{1}{2}(\hbar^2/ma^2)(a^2/\alpha^2). \tag{8}$$

Hence, in atomic units,

$$T = 1/2\alpha^2. \tag{9}$$

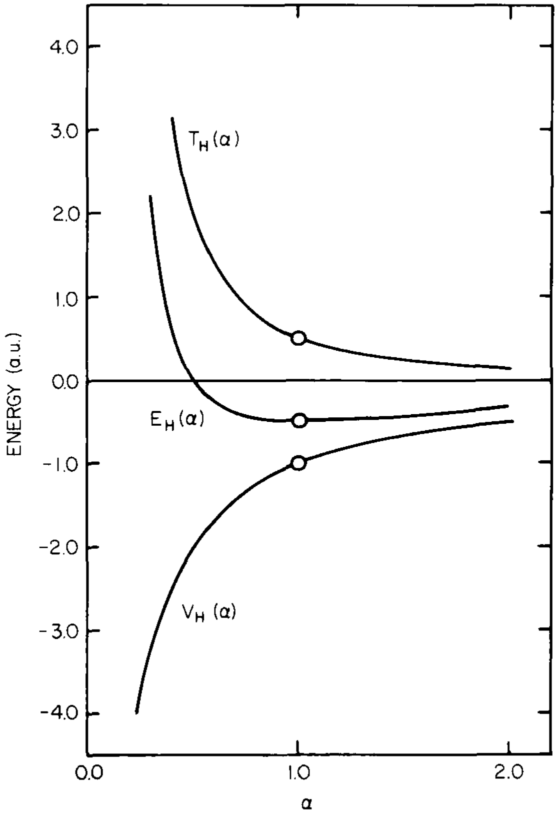

Fig. 1. Competition between kinetic and potential energy in determining the ground state of atomic hydrogen.

3. Virial Theorem for Atoms

In any atomic system, the virial theorem

$$2T + V = 0 \tag{10}$$

holds for the true wave function. More generally, it holds for any function whose energy is minimized with respect to a "scale parameter" (Fock, 1930). For example, if a trial function $\zeta^{3/2} f(\zeta r)$ is assumed for hydrogen, and if ζ is determined by energy minimization, then the virial theorem is fulfilled regardless of the form of $f(r)$. "Scaling" can be considered as the simplest and most descriptive type of contraction–expansion variation, and ***here the virial theorem can be used instead of the variation principle for finding*** *the point of optimal compromise in the competition between T and V.*

In the case of the hydrogen atom, for example, this can be done as follows. From the electrostatic relation (3) for the potential energy and the result of the uncertainty principle (9) for the kinetic energy, the relation

$$2T/V^2 = 1 \tag{11}$$

holds for any scale variation. Combining this with the virial theorem

$$2T/V = -1, \tag{12}$$

one finds immediately the result

$$T = \tfrac{1}{2}, \qquad V = -1, \qquad E = -\tfrac{1}{2}. \tag{13}$$

The virial theorem can therefore be regarded as an *indicator* characterizing the optimal compromise in the competition between T and V under scale variations.

4. *Virial Theorem for Molecules*

Within the Born–Oppenheimer approximation, a more general form of the virial theorem, namely,

$$2T + V + R(dE/dR) = 0, \tag{14}$$

holds for diatomic molecules (Slater, 1933). This relation is valid regardless of whether the nuclear repulsion is included or not. *If* it is included, then Eq. (14) reduces, at the equilibrium distance, to the form of Eq. (10), i.e., the form valid for the separated atoms. Therefore, a virial relationship

$$\Delta E = -\Delta T = \tfrac{1}{2}\,\Delta V \tag{15}$$

holds also for the energy *differences* between the molecule at the equilibrium distance and the separated atoms.

The molecular virial theorem in the form (14) is not only valid for the true solution but also for any function whose energy is minimized with respect to a somewhat more general scale variation (Löwdin, 1959). It is defined by a variation function of the form

$$\begin{aligned} &F(\mathbf{r}_1, \mathbf{r}_2, \ldots; \mathbf{R}_A, \mathbf{R}_B, \ldots; t) \\ &\quad = t^{3N/2} f(t\mathbf{r}_1, t\mathbf{r}_2, \ldots; t\mathbf{R}_A, t\mathbf{R}_B, \ldots), \end{aligned} \tag{16}$$

where $\mathbf{r}_1$, $\mathbf{r}_2$, ... are electronic coordinates and $\mathbf{R}_A$, $\mathbf{R}_B$, ... are nuclear positions. If the wave function is expressed in terms of atomic orbitals, such a scale variation is seen to be equivalent to multiplying all orbital exponents by t. Therefore, this variation corresponds to a uniform and simultaneous contraction or expansion of the electronic cloud *towards all nuclei* and is therefore analogous to that discussed in the atomic case.[2]

If, after minimization with respect to t, the function (16) is not the true solution, then the simple form of the virial theorem, as expressed by Eqs. (10) and (15), holds *at the equilbrium positions predicted by this approximation*, and not at the actual equilibrium position.

III. Wave Functions and Densities in the Ground State

A. Wave Functions

In the present investigation, we consider two wave functions for the binding state of the hydrogen molecule-ion: The simple molecular orbital of Finkelstein and Horowitz (1928) and the rather accurate approximation of Guillemin and Zener (1929). Both of these functions can be written in the form

$$\Phi = [A + B][2(1 + S)]^{-1/2}, \tag{17}$$

where A and B are appropriate normalized atomic orbitals on nuclei A and B, respectively, and S is the overlap integral

$$S = \int d\tau\, AB. \tag{18}$$

It is frequently said that, in a molecule such as H_2^+, the electron is *shared* between the atoms. *We contend that this picture expresses the fact that the molecular wave amplitude can be interpreted as a superposition of two atomic wave amplitudes.*

The simplest choice of atomic orbitals is that of Finkelstein and Horowitz (FH), namely, 1*s* orbitals:

$$\begin{aligned} A_{\mathrm{FH}}(\zeta) &= (\zeta^3/\pi)^{1/2} \exp(-\zeta r_A) \\ B_{\mathrm{FH}}(\zeta) &= (\zeta^3/\pi)^{1/2} \exp(-\zeta r_B), \end{aligned} \tag{19}$$

where the orbital exponent, ζ, is a variation parameter whose meaning has been discussed in Eqs. (1)–(5). The corresponding molecular orbital will be called $\Phi_{\mathrm{FH}}(\zeta)$.

---

[2] Contraction does not have to be described by a variation of orbital exponents. It is well known that minimization with respect to orbital exponents is less important the larger the basis set of atomic orbitals is chosen. In this case, the virial theorem can be fulfilled by minimization with respect to linear superposition coefficients only. Under these conditions, contraction is achieved by orbital mixing. Contraction is therefore a more fundamental concept than scaling.

The Guillemin–Zener (GZ) function is defined by choosing A and B in Eq. (17) as the normalized functions

$$\begin{aligned} A_{\mathrm{GZ}}(\zeta_A, \zeta_B) &= C\exp(-\zeta_A r_A - \zeta_B r_B) \\ B_{\mathrm{GZ}}(\zeta_A, \zeta_B) &= C\exp(-\zeta_B r_A - \zeta_A r_B), \end{aligned} \tag{20}$$

where C is a normalization constant given explicitly in Appendix A. The corresponding molecular orbital will be called $\Phi_{\mathrm{GZ}}(\zeta_A, \zeta_B)$. The functions of Eq. (20) may be regarded as approximating distorted 1*s* atomic orbitals.[3]

In confocal elliptic coordinates [$\xi = (r_A + r_B)/R$, $\eta = (r_A - r_B)/R$, $R =$ the internuclear distance], both the FH and GZ orbitals have the form

$$\begin{aligned} \bar{A}(\zeta_1, \zeta_2) &= C\exp[-\tfrac{1}{2}R(\zeta_1\xi + \zeta_2\eta)] \\ \bar{B}(\zeta_1, \zeta_2) &= C\exp[-\tfrac{1}{2}R(\zeta_1\xi - \zeta_2\eta)], \end{aligned} \tag{21}$$

where

$$\zeta_1 = \zeta_A + \zeta_B, \qquad \zeta_2 = \zeta_A - \zeta_B, \qquad \text{for GZ},$$

$$\zeta_1 = \zeta_2 = \zeta, \qquad \text{for FH}.$$

For the FH case, the ξ and η directions are scaled equally. In contrast, the GZ function allows for different scaling in the ξ and η directions. The difference $(\zeta_1 - \zeta_2)/2 = \zeta_B$ can be regarded as a measure of distortion polarization or departure from the spherical symmetry of the 1*s* orbital.

The present discussion is based upon the nonrelativistic Hamiltonian

$$\mathscr{H} = -\tfrac{1}{2}\nabla^2 - r_A^{-1} - r_B^{-1} + R^{-1}. \tag{22}$$

The most recent calculations of the optimal values of ζ, ζ_1, and ζ_2 as functions of R have been published by Kim *et al.* (1965). An independent calculation with the FH function for a larger range of R values had been carried out previously by one of the present authors (E.L.M.) and is reported in Appendix B. Table I summarizes pertinent results for both wave functions. The optimized FH and GZ functions will be denoted by Φ_{FH} and Φ_{GZ}, respectively.

It is seen that the FH and GZ functions yield very slightly different equilibrium positions. For convenience, the calculations in the sequel are based on the intermediate internuclear distance $R = 2.0$ au. From Table I, it is evident that this adjustment of R in the third decimal place has no bearing on energetic considerations.

---

[3] Actually, A_{GZ} has a little cusp at the position of atom B. For the internuclear distances of interest here, this discontinuity in the derivative is, however, so small that it does not affect the interpretation given in the text.

TABLE I

ENERGIES AND VARIATION PARAMETERS FOR THE H_2^+ BINDING STATE AT THE MINIMUM

	Finkelstein–Horowitz		Guillemin–Zener	
	$R_{eq} = 2.0033$	$R = 2.0$	$R_{eq} = 1.9979$	$R = 2.0$
ζ	1.2380	1.2387	—	—
ζ_A	—	—	1.1366	1.1365
ζ_B	—	—	0.2176	0.2174
T	0.5865	0.5871	0.6022	0.6020
V	−1.1730	−1.1736	−1.2047	−1.2044
E	−0.5865	−0.5865	−0.6024	−0.6024
E^B	−0.0865	−0.0865	−0.1024	−0.1024

B. Comparison of Molecule and Separated Atoms

In Section II we emphasized the need for constructing virtual intermediate states $\tilde{\Phi}_R$ and $\tilde{\Phi}_P$ whose energies can be related to each other by a suitable interpretation. In the present problem we chose $\tilde{\Phi}_R$ identical to $\Phi_R = \Phi_H(\zeta = 1) = \Phi_H$, the ground state of the hydrogen atom as given in Eq. (1). For the hydrogen molecule-ion, we choose $\tilde{\Phi}_P = \Phi_{FH}(\zeta = 1) = \tilde{\Phi}_{FH}$, the superposition of 1*s* orbitals of the two constituent atoms, at $R = 2.0$ au, without change in the orbital exponents. In the present context we furthermore identify Φ_{GZ} with Φ_P, the true solution of the molecule-ion. Thus, we can describe the transition from the atomic wave function Φ_H to the molecular wave function Φ_P in terms of the following three steps:

$$\Phi_R = \Phi_H \xrightarrow{(I)} \tilde{\Phi}_{FH} \xrightarrow{(II)} \Phi_{FH} \xrightarrow{(III)} \Phi_{GZ} = \Phi_P, \qquad (23)$$

where Φ_{FH} is the FH function with optimal ζ and Φ_{GZ} is the GZ function with optimal ζ_A and ζ_B.

Frequently, the comparison of properties derived from $\tilde{\Phi}_{FH}$ with those derived from Φ_H requires a further decomposition of the first of the steps indicated in Eq. (23). The density of $\tilde{\Phi}_{FH}$ is written in the form

$$\tilde{\Phi}_{FH}^2 = \tfrac{1}{2}\{A_{FH}^2(\zeta = 1) + B_{FH}^2(\zeta = 1)\} + \text{"remainder,"} \qquad (24)$$

and the transition from the atomic density to the molecular density is described in terms of the four steps

$$\Phi_H{}^2 \xrightarrow{(Ia)} \tfrac{1}{2}\{A_{FH}^2(1) + B_{FH}^2(1)\} \xrightarrow{(Ib)} \tilde{\Phi}_{FH}^2 \xrightarrow{(II)} \Phi_{FH}^2 \xrightarrow{(III)} \Phi_{GZ}^2. \qquad (25)$$

The first term on the right side of Eq. (24) is merely the mean value of the densities of the two atoms and it therefore turns out to be relatively easy to establish quantitative relations corresponding to Step (Ia) of Eq. (25). The contributions of various properties arising from the "remainder" of Eq. (24), which furnish Step (Ib) of Eq. (25), can also be assessed without difficulty.

These steps are illustrated by the diagrams given in Fig. 2. The five parts exhibit plots for the following quantities along the internuclear axis:

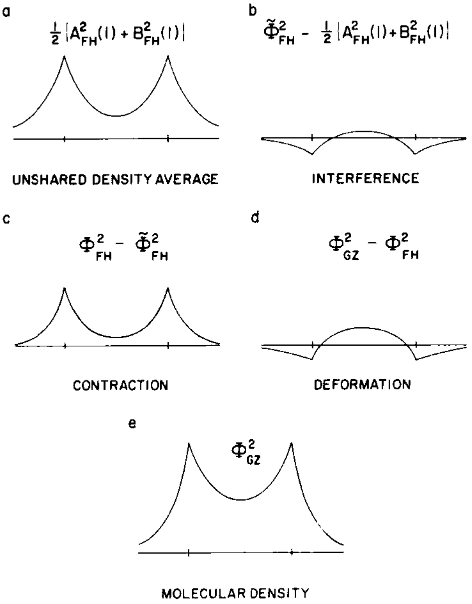

Fig. 2. Transition from atomic density to molecular density according to Eq. (25).

Fig. 2a: $\frac{1}{2}\{A^2_{FH}(1) + B^2_{FH}(1)\}$;
Fig. 2b: $\tilde{\Phi}^2_{FH} - \frac{1}{2}\{A^2_{FH}(1) + B^2_{FH}(1)\}$ = "remainder" of Eq. (24);
Fig. 2c: $\Phi^2_{FH} - \tilde{\Phi}^2_{FH}$;
Fig. 2d: $\Phi^2_{GZ} - \Phi^2_{FH}$;
Fig. 2e: Φ^2_{GZ}.

The omitted transition from the density of the separated atoms to the density of Fig. 2a can be imagined by first bringing a proton up to a distance of $R = 2.0$ au from a hydrogen atom and then dividing the electron density equally between the two centers.

Figure 2b shows that the density of the wave function $\tilde{\Phi}_{FH}$ differs from the average of the atomic densities by an accumulation of charge in the central region. This charge is taken away from two regions located more or less symmetrically around each of the two nuclei.

Figure 2c shows that the next best approximation, Φ_{FH}, differs from $\tilde{\Phi}_{FH}$ by a contraction of electronic charge toward the two nuclei which is a result of the increase in ζ from 1 to 1.2387.

Figure 2d illustrates that the true solution differs from Φ_{FH} by a deformation which transfers charge in a direction parallel to the nuclear axis from a region outside the two centers to the region between them.

The density differences characterized by Figs. 2b–d will, in the sequel, be referred to as interference, contraction, and deformation, respectively. The word "interference" has been chosen because the "remainder" in Eq. (24) represents the difference between the square of a sum of two wave amplitudes and the sum of the squares of the two amplitudes, with appropriate normalizations. It can also be regarded as the difference between electron sharing, as defined after Eq. (18), and density averaging.

IV. The Origin of Binding in the Ground State

A. Variational Considerations

Let us focus our attention on the first two steps in Eq. (23), namely, the transition from Φ_H to Φ_{FH}. Figure 3 gives two sets of curves. The dashed curves, an enlargement of Fig. 1, give the kinetic, potential, and total energies of the hydrogen atom trial function of Eq. (1) as functions of α, near the minimum, $\alpha = 1.0$. The solid curves represent the analogous quantities which result for the molecule-ion if the FH trial function $\Phi_{FH}(\zeta)$ is used.

In comparing the two sets of curves, we note the following characteristics:

(a) The *overall behavior* of the H_2^+ curves is very similar to that of the H atom curves. The interatomic interactions merely result in a moderate *shift of the curves.*

(b) The kinetic energy curve is "responsible" for the characteristics of the *shift* in the total energy curve: For *any* α, there is a decrease in the kinetic energy and an increase in the potential energy, such that the former outweighs the latter. Hence, the molecular energy curve of H_2^+ lies below that of the H atom for a wide range of $\alpha < 1.23$. This is indicated by the text on the left-hand side of Fig. 3.

(c) The *minimum* for H_2^+ lies at approximately $\alpha = 0.8$ as compared to $\alpha = 1$ for the atom.

(d) The kinetic energy is also "responsible" for the *shift in the minimum.*

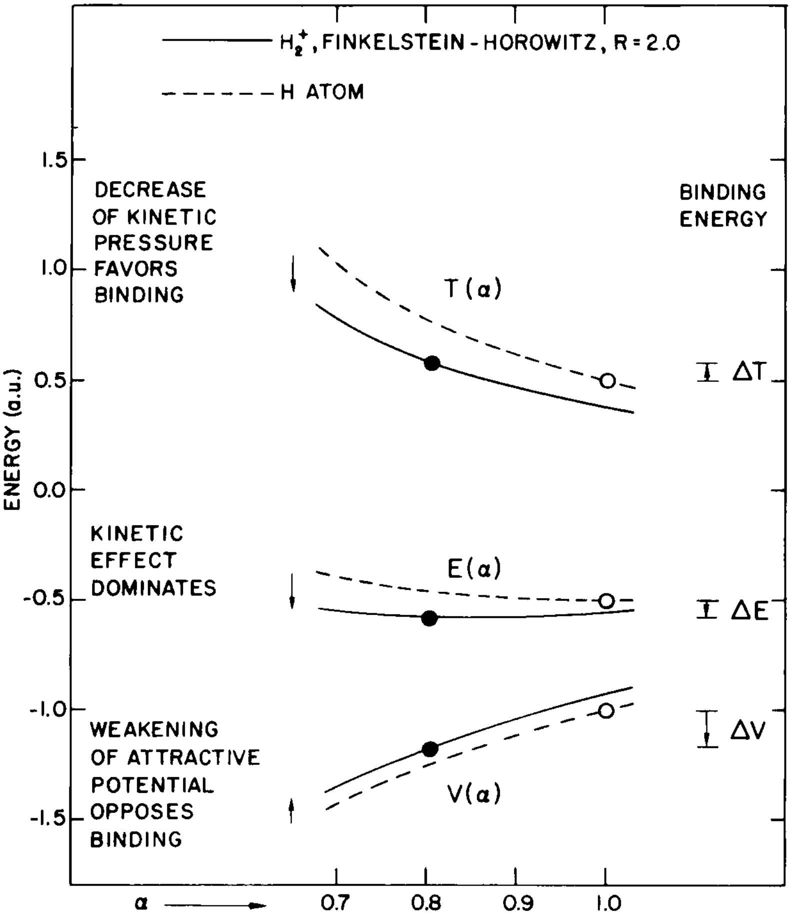

Fig. 3. Competition between kinetic and potential energy in the FH approximation to the H_2^+ molecule and comparison with the H atom.

This is so since, at $\alpha = 1$, one finds $T(H_2^+) < |\frac{1}{2}V(H_2^+)|$, whereas the minimum is characterized by the virial theorem, $T(H_2^+) = |\frac{1}{2}V(H_2^+)|$. Since the overall character of the T-V competition is still similar to that of the free atom, it is clear that only by going to $\alpha < 1$ can $T(H_2^+)$ be increased until it equals $|\frac{1}{2}V(H_2^+)|$. Using the concepts formulated in Section II, one may say: *Because the virtual kinetic energy pressure is lower in H_2^+ than in H, the nuclear suction is somewhat more successful in contracting and localizing the electron cloud near the nuclei.*

Let us now consider the first two steps of Eq. (23) separately. The first step, $\Phi_H \rightarrow \tilde{\Phi}_{FH}$, corresponds to going from the H curves to the H_2^+ curves for $\alpha = 1.0$ It is seen that even for this wave function, $\tilde{\Phi}_{FH}$, binding occurs, but it must be noticed that in this case binding results *because of a drop in kinetic energy in spite of an increase in potential energy.* The second step of Eq. (23) leads from $\tilde{\Phi}_{FH}$ to Φ_{FH}, that is, from $\alpha = 1.0$ to $\alpha = 0.8$ on the solid curves of Fig. 3. After completion of the second step, binding is seen to arise from a *drop in potential energy in spite of an increase in kinetic energy*, as indicated by ΔE, ΔT, and ΔV on the right-hand side of Fig. 3. The differences in the wave functions $\tilde{\Phi}_{FH}$ and Φ_{FH} are therefore significant.

If we finally consider the third step of Eq. (23), it is clear that the energy is further lowered due to the additional flexibility in the wave function permitting deformation of the atomic orbitals.

Each of the three steps in Eq. (23) corresponds, therefore, to a lowering of the total energy. In order to carry out the program suggested in Section II, it is now necessary to provide physical pictures to account for these lowerings. In the present section, this problem will be solved by partitioning the energy according to a geometric division of the molecule into atomic and bond regions; in Section V the same problem will be analyzed from an orbital viewpoint.

B. Geometric Partitioning of the Kinetic Energy

1. Cartesian Components of the Kinetic Energy

The kinetic energy is a unique sum of three components,

$$T = T_x + T_y + T_z, \tag{26}$$

where the z axis is chosen collinear with the internuclear axis, and x and y denote two axes perpendicular to it. It is of interest to examine the relationship between the behavior of the total kinetic energy, discussed in the preceding section, and that of its three components.

Table II gives a breakdown of the total kinetic energy in terms of the Cartesian components, defined in Eq. (26), for the following six systems:

(i) the ground state H atom;
(ii) the contracted H atom described by function (19) for $\zeta = 1.2387$;
(iii) the deformed contracted atom described by function (20) with $\zeta_A = 1.1365$ and $\zeta_B = 0.2174$;
(iv) the virtual molecular function $\tilde{\Phi}_{FH}$, i.e., the FH function with $\zeta = 1.0$;
(v) the molecular function Φ_{FH} with $\zeta = 1.2387$;
(vi) the true molecular function Φ_{GZ}.

TABLE II

CARTESIAN COMPONENTS OF KINETIC ENERGY

		FH ($\zeta = 1.0$)	FH ($\zeta = 1.2387$)	GZ ($\zeta_A = 1.1365$) ($\zeta_B = 0.2174$)
Atom	T_x	0.1667	0.2557	0.2550
	T_y	0.1667	0.2557	0.2550
	T_z	0.1667	0.2557	0.2319
	T	0.5000	0.7671	0.7419
Molecule	T_x	0.1477	0.2257	0.2311
	T_y	0.1477	0.2257	0.2311
	T_z	0.0908	0.1357	0.1398
	T	0.3862	0.5871	0.6020

The following observations are apparent from this table:

(a) For fixed values of ζ, ζ_A, ζ_B, the molecular kinetic energy is lower than the corresponding atomic value, essentially *because of a sharp drop in the contribution of the z component.* It is reasonable to compare this behavior of T_z, with the decrease in kinetic energy of a particle in a one-dimensional box as the box length is increased. Indeed, if a box of length 5.5 au, whose free electron energy is identical to the atomic T_z value of 0.167 au, is lengthened to (5.5 + 2.0) au, then the free electron energy of the enlarged box becomes 0.087 au, i.e., almost equal to the molecular T_z value of 0.091.

(b) There is an increase in going from the first column to the second column *for the molecule as well as for the atom.* It is noteworthy that the increase occurs for all three components of the molecular kinetic energy. In fact in every one of the eight rows the kinetic energy increases by approximately the same ratio, $1.5 \approx (1.2387)^2$.[3] This appears to suggest that even in the molecule this increase is due to a contraction of an atomic character and this will be confirmed below.

(c) For the free atom, there is a decrease of the T_z component in going from the second to the third column. This must be attributed to a stretching of the atomic orbital in the z direction by introducing the type of atomic deformation defined in Eq. (20). In contrast, there is an *increase* in the components of the *molecular* kinetic energy in going from the second to the

---

[3] It may be noted that the decrease of T_z, in going from the atom to the molecule at $\zeta = 1.0$, is so strong that the *final* value of T_z is still slightly less than that of the free atom, although the subsequent contraction increases T_z in approximately the same ratio as T_x and T_y.

third column. This suggests that the deformation rearrangement illustrated by Fig. 2d shifts charge into regions where $|\nabla\Phi|$ is larger.

2. *Basis of Atomic and Bond Decomposition*

The results just found suggest that it may be informative to divide the molecule into atomic and bond regions and to examine the corresponding energy contributions. It appeared simplest to choose as boundaries separating the three regions a two-sheet hyperboloid defined by $\eta = \pm\eta_0 =$ constant, where $\eta = (r_A - r_B)/R$ is one of the elliptic coordinates mentioned between Eqs. (20) and (21). The qualitative character of the results to be reported changes little if η_0 is chosen anywhere in the range $0.3 \gtrsim \eta_0 \gtrsim 0.7$. As illustrations, results for $\eta_0 = 0.4, 0.5, 0.6$ will be quoted. Values of η_0 outside this range would make either the atomic regions or the bond region unreasonably small. Figure 4 shows the regions corresponding to the choice $\eta_0 = \pm 0.5$.

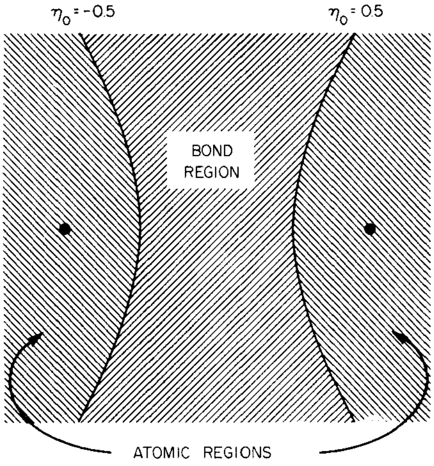

Fig. 4. Atomic and bond regions in H_2^+ for $\eta_0 = \pm 0.5$

In calculating contributions to the kinetic energy arising from parts of space, a decision has to be made whether the formula

$$T = \int d\tau \Psi(-\tfrac{1}{2}\nabla^2)\Psi \tag{27}$$

or the expression

$$T = \tfrac{1}{2}\int d\tau (\nabla\Psi)^2 \tag{28}$$

is used. Equations (27) and (28) are equivalent if applied to *all* space but differ if applied to *parts* of space. There is no *a priori* reason to prefer one or the other. In particular, *under no circumstances can any integral* over a part of space *be interpreted as an observable expectation value of the energy characteristic of the electronic motion in that part of space.* The only objective we have here is to partition the total integral into local contributions whose quantitative behavior can be consistently analyzed so that one can thereby deduce the behavior of the *total* kinetic energy integral.

To this end, Eq. (28) is by far the more practical expression because, in this representation, every volume element makes a positive contribution to the kinetic energy integral. In contrast, in Eq. (27) positive and negative local contributions arise which make the reasoning much more difficult. Moreover, it is considerably easier to discuss the character of the gradient than that of the curvature of Ψ. Therefore, all local kinetic energy contributions referred to in the sequel are based on Eq. (28).

3. *Atomic and Bond Contributions to the Kinetic Energy*

Each of the twelve values referring to the *molecular* kinetic energy in Table II is broken down into a contribution from the bond region and the atomic regions as indicated in Fig. 4. The results are given in Table III.

TABLE III

ATOMIC AND BOND COMPONENTS TO MOLECULAR KINETIC ENERGY

Cartesian component	$\eta_0 = 0.4$		$\eta_0 = 0.5$		$\eta_0 = 0.6$		Total (At + Bo)
	Atomic	Bond	Atomic	Bond	Atomic	Bond	
	Φ_{FH} = Finkelstein–Horowitz, $\zeta = 1.0$						
T_x	0.0930	0.0547	0.0769	0.0708	0.0597	0.0880	0.1477
T_y	0.0930	0.0547	0.0769	0.0708	0.0597	0.0880	0.1477
T_z	0.0889	0.0019	0.0868	0.0040	0.0832	0.0076	0.0908
T	0.2749	0.1113	0.2406	0.1456	0.2026	0.1836	0.3862
	Φ_{FH} = Finkelstein–Horowitz, $\zeta = 1.2387$						
T_x	0.1568	0.0689	0.1341	0.0916	0.1079	0.1178	0.2257
T_y	0.1568	0.0689	0.1341	0.0916	0.1079	0.1178	0.2257
T_z	0.1322	0.0035	0.1289	0.0068	0.1240	0.0117	0.1357
T	0.4458	0.1413	0.3971	0.1900	0.3398	0.2473	0.5871
	Φ_{GZ} = Guillemin–Zener, $\zeta_A = 1.1365$, $\zeta_B = 0.2174$						
T_x	0.1403	0.0908	0.1149	0.1162	0.0882	0.1429	0.2311
T_y	0.1403	0.0908	0.1149	0.1162	0.0882	0.1429	0.2311
T_z	0.1369	0.0029	0.1336	0.0062	0.1279	0.0119	0.1398
T	0.4175	0.1845	0.3634	0.2386	0.3043	0.2977	0.6020

A study of these decompositions leads to the following conclusions:

(a) The small value of T_z arises from the fact that the bond region contributes about ten times less to this component than to each of the other components, T_x and T_y. This is clearly related to the fact that the z component of the gradient for the molecular wave function is very small in the bond region.

(b) The increase in the kinetic energy, which occurs with the contraction described by the increase in ζ from 1.0 to 1.2387, arises mostly from the atomic regions. We conclude that the increase in kinetic energy associated with an increase in ζ is mostly contributed by the increase in all components of the gradient in the neighborhood of the nuclei.

(c) The changes in going from Φ_{FH} to Φ_{GZ}, although small, can be understood in terms of the transfer of charge previously illustrated in Fig. 2d, if one keeps in mind that $|\partial\Phi/\partial x|$ and $|\partial\Phi/\partial y|$ are larger in the bond region than on the outside of the atomic regions, and that $|\nabla\Phi|$ is larger in the inner part of the atomic regions than in their outer parts.

The qualitative content of all aforementioned conclusions is seen to be the same for the three η_0 values considered in Table III.

C. Geometric Partitioning of the Potential Energy

1. Coulombic Interactions

Since the potential energy depends only on the electron density, the four intermediate steps, which were introduced in Eq. (25), can be used to analyze the difference between the atomic and the molecular value.

The potential energy change (including the nuclear repulsion) associated with Step (Ia) can be assessed as follows. *First*, proton B is brought from infinity to the distance 2.0 au from a hydrogen atom A in its ground state. This yields the energy change

$$\begin{aligned}\int d\tau A_{\mathrm{FH}}^2(1)(-r_B^{-1}) + R^{-1} &= -0.4725 + 0.5000 \\ &= 0.0275 \quad \text{au.}\end{aligned} \tag{29}$$

The quantitative result is a consequence of Newton's potential theorem for spherical space charges, i.e.,

$$\int d\tau A^2(r_B^{-1}) = R^{-1} \int_{r_A<R} d\tau A^2, \tag{30}$$

in conjunction with the fact that a sphere of radius 2.0 au around the H atom contains the electronic charge -0.9450, that is, almost the entire electron. Thus, bringing the proton into this position generates a nuclear-electronic attraction almost identical to, but slightly less than, the simultaneously arising nuclear repulsion. *Secondly*, half of the electronic density is moved from atom A to proton B, thereby establishing the density of Fig. 2a with the potential energy

$$\int d\tau \tfrac{1}{2}\{A_{\mathrm{FH}}^2(1) + B_{\mathrm{FH}}^2(1)\}\{-r_A^{-1} - r_B^{-1}\} + R^{-1}. \tag{31}$$

This symmetrization of the density does not change the potential energy of the system.

The further potential energy differences, which correspond to Steps (Ib), (II), and (III), and lead to $\tilde{\Phi}_{\mathrm{FH}}$, Φ_{FH}, and Φ_{GZ}, respectively, can now be analyzed by a geometric partitioning of the molecular space.

2. *Basis of Geometric Partitioning*

For the geometric partitioning of the potential energy it must be kept in mind that the electron is attracted by both nuclei. Because of this, it is useful to divide the bond region, introduced in connection with Fig. 4, into a left and right part separated by the symmetry plane perpendicular to the internuclear axis. We can now distinguish four contributions to the electronic potential energy as illustrated in Fig. 5.

The first two rows of the *first* column of Fig. 5 illustrate the two kinds of nuclear attractions operative upon the "atomic parts" of the electron cloud: The first is the interaction of each nucleus with the electron charge in its own atomic region; the second is the interaction of each nucleus

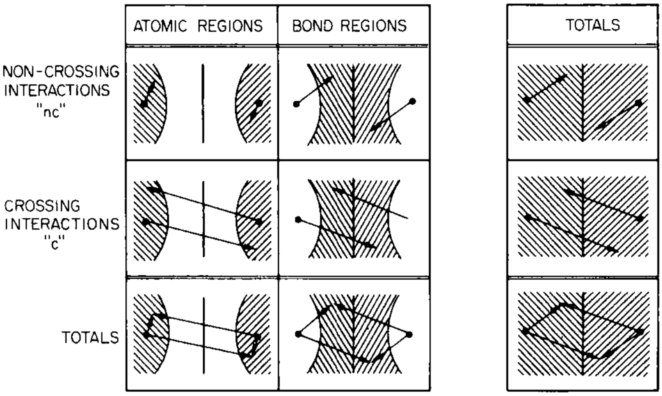

Fig. 5. Geometric partitioning of electronic-nuclear interactions.

with the electron cloud in the opposite atomic region. The former we shall denote as *noncrossing* interactions, the latter as *crossing* interactions. The sum of the two, containing all interactions of the electronic charge in the atomic regions, is illustrated in the third row of the first column.

The first two rows of the *second* column of Fig. 5 illustrate the two kinds of nuclear attractions operative upon the " bond part " of the electron cloud: The first is the interaction of each nucleus with the electronic charge in the bond region adjacent to it; the second is the interaction of each nucleus with the electronic cloud in the bond region opposite it. As before, the former will be called *noncrossing* and the latter, *crossing* interactions. The sum of the two, containing all interactions of the electronic charge in the bond region, is illustrated in the third row of the second column.

In the *third* column, the first row illustrates the interactions of each nucleus with the entire electronic charge located on the same side of the central plane and represents the sum of the noncrossing interactions in both the atomic and bond region. The second row is the sum of the two crossing interactions and represents the attraction of each nucleus with the charge on the opposite side of the center plane. The third row represents the total electronic potential energy. It is the sum of the two entries above it or to the left of it.

3. *Quantitative Results*

As in the case of the kinetic energy, the numerical values of the local contributions to the potential energy depend upon the choice of η_0 and, as before, the results for $\eta_0 = 0.4, 0.5, 0.6$ will be quoted. They are given in Table IV, which combines the conceptual steps introduced in Eq. (25) with the geometric partitioning defined in Fig. 5.

Of these, Step (Ia) has already been quantitatively discussed in connection with Eqs. (29), (30), and (31). It leads to the average atomic density $\frac{1}{2}\{A_{\text{FH}}^2(1) + B_{\text{FH}}^2(1)\}$ whose potential energy was given in Eq. (31). The geometric partitioning of its *electronic part* is contained in the first section of Table IV. The potential energy *changes* corresponding to Steps (Ib), (II), and (III) of Eq. (25) are contained in the second, third, and fourth sections of Table IV, respectively.

Each of the sections of Table IV is arranged and labeled according to the pattern of Fig. 5, with the exception that the division into atomic and bond parts is given three times, for $\eta_0 = 0.4$, $\eta_0 = 0.5$, and $\eta_0 = 0.6$, whereas the total is given only once, namely in the last column. Since the results for the three η_0 values are qualitatively similar, only those for $\eta_0 = 0.5$ are explicitly referred to in the following text.

TABLE IV

ATOMIC AND BOND CONTRIBUTIONS TO ELECTRONIC POTENTIAL ENERGY

Potential interactions	$\eta_0 = 0.4$		$\eta_0 = 0.5$		$\eta_0 = 0.6$		Total (At + Bo)
	Atomic	Bond	Atomic	Bond	Atomic	Bond	
			$\frac{1}{2}\{A_{FH}^2(1) + B_{FH}^2(1)\}$				
nc	−0.8347	−0.2055	−0.7589	−0.2813	−0.6661	−0.3741	−1.0402
c	−0.2773	−0.1550	−0.2365	−0.1958	−0.1936	−0.2387	−0.4323
Total	−1.1120	−0.3605	−0.9954	−0.4771	−0.8597	−0.6128	−1.4725
			$\tilde{\Phi}_{FH}^2 - \frac{1}{2}\{A_{FH}^2(1) + B_{FH}^2(1)\}$, Interference				
nc	0.0834	−0.0401	0.0886	−0.0453	0.0893	−0.0460	0.0433
c	0.0206	−0.0314	0.0235	−0.0343	0.0238	−0.0346	−0.0108
Total	0.1040	−0.0715	0.1121	−0.0796	0.1131	−0.0806	0.0325
			$\Phi_{FH}^2 - \tilde{\Phi}_{FH}^2$, Contraction				
nc	−0.2039	−0.0009	−0.1970	−0.0078	−0.1843	−0.0205	−0.2048
c	−0.0324	0.0036	−0.0309	0.0021	−0.0278	−0.0010	−0.0288
Total	−0.2363	0.0027	−0.2279	−0.0057	−0.2121	−0.0215	−0.2336
			$\Phi_{GZ}^2 - \Phi_{FH}^2$, Deformation				
nc	0.0583	−0.0610	0.0708	−0.0735	0.0793	−0.0820	−0.0027
c	0.0167	−0.0448	0.0222	−0.0503	0.0247	−0.0528	−0.0281
Total	0.0750	−0.1058	0.0930	−0.1238	0.1040	−0.1348	−0.0308

Examination of Table IV leads to the following conclusions:

a. Coulombic Interactions. For the density $\frac{1}{2}\{A_{\mathrm{FH}}^2(1) + B_{\mathrm{FH}}^2(1)\}$, the most interesting observation is that the value of the total *noncrossing* interactions (−1.0402) is very similar to the potential energy of the free H atom, and that the value of all *crossing* interactions (−0.4323) is correspondingly close to the interaction of a proton with the electronic cloud of the H atom as discussed in connection with Eqs. (29) and (30).

b. Interference. According to Fig. 2b, electronic charge is moved from a region of deep electrostatic potential near the nuclei to a region of shallow potential in the bond. Correspondingly, there occurs a net increase (0.0325) in the potential energy which is the result of a strong increase (0.1121) in the atomic region and a lesser decrease (−0.0796) in the bond region.

More specifically, it can be imagined that charge from the atomic regions is transferred to the bond region adjacent to it. This charge is therefore moved away from its own nucleus and closer to the opposite nucleus. Hence, the total noncrossing energy increases (0.0433) whereas the total crossing energy decreases (−0.0108), understandably by a smaller amount.

The pictures just given also explain the values of the individual atomic and bond, crossing and noncrossing contributions.

c. Contraction. According to Fig. 2c, electronic charge is accumulated close to the nuclei in the atomic regions where the attractive nuclear potential is very deep. It is taken away from distant parts of the atomic and bond regions where the nuclear attractions are small. This results in an exceedingly large decrease of the noncrossing atomic contribution (−0.1970) and a considerably smaller decrease of the crossing atomic contribution (−0.0309). The changes in the bond region are very small (−0.0057). Hence, the total decrease in potential energy (−0.2336) arises almost entirely from the atomic region (−0.2279).

d. Atomic Deformation. The charge transfer due to deformation, Fig. 2d, is somewhat similar to that due to interference, Fig. 2b; there is a characteristic difference, however. The recipient region in Fig. 2d lies not only in the center of the bond but extends over the major part of the internuclear distance. Concommitantly, only a negligible part of the dative region lies between the nuclei. Most of it lies to the outside.

This charge rearrangement affects the total noncrossing interaction very little (−0.0027) since, here, charge is merely shifted from one side of a nucleus to the other. The total crossing interactions, on the other hand, are considerably lowered (-0.0281) since charge on the right side, say, is shifted closer to the nucleus on the left. This lowering clearly consists of an increase (0.0222) of the atomic crossing interaction energy and a larger decrease (-0.0503) of the bond crossing interaction energy. Thus, the total (-0.0308) is negative because the charge cloud on each side of the molecule is polarized in such a way that the attraction by the nucleus on the opposite side is enhanced without greatly affecting the interaction with the nucleus on the same side.

e. Total Potential Binding Energy. A revealing insight is obtained by decomposing the potential binding energy

$$V_{\mathrm{el}}(\mathrm{GZ}) + V(\mathrm{Nucl.\ Rep.}) - \mathrm{V}(\mathrm{H\ Atom}) = -0.2044$$

into the following five components:

$$\begin{aligned}
V_{\mathrm{el}}^{\mathrm{c}}(\mathrm{GZ}) + V(\mathrm{Nucl.\ Rep.}) &= 0.0000 \\
V_{\mathrm{el}}^{\mathrm{nc}}(\mathrm{GZ}) - V_{\mathrm{el}}^{\mathrm{nc}}(\mathrm{FH}) &= -0.0027 \\
V_{\mathrm{el}}^{\mathrm{nc,\,bond}}(\mathrm{FH}) - V_{\mathrm{el}}^{\mathrm{nc,\,bond}}(\widetilde{\mathrm{FH}}) &= -0.0078 \\
V_{\mathrm{el}}^{\mathrm{nc,\,atomic}}(\mathrm{FH}) - V_{\mathrm{el}}^{\mathrm{nc,\,atomic}}(\widetilde{\mathrm{FH}}) &= -0.1970 \\
V_{\mathrm{el}}^{\mathrm{nc}}(\widetilde{\mathrm{FH}}) - V(\mathrm{H\ Atom}) &= 0.0031
\end{aligned}$$

which are readily obtained from Table IV. They show that the large negative value of the potential binding energy arises from the *contractive change* of the *atomic contribution* to the *noncrossing portion* of the electronic potential energy.

D. Analysis of the Binding Energy

The results of the quantitative analysis developed in the preceding sections must now be synthesized to yield a conceptual explanation of the chemical bond in H_2^+. To this end, the salient features are collected in Table V. The total energy changes given in the last column correspond to energy changes described in Section IV.A. The rest of the table contains physical explanations of the kind sought at the end of that section. Taking into account these physical pictures, as well as the variational considerations of Section IV.A, the following observations can now be made regarding the binding process:

(a) The kinetic energy curve in Fig. 3 is lowered because, in the bond region, molecular wave functions have an extremely small gradient parallel to the internuclear axis. Table V contains the numerical results for Step (I) of Eq. (23), i.e., for $\zeta = 1$. The results of Tables II and III showed that the same interpretation is valid for all values of ζ.

(b) Because the kinetic energy curve is lowered, the variation principle requires the contraction towards the two nuclei, embodied in Step (II), which establishes the virial relationship, as required for a scale variation. This contraction is characterized by two features: The lowering of the total energy is due to the potential energy which decreases below the atomic value; whereas the kinetic energy increases above the atomic value.

(c) The difference between the atomic and molecular potential energy curves of Fig. 3 is illustrated by the potential energy increase shown in Table V for Step (I). Although this step corresponds to $\zeta = 1$, the interpretation given is equally valid for other ζ values, as was the case for the kinetic energy. The increase is most conveniently understood as the sum of the coulombic interaction of a proton with a neutral hydrogen atom [Step (Ia)] and the potential energy change associated with the charge rearrangement characteristic for electron sharing, called here interference [Step (Ib)]. Both changes are positive for the reasons discussed and considerably smaller than the potential energy drop arising from contraction [Step (II)].

(d) In Step (III), each half of the charge cloud is polarized towards the opposite nucleus. This deformation of the density increases the attraction by the further nucleus without essentially changing that by the nearer nucleus. Because the virial theorem is preserved during this step, the kinetic energy must increase; but since it changes only by half the potential energy, the readjustment leads to a lowering of the total energy.

(e) The polarization of Step (III) is an example of a density rearrangement which, through an accumulation of charge in the bond, *lowers* the potential energy. In contrast, the interference of Step (Ib) represents a density rearrangement which, through an accumulation of charge in the bond, *increases* the potential energy. The reason is that polarization removes charge from *outside regions*, whereas interference takes it away from the *immediate neighborhood of the nuclei.* It is remarkable that the potential energy effects of these two rearrangements very nearly cancel each other out, so that the total change of the potential energy is essentially the sum of the small coulombic repulsion [Step (Ia)] and the dominating drop due to contraction [Step (II)].

(f) These observations can be combined to the following overall description.

In the atom as well as in the molecule (at the equilibrium distance) the nuclear suction concentrates charge as much as possible, i.e., until T increases to $\frac{1}{2}|V|$. The difference is that in the atom the charge cloud gravitates toward one center whereas in the molecule it can gravitate toward

TABLE V

ORIGIN OF BINDING ENERGY IN H_2^+ GROUND STATE

Steps in Eq. (23) (25)		Change in Φ	Density changes		Potential energy changes		Kinetic energy changes		Total energy changes
			Physical picture	Name	Physical picture	Num. value	Physical picture	Num. value	
I	Ia	$\Phi_H \downarrow \tilde{\Phi}_{FH}$	H^+ is brought from ∞ to distance 2.0 au from H atom. Density is symmetrized	Unshared density average	H^+ is slightly repelled by a proton which is almost completely shielded by a spherical electronic cloud	0.0275			-0.0538
	Ib		Charge is transferred from nuclear neighborhoods to to bond region due to electron sharing	Interference	Potential in the recipient bond region is much shallower than in the dative atomic regions	0.0325	T_z decreases because the z component of the gradient of the molecular wave function is very small in the bond region	-0.1138	

II	II	$\tilde{\Phi}_{FH}$ $\downarrow$ Φ_{FH}	Charge is contracted towards both nuclei	Contraction	Charge is accumulated near the two centers of attraction, mainly in the atomic regions	−0.2336	All components increase because all gradients increase essentially in the atomic regions	0.2009	−0.0327
III	III	Φ_{FH} $\downarrow$ Φ_{GZ}	Charge is transferred essentially parallel to molecular axis from outside the nuclei into the region between them	Polarization	Attraction by the farther nucleus is increased without change in attraction by the nearer nucleus	−0.0308	Slight increase because the components of the gradient are slightly higher in the bond than outside the atoms	0.0149	−0.0159
I + II + III		Φ_H $\downarrow$ Φ_{GZ}	$H + H^+ \rightarrow H_2^+$		Mostly contraction	−0.2044	Mostly interference and contraction	0.1020	−0.1024

two. *Because of this two-center character, the kinetic energy pressure is lower in the molecule than in the atom, i.e., a given amount of virtual negative potential energy can be acquired with a smaller concomitant increase in virtual positive kinetic energy. As a consequence, the optimal balance, as characterized by the virial theorem, is reached for a lower potential and, hence, total energy.*

The lowering of the kinetic energy pressure originates from the behavior of the longitudinal component of the wave function gradient in the bond region, or, more generally speaking, from the intrinsic delocalization from one to two atoms along the internuclear axis associated with electron sharing.

In the virtual potential energy, interatomic and bond contributions cancel almost entirely except for a small coulombic remnant. In the variational competition, the potential energy behavior is, therefore, almost exactly like that of the free atom or, equivalently, like that of two noninteracting "half atoms." Thus, the final lowering of the potential energy is due to a firmer atomic-type attachment of the electron cloud to the two nuclei.

The final increase of the kinetic energy is the combined result of the aforementioned decreasing influences on T_z *and an increase in all components concomitant with the firmer atomic-type attachment to the centers.*

Only the recognition of the interplay between kinetic and potential energy, i.e., between nuclear attractions and uncertainty principle, does justice to the binding process within the context of the variation principle.

V. Orbital Analysis of the Ground State

A. Basis for Orbital Partitioning

The three steps of Eq. (23), which formed the basis for the preceding analysis, were selected in such a way that the energy integral was lowered in each of them. This choice was convenient for variational reasoning, but it entailed the need for a geometrical analysis in order to extract the two essential ingredients of bond formation. These were the lowering of the kinetic energy pressure in the longitudinal direction, which has "bond character," and the contraction of the electron cloud towards the nuclei which has "atomic character" and affects both kinetic and potential energy.

We wish now to extend the analysis in a way which will bring out these bond-forming elements more clearly. To this end we consider, in addition to the steps of Eq. (23), also the following sequence of conceptual intermediates:

$$\Phi_R = \Phi_H \xrightarrow{(I')} \tilde{\Phi}_H \xrightarrow{(II')} \hat{\Phi}_H \xrightarrow{(III')} \Phi_{GZ} = \Phi_P . \qquad (32)$$

Here the virtual atomic state, $\tilde{\Phi}_H$, is defined by

$$\tilde{\Phi}_H = \mathcal{A}_{FH}(\zeta = 1.2387); \tag{32a}$$

that is, it represents an isolated hydrogen atom contracted to the optimal FH ζ value, and Step (I′) will be called *contractive promotion.* The second virtual atomic state, $\hat{\Phi}_H$, is defined by

$$\hat{\Phi}_H = \mathcal{A}_{GZ}(\zeta_A = 1.1365,\ \zeta_B = 0.2174) \tag{32b}$$

and represents a deformed contracted isolated hydrogen atom as described by the atomic component [see Eq. (20)] of the optimal GZ function. Step (II′) will be referred to as *deformation promotion.*

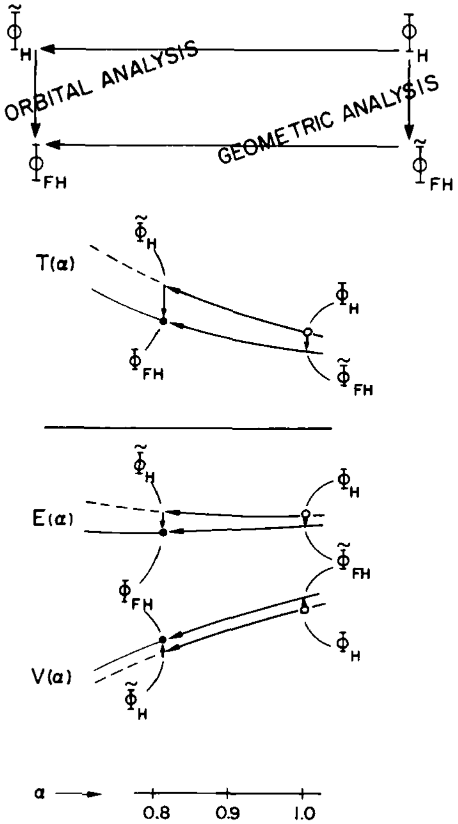

Fig. 6. Relation between the geometric analysis and the orbital analysis of the FH approximation.

Whereas previously in Eq. (23) the intermediates were virtual *molecular* states, the intermediates of Eq. (32) are promoted virtual *atomic* states, and the ensuing analysis can therefore be based on a partitioning by atomic orbitals in lieu of a partitioning by geometric regions. This approach is similar to traditional methods of building molecules from atoms in their valence states; it permits an analysis of the relation between overlap and chemical binding; and it is more easily extended to complex systems than is the geometric analysis. It is true that the first two steps of Eq. (32) are associated with an energy *increase* and this seemingly introduces an element of arbitrariness into the application of the variation principle. It will transpire, however, that the orbital interpretation is in substantial agreement with the geometric analysis.

The difference between the two approaches can be simply illustrated for the FH approximation. The two sets of steps, leading from the H atom to the FH wave function, are indicated in Fig. 6, which contains the same curves as Fig. 3.

B. Orbital Partitioning of Molecular Density

Let us focus our attention again on Step (I), Eq. (23), of the previous analysis. It resulted in a potential energy increase which could be understood by introducing the two substeps (Ia) and (Ib) according to Eq. (25). Let us examine in greater detail the density decomposition, given by Eq. (24), which formed the basis for these two substeps.

To this end, we introduce a density partitioning for the *general* wave function of Eq. (17) by the following definitions:

$$\rho = \rho^{\mathrm{QC}} + \rho^{\mathrm{I}}, \tag{33}$$

where

$$\rho = \Phi^2 = (A + B)^2/2(1 + S) \tag{34}$$

$$\rho^{\mathrm{QC}} = \tfrac{1}{2}(A^2 + B^2) \tag{35}$$

$$\rho^{\mathrm{I}} = (1 + S)^{-1}\{AB - \tfrac{1}{2}S[A^2 + B^2]\}. \tag{36}$$

The term ρ^{I} owes its appearance to the fact that an approximate molecular density is obtained by *first superposing* atomic orbitals and *then squaring* the superposition, and *not* by *first squaring* the atomic orbitals and *then superposing* the atomic densities. The latter, which is given by Eq. (35), would represent a reasonable approximation if the electron densities themselves were subject to linear homogeneous differential equations, as is the case in classical electrostatics, and for this reason it is called the *quasi-*

classical density part. Actually, however, the quantum mechanical density is defined as the square of an amplitude function. It is the *latter* which is determined by a linear homogeneous differential equation and, therefore, can be approximated with the help of the superposition principle. This is essential for a wave theory and is known to lead to phenomena of interference. The density term, ρ^I, of Eq. (36), which is the difference between the wave mechanical and the quasi-classical density, ρ^{QC}, describes the effect of the *constructive interference* of the atomic orbitals A and B. This was already noted at the end of Section III, where it was also pointed out that the superposition of atomic orbital amplitudes must be identified with the concept of *electron sharing*.

Application of the partitioning just introduced to the wave function $\tilde{\Phi}_{FH} = \Phi_{FH}(\zeta = 1)$ yields the decomposition of Eq. (24) with an explicit definition for the "remainder." For this wave function, graphical representations of ρ^{QC} and ρ^I were given in Figs. 2a and 2b and discussed at that occasion. We recall that the interference density (Fig. 2b) represents a transfer of charge from the neighborhood of the nuclei into the bond.

The definitions (33)–(36) are, however, general and we shall now proceed to apply them to the wave functions $\Phi_{FH} = \Phi_{FH}(\zeta = 1.2387)$ and Φ_{GZ}. The character of the resulting terms ρ^{QC} and ρ^I is illustrated in Fig. 7. The first column of this figure contains ρ^{QC}, ρ^I, and ρ for the wave function

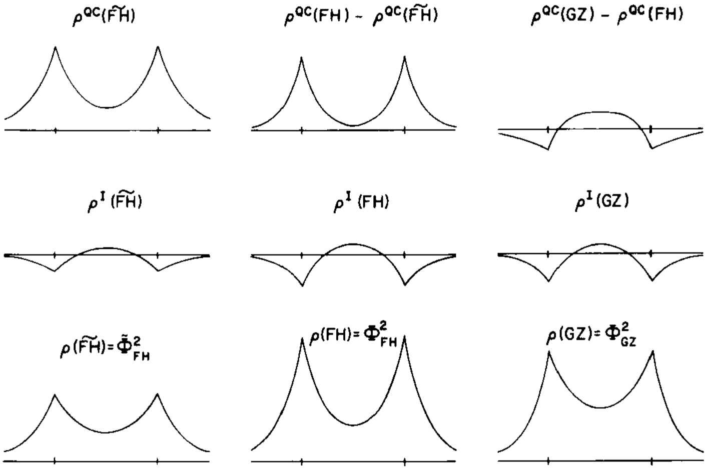

Fig. 7. Quasi-classical and interference densities for the wave functions $\tilde{\Phi}_{FH}$, Φ_{FH}, and Φ_{GZ}. $\rho^{QC}(\widetilde{FH}) = \frac{1}{2}\{A^2_{FH}(1) + B^2_{FH}(1)\}$; $\rho^{QC}(FH) = \frac{1}{2}\{A^2_{FH}(1.2387) + B^2_{FH}(1.2387)\}$; $\rho^{QC}(GZ) = \frac{1}{2}\{A^2_{GZ} + B^2_{GZ}\}$.

$\tilde{\Phi}_{\mathrm{FH}}$ which has been discussed before. The second and the third entries in the first row illustrate how ρ^{QC} is modified if one goes from $\Phi_{\mathrm{FH}}(\zeta = 1)$ to Φ_{FH}, and then from Φ_{FH} to Φ_{GZ}. In other words, they show the change in the quasi-classical density due to contractive promotion and deformation promotion, respectively. The last row contains the total densities of $\tilde{\Phi}_{\mathrm{FH}}$, Φ_{FH}, and Φ_{GZ}, respectively. The middle row contains the interference densities, ρ^{I}, corresponding to the three wave functions. Figure 7 exhibits all the familiar features which we have encountered before. Contraction and deformation of the quasi-classical terms are similar in character to those found earlier for the total densities (see Figs. 2c and 2d). The interference terms of Φ_{FH} and Φ_{GZ} are similar in character to that of $\tilde{\Phi}_{\mathrm{FH}}$ which is identical to Fig. 2b.

C. Orbital Partitioning of Molecular Energies

1. Potential Energy

With the help of the density partitioning given in Eqs. (33)–(36), the potential energy arising from the molecular Hamiltonian, given in Eq. (22), can be partitioned as follows:

$$V = V^{\mathrm{A}} + V^{\mathrm{QC}} + V^{\mathrm{I}}, \tag{37}$$

where

$$V^{\mathrm{A}} = -\tfrac{1}{2}\int d\tau\{A^2 r_A^{-1} + B^2 r_B^{-1}\} = -\int d\tau A^2 r_A^{-1} \tag{38}$$

$$\begin{aligned} V^{\mathrm{QC}} &= -\tfrac{1}{2}\int d\tau\{A^2 r_B^{-1} + B^2 r_A^{-1}\} + R^{-1} \\ &= -\int d\tau A^2 r_B^{-1} + R^{-1} \end{aligned} \tag{39}$$

$$\begin{aligned} V^{\mathrm{I}} &= \int d\tau \rho^{\mathrm{I}}(-r_A^{-1} - r_B^{-1}) \\ &= (1+S)^{-1}\int d\tau\{AB - \tfrac{1}{2}S[A^2 + B^2]\}\{-r_A^{-1} - r_B^{-1}\}. \end{aligned} \tag{40}$$

The sum $(V^{\mathrm{A}} + V^{\mathrm{QC}})$ arises from the quasi-classical density of Eq. (35).

Assuming the possibility that the atomic orbital A may not be the true ground state orbital, we denote V^{A} as the promoted atomic potential energy. The second term, V^{QC}, represents the electrostatic energy of a promoted neutral H atom in the field of a proton at the distance R and will be called the quasi-classical potential energy. Finally, the last term, V^{I}, represents the change in the potential energy resulting from the charge rearrangement associated with interference.

For the case of Step (I), Eq. (23), the atomic term V^A is identical with that of the unpromoted H atom and the terms V^{QC} and V^I correspond to the potential energy changes listed under Steps (Ia) and (Ib) in Table V. These were discussed in considerable detail in Section IV.C.

For the FH and GZ wave functions the scheme (37)–(40) yields the following decompositions of the potential energy part of the binding energy:

$$\begin{aligned} V(\mathrm{FH}) - V(\mathrm{H}) &= [V^A(\mathrm{FH}) - V(\mathrm{H})] + V^{QC}(\mathrm{FH}) + V^I(\mathrm{FH}) \\ &= V^{AC} + V^{QC}(\mathrm{FH}) + V^I(\mathrm{FH}) \end{aligned} \tag{41}$$

$$\begin{aligned} V(\mathrm{GZ}) - V(\mathrm{H}) &= [V^A(\mathrm{FH}) - V(\mathrm{H})] + [V^A(\mathrm{GZ}) - V^A(\mathrm{FH})] \\ &\quad + V^{QC}(\mathrm{GZ}) + V^I(\mathrm{GZ}) \\ &= V^{AC} + V^{AD} + V^{QC}(\mathrm{GZ}) + V^I(\mathrm{GZ}). \end{aligned} \tag{42}$$

In this partitioning, the concepts

$$V^{AC} = V^A(\mathrm{FH}) - V(\mathrm{H}) = \textit{atomic}\text{ potential energy change due to }\textit{contractive}\text{ promotion} \tag{43}$$

and

$$V^{AD} = V^A(\mathrm{GZ}) - V^A(\mathrm{FH}) = \textit{atomic}\text{ potential energy change due to }\textit{deformation}\text{ promotion of contracted atom} \tag{44}$$

have been introduced.

2. *Kinetic Energy*

In complete analogy to the potential energy partitioning we can write down the following partitioning of the kinetic energy for wave functions of the type Eq. (17):

$$T = T^A + T^I, \tag{45}$$

where

$$\begin{aligned} T^A &= \tfrac{1}{2}\int d\tau\{A(-\tfrac{1}{2}\nabla^2)A + B(-\tfrac{1}{2}\nabla^2)B\} \\ &= \int d\tau\{A(-\tfrac{1}{2}\nabla^2)A\} \end{aligned} \tag{46}$$

$$\begin{aligned} T^I &= (1 + S)^{-1}\int d\tau\{A(-\tfrac{1}{2}\nabla^2)B - \tfrac{1}{2}S[A(-\tfrac{1}{2}\nabla^2)A + B(-\tfrac{1}{2}\nabla^2)B]\} \\ &= (1 + S)^{-1}\int d\tau\{A(-\tfrac{1}{2}\nabla^2)B - S[A(-\tfrac{1}{2}\nabla^2)A]\}. \end{aligned} \tag{47}$$

Comparison of Eq. (47) with the analogous potential term of Eq. (40) suggests that the kinetic energy change T^{I} must also be associated with the density change ρ^{I} of Eq. (36). It will therefore be called the kinetic energy due to interference. This interpretation is substantiated by observing that it correctly explains the negative value of T^{I}. For, adding the interference density to the quasi-classical density raises the latter in the bond and lowers it near the nuclei. Thus, it not only accumulates charge in the bond, but it also lowers the z component of the *gradient* of the density at all points.

For the case of Step (I), Eq. (23), T^{A} is identical with the kinetic energy of the unpromoted H atom and T^{I} is given by the kinetic energy change listed under Step (I) of Table V which was discussed in Section IV,B. For the FH and GZ wave functions, the partitioning given by Eqs. (45)–(47) yields the following decomposition of the kinetic part of the binding energy:

$$\begin{aligned} T(\mathrm{FH}) - T(\mathrm{H}) &= [T^{\mathrm{A}}(\mathrm{FH}) - T(\mathrm{H})] + T^{\mathrm{I}}(\mathrm{FH}) \\ &= T^{\mathrm{AC}} + T^{\mathrm{I}}(\mathrm{FH}) \end{aligned} \tag{48}$$

$$\begin{aligned} T(\mathrm{GZ}) - T(\mathrm{H}) &= [T^{\mathrm{A}}(\mathrm{FH}) - T(\mathrm{H})] + [T^{\mathrm{A}}(\mathrm{GZ}) - T^{\mathrm{A}}(\mathrm{FH})] \\ &\quad + T^{\mathrm{I}}(\mathrm{GZ}) \\ &= T^{\mathrm{AC}} + T^{\mathrm{AD}} + T^{\mathrm{I}}(\mathrm{GZ}), \end{aligned} \tag{49}$$

where the concepts

$$T^{\mathrm{AC}} = T^{\mathrm{A}}(\mathrm{FH}) - T(\mathrm{H}) = \textit{atomic}\text{ kinetic energy change due to }\textit{contractive}\text{ promotion} \tag{50}$$

and

$$T^{\mathrm{AD}} = T^{\mathrm{A}}(\mathrm{GZ}) - T^{\mathrm{A}}(\mathrm{FH}) = \textit{atomic}\text{ kinetic energy change due to }\textit{deformation}\text{ promotion of the contracted atom} \tag{51}$$

have been introduced.

3. *Binding Energy*

Combining the results for the kinetic and potential energies, one obtains the following orbital decomposition for the total binding energy:

$$E(\mathrm{GZ}) - E(\mathrm{H}) = E^{\mathrm{AC}} + E^{\mathrm{AD}} + E^{\mathrm{QC}}(\mathrm{GZ}) + E^{\mathrm{I}}(\mathrm{GZ}), \tag{52}$$

where

$$E^{\mathrm{AC}} = T^{\mathrm{AC}} + V^{\mathrm{AC}} \tag{53}$$

$$E^{\mathrm{AD}} = T^{\mathrm{AD}} + V^{\mathrm{AD}} \tag{54}$$

$$E^{\mathrm{QC}}(\mathrm{GZ}) = V^{\mathrm{QC}}(\mathrm{GZ}) \tag{55}$$

$$E^{\mathrm{I}}(\mathrm{GZ}) = T^{\mathrm{I}}(\mathrm{GZ}) + V^{\mathrm{I}}(\mathrm{GZ}). \tag{56}$$

For the FH approximation, the above equations simplify to

$$E(\mathrm{FH}) - E(\mathrm{H}) = E^{\mathrm{AC}} + E^{\mathrm{QC}}(\mathrm{FH}) + E^{\mathrm{I}}(\mathrm{FH}), \tag{57}$$

where

$$E^{\mathrm{AC}} = T^{\mathrm{AC}} + V^{\mathrm{AC}} \tag{58}$$

$$E^{\mathrm{QC}}(\mathrm{FH}) = V^{\mathrm{QC}}(\mathrm{FH}) \tag{59}$$

$$E^{\mathrm{I}}(\mathrm{FH}) = T^{\mathrm{I}}(\mathrm{FH}) + V^{\mathrm{I}}(\mathrm{FH}). \tag{60}$$

D. Orbital Analysis of Binding Energy

The quantitative results for the various energy fragments occurring in the preceding equations are listed in Table VI. The first column contains essentially the results of Step (I) of Table V. The second and third columns contain the partitionings for the FH and GZ functions, respectively. In addition, the kinetic energy values of Table VI have been decomposed into x, y, and z components and these are tabulated in Table VII. An examination of these tables yields the following observations:

(a) In agreement with the previous results the largest energy changes are those due to contractive promotion in the first row (Table VI). They appear now isolated as inner-atomic effects.

(b) The next largest effects are the kinetic energy decreases which, in the fourth row, appear as negative interference energy values. They are similar in magnitude for all three wave functions and, as apparent from Table VII, are essentially due to the z components. It is evident that constructive interference between two overlapping orbitals at different centers represents the orbital description equivalent to the wave amplitude delocalization which, according to the discussion in Section IV. B, lowers the kinetic energy pressure in the longitudinal direction.

(c) A comparison of the $\widetilde{\mathrm{FH}}$ terms with the FH terms in Table VI sheds new light on the origin of the orbital contraction.

In going from $\widetilde{\mathrm{FH}}(\zeta = 1)$ to $\mathrm{FH}(\zeta = 1.2387)$ there occur an *increase* in the contractive promotion energy, a *decrease* in the quasi-classical electrostatic energy, and a *decrease* in the interference energy. The first arises because $\zeta = 1$ is the minimum for the free atom; the second arises because contraction increases the shielding discussed in connection with Eqs. (29) and (30).

The increase in the absolute values of the interference energies is related to the fact that the orbital energy of an atomic orbital increases in absolute value when such an orbital contracts. This point will be discussed in greater detail in Section V.E; here we merely note that, *for similar values of*

TABLE VI

Orbtial Partitioning of the Binding Energy

Energy changes due to	$\widetilde{\mathrm{FH}}(\zeta = 1.0)$			$\mathrm{FH}(\zeta = 1.2387)$			GZ		
	T	V	E	T	V	E	T	V	E
Contractive promotion	0.0	0.0	0.0	0.2672	−0.2387	0.0285	0.2672	−0.2387	0.0285
Deformation promotion	0.0	0.0	0.0	0.0	0.0	0.0	−0.0253	0.0384	0.0131
Quasi-classical electrostatic	0.0	0.0275	0.0275	0.0	0.0123	0.0123	0.0	−0.0507	−0.0507
Constructive interference	−0.1138	0.0325	−0.0813	−0.1801	0.0528	−0.1273	−0.1400	0.0466	−0.0934
Binding	−0.1138	0.0600	−0.0538	0.0871	−0.1736	−0.0865	0.1020	−0.2044	−0.1024

TABLE VII

ORBITAL PARTITIONING OF CARTESIAN KINETIC ENERGY COMPONENTS

Kinetic energy changes due to	FH($\zeta = 1.0$)			
	T_x	T_y	T_z	T
Contractive promotion	0.0	0.0	0.0	0.0
Deformation promotion	0.0	0.0	0.0	0.0
Constructive interference	−0.0190	−0.0190	−0.0758	−0.1138
Binding	−0.0190	−0.0190	−0.0758	−0.1138

Kinetic energy changes due to	FH($\zeta = 1.2387$)			
	T_x	T_y	T_z	T
Contractive promotion	0.0891	0.0891	0.0891	0.2672
Deformation promotion	0.0	0.0	0.0	0.0
Constructive interference	−0.0300	−0.0300	−0.1201	−0.1801
Binding	0.0590	0.0590	−0.0310	0.0871

Kinetic energy changes due to	GZ			
	T_x	T_y	T_z	T
Contractive promotion	0.0891	0.0891	0.0891	0.2672
Deformation promotion	−0.0007	−0.0007	−0.0239	−0.0253
Constructive interference	−0.0239	−0.0239	−0.0922	−0.1400
Binding	0.0645	0.0645	−0.0270	0.1020

the overlap integral, tightly bound atomic orbitals yield stronger interference energies than weakly bound ones. More specifically, the strong decrease in the interference energy results from its kinetic part T^{I}. The potential part is much smaller, and so is its increase (it approximately cancels the decrease in the quasi-classical potential energy).

In Section V.E it will also be seen that, for ζ near $\zeta = 1$, the kinetic interference energy T^{I} decreases rather briskly with increasing ζ, whereas on the other hand, the promotion energy increases only slowly (it is given by $\frac{1}{2}[\zeta - 1]^2$). Hence T^{I} predominates, and the change in ζ from 1 to 1.2387 can also be interpreted as the *result of the competition between the total energy increase due to promotion and the kinetic energy decrease due to interference.*

The contractive promotion entails the inner-atomic readjustment in kinetic and potential energies, which has been discussed at length.

(d) In going from FH($\zeta = 1.2387$) to GZ, i.e., from the second to the third column, the energy lowering is manifestly due to the decrease in the quasi-classical potential energy by $(-0.0507 - 0.0123) = -0.0630$ au. It occurs because the charge around one nucleus is polarized in such a way as to increase the attraction by the other nucleus. This conclusion is again in agreement with the interpretation given in Section IV.C.

The values for the deformation promotion arise because the deformation defined by Eq. (32b) represents an elongation of the atomic orbitals in the z direction toward the other nucleus; the kinetic energy is lowered because of delocalization, the potential energy is raised since charge is moved away from the nucleus.

The decrease in absolute values of the interference energies is associated with the increase in atomic-orbital overlap in going from the second to the third column. The relation between overlap and interference will also be discussed in Section V.E.

(e) Let us finally consider the sequence of steps defined in Eq. (32). It corresponds to first going from left to right in the first row and then down in the last column of Table VI.

In spite of the large quasi-classical energy lowering, nevertheless the quasi-classical, deformation, and interference contributions to the potential energy together add up to a positive value. (The difference between the second and the third column is merely that this sum is smaller in the latter.) Hence, the lowering of the total potential energy must still be identified with that of contractive promotion, in agreement with our previous conclusions.

The two kinetic energy contributions which are not due to contractive promotion, i.e., those associated with deformation promotion and interference, are both lowerings which arise from delocalization of the wave function in the z direction. This too is in agreement with Section IV.

(f) In summary then, the orbital partitioning leads to the same physical concepts as the geometric partitioning of Section IV, namely:
(1) *Electron sharing lowers the kinetic energy pressure along the internuclear axis because of atomic orbital interference, which is equivalent to wave amplitude delocalization;* (2) *Orbital contraction, which describes the firmer attachment to the nuclei, rearranges the kinetic and the potential energy;* (3) *Orbital deformation lowers the potential energy somewhat by quasi-classical polarization.*

Moreover, the orbital partitioning furnishes an additional viewpoint which makes it possible to understand the orbital contraction without invoking the virial theorem: *Orbital contraction raises the absolute values of both the positive promotion energy and the negative interference energy. These two effects oppose each other variationally. The actually occurring* *contraction can therefore be interpreted as the balance resulting from the competition between these two tendencies.*

It may be mentioned that our numerical values for deformation promotion and interference result from the particular partitioning entailed by the definition adopted in Eq. (32b) for the deformed atomic orbitals. Different definitions of deformed orbitals are possible, and some may well yield a more clear-cut and, hence, preferable numerical separation of the two categories, in particular as regards the kinetic energy. This problem will be taken up in a subsequent investigation (Wasserman and Ruedenberg, to be published) with the aim of improving the definition of the deformed atomic orbital.

E. Overlap, Interference, and Covalent Binding

It has been recognized for a long time that atomic orbitals must overlap in order that electrons can be shared between them. More specifically, Mulliken (1949), recognizing that the "resonance integral"

$$\langle A|\mathscr{H}|B\rangle - \tfrac{1}{2}S\{\langle A|\mathscr{H}|A\rangle + \langle B|\mathscr{H}|B\rangle\} \tag{61}$$

plays an essential role in the binding energy, suggested that in qualitative reasoning it might be considered proportional to the overlap integral and the average of the orbital energies of A and B. We note that the interference energy E^{I} of Eq. (56) or Eq. (60) is the product of the "bond order" $(1 + S)^{-1}$ and the resonance integral (61). We can therefore give a more precise meaning to Mulliken's observation: It is the kinetic part of the resonance integral which is essential for binding in H_2^+. The question therefore arises whether it is possible for us to establish a quantitative relationship between the kinetic interference energy, T^{I}, the corresponding overlap integral, S, and the orbital energies of the interfering atomic orbitals. For the sake of simplicity we limit ourselves here to the FH wave function which will bring out the aspects important to this discussion.

1. *Interference Population and Overlap*

In looking for a single number which could be used as a measure of the "strength" of interference for a specific interference density, ρ^{I}, one thinks immediately of the amount of charge which is transferred from the atomic regions into the bond region. We shall call this quantity the *interference population* q^{I}. Inserting the atomic orbitals, given in Eq. (19) for the FH approximation, into the definition (36) of the interference density, we obtain for the latter the expression

$$\rho^{\mathrm{I}} = (1 + S)^{-1}\bar{\rho}^{\mathrm{I}}, \tag{62}$$

where, in elliptic coordinates [see before Eq. (21)], $\bar{\rho}^{\mathrm{I}}$ can be written as

$$\begin{aligned}\bar{\rho}^{\mathrm{I}} &= A_{\mathrm{FH}}B_{\mathrm{FH}} - \tfrac{1}{2}S[A_{\mathrm{FH}}^2 + B_{\mathrm{FH}}^2] \\ &= (\zeta^3/\pi)\exp(-\zeta R\xi)[1 - S(\zeta R)\cosh(\zeta R\eta)]. \qquad (63)\end{aligned}$$

Thus, the recipient bond region and the dative atomic regions are seen to be separated by the two-sheet hyperboloid $\eta = \pm\eta^{\mathrm{I}}$, where $\eta^{\mathrm{I}}(\zeta R)$ is defined as the solution of the equation

$$S(\zeta R)\cosh(\zeta R\eta^{\mathrm{I}}) = 1 \qquad (64)$$

and $S(\zeta R)$ is given in Appendix A. Graphical representations of the interference density $\bar{\rho}^{\mathrm{I}}$ were given in Figs. 1 and 2 of Ruedenberg (1962). The interference population q^{I} is then given by

$$q^{\mathrm{I}} = (1 + S)^{-1}\bar{q}^{\mathrm{I}}, \qquad (65)$$

where $\bar{q}^{\mathrm{I}}$ is the integral

$$\bar{q}^{\mathrm{I}} = \int_{-\eta^{\mathrm{I}}}^{\eta^{\mathrm{I}}} d\eta \int_{1}^{\infty} d\xi \int_{0}^{2\pi} d\varphi(\tfrac{1}{2}R)^3(\xi^2 - \eta^2)\bar{\rho}^{\mathrm{I}}. \qquad (66)$$

A plot of $\bar{q}^{\mathrm{I}}$ against S is contained in Fig. 8. The behavior of $\bar{q}^{\mathrm{I}}$ is almost

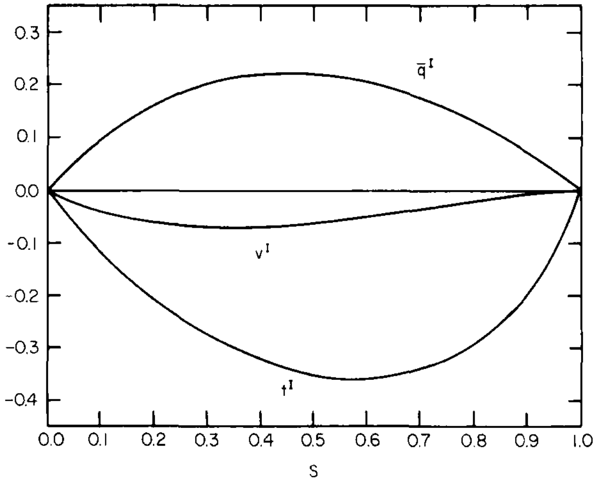

Fig. 8. Overlap dependence of interference population and kinetic and potential interference energies for Φ_{FH}.

parabolic in S and can be expressed by the numerical approximations

$$\bar{q}^{\mathrm{I}} \simeq 0.90322S(1 - |S|) \tag{67}$$

$$\bar{q}^{\mathrm{I}} \simeq 0.738087S(1 - S^2)(1 - 0.576997S^2) \tag{68}$$

with an absolute mean deviation of 0.01. Note should be taken of the fact that *the interference population*, q^{I}, *vanishes for* $R = 0$ *as well as for* $R = \infty$. From the definitions (33)–(36), it is indeed obvious that the interference density, ρ^{I}, itself vanishes at both limits.

In view of the preceding orbital analysis, it is to be expected that the quantity $\bar{q}^{\mathrm{I}}$, rather than the overlap integral, is a qualitative measure of the resonance integral, Eq. (61), and we shall therefore examine whether the interference energies depend on S in the way predicted for q^{I} by combining Eq. (65) with (67).

2. *Interference Energies and Overlap*

By virtue of Eqs. (A.20) and (A.25) in Appendix A, the potential and kinetic interference energies can be written in the following form:

$$T^{\mathrm{I}} = T_{\mathrm{H}}(\zeta)\, t^{\mathrm{I}}/(1 + S) \tag{69}$$

$$V^{\mathrm{I}} = V_{\mathrm{H}}(\zeta)\, v^{\mathrm{I}}/(1 + S), \tag{70}$$

where $T_{\mathrm{H}}(\zeta)$ and $V_{\mathrm{H}}(\zeta)$ are the kinetic and potential energies of the atomic orbital [see Eqs. (2) and (3)]. The factors t^{I} and v^{I} depend only upon the product ζR. Since, on the other hand, the overlap integral $S = S(\zeta R)$, too, is a unique function of ζR [see Eq. (A.4) of Appendix A], t^{I} and v^{I} can also be considered as functions of S, i.e.,

$$t^{\mathrm{I}} = t^{\mathrm{I}}(\zeta R) = t^{\mathrm{I}}(S) \tag{71}$$

$$v^{\mathrm{I}} = v^{\mathrm{I}}(\zeta R) = v^{\mathrm{I}}(S). \tag{72}$$

Plots of these quantities as functions of S are also contained in Fig. 8 and it is apparent that these curves exhibit the same overall character as $\bar{q}^{\mathrm{I}}$. They are given by the approximations

$$t^{\mathrm{I}} \simeq -0.902957S(1 - S^2)(1 + 0.310693S^2) \tag{72a}$$

$$v^{\mathrm{I}} \simeq -0.234145S(1 - S^2)(1 + 0.000172S^2) \tag{72b}$$

with an absolute mean deviation of 0.01. Such behavior is not limited to

$1s$ orbitals[4] and, by inserting explicit correlations of this type in Eqs. (69) and (70), one can obtain improved forms of Mulliken's approximation which was mentioned after Eq. (61). It may roughly be said that these improvements result from *replacing the "overlap population"* $(S/1 + S)$ *by the interference population* q^{I} *and by treating the kinetic and the potential parts separately.*

The relationships between interference energies, overlap integrals, and the orbital kinetic and potential energies T_{H} and V_{H}, which were discussed here, furnish the explicit reason for the related conclusions in Section V,D.

3. *Binding Energy and Overlap*

It is possible to exploit the explicit dependence upon S to gain additional insight into the binding process. In order to accomplish this, we note that, according to Eq. (A.18) of Appendix A, the quasi-classical energy V^{QC} of Eq. (39) can also be written in the form

$$V^{\mathrm{QC}} = V_{\mathrm{H}}(\zeta)v^{\mathrm{QC}}, \tag{73}$$

where v^{QC} is again a function of ζR, so that

$$v^{\mathrm{QC}} = v^{\mathrm{QC}}(\zeta R) = v^{\mathrm{QC}}(S). \tag{74}$$

The total kinetic and potential energies of the FH variational function can then be expressed as follows:

$$T = T_{\mathrm{H}}(\zeta)\, t(S), \qquad V = V_{\mathrm{H}}(\zeta)\, v(S) \tag{75}$$

with

$$t(S) = 1 + (1 + S)^{-1} t^{\mathrm{I}}(S) \tag{76}$$

$$v(S) = 1 + (1 + S)^{-1} v^{\mathrm{I}}(S) + v^{\mathrm{QC}}(S). \tag{77}$$

Plots of $t(S)$ and $v(S)$ against S are given in Fig. 9, which also contains a graph of $q^{\mathrm{I}}(S)$ for comparison. From this figure it is apparent that in the region of interest, $0.4 \leq S \leq 0.6$, $t(S)$ and $v(S)$ are given fairly well by the simplified approximations

$$t(S) \simeq 1 - 0.95S(1 - S) \tag{78}$$

$$v(S) \simeq 1 - 0.05. \tag{79}$$

Almost identical expressions are obtained by inserting the approximations of Eqs. (72a) and (72b) into (76) and (77) (the term v^{QC} is negligibly small).

[4] In a previous investigation (Ruedenberg, 1961), it was shown that, for two $2p\pi$ orbitals with identical ζ values, the relation

$$\langle A|-\tfrac{1}{2}\nabla^2|B\rangle \simeq S^2\langle A|-\tfrac{1}{2}\nabla^2|A\rangle$$

holds for $S > 0$. Inserting this in the definition of t^{I}, one obtains the similar relation

$$t^{\mathrm{I}} = -S(1 - |S|).$$

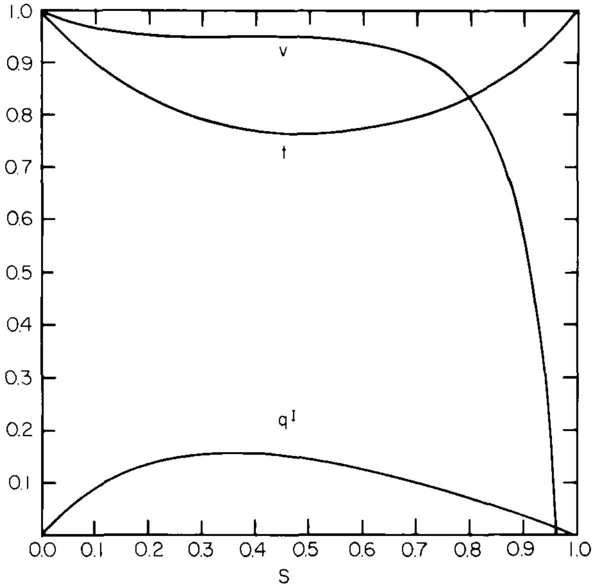

Fig. 9. Overlap dependence of kinetic and potential energy factors for Φ_{FH}.

These equations, in conjunction with Eq. (75) clearly substantiate and emphasize again the previous conclusions, i.e., that the dominating features of bond formation are atomic contraction and kinetic-energy-pressure lowering in the bond due to interference.

Let us use the resulting energy expression

$$E(\zeta, R) \simeq \tfrac{1}{2}\zeta^2\{1 - 0.95S(1 - S)\} - 0.95\zeta \qquad (80)$$

for finding the solution at the equilibrium distance. The latter is determined by the two minimum conditions

$$\left(\frac{\partial E}{\partial \zeta}\right)_R = 0 \qquad (81)$$

$$\frac{dE}{dR} = \left(\frac{\partial E}{\partial \zeta}\right)_R \frac{d\zeta}{dR} + \left(\frac{\partial E}{\partial R}\right)_\zeta = \left(\frac{\partial E}{\partial R}\right)_\zeta = 0. \qquad (82)$$

But they can be replaced by

$$0 = \left(\frac{\partial E}{\partial \zeta}\right)_S = \zeta\{1 - 0.95S(1 - S)\} - 0.95 \qquad (83)$$

$$0 = \left(\frac{\partial E}{\partial S}\right)_\zeta = 0.95\zeta^2(S - 0.5). \qquad (84)$$

From Eq. (84) one obtains $S = 0.5$ and substitution of this in Eq. (83) yields $\zeta = 1.247$. The internuclear distance follows from the implicit relation $S(1.247R) = 0.5$ which yields $R = 1.9$. These values are quite close to the exact values, which confirms that Eqs. (78) and (79) are *bona-fide* approximations.

3. Contractive Promotion and Overlap

A very close comparison with the analyses developed in the preceding sections can be achieved by inserting, in Eqs. (75), (78) and (79), the equilibrium distance and then minimizing with respect to ζ. This is relatively simple since, because of the parabolic dependence on S, the quantity t^{I} changes only very little if R lies near the equilibrium value and ζ varies between 0.8 and 1.3. For $R = R_{\mathrm{eq}}$ one has therefore approximately

$$E(\zeta, R_{\mathrm{eq}}) \simeq \tfrac{1}{2}\zeta^2(1 - 0.236) - \zeta(1 - 0.05). \tag{85}$$

This equation can now be interpreted in two ways. In the form[5]

$$E(\zeta) \simeq (0.764)\tfrac{1}{2}\zeta^2 - 0.95\zeta \tag{86}$$

it exhibits the modified competition between kinetic and potential energy (modified as compared to the free atom) which was the basis of the discussion in Section IV.A. Alternatively we may write

$$E(\zeta) \simeq [\tfrac{1}{2}\zeta^2 - \zeta] + \tfrac{1}{2}\zeta^2(-0.236) + 0.05\zeta, \tag{87}$$

and this form exhibits the competition between the promotion energy, $\frac{1}{2}\zeta^2 - \zeta$, and the kinetic energy lowering from interference, $(-0.118)\zeta^2$, which was described in Section V.D. The last term in Eq. (87) has a negligible influence on this competition. As discussed in Section V.D, minimization with respect to ζ leads to contraction because the promotion energy increases only slowly near its minimum, $\zeta = 1$, whereas the negative kinetic interference energy, which is proportional to the kinetic energy of the atomic orbital, $T_{\mathrm{H}}(\zeta) = \frac{1}{2}\zeta^2$, can be substantially enhanced by increasing ζ.

4. Remarks on Overlap

(1) It should be noted that, because of the contractive effect, the overlap integral in the molecule ($S = 0.4637$) is smaller than that between two ground state hydrogen atomic orbitals ($S = 0.5865$ at $R = 2.0$ au). It is therefore seen that *the principle of maximum overlap does not apply to the overlap variation arising from orbital exponent variation.*

---

[5] Equation (86) is almost identical with the intuitively proposed Eq. (7.6) of Ruedenberg (1962).

(2) Not infrequently one finds the statement that the accumulation of charge in the bond, which results from the overlap of neighboring atomic orbitals, lowers the potential energy of the system. On the basis of the present analysis it must be concluded that *there exists no justification for identifying overlap with any kind of potential energy lowering.*

VI. Orbital Analysis of the Antibinding State

A. Wave Functions and Energies for the Antibinding State

The wave function for the antibinding state has the form

$$\Psi = [A - B][2(1 - S)]^{-1/2} \tag{88}$$

and we consider again the two choices of atomic orbitals defined in Eqs. (19) and (20). Since the antibinding state does not have an equilibrium position, we shall discuss the results at the equilibrium distance of the binding state, $R = 2.0$ au. This corresponds to a "vertical transition" and is convenient for comparison with the binding state. The results of the energy minimization are listed in Table VIII.

TABLE VIII

ENERGIES AND VARIATION PARAMETERS FOR THE H_2^+ MOLECULE ION ANTIBINDING STATE AT $R = 2.0$ au

	Finkelstein–Horowitz	Guillemin–Zener
ζ	0.9010	—
ζ_A	—	0.9003
ζ_B	—	−0.0020
T	0.8095	0.8087
V	−0.9753	−0.9745
E	−0.1658	−0.1658
E^B	0.3342	0.3342

The results for the FH-type wave function, Ψ_{FH}, were determined by one of the authors (E.L.M.), whereas results for the GZ-type wave function, Ψ_{GZ}, were taken from the paper of Kim *et al.* (1965). It is apparent that for $R = 2.0$ au, Ψ_{GZ} does not significantly differ from Ψ_{FH}; the additional flexibility offered by the parameter ζ_B in Ψ_{GZ} is essentially useless. The subsequent discussion will therefore be based on the FH-type approximation.

B. Origin of the Antibinding Energy

As in the case of the binding state, the origin of the increase in energy in the antibinding state is most easily understood by considering kinetic, potential, and total energy as a function of the variation parameter, α, and examining the characteristics of that wave function which is selected by the variation principle. These curves are plotted in Fig. 10, which, similar to Fig. 3, also contains the free atom graphs.

The curves for the antibinding state show a behavior opposite to that of the curves for the binding state in Fig. 3: The kinetic energy curve lies

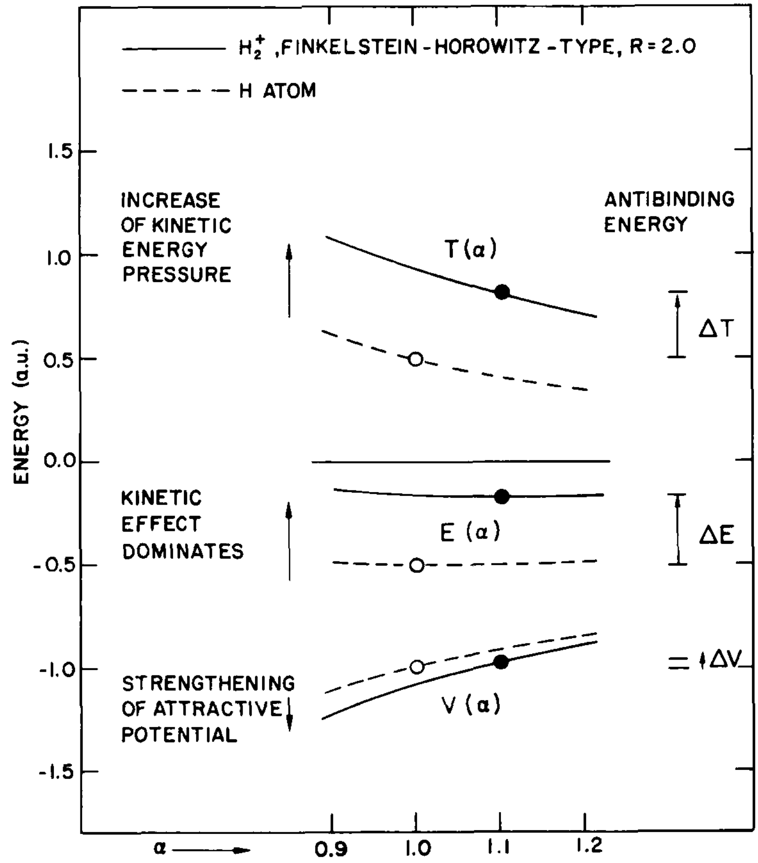

Fig. 10 Competition between kinetic energy and potential energy in the antibinding state of the H_2^+ molecule and comparison with the H atom.

considerably *above* that of H, whereas the potential energy curve lies slightly *below* that of H; the slopes of the two curves show the corresponding changes. As a consequence, the minimum of the energy curve is shifted to a value $\alpha > 1$, and we may say the following: Because the kinetic energy pressure is higher in the H_2^+ antibinding state than in H, the nuclear suction is slightly less successful in holding the electron cloud close to the nuclei, i.e., the average distance from the nuclei is larger than in H.

The increase of the kinetic energy pressure, in going from H to H_2^+, is therefore crucial for the antibinding effect. Again, it is a typical consequence of the wave nature of the electron: The wave function of the antibinding state can be conceptually constructed by first delocalizing the electron from one to two atoms and then exciting it into a state whose wave function contains a nodal plane. The corresponding excitation energy is kinetic in character and much larger than the drop in kinetic energy associated with delocalization.

For the antibinding state the similarity to the case of a particle in a box is closer than for the binding state. It is true, as it was for the latter, that the change in α counteracts the difference in the kinetic and potential energy established by the shift of the curves in Fig. 10. However, the potential energy contribution to the antibinding energy is barely reversed, and the kinetic energy contribution is not at all reversed, when α is changed from 1 to 1.11.

Thus, at the equilibrium position, the antibinding energy is almost entirely given by the rise in kinetic energy associated with the formation of a nodal plane in the electron wave; the potential energy change is small.

C. Orbital Partitioning of the Antibinding State

The orbital analysis of the antibinding state follows the same pattern as that of the binding state. In analogy to Eqs. (33)–(36), we now define the following density partitioning for Ψ of Eq. (88):

$$\rho_a = \rho_a^{QC} + \rho_a^{I}, \tag{89}$$

where

$$\rho_a = \Psi^2 = (A - B)^2/2(1 - S) \tag{90}$$

$$\rho_a^{QC} = \tfrac{1}{2}\{A^2 + B^2\} \tag{91}$$

$$\rho_a^{I} = -(1 - S)^{-1}\{AB - \tfrac{1}{2}S[A^2 + B^2]\}. \tag{92}$$

In analogy to Eqs. (37)–(40), we define the corresponding potential energy parititioning

$$V_a = V_a^{\mathrm{A}} + V_a^{\mathrm{QC}} + V_a^{\mathrm{I}}, \tag{93}$$

where V_a^{A} and V_a^{QC} are again given by the definitions (38) and (39) and the interference term V_a^{I} is now

$$V_a^{\mathrm{I}} = -(1-S)^{-1} \int d\tau \{AB - \tfrac{1}{2}S[A^2 + B^2]\}\{-r_A^{-1} - r_B^{-1}\}. \tag{94}$$

In analogy to Eqs. (45)–(47), we define the corresponding kinetic energy partitioning

$$T_a = T_a^{\mathrm{A}} + T_a^{\mathrm{I}}, \tag{95}$$

where T_a^{A} is again given by the definition (46) and the interference term T_a^{I} is now

$$T_a^{\mathrm{I}} = -(1-S)^{-1} \int d\tau \{A(-\tfrac{1}{2}\nabla^2)B - \tfrac{1}{2}S[A(-\tfrac{1}{2}\nabla^2)A + B(-\tfrac{1}{2}\nabla^2)B]\}. \tag{96}$$

Figure 11 illustrates the meaning of the interference density for the antibinding state. It is evident that the addition of the interference density ρ_a^{I} to the quasi-classical density ρ_a^{QC} generates the node of the antibinding state, displaces charge density from the bond region into regions near the nuclei, and concomitantly creates a strong increase in the gradient at all points. With reference to the effects in the bond regions, we call this *destructive interference* between the atomic orbitals in contrast to the *constructive interference* in the *binding state.*

In view of the charge shift towards the nuclei, it is clear that destructive interference will lead to a potential energy *decrease* in contrast to the increase due to constructive interference in the binding state. Likewise, the increase in the gradient, arising from destructive interference, mainly in the z direction, will lead to an *increase* in the kinetic energy in contrast to the kinetic energy decrease due to constructive interference in the binding state. Moreover, the interference effects are stronger for the antibinding wave function than for the binding wave function because $(1 - S)^{-1}$ is larger than $(1 + S)^{-1}$.

Since these arguments about the kinetic and potential interference energies are valid for any value of ζ, they explain the position of the molecular T and V curves with respect to the atomic T and V curves in Fig. 10. To be sure, the molecular potential energy also contains the quasi-classical energy V_a^{QC} of Eq. (93). It is positive as in the case of the binding state but,

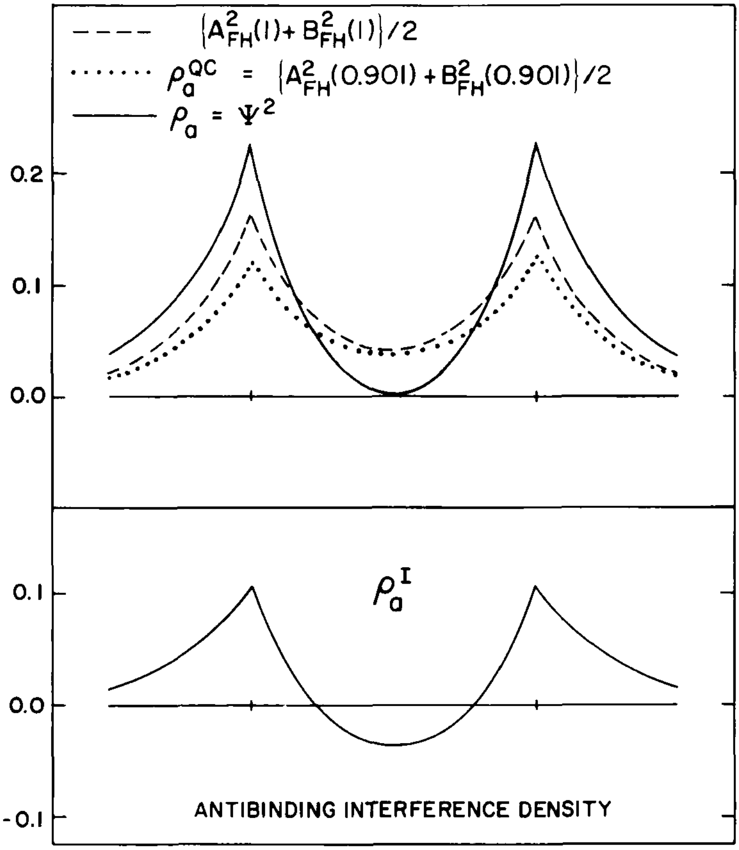

Fig. 11. Quasi-classical and interference density for the antibinding state.

although somewhat larger (because the decrease in ζ decreases the shielding slightly), still only a fraction of the interference potential energy.

D. Expansive Promotion

In the antibinding state, it is not possible to use the virial theorem to predict the result of the minimization process. However, an analysis based on the behavior of the interference energy elucidates the reasons why the variation principle leads to an expansion of the atomic orbitals.

If one uses the interference energy definitions of Eqs. (94) and (96) instead of those of the binding state, then Eq. (75) becomes

$$T_a = T_H(\zeta)\, t_a(S), \qquad V_a = V_H(\zeta)\, v_a(S), \tag{97}$$

where now

$$t_a(S) = 1 - (1 - S)^{-1}\, t^{\mathrm{I}}(S) \tag{98}$$

$$v_a(S) = 1 + v^{\mathrm{QC}}(S) - (1 - S)^{-1}\, v^{\mathrm{I}}(S). \tag{99}$$

Plots of $v_a(S)$ and $t_a(S)$ are given in Fig. 12. From these, it is apparent that in the region of interest one has approximately

$$V_a = V_{\mathrm{H}}(\zeta)\,\{1 + 0.1\} \tag{100}$$

$$T_a = T_{\mathrm{H}}(\zeta)\,\{1 + 0.95S(1 + S)\}. \tag{101}$$

Nearly identical expressions are obtained by inserting the approximations of Eqs. (72a) and (72b) into Eqs. (98) and (99). It is therefore evident that Eqs. (100) and (101) are consistent with Eqs. (78) and (79), since both are explained by the approximations of Eqs. (72a) and (72b).

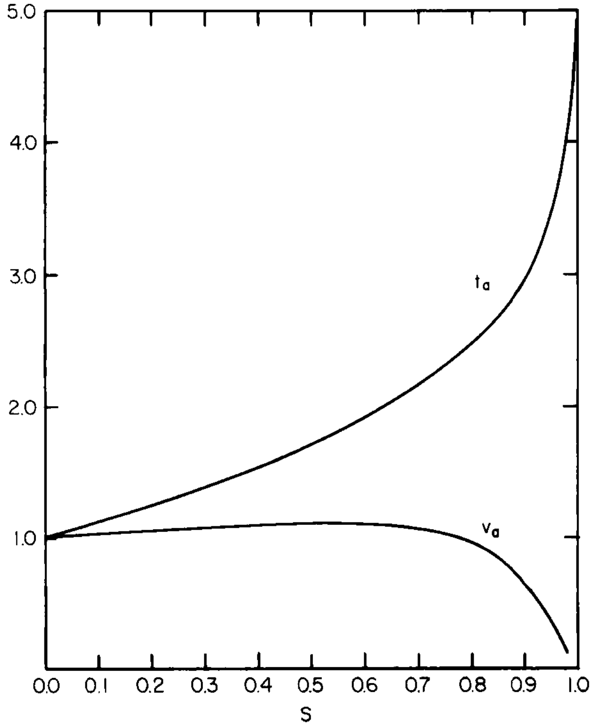

Fig. 12. Overlap dependence of kinetic and potential energy factors in the antibinding state.

From Eqs. (97), (100) and (101) one obtains now

$$E_a[\zeta, S(\zeta R_{eq})] \simeq \{\tfrac{1}{2}\zeta^2 - \zeta\} + \tfrac{1}{2}\zeta^2[0.95S(1 + S)] - 0.1\zeta. \qquad (102)$$

For ζ in the neighborhood of $\zeta = 1$, the variation of E_a is again dominated by that of the kinetic interference energy, i.e., the second term of Eq. (102) and the variation of the latter is again essentially determined by the factor $\frac{1}{2}\zeta^2 = T_H(\zeta)$, representing the kinetic energy of the atomic orbital (the variation of $S(\zeta R_{eq})[1 + S(\zeta R_{eq})]$ is relatively small). Since the kinetic interference energy is now positive, ζ decreases from $\zeta = 1.0$ ($S = 0.5865$) to $\zeta = 0.9010$ ($S = 0.6407$).

E. Orbital Analysis of the Antibinding Energy

In analogy to Eqs. (57)–(60), the antibinding energy of the FH approximation can now be expressed as follows:

$$E_a(\text{FH}) - E(\text{H}) = E_a^{\text{AE}} + E_a^{\text{QC}}(\text{FH}) + E_a^{\text{I}}(\text{FH}), \qquad (103)$$

where

$$E_a^{\text{AE}} = T_a^{\text{AE}} + V_a^{\text{AE}} \qquad (104)$$

$$E_a^{\text{QC}}(\text{FH}) = V_a^{\text{QC}}(\text{FH}) \qquad (105)$$

$$E_a^{\text{I}}(\text{FH}) = T_a^{\text{I}}(\text{FH}) + V_a^{\text{I}}(\text{FH}) \qquad (106)$$

and where, in analogy to Eqs. (43) and (50), we define potential and kinetic energy changes due to *expansive* promotion as

$$V_a^{\text{AE}} = V_a^{\text{A}}(\text{FH}) - V(\text{H}) \qquad (107)$$

$$T_a^{\text{AE}} = T_a^{\text{A}}(\text{FH}) - T(\text{H}). \qquad (108)$$

In Eqs. (103)–(108) the symbol "FH" implies use of the ζ values appropriate to the antibinding state.

The numerical values for this partitioning are summarized in Table IX.

TABLE IX

ORBITAL PARTITIONING OF THE ANTIBINDING ENERGY
FH APPROXIMATION, $R = 2.0$ au

Energy changes due to	T	V	E
Expansive promotion	−0.0941	0.0990	0.0049
Quasi-classical electrostatic	—	0.0381	0.0381
Destructive interference	0.4036	−0.1124	0.2912
Binding energy	0.3095	0.0247	0.3342

It provides the quantitative substantiation of the preceding interpretation and suggests the following additional observations:

(a) the expansive promotion found in the antibinding state is conconsiderably weaker energetically than the contractive promotion in the binding state;
(b) quasi-classical and interference potential energies cancel each other in part;
(c) the kinetic interference energy is by far the most important contribution.

In conclusion, then, the energy increase in the antibinding state is essentially due to a kinetic energy increase associated with destructive interference of the atomic orbitals. Within the context of the variation principle, the concomitantly occurring expansive promotion can be viewed as an attempt to mitigate this large kinetic energy increase without sacrificing too much potential energy.

VII. Dependence upon the Internuclear Distance

A. Orbital Partitioning

In the present section we discuss the energetic behavior of the FH and the GZ wave functions as a function of the internuclear distance R. The differences between the molecular total, potential, and kinetic energies and their atomic counterparts are given by

$$E(\mathrm{H}_2^+; R) - E(\mathrm{H}) = E(\mathrm{H}_2^+; R) + \tfrac{1}{2} \tag{109}$$

$$V(H_2^+; R) - V(\mathrm{H}) = V(\mathrm{H}_2^+; R) + 1 \tag{110}$$

$$T(H_2^+; R) - T(\mathrm{H}) = T(\mathrm{H}_2^+; R) - \tfrac{1}{2}. \tag{111}$$

A formal understanding of the behavior of the T and V curves can be derived from the molecular virial theorem, Eq. (14). This equation, in conjunction with the relation $T + V = E$, yields

$$T = -E - R(dE/dR) \tag{112}$$

$$V = 2E + R(dE/dR) \tag{113}$$

as was first pointed out by Slater (1933).

1. Binding State

Plots of the energy differences defined in Eqs. (109)–(111) are given in Figs. 13a and 14a for the FH and GZ functions, respectively. In order to provide a further understanding, Figs. 13 and 14 also show how the decompositions in promotional, quasi-classical, and interference contributions vary with the internuclear distance. The curves in Fig. 13 suggest the following conclusions for the FH approximation.

At large distances there is neither contractive promotion nor quasi-classical interaction. Here, the attraction is due to a drop in kinetic energy

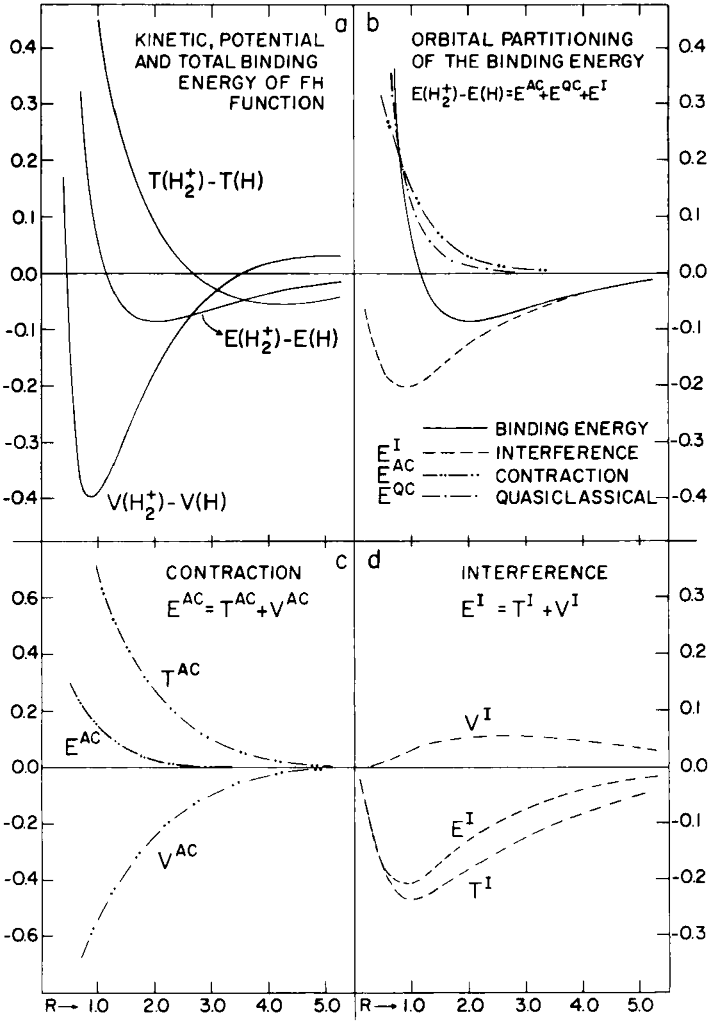

Fig. 13. Energy partitioning of the H_2^+ binding state (FH approximation) as functions of the internuclear distance.

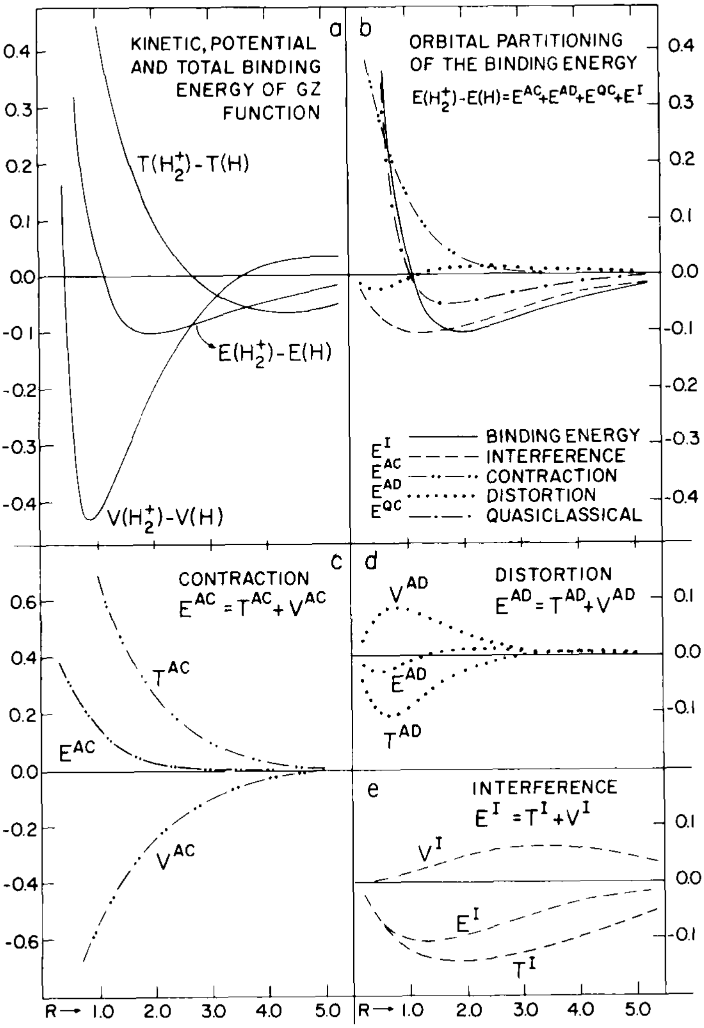

Fig. 14. Energy partitioning of the H_2^+ binding state (GZ approximation) as functions of the internuclear distance.

arising from interference delocalization. From about $2.5R_{eq}$ in, contractive promotion becomes a contributing factor and starts to swing the potential and kinetic energy curves the other way. It increases steadily toward smaller R values, causing the curves to cross, until the previously discussed equilibrium situation is reached for $R = R_{eq}$. Quasi-classical interaction comes into play only for $R = 1.5R_{eq}$. The repulsion at R_{eq} is due to the steep kinetic energy curve, i.e., it is connected to the uncertainty principle, and not due to the potential energy which is still falling toward shorter R. The latter turns repulsive only for $R \simeq \frac{1}{2}R_{eq}$, where its quasi-classical component now becomes dominant due to the nuclear repulsion.

The observations made for the FH approximation remain valid for the GZ curves of Fig. 14, except for a remark concerning the quasi-classical interaction. In the GZ case the latter is not only attractive in the entire range $R > R_{eq}$ but, more important, it extends to much larger internuclear distances. Nevertheless, this induced dipole–monopole interaction is weaker than the interference interactions for $R \leq 5R_{eq}$. The GZ graphs, in addition, contain the deformation promotion curves. The behavior discussed earlier at the equilibrium distance tapers off toward larger R values. At small R values, the behavior changes because of the transition to the united atom.

2. *Antibinding State*

For a large range of R values the GZ wave function is practically identical with the FH wave function in the antibinding state, as was already discussed for $R = R_{eq}$, the equilibrium distance of the binding state. For this reason, the following discussion is limited to the FH approximation.

In Fig. 15, there are plotted the energy differences defined in Eqs. (109)–(111), applied to the antibinding state, as well as their decompositions into promotion, quasi-classical and interference parts. The overall behavior of T and V, shown in Fig. 15a, can again be related to that of E with the help of Eqs. (112) and (113). The decompositions given in Figs. 15b–d suggest the following interpretations.

At large distances there is no quasi-classical interaction. The repulsion is due to the large increase of the kinetic energy caused by destructive interference. Further, the promotional energy has a slightly contractive effect in this region. From $R = 1.5R_{eq}$ in, the promotion becomes expansive and starts to swing both the kinetic energy and the potential energy curves the other way. For the same distance the quasi-classical interaction becomes effective as well.

Towards smaller R values, expansive promotion steadily increases, but the kinetic energy remains dominated by the strong antibinding destructive interference component until about $\frac{1}{4}$ R_{eq}. The potential curve, in contrast to that of the binding state, exhibits no further change in curvature, since expansive promotion and interference reinforce each other all

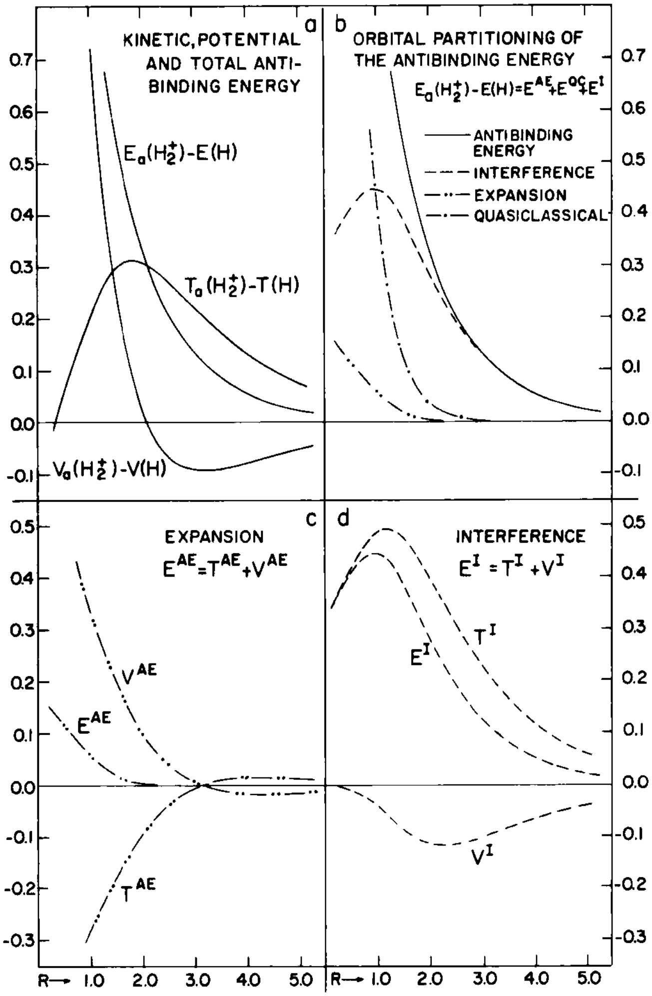

Fig. 15. Energy partitioning of the H_2^+ antibinding state as functions of the internuclear distance.

the way. Hence, the potential energy becomes antibinding from about R_{eq} in, and is dominating for smaller R values where the kinetic energy turns binding. The quasi-classical component, i.e., the nuclear repulsion, begins to dominate the potential energy from $R = \frac{3}{4} R_{eq}$ in.

B. Competition between Promotion and Interference

The partitioning of Section VII.A showed that contraction and expansion do not occur for large internuclear distances. Here, constructive and destructive interference are the only energetic effects. The reasons for these changes in the character of the binding and antibinding processes can be adequately discussed on the basis of the FH approximation.

By virtue of Eqs. (69), (70), (75)–(77), and (97)–(99) the energy difference between the molecule and the atom can be written as follows:

$$\begin{aligned}\Delta E &= E(\mathrm{H}_2^+) - E(\mathrm{H}) = E^{\mathrm{P}} + E^{\mathrm{I}} + E^{\mathrm{QC}} \\ &= \Delta T + \Delta V \qquad (114)\end{aligned}$$

$$\Delta T = T(\mathrm{H}_2^+) - T(\mathrm{H}) = T^{\mathrm{P}} + T^{\mathrm{I}} \qquad (115)$$

$$\Delta V = V(\mathrm{H}_2^+) - V(\mathrm{H}) = V^{\mathrm{P}} + V^{\mathrm{I}} + V^{\mathrm{QC}}, \qquad (116)$$

where E^{P}, T^{P}, V^{P} denote promotion energies previously denoted by E^{AC}, V^{AC}, T^{AC}, or by E^{AE}, V^{AE}, T^{AE}. The individual terms are

$$T^{\mathrm{P}} = \tfrac{1}{2}(\zeta^2 - 1) \qquad (117)$$

$$V^{\mathrm{P}} = -\zeta + 1 \qquad (118)$$

$$T^{\mathrm{I}} = \pm(1 \pm S)^{-1}\tfrac{1}{2}\zeta^2 t^{\mathrm{I}}(S) \qquad (119)$$

$$V^{\mathrm{QC}} + V^{\mathrm{I}} = -\zeta\{v^{\mathrm{QC}}(S) \pm (1 \pm S)^{-1} v^{\mathrm{I}}(S)\}, \qquad (120)$$

where the plus and minus signs apply to the binding and antibinding states, respectively.

In Sections V.E and VI.D, it was found that at $R = 2.0$ au the wave function resulted from the variational competition between the promotion and interference components of the total energy, i.e., E^{P} and E^{I}. We will now examine the nature of this competition at other internuclear distances.

1. Binding State

For the binding state, the nature of the variational competition implied in Eqs. (114)–(120) is graphically represented in Fig. 16 for the internuclear distances $R = 1.6, 2.0, 3.0, 4.0, 5.0$ and infinite separation.

Consider first the plots for the equilibrium distance, $R = 2.0$ au. The curves in the first column show ΔE, ΔT, and ΔV as functions of the variation parameter $\zeta = \alpha^{-1}$. As discussed before, for $\zeta = 1.0$, the drop ΔE results from the drop ΔT, in spite of the increase ΔV. In contrast, the virial theorem $\Delta E = -\Delta T = \frac{1}{2}\Delta V$ is satisfied for the variational minimum,

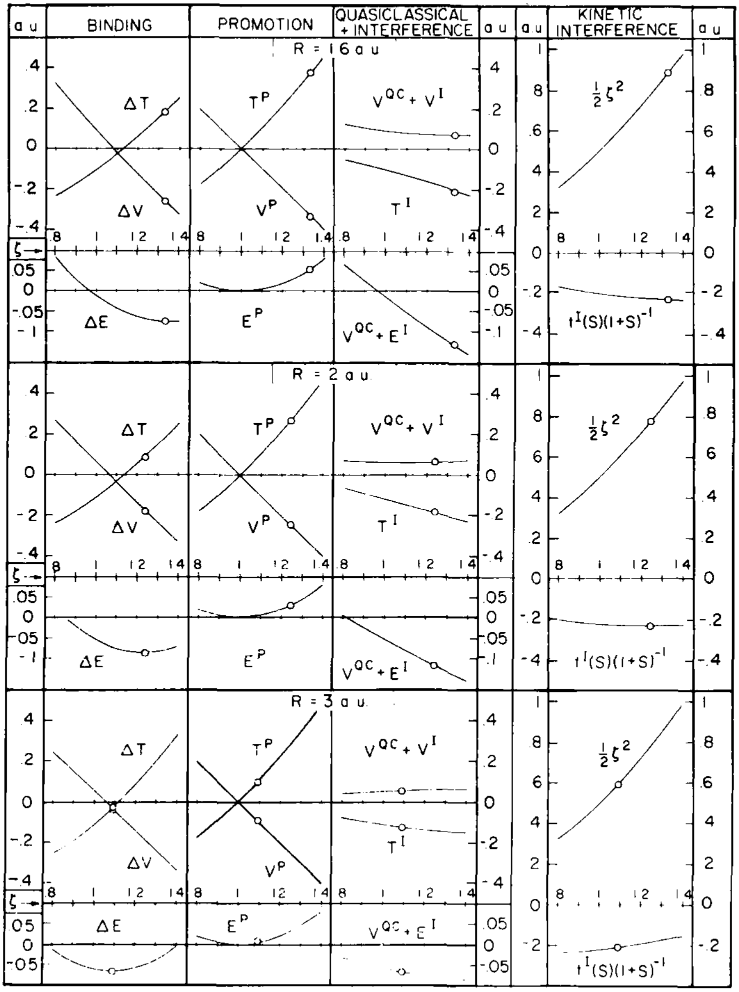

Fig. 16. Variational competition in the binding state (FH

$\zeta = 1.2387$ (increasing ζ corresponds to orbital contraction). The curves in the next two columns show the terms on the right-hand side of Eqs. (115) and (116) as functions of ζ. The following observations are apparent: The minimum in ΔE is the result of the compromise between the increase in E^P and the sharp drop in $(V^{QC} + E^I)$ with increasing ζ; the behavior of E^P is the result of the increase of T^P and the decrease of V^P upon contraction; the strong decrease in $(V^{QC} + E^I)$ upon contraction is due solely to the

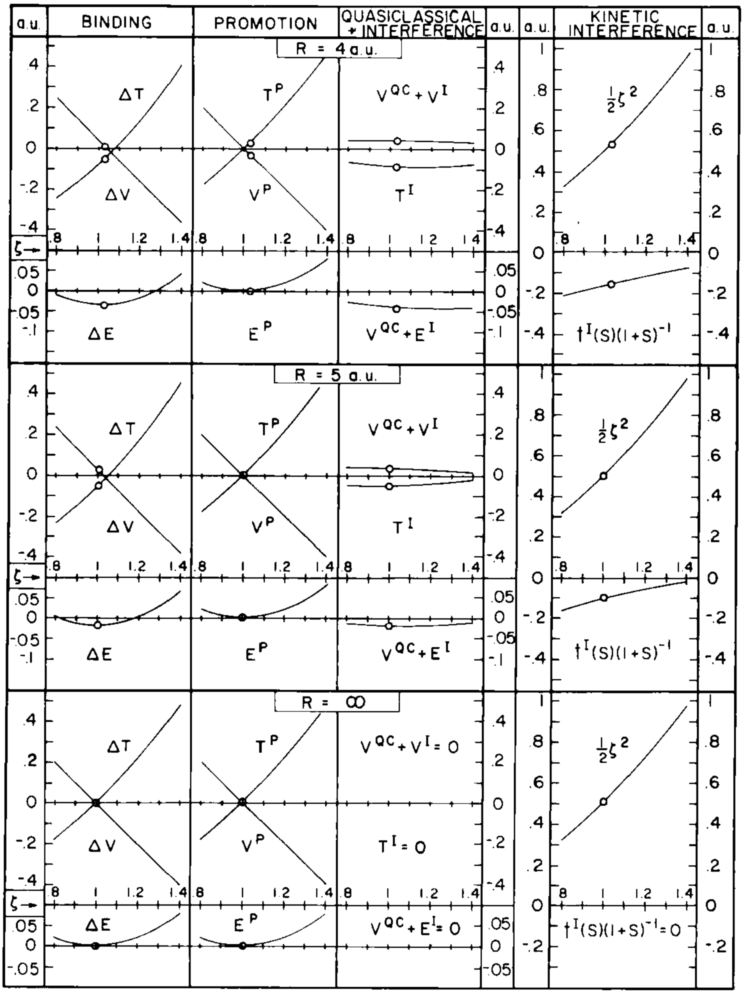

approximation) as a function of internuclear distance.

similar behavior of T^{I} since ($V^{\text{QC}} + V^{\text{I}}$) is approximately constant. Finally, according to Eq. (119), T^{I} is the product of the two quantities plotted in the last column of Fig. 16, and it is seen that while the negative character of T^{I} results from $t^{\text{I}}(S)$, the rapid variation of T^{I} with ζ comes from the factor $\frac{1}{2}\zeta^2$.

These diagrams therefore furnish a graphic illustration of the competition between T^{I} and E^{P}, discussed in Section V.E, resulting in the

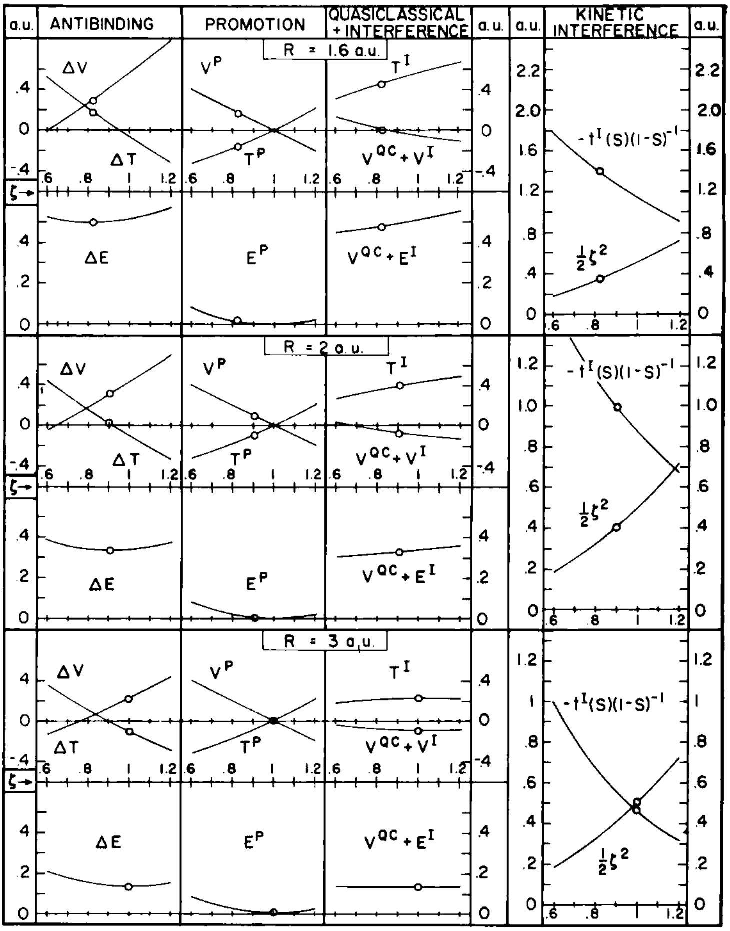

Fig. 17. Variational competition in the antibinding state

preponderance of T^I over E^P, not withstanding the fact that the overall changes ΔT and ΔV reflect the behavior of T^P and V^P as functions of ζ. Although there is a slight difference in viewpoint as compared to Section IV, there is complete agreement as to the central role of T^I at $R = 2.0$ au.

For other internuclear distances a similar competition between T^I and E^P occurs. In fact, the curves for T^P and V^P are the same for all R and the small changes in the curves for $(V^{QC} + V^I)$ are of little consequence. However, the *character of the competition does change for different R values*

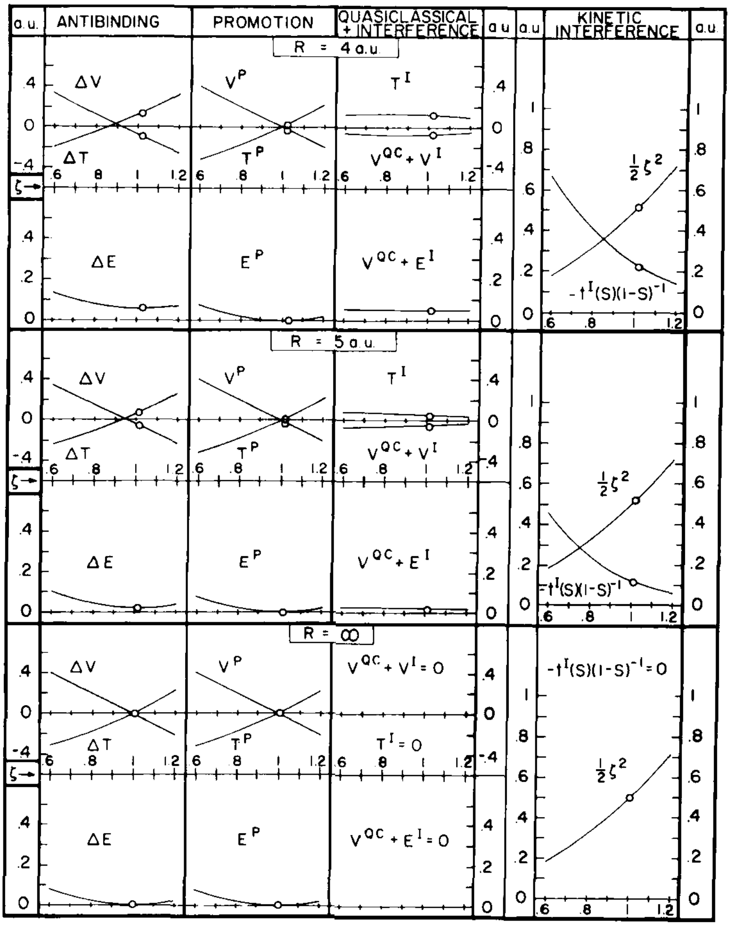

(FH approximation) as a function of internuclear distance.

because the T^1 versus ζ curves undergo significant changes in slope as R varies: For $R = 1.6$ au this slope is strongly negative; as R increases, it becomes less so; for $R \simeq 4.0$ au, it is essentially zero; for $R \simeq 5.0$ au and larger, it turns slightly positive. It is apparent that a negative slope for T^1 forces a contraction of the atomic orbital, whereas a positive slope leads to an expansion. This explains why we find a strong contractive effect for small internuclear distances and practically no change in ζ for large internuclear distances. It moreover explains why at certain large distances

ζ becomes in fact slightly *less* than unity (see Table B.I of Appendix B).

The aforementioned behavior of the T^{I} curves can be further analyzed by examining the two factors of T^{I} which are plotted in the last column of Fig. 16, namely $\frac{1}{2}\zeta^2$ and $(1 + S)^{-1}t^{\mathrm{I}}(S)$. It is apparent that the changes in the slope of T^{I} results from the corresponding changes in the slope of $(1 + S)^{-1}t^{\mathrm{I}}(S)$. In turn, the changes in the slope of the latter quantity are readily understood by reference to the S dependence of $t = 1 + (1 + S)^{-1}t^{\mathrm{I}}(S)$ displayed in Fig. 9. For example, at $R = 2.0$ au, $S \simeq 0.5$, and, hence, t as well as $(1 + S)^{-1}t^{\mathrm{I}}(S)$ have almost vanishing slope so that the slope of $\frac{1}{2}\zeta^2$ predominates. In contrast, for $R = 5.0$ au, the overlap integral S is approximately 0.1. Hence, t increases strongly with S and, correspondingly, the absolute value of $(1 + S)^{-1}t^{\mathrm{I}}(S)$ decreases so strongly with increasing ζ (orbital contraction) that it determines the slope of T^{I}.

In summary, it is because of the characteristic S dependence of the interference population, q^{I}, that orbital contraction substantially increases the strength of T^{I} for internuclear distances in the neighborhood of $R =$ 2.0 au, whereas it slightly weakens the strength of T^{I} at large values of R. Consequently, orbital contraction occurs only for small values of R.

2. *Antibinding State*

The variational competition in the antibinding state is displayed in Fig. 17 for the same internuclear distances as above. The terms T^{P} and V^{P} are identical to those in the binding state, but T^{I} is now positive and $(V^{\mathrm{QC}} + V^{\mathrm{I}})$ is negative, in agreement with the discussion of Section VI,D. Again the behavior of T^{I} versus ζ and the change of its slope with R are the crucial elements. Since now $-(1 - S)^{-1}t^{\mathrm{I}}(S)$ has the opposite sign from the corresponding quantity $(1 + S)^{-1}t^{\mathrm{I}}(S)$ for the binding case, substantial *expansion* (decrease in ζ) results in the neighborhood of $R =$ 2.0 au, no change in ζ occurs for very large R, and a very slight contraction occurs for certain large R values (see Table B.I of Appendix B). The detailed explanation of these observations is completely analogous to the reasoning given for the binding state except that the overlap dependence of $1 - (1 - S)^{-1}t^{\mathrm{I}}(S)$ is that of Fig. 12.

C. Differences between the United Atom and the Molecule

In the united atom model, the overall lowering of the potential energy in the bonding state upon molecule formation is ascribed to the fact that the two protons, though separated, act similar to a He nucleus in contracting the electronic wave function. From a physical point of view this interpretation is difficult to visualize, because the majority of the electronic charge is located in the immediate neighborhood of the two hydrogen nuclei and in the bond region between them, and these regions really have no counterpart in the He atom. Only for the very small amount of charge far out do the two protons begin to resemble a He nucleus. Moreover, the kinetic and potential electronic energies at the equilibrium distance are much closer in value to those of the separated atoms than to those of the united atom. The following considerations, which are based on the FH approximation, suggest that the united atom description is in fact not compatible with the present analysis.

1. Binding State

A similarity appears to exist between the united atom and the FH wave function of the molecule in as much as both exhibit a contraction in the atomic orbital (s), and in that the value of α decreases monotonically from 0.8 to 0.5, when the internuclear distance is varied from R_{eq} to zero (see Appendix B). This superficial similarity disappears, however, when the reasons for the contraction in both systems are examined more closely.

The discussion in Section IV.A in connection with Fig. 3 showed that, at the equilibrium position, the shrinkage in α form 1 to 0.8 is a consequence of the change in the kinetic energy curve and not in the potential energy curve. If the analogous diagram is drawn, however, for the He^+ ion, then it is found, of course, that the kinetic energy curve $T(\alpha)$ is identical to that of the H atom, whereas now the potential energy curve (after omission of the infinite nuclear replusion constant) has a slope twice as steep as that of the hydrogen atom. Therefore, the value of $\alpha(He^+) = 0.5$ is in this case a result of the change in the potential energy curve.

A quantitative formulation of this matter can be obtained by analyzing the reasons why the derivative of the total energy curve in Fig. 3 is positive for $\alpha = 1$. (The positive value of this derivative implies the shift of the minimum towards smaller α.) While Fig. 3 applies to the equilibrium distance, analogous plots can be made for other R values and here, too, the derivative $\partial E(R, \alpha)/\partial\alpha$ can be examined for $\alpha = 1$. These derivatives can be decomposed into their kinetic and potential components, i.e.,

$$\left[\frac{\partial E(R,\alpha)}{\partial\alpha}\right]_{\alpha=1} = \left[\frac{\partial T(R,\alpha)}{\partial\alpha}\right]_{\alpha=1} + \left[\frac{\partial V(R,\alpha)}{\partial\alpha}\right]_{\alpha=1} \qquad (121)$$

and one can then examine how the potential and the kinetic slopes contribute to that of the total energy. Numerical values for the three slopes are plotted in Fig. 18 as functions of R, and it is obvious that the total energy slope is determined by the *deviations* of the kinetic and potential slopes

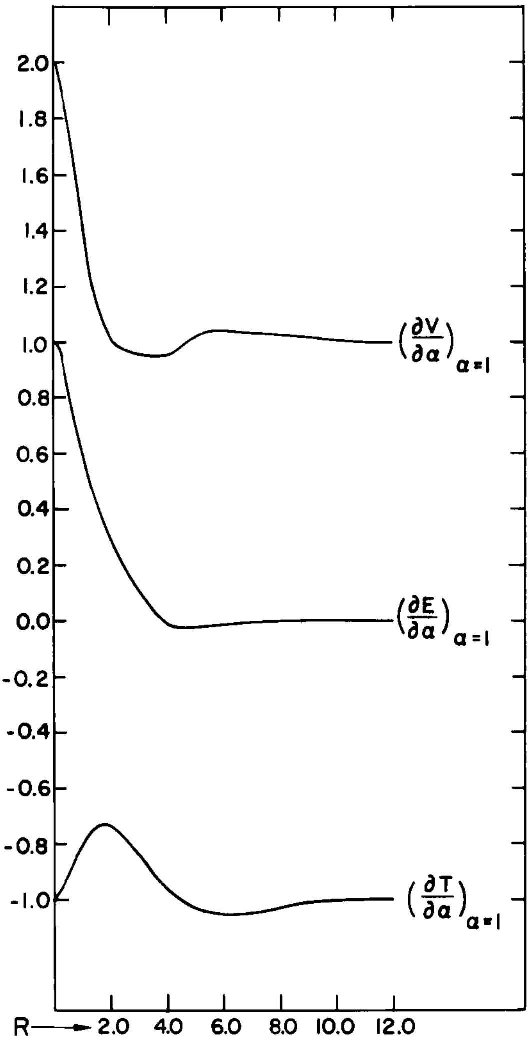

Fig. 18. Dependence upon the internuclear distance for the quantities of Eq. (121).

from their separated atom values ($R = \infty$), which balance each other. It is now apparent that at the equilibrium distance one has

$$\left[\frac{\partial E(R_{eq},\alpha)}{\partial \alpha}\right]_{\alpha=1} = \left[\frac{\partial T(R_{eq},\alpha)}{\partial \alpha}\right]_{\alpha=1} - \left[\frac{\partial T(\infty,\alpha)}{\partial \alpha}\right]_{\alpha=1} \tag{122}$$

whereas, for the united atom, one finds

$$\left[\frac{\partial E(0,\alpha)}{\partial\alpha}\right]_{\alpha=1} = \left[\frac{\partial V(0,\alpha)}{\partial\alpha}\right]_{\alpha=1} - \left[\frac{\partial V(\infty,\alpha)}{\partial\alpha}\right]_{\alpha=1} \tag{123}$$

Thus, at R_{eq}, it is the kinetic energy which changes the balance between the slopes from what it is $R = \infty$, but it is the potential energy at $R = 0$.

It is to be concluded that the atomic orbital contraction in the molecule is a result of the weakening in virtual kinetic energy pressure, whereas the contraction in the united atom is a consequence of the strengthened nuclear suction. Between R_{eq} and $R = 0$, a continuous transition occurs from one extreme to the other and, at about $R = 1.25$ au, the contractive promotion is due in about equal parts to the increase of the potential and kinetic slopes above their separated atom values.

2. *Antibinding State*

The antibinding state of H_2^+, too, differs from its united atom counterpart, the $2p$ state of He^+, in essential respects.

First, the overall extension of the excited (antibinding) state wave function in H_2^+ is about as large as that of the ground state. In He^+, however, it is considerably larger than that of the ground state. Consequently, the H_2^+ excitation resembles largely that of a particle in a box, involving an increase in kinetic energy. In contrast, the kinetic energy of the $2p$ state of He^+ is *lower* than that of the $1s$ state in spite of the fact that the wave function has acquired a node.

Secondly, the attractive nuclear point charges lie *near* the points of greatest electron density in the antibinding state of H_2^+, so that not too much (negative) potential energy is lost by putting a nodal plane in the wave function. In He^+, however, the attractive center lies on the nodal plane itself. This fact, together with the aforementioned expansion of the wave function, has the consequence that the $2p$ state possesses considerably less (negative) potential energy than the $1s$ state.

The numerical results agree with these considerations. In H_2^+, the energy increase from the binding to the antibinding state is 50% kinetic and 50% potential in origin (compare Tables I and VIII). But in He^+, the $1s - 2p$ excitation energy arises solely from an *increase* in potential energy, in spite of a *decrease* in kinetic energy, the latter being half as large in absolute magnitude as the former. In fact, whereas the virial theorem is satisfied for the $2p$ state of He^+, this is not the case for the antibinding state of H_2^+ at $R = R_{eq}$. From these observations, it is apparent that the united atom model is valid for Rydberg states only.

VII. Conclusion

The foregoing analysis confirms conclusions which had been reached previously, from more general considerations, in the investigation of Ruedenberg (1962). There it had also been found that chemical binding has essentially the same character in H_2 as it has in H_2^+. In the investigations referred to in Section I it became furthermore apparent that similar concepts are also useful in interpreting binding by L-shell electrons. Here, a new element comes into play, however: The possibility of energy lowering through polarization by $2s$-$2p$ hybridization, which requires considerably less promotion energy than does K-shell deformation. We hope to take up this question in future work.

Appendix A

A. Integrals over Atomic Orbitals

We list here the one-electron integrals which are needed for the explicit evaluation of the energies and other quantities discussed in the text. The integrals are given for both the GZ and FH atomic orbitals defined in Eqs. (19)–(21). The FH integrals may be obtained by setting $\zeta_1 = \zeta_2 = \zeta$ in the GZ formulas. In the sequel, the following definitions are used:

$$\rho = \zeta R$$

$$\rho_1 = \zeta_1 R, \qquad \alpha = \tfrac{1}{2}\rho_1$$

$$\rho_2 = \zeta_2 R, \qquad \beta = \tfrac{1}{2}\rho_2$$

$$A_n(t) = \int_1^\infty e^{-tx} x^n \, dx$$

$$B_n(t) = \int_{-1}^1 e^{-tx} x^n \, dx.$$

(1) Atomic orbital normalization:

$$C_{GZ}^2 = (4/\pi R^3)\{A_2(\rho_1)B_0(\rho_2) - A_0(\rho_1)B_2(\rho_2)\}^{-1} \qquad (A.1)$$

$$C_{FH}^2 = \zeta^3/\pi. \qquad (A.2)$$

(2) Overlap, S:

$$\langle A_{GZ} | B_{GZ} \rangle = \tfrac{1}{2}\pi C^2 R^3 \{A_2(\rho_1) - A_0(\rho_1)/3\} \qquad (A.3)$$

$$\langle A_{FH} | B_{FH} \rangle = e^{-\rho}(1 + \rho + \rho^2/3) = S(\rho). \qquad (A.4)$$

(3)

$$\langle A_{GZ}| -r_A^{-1} |A_{GZ}\rangle = -\tfrac{1}{2}\pi C^2R^2\{A_1(\rho_1)B_0(\rho_2) - A_0(\rho_1)B_1(\rho_2)\} \quad (A.5)$$

$$\langle A_{FH}| -r_A^{-1} |A_{FH}\rangle = -\zeta. \quad (A.6)$$

(4)

$$\langle A_{GZ}| -r_B^{-1} |A_{GZ}\rangle = -\tfrac{1}{2}\pi C^2R^2\{A_1(\rho_1)B_0(\rho_2) + A_0(\rho_1)B_1(\rho_2)\} \quad (A.7)$$

$$\langle A_{FH}| -r_B^{-1} |A_{FH}\rangle = -\zeta\{\rho^{-1} - e^{-2\rho}(1 + \rho^{-1})\}. \quad (A.8)$$

(5)

$$\langle A_{GZ}| -r_A^{-1} |B_{GZ}\rangle = -\pi C^2R^2A_1(\rho_1) \quad (A.9)$$

$$\langle A_{FH}| -r_A^{-1} |B_{FH}\rangle = -\zeta e^{-\rho}(1 + \rho). \quad (A.10)$$

(6)

$$\begin{aligned}\langle A_{GZ}| -\tfrac{1}{2}\nabla^2 |A_{GZ}\rangle = -\tfrac{1}{2}\pi C^2R\{&(\beta^2 - \alpha^2)A_0(\rho_1)B_0(\rho_2)\\ &+ B_0(\rho_2)[-\rho_1A_1(\rho_1) + \alpha^2A_2(\rho_1)]\\ &+ A_0(\rho_1)[\rho_2B_1(\rho_2) - \beta^2B_2(\rho_2)]\}\end{aligned} \quad (A.11)$$

$$\langle A_{FH}| -\tfrac{1}{2}\nabla^2 |A_{FH}\rangle = \tfrac{1}{2}\zeta^2. \quad (A.12)$$

(7)

$$\begin{aligned}\langle A_{GZ}| -\tfrac{1}{2}\nabla^2 |B_{GZ}\rangle = -\pi C^2R\{&[(2/3)\beta^2 - \alpha^2]A_0(\rho_1)\\ &- \rho_1A_1(\rho_1) + \alpha^2A_2(\rho_1)\}\end{aligned} \quad (A.13)$$

$$\langle A_{FH}| -\tfrac{1}{2}\nabla^2 |B_{FH}\rangle = \tfrac{1}{2}\zeta^2(1 + \rho - \rho^2/3)e^{-\rho}. \quad (A.14)$$

B. Orbital Partitoning of the FH Molecular Energy

In view of Eqs. (37) and (45), the molecular potential and kinetic energies for the FH trial function are given by

$$V(\mathrm{FH}) = V^{\mathrm{A}}(\mathrm{FH}) + V^{\mathrm{QC}}(\mathrm{FH}) + V^{\mathrm{I}}(\mathrm{FH}) \quad (A.15)$$

$$T(\mathrm{FH}) = T^{\mathrm{A}}(\mathrm{FH}) + T^{\mathrm{I}}(\mathrm{FH}). \quad (A.16)$$

According to Eqs. (38)–(40) and (A.6)–(A.10), the three potential energy contributions to (A.15) are explicitly given by

$$\begin{aligned} V^{A}(\mathrm{FH}) &= \langle A_{\mathrm{FH}}| -r_{A}^{-1} |A_{\mathrm{FH}}\rangle \\ &= -\zeta = V_{\mathrm{H}}(\zeta) \end{aligned} \tag{A.17}$$

$$\begin{aligned} V^{\mathrm{QC}}(\mathrm{FH}) &= \langle A_{\mathrm{FH}}| -r_{B}^{-1} |A_{\mathrm{FH}}\rangle + R^{-1} \\ &= V_{\mathrm{H}}(\zeta) v^{\mathrm{QC}}(\rho) \end{aligned} \tag{A.18}$$

$$v^{\mathrm{QC}}(\rho) = -e^{-2\rho}(1 + \rho^{-1}) \tag{A.19}$$

$$\begin{aligned} V^{\mathrm{I}}(\mathrm{FH}) &= (1 + S)^{-1}\{2\langle A_{\mathrm{FH}}| -r_{A}^{-1} |B_{\mathrm{FH}}\rangle \\ &\quad - S[\langle A_{\mathrm{FH}}| -r_{A}^{-1} |A_{\mathrm{FH}}\rangle + \langle A_{\mathrm{FH}}| -r_{B}^{-1} |A_{\mathrm{FH}}\rangle]\} \\ &= V_{\mathrm{H}}(\zeta) v^{\mathrm{I}}(\rho)/(1 + S) \end{aligned} \tag{A.20}$$

$$v^{\mathrm{I}}(\rho) = 2e^{-\rho}(1 + \rho) - S(\rho)[1 + \rho^{-1} - e^{-2\rho}(1 + \rho^{-1})]. \tag{A.21}$$

Thus, Eq. (A.15) may be written as

$$V(\mathrm{FH}) = V_{\mathrm{H}}(\zeta) v(\rho) \tag{A.22}$$

with

$$v(\rho) = 1 + v^{\mathrm{QC}}(\rho) + [1 + S(\rho)]^{-1} v^{\mathrm{I}}(\rho). \tag{A.23}$$

Likewise, in accordance with Eqs. (46), (47), (A.12), and (A.14) we have for the kinetic energy

$$\begin{aligned} T^{A}(\mathrm{FH}) &= \langle A_{\mathrm{FH}}| -\tfrac{1}{2}\nabla^{2} |A_{\mathrm{FH}}\rangle \\ &= \tfrac{1}{2}\zeta^{2} = T_{\mathrm{H}}(\zeta) \end{aligned} \tag{A.24}$$

$$\begin{aligned} T^{\mathrm{I}}(\mathrm{FH}) &= (1 + S)^{-1}\{\langle A_{\mathrm{FH}}| -\tfrac{1}{2}\nabla^{2} |B_{\mathrm{FH}}\rangle - S\langle A_{\mathrm{FH}}| -\tfrac{1}{2}\nabla^{2} |A_{\mathrm{FH}}\rangle\} \\ &= T_{\mathrm{H}}(\zeta) t^{\mathrm{I}}(\rho)/(1 + S) \end{aligned} \tag{A.25}$$

$$t^{\mathrm{I}}(\rho) = -(2/3)\rho^{2} e^{-\rho}. \tag{A.26}$$

Thus, Eq. (A.16) may be written as

$$T(\mathrm{FH}) = T_{\mathrm{H}}(\zeta) t(\rho) \tag{A.27}$$

$$t(\rho) = 1 + [1 + S(\rho)]^{-1} t^{\mathrm{I}}(\rho). \tag{A.28}$$

Appendix B

Application of the variation principle $(\partial E/\partial \alpha) = 0$, to Eqs. (A.22) and (A.27) in the form

$$T = \tfrac{1}{2}\alpha^{-2}t(\rho) \tag{B.1}$$

$$V = -\alpha^{-1}v(\rho), \tag{B.2}$$

where

$$\rho = R/\alpha, \tag{B.3}$$

yields the equation

$$\rho = Rf(\rho) \tag{B.4}$$

$$f(\rho) = [v(\rho) + \rho v'(\rho)]/[t(\rho) + \tfrac{1}{2}\rho t'(\rho)]. \tag{B.5}$$

TABLE B.I

Optimal $\alpha(R)$ for the FH Binding and Antibinding States

R	Binding	Antibinding	R	Binding	Antibinding
0	0.5	2.5	4.1	0.97628	0.98397
0.1	0.50507	2.38172	4.3	0.98295	0.98353
0.3	0.53010	2.15486	4.5	0.98845	0.98356
0.5	0.56215	1.94514	4.7	0.99293	0.98394
0.7	0.59687	1.75634	4.9	0.99649	0.98456
0.9	0.63248	1.59191	5.1	0.99927	0.98535
1.1	0.66777	1.45376	5.3	1.00138	0.98624
1.3	0.70195	1.34157	5.5	1.00293	0.98719
1.5	0.73452	1.25295	5.7	1.00400	0.98816
1.7	0.76519	1.18432	5.9	1.00470	0.98913
1.9	0.79379	1.13185	6.0	1.00494	0.98960
2.1	0.82027	1.09204	7.0	1.00474	0.99377
2.3	0.84460	1.06201	8.0	1.00306	0.99658
2.5	0.86680	1.03946	9.0	1.00169	0.99823
2.7	0.88692	1.02265	10.0	1.00085	0.99913
2.9	0.90502	1.01022	11.0	1.00041	0.99959
3.1	0.92118	1.00114	12.0	1.00019	0.99981
3.3	0.93549	0.99462	13.0	1.00009	0.99991
3.5	0.94804	0.99006	14.0	1.00004	0.99996
3.7	0.95895	0.98699	15.0	1.00002	0.99998
3.9	0.96832	0.98505	16.0	1.00001	0.99999
			17.0	1.00000	1.00000

Equation (B.4) in conjunction with Eq. (B.3) determines the optimal value of $\alpha(R)$. A convenient method of solution consists of first finding the corresponding value of $\rho(R)$ by successive iterations based on the equation

$$\rho^{(n+1)} = Rf[\rho^{(n)}], \qquad \rho^{(0)} = 1. \tag{B.6}$$

When $\rho(R)$ has been found then $\alpha(R)$ is given by

$$\alpha(R) = \{f[\rho(R)]\}^{-1}. \tag{B.7}$$

The optimal $\alpha(R)$ values for the antibinding state can be found by a completely analogous procedure except that $t_a(\rho)$ and $v_a(\rho)$ [see Eqs. (97)–(99)] replace $t(\rho)$ and $v(\rho)$ in Eqs. (B.1) and (B.2), respectively. Table B.I reports $\alpha(R)$ values over a wide range of internuclear distances for both the binding and antibinding states.

ACKNOWLEDGMENTS

Part of this work was done under a National Science Foundation Postdoctoral Fellowship (1963–1965) held by M. J. F. first at the Johns Hopkins University and then at Iowa State University. The support and hospitality of both institutions and the support by the NSF is gratefully acknowledged. M.J.F. also expresses gratitude for support through a Tufts Faculty Research Fellowship (1966) and the Tufts Faculty Research Fund. Finally, the authors gratefully acknowledge support by the Petroleum Research Fund of the American Chemical Society.

REFERENCES

EDMISTON, C. and RUEDENBERG, K. (1964). *J. Phys. Chem.* **68**, 1628.
FINKELSTEIN, B. N. and HOROWITZ, G. E. (1928). *Z. Physik*, **48**, 118.
FOCK, V. (1930). *Z. Physik*. **63**, 855.
GUILLEMIN, V. and ZENER, C. (1929). *Proc. Natl. Acad. Sci. U.S.* **15**, 314.
KIM, S., CHANG, T. Y., and HIRSCHFELDER, J. O. (1965). *J. Chem. Phys.* **43**, 1092.
LAYTON, E. M., Jr., and RUEDENBERG, K. (1964). *J. Phys. Chem.* **68**, 1654.
LOWDIN, P. O. (1959). *Mol. Spectry.* **3**, 46.
MULLIKEN, R. S. (1949). *J. Chim. Phys.* **46**, 497.
POPKIE, H. E. and MOFFATT, L. B. (1968). *Intern. J. Quantum Chem.* **2**, *565*.
RUE, R. R. and RUEDENBERG, K. (1964). *J. Phys. Chem.* **68**, 1676
RUEDENBERG, K. (1961). *J. Chem. Phys.* **34**, 1892.
RUEDENBERG, K. (1962). *Rev. Mod. Phys.* **34**, 326.
SLATER, J. C. (1933). *J. Chem. Phys.* **1**, 687.
WASSERMAN, A. L. and RUEDENBERG, K. (To be published).

Adiabatic Approximation and Its Accuracy

WŁODZIMIERZ KOŁOS

Department of Theoretical Chemistry
University of Warsaw
Warsaw, Poland

I. Introduction

The adiabatic approximation, its accuracy, as well as its shortcomings, can be studied both analytically and numerically. An analytical study usually results in some general conclusions which, however, depending on the problem, can be either completely satisfactory or of little value. Development of the theory, qualitative explanations or predictions of physical phenomena, and estimations of orders of magnitude of various effects represent obviously the first crucial step in the theoretical approach to the many-particle systems. However, only the second step, which consists in a quantitative comparison of the theory with experiment, if successful, can result in final conclusions with regard to the theory employed, and with regard to our quantitative understanding of the phenomena under consideration. It is well known that the second step in the theory of many-particle systems requires very complex numerical computations and therefore significant progress in this direction could be achieved only when the high-speed computers became available. This is why during the last decade considerable activity has been developed in the study of some basic approximations appearing in various theories of molecular structure. This includes the adiabatic approximation and other problems arising from the finite mass of the nuclei.

It is natural that in these efforts, explicitly or implicitly directed towards a better understanding of the coupling between electronic and nuclear motion, the objects under consideration are usually the simplest possible molecular systems for which relatively accurate numerical computations can be carried out. This obviously applies, first of all, to the one- and two-electron molecules.

In the present article the adiabatic theory for nondegenerate electronic states of diatomic molecules is reviewed and its possible refinements are discussed. Recent numerical results obtained for one- and two-electron molecules are used to discuss the accuracy of the adiabatic approximation by comparing the adiabatic results with the nonadiabatic or experimental ones, and also with those which result in the Born–Oppenheimer (clamped nuclei) approximation.

II. Separation of Electronic and Nuclear Motion

A. Separation of the Center of Mass Motion

In atomic units the nonrelativistic Hamiltonian for an n-electron diatomic molecule in a laboratory-fixed reference system is

$$H = -\frac{1}{2M_a}\Delta_a - \frac{1}{2M_b}\Delta_b - \frac{1}{2}\sum_{i=1}^{n}\Delta_i + V, \tag{1}$$

where the subscripts a and b denote the two nuclei, respectively, and the index i labels the electrons.

If there are no external fields, the potential energy V is a function of the interparticle distances only, and one can easily separate off the translational motion of the center of mass of the system. The choice of the internal coordinates is, however, not unique, and various coordinates have been proposed and used by various authors. One possible set can be defined (Kołos and Wolniewicz, 1963) as

$$\mathbf{R} = \mathbf{R}_a - \mathbf{R}_b, \qquad \mathbf{r}_i = \xi_i - \tfrac{1}{2}(\mathbf{R}_a + \mathbf{R}_b) \tag{2}$$

and another (see, for example, Dalgarno and McCarroll, 1956) as

$$\mathbf{R} = \mathbf{R}_a - \mathbf{R}_b, \qquad \mathbf{r}_i = \xi_i - (M_a\mathbf{R}_a + M_b\mathbf{R}_b)/(M_a + M_b), \tag{3}$$

where $\mathbf{R}_a$, $\mathbf{R}_b$ denote the radius vectors and M_a, M_b the masses of the two nuclei, respectively, and ξ_i denotes the radius vector of the ith electron in the laboratory reference system.

If Eqs. (2) are employed, the electronic coordinates $\mathbf{r}_i$ are measured from the geometrical center of the molecule. In the case of Eqs. (3) they are referred to the mass center of the two nuclei.

Other coordinate systems can also be introduced and they may be useful for some particular purposes. Thus, for example, Pack (1966) employed a separated atom coordinate system in which the positions of n_a electrons are referred to the nucleus a, and those of $n_b = n - n_a$ electrons to the nucleus b. This is a natural coordinate system for treatment of the long-range interaction in the adiabatic approximation. Still other coordinates have been discussed by Jepsen and Hirschfelder (1960).

A straightforward transformation of the kinetic energy operator to the center of mass coordinates (X, Y, Z) and those defined by Eqs. (2) results in

$$T = -\frac{1}{2M}\Delta_{XYZ} - \frac{1}{2\mu}\Delta_R - \frac{1}{2}\sum_{i=1}^{n}\Delta_{r_i} - \frac{1}{8\mu}\left(\sum_{i=1}^{n}\nabla_{r_i}\right)^2 - \frac{1}{2\mu_a}\nabla_R\sum_{i=1}^{n}\nabla_{r_i}, \quad (4)$$

where

$$M = M_a + M_b + n, \qquad \mu^{-1} = M_a^{-1} + M_b^{-1}, \qquad \mu_a^{-1} = -M_a^{-1} + M_b^{-1}. \quad (5)$$

The cross-terms of the form $\nabla_i\nabla_j$ represent the so-called mass polarization. They also appear in many-electron atoms as a result of the separation of the center of mass motion (see, for example, Bethe and Salpeter, 1957). In the same coordinates the potential energy reads

$$V = \frac{Z_a Z_b}{R} - \sum_{i=1}^{n}\frac{Z_a}{|\mathbf{r}_i - \frac{1}{2}\mathbf{R}|} - \sum_{i=1}^{n}\frac{Z_b}{|\mathbf{r}_i + \frac{1}{2}\mathbf{R}|} + \sum_{i>j=1}^{n}\frac{1}{|\mathbf{r}_i - \mathbf{r}_j|}, \quad (6)$$

where Z_a and Z_b denote the nuclear charges of atoms a and b, respectively.

If one uses the coordinates (3) rather than those defined by Eqs. (2) one gets the kinetic energy

$$T = -\frac{1}{2M}\Delta_{XYZ} - \frac{1}{2\mu}\Delta_R - \frac{1}{2}\sum_{i=1}^{n}\Delta_{r_i} - \frac{1}{2(M_a + M_b)}\left(\sum_{i=1}^{n}\nabla_{r_i}\right)^2. \quad (7)$$

There is no mass-polarization term of the type $\nabla_R\nabla_{r_i}$ in (7) and Eqs. (3) are seen to give, in principle, a simpler expression for the kinetic energy. However, in this case the coordinates $\mathbf{r}_i$ depend on the nuclear masses, which makes the calculation of the potential energy prohibitively complicated. Set (3) has been used (e.g., by Dalgarno and McCarroll, 1956) to obtain some general results; however, in practical applications the formulas have been employed only to the homonuclear molecules for which the coordinates (2) and (3) become identical.

B. Separation of Rotations

In the center of mass system we shall use the Hamiltonian resulting from Eqs. (4) and (6):

$$H = H_0 + H' \tag{8}$$

$$H_0 = -\tfrac{1}{2}\sum_{i=1}^{n}\Delta_{r_i} + V \tag{9}$$

$$H' = -\frac{1}{2\mu}\Delta_R - \frac{1}{8\mu}\left(\sum_{i=1}^{n}\nabla_{r_i}\right)^2 - \frac{1}{2\mu_a}\nabla_R\sum_{i=1}^{n}\nabla_{r_i} \tag{10}$$

Two coordinates describing the overall rotation of the molecule can easily be removed from the complete Schrödinger equation (Hirschfelder and Wigner, 1935). In the present article this will be performed by transforming the Hamiltonian to the angular momentum representation in which the operators $\mathbf{K}^2$, $K_{Z'}$, and $(R^{-1})\mathbf{RK}$ are diagonal (Kołos and Wolniewicz, 1963). The operator $\mathbf{K}^2$ denotes the square of the total angular momentum of the molecule in the space-fixed reference system. Since the theory will be applied only to the one- and two-electron molecules, one may neglect the spin contribution to the total angular momentum. The term $K_{Z'}$ denotes the component of $\mathbf{K}$ in the direction of the space-fixed axis Z', and $(R^{-1})\mathbf{RK}$ the component of $\mathbf{K}$ in the direction of the molecular axis which will be called the Z direction. The latter operator can easily be shown to be equal to the Z component of the electronic angular momentum L_Z. The quantum numbers corresponding to the above operators will be denoted by K, M_K, and Λ, respectively. Since L_Z does not commute with H', the complete Hamiltonian (8) is not diagonal in the representation in which the above three operators have the diagonal form.

Thus, for given values of K and M_K, the spinless eigenfunctions of H can be represented (Wigner, 1959) in the form

$$\Psi = \sum_{\Lambda=-K}^{K}\Omega^{K}_{M_K,\Lambda}\,u_{\Lambda}{}^{K}, \tag{11}$$

where $\Omega^{K}_{M_K,\Lambda}$ denotes the eigenfunctions of $\mathbf{K}^2$, $K_{Z'}$, and L_Z which, due to the axial symmetry of the problem, are identical with wave functions of a symmetric top. The $u_\Lambda{}^K$ functions depend only on the relative positions of the particles. Using (11) it is convenient to introduce a coordinate system rotating with the molecule, following, for example, the procedure of Valatin (1947). By transforming the Hamiltonian to the rotating coordinate system and integrating over the angles, one gets (Kołos and Wolniewicz, 1963) the following nonvanishing matrix elements of the Hamiltonian:

$$\begin{aligned}
\langle\Lambda|\,H\,|\Lambda\rangle &= -\tfrac{1}{2}\sum_j \langle\Lambda|\,\Delta_{r_j}\,|\Lambda\rangle + V + \frac{1}{8\mu}\langle\Lambda|\,P^2\,|\Lambda\rangle \\
&\quad - \frac{1}{2\mu}\biggl[\frac{\partial^2}{\partial R^2} + \frac{2}{R}\frac{\partial}{\partial R} \\
&\qquad\qquad - \frac{K(K+1)-\Lambda(\Lambda+1)}{R^2} - \frac{1}{R^2}\langle\Lambda|\,L^+L^-\,|\Lambda\rangle\biggr] \\
&\quad - \frac{i}{2\mu_a}\biggl[P_z\frac{\partial}{\partial R} + \frac{1}{2R}\langle\Lambda|\,P^+L^- - P^-L^+\,|\Lambda\rangle\biggr]
\end{aligned} \tag{12}$$

$$\begin{aligned}
\langle\Lambda+1|\,H\,|\Lambda\rangle &= [(K+\Lambda+1)(K-\Lambda)]^{1/2} \\
&\quad \times \biggl[\frac{1}{2\mu R^2}\langle\Lambda+1|\,L^+\,|\Lambda\rangle - \frac{1}{4\mu_a R}\langle\Lambda+1|\,P^+\,|\Lambda\rangle\biggr]
\end{aligned}$$

$$\begin{aligned}
\langle\Lambda-1|\,H\,|\Lambda\rangle &= [(K+\Lambda)(K-\Lambda+1)]^{1/2} \\
&\quad \times \biggl[\frac{1}{2\mu R^2}\langle\Lambda-1|\,L^-\,|\Lambda\rangle + \frac{1}{4\mu_a R}\langle\Lambda-1|\,P^-\,|\Lambda\rangle\biggr],
\end{aligned}$$

where

$$L^{\pm} = L_x \pm iL_y, \qquad P^{\pm} = P_x \pm iP_y$$

and L_x, L_y and P_x, P_y are the components of the electronic angular momentum and of the impulse operator, respectively, in the rotating reference system. Hence, for a given value of K, the exact Schrödinger equation for a diatomic molecule is represented by a set of $2K+1$ equations for the $2K+1$ components u_Λ of the wave function:

$$\begin{gathered}
\langle\Lambda|\,H\,|\Lambda-1\rangle u_{\Lambda-1} + [\langle\Lambda|\,H\,|\Lambda\rangle - E]u_\Lambda + \langle\Lambda|\,H\,|\Lambda+1\rangle u_{\Lambda+1} = 0 \\
\Lambda = -K, -K+1, \ldots, K,
\end{gathered} \tag{13}$$

where, for simplicity, the superscript K in $u_\Lambda{}^K$ has been omitted.

The above equations show that only for the nonrotational Σ states ($K = 0$) does one get a Schrödinger-type equation for the wave function u_Λ (u_0 in this case) which depends on the relative coordinates and describes the internal motion of the particles in the molecule. If $K \neq 0$, i.e., for $\Lambda \neq 0$, or for rotationally excited Σ states, a coupling of the states with different Λ values occurs, as represented by Eqs. (13). It is also seen that the lowest-order correction will be due to the interaction of states whose Λ values differ by one unit. The coupling is responsible for the well-known heterogeneous perturbations in molecular energy levels (Mulliken, 1937). On the other hand, since the complete Hamiltonian is diagonal in K, no interaction of states with different K values is possible, and a rigorous selection rule $\Delta K = 0$ holds for perturbations in the molecular spectra under consideration.

C. Separation of Vibrations. The Adiabatic Approximation

To introduce the adiabatic approximation (Born, 1951; Born and Huang, 1956) let us consider again the complete Hamiltonian (8). Suppose that the electronic Schrödinger equation has been solved for all states

$$H_0 \psi_n(\mathbf{r}; R) = U_n(R) \psi_n(\mathbf{r}; R), \tag{14}$$

where $\mathbf{r}$ represents the coordinates of all electrons in the molecule, and n the proper set of electronic quantum numbers. The eigenfunctions ψ_n and eigenvalues U_n depend on the parameter R, defined in (2) as the internuclear distance. For all values of R the eigenfunctions are assumed to be normalized, and are chosen to be real. Since they form a complete set in the space of $\mathbf{r}$ one may assume (Born, 1951) the solution of the complete Schrödinger equation

$$H\Psi = E\Psi \tag{15}$$

in the form of the expansion

$$\Psi = \sum_n \psi_n(\mathbf{r}; R)\chi_n(\mathbf{R}), \tag{16}$$

where the sum denotes summation over the discrete spectrum and integration over the continuum. For a nonrotational Σ state χ_n can be expressed as $\Omega_{00}^0 f_n(R)$ and $\sum_n \psi_n f_n$ is identical with the $u_0{}^0$ function in the expansion (11). For a $\Lambda \neq 0$ state the angular function Ω contains a $(2\pi)^{-1/2} \exp(i\Lambda\phi)$ factor, where ϕ describes a simultaneous rotation of all electrons around the Z axis. This factor is usually included in the electronic function ψ_n.

Substituting the expansion (16) into Eq. (15), multiplying from the left by ψ_m, and integrating over the electronic coordinates one gets the following set of equations for the functions $\chi_n(\mathbf{R})$:

$$\left[-\frac{1}{2\mu}\Delta_R + U_n(R) + H'_{nn} - E\right]\chi_n(\mathbf{R}) = -\sum_{m\neq n}(H'_{nm} - \mathbf{B}_{nm}\nabla_R)\chi_m(\mathbf{R}), \quad (17)$$

where

$$H'_{nm}(R) = \int \psi_n H' \psi_m \, d\mathbf{r} \quad (18)$$

$$\mathbf{B}_{nm}(R) = -\int \psi_n\left(\frac{1}{\mu}\nabla_R + \frac{1}{2\mu_a}\sum_i \nabla_{r_i}\right)\psi_m \, d\mathbf{r}. \quad (19)$$

Since $\mathbf{B}_{nn} = 0$, one can define the operator

$$C_{nm}(R) = H'_{nm} + \mathbf{B}_{nm}\nabla_R \quad (20)$$

and Eq. (17) can be rewritten in the form

$$\left[-\frac{1}{2\mu}\Delta_R + U_n(R) + C_{nn}(R) - E\right]\chi_n(\mathbf{R}) = -\sum_{m\neq n} C_{nm}(R)\chi_m(\mathbf{R}). \quad (21)$$

From the above derivation it is clear that Eqs. (21) represent a rigorous set of equations; however, they can be solved only if the complete set of the electronic wave functions ψ_n is available.

Following Born (1951) and Born and Huang (1956), the adiabatic approximation can now be introduced by neglecting the right-hand side of Eqs. (21), i.e., by neglecting the nondiagonal correction terms C_{nm}. This corresponds to using only one term in the expansion (16).

The resulting Schrödinger-type equation

$$\left[-\frac{1}{2\mu}\Delta_R + U_n'(R) - E\right]\chi_n(\mathbf{R}) = 0 \quad (22)$$

describes free rotations and vibrations of the molecule, the latter occurring under the influence of the adiabatic potential, defined as

$$U_n'(R) = U_n(R) + C_{nn}(R), \quad (23)$$

which, in addition to the usual clamped nuclei potential U_n, includes the diagonal correction term C_{nn}. Assuming

$$\chi(\mathbf{R}) = R^{-1} f(R)\, Y(\theta, \varphi) \quad (24)$$

one can immediately separate off the rotations. This yields the following equation for the vibrational wave function $f(R)$:

$$\left[-\frac{1}{2\mu}\frac{d^2}{dR^2}+U_n'(R)+\frac{K(K+1)}{2\mu R^2}-E_{nvK}\right]f_{nvK}(R)=0, \qquad (25)$$

where v and K denote the vibrational and rotational quantum numbers, respectively.

In the case of the $\Lambda \neq 0$ states, C_{nn} can be shown to contain the $-\Lambda^2/2\mu R^2$ term [see Eq. (35)], and this term is usually taken into account, in the calculations, even if the remaining part of C_{nn} is ignored. This gives an approximate vibrational equation in the form

$$\left[-\frac{1}{2\mu}\frac{d^2}{dR^2}+U_n(R)+\frac{K(K+1)-\Lambda^2}{2\mu R^3}-E_{nvK}\right]f_{nvK}(R)=0. \qquad (26)$$

Hence, the adiabatic wave function represented by the first term in the expansion (16) is

$$\Psi_{\mathrm{ad}}=\psi_n(\mathbf{r};R)R^{-1}f_{nvK}(R)Y_K{}^M(\theta,\varphi), \qquad (27)$$

with ψ_n and f_{nvK} determined by Eqs. (14) and (25), respectively, and $Y_K{}^M$ denoting the spherical harmonic.

Thus, the adiabatic approach represents a strict treatment of the problem based on the approximate form (27) of the wave function. The Born–Oppenheimer (1927), or clamped nuclei, approximation, on the other hand, is obtained if, in addition to using the wave function (27) the diagonal correction term C_{nn} is also neglected in (23), and the potential energy for nuclear motion is defined simply as the eigenvalue U_n of the electronic Hamiltonian in Eq. (14).

The electronic wave function $\psi_n(\mathbf{r};R)$ describes the motion of the light particles (electrons) for fixed positions (R) of the heavy particles (nuclei), i.e., for infinitely slow changes of R. Therefore, the adiabatic approximation is applicable only if the heavy particles are significantly heavier than the light ones.

If more than one term is taken in the expansion (16), and all the electronic wave functions ψ_n have the same value of Λ, the additional terms account for the homogeneous perturbations in molecular energy levels (Mulliken, 1937). Note, however, that irregularities which may be classified as the homogeneous perturbations (Mulliken, 1966) may also appear if in the adiabatic wavefunction (27) the single electronic function ψ_n can be represented as a superposition of configurations, each of which is suitable for representing approximately ψ_n in a different region of the internuclear separation. This case will be discussed in Section IV,B,2.

Let us consider now the expectation value of the complete Hamiltonian calculated with the adiabatic wave function (27) for the lowest energy state

$$\mathscr{E} = \int \Psi_{\mathrm{ad}} H \Psi_{\mathrm{ad}} \, d\mathbf{r} \, d\mathbf{R}. \tag{28}$$

If ψ_n and f_{nvK} in (27) are solutions of Eqs. (14) and (25), respectively, one can easily show (Wolniewicz, 1966) that

$$\mathscr{E} = E_{n00}, \tag{29}$$

where E_{n00} is the energy of the molecule for the $v = K = 0$ state calculated in the adiabatic approximation by solving Eq. (25). Hence the adiabatic energy represents an upper bound to the exact eigenvalue of the complete Hamiltonian. It can also be shown (Brattsev, 1965; Epstein, 1966) that in the Born–Oppenheimer approximation the accurate total energy represents a lower bound. However, the deviations of the lower bound from the exact energy is of a lower order than that of the upper bound. In addition a wave function not sufficiently flexible may yield even in the Born–Oppenheimer approximation an energy which is higher than the exact value. Therefore the lower bound, as given by this approximation, seems to be of little practical importance.

III. Limiting Values of the Adiabatic Corrections

The diagonal nuclear motion corrections, resulting from the Hamiltonian (10), can be expressed as

$$C_{nn} = D_{nn} + S_{nn} + [L(L+1) - 2\Lambda^2]/2\mu R^2, \tag{30}$$

where

$$D_{nn} = -(1/2\mu)\langle n|\,\Delta_R\,|n\rangle - [L(L+1) - 2\Lambda^2]/2\mu R^2 \tag{31}$$

$$S_{nn} = -(1/8\mu)\langle n|\sum_{i,j} \nabla_{r_i}\nabla_{r_j}|n\rangle \tag{32}$$

and L denotes the quantum number corresponding to the orbital angular momentum of the united atom.

Leaving out the trivial term proportional to $K(K+1)$ the angular part of the first term in D_{nn} is [see, for example, Kołos and Wolniewicz 1963, Eq. (17)]

$$(1/2\mu R^2)[\langle n|\,L^+ L^-\,|n\rangle - \Lambda(\Lambda+1)], \tag{33}$$

where $L^{\pm} = L_x \pm iL_y$. The expression (33) is obviously equal to

$$(1/2\mu R^2)[\langle n|L^2|n\rangle - 2\Lambda^2] \tag{34}$$

or

$$(1/2\mu R^2)[\langle n|L_x{}^2 + L_y{}^2|n\rangle - \Lambda^2], \tag{35}$$

which at $R = 0$ cancels exactly the second term in D_{nn}, and D_{nn} is seen to be finite at $R = 0$. Since S_{nn} is also finite, the total correction C_{nn}, as given by Eq. (30), is finite at $R = 0$ only if $L(L + 1) = 2\Lambda^2$. Thus $C_{nn} = \infty$ if $L \neq 0$ for the Σ states or $L \neq 1$ for the Π states. The infinite value of the nuclear motion correction at $R = 0$, e.g., for a Σ_u state, has obviously no physical meaning and results from the failure of the perturbation treatment at this limiting value of the internuclear distance (Van Vleck, 1936). In the perturbation theory approach one assumes that the electronic charge cloud rotates with the nuclei, whereas for small values of R a decoupling of the two rotational motions occurs. Therefore for $R \to 0$ the perturbation theory is not applicable. For intermediate values of R ($R \approx R_e$), the decoupling has usually only started, and the perturbation theory approach is still justified. However, if the numerator in the last term in C_{nn} does not vanish, it gives also in this region an abnormally large contribution to C_{nn}. Therefore one may expect that for those states for which $L(L + 1) - 2\Lambda^2 \neq 0$, the R dependence of C_{nn}, at least for intermediate and small values of R, is determined mainly by the last term in C_{nn}. Hence, in this case, it seems to be more appropriate to use the vibrational equation

$$\left\{-\frac{1}{2\mu}\frac{d^2}{dR^2} + U_n(R) + \frac{1}{2\mu R^2}[L(L + 1) - 2\Lambda^2 + K(K + 1)] - E_{nvK}\right\}f_{nvK} = 0 \tag{36}$$

rather than to neglect C_{nn} completely.

For large values of the internuclear distance the coupling between electronic and nuclear motion requires also some comments. The correction $C_{nn} = H'_{nn}$ to the potential (23) is obtained by using in Eq. (18) the electronic wave function resulting from Eq. (14). Thus the potential is calculated in the first order of the perturbation theory and is accurate only up to the order of m/M at all values of R. Therefore, even for the hydrogen molecule, or for the hydrogen molecular ion, using a wave function which in the Born–Oppenheimer approximation describes properly the dissociation of the system, one gets at $R = \infty$ the energy of the atoms accurate only up to the order of m/M. This has an undesirable consequence. The adiabatic energy for the lowest vibrational state E_0 represents an upper bound;

however, since the energy of the dissociation products, $E(R = \infty)$, in the adiabatic approximation also represents an upper bound, the dissociation energy, $D_0 = E(R = \infty) - E_0$, does not represent any bound at all. In some cases the above deficiency can be removed (Hunter 1966, Hunter *et al.*, 1966, 1967) by introducing a scaling parameter γ into the wave function (27):

$$\Psi = \psi(\gamma\mathbf{r}; \gamma R)R^{-1}f_{nvK}(R)Y_K{}^M(\theta, \varphi). \tag{37}$$

Using (Kołos and Wolniewicz, 1969b) for γ the value

$$\gamma_{\min} = 2\mu/(2\mu + M) \tag{38}$$

one gets for the symmetric hydrogen molecules (H_2, D_2, T_2) the exact energy of the dissociation products, and in consequence the calculated dissociation energy represents a lower bound. For the nonsymmetric molecules, such as HD, one can also get a lower bound for D_0 by simply using the sum of the exact atomic energies as $E(R = \infty)$. It should also be pointed out that the scaling procedure goes beyond the adiabatic approximation as defined in Section II,C.

The error in the adiabatic energy at $R = \infty$ is usually very small. However, it becomes considerably larger (Kołos and Wolniewicz, 1969b) in some excited electronic states of the nonsymmetric homonuclear molecules such as HD if they dissociate into differently excited atoms. If the molecule dissociates into two atoms with energies E_1 and E_2, where $E_1 < E_2$, then there are two possible states at $R = \infty$ corresponding to $E_1(\mathrm{H}) + E_2(\mathrm{D})$ and $E_1(\mathrm{D}) + E_2(\mathrm{H})$, the latter being the lower one. However, the nuclear motion correction resulting from the adiabatic theory is proportional to the inverse of the reduced mass of the nuclei at all values of R and does not distinguish between the two possibilities at $R = \infty$. Hence, at $R = \infty$ the adiabatic energy represents an average value for the two possible combinations of atomic states. It still represents an upper bound for the lower state but the error may be considerable.

The asymptotic behavior of the diagonal nuclear motion corrections has also been studied by several authors. Dalgarno and McCarroll (1956, 1957) concluded that if at least one of the separated atoms has a nonzero angular momentum, the diagonal correction for nuclear motion goes like R^{-2} for large R:

$$\Delta E(R) = C_{nn}(R) - C_{nn}(\infty) = (\hbar^2/2\mu)[L(L+1) + L'(L'+1) - \Lambda^2]R^{-2}, \tag{39}$$

where L and L' are the total azimuthal quantum numbers for the respective separated atoms. The above correction clearly results from the angular part of the first term in D_{nn}, as given by Eq. (35). Since the dominant term in the long-range clamped nuclei interaction energy is usually proportional to a higher than second power of R^{-1}, for sufficiently large values of the internuclear distance the diagonal nuclear motion correction seems to become larger than the clamped nuclei interaction energy.

This point has been recently taken up by Laue (1967). He noticed that for large R the adiabatic approach should be reformulated. The usual procedure, which has also been followed in the present article, consists in introducing a rotating coordinate system. This raises no objections as long as the interaction energy is relatively large. However, if the interaction between the atoms becomes weak, their electronic angular momenta retain their orientations with respect to a space fixed coordinate system rather than with respect to the molecular axis. Therefore in this case a nonrotating coordinate system is more appropriate, and this according to Laue (1967) accounts for the failure of the usual adiabatic approach, if the latter is applied to rotating states and very large values of the internuclear distance.

It should also be noted that in the conventional calculation of the long-range interaction energy the van der Waals coefficients are calculated in the Born–Oppenheimer approximation. This corresponds to dissociation of the molecule into two atoms with infinitely heavy nuclei. The appropriate adiabatic correction is due to the $-(8\mu)^{-1}(\Sigma\nabla_{r_i})^2$ term in the Hamiltonian (10) and if taken into account it results in different van der Waals coefficients for different isotopes (Dalgarno and McCarroll, 1956; Pack, 1966).

IV. Refinements of the Adiabatic Approximation

A. Nonadiabatic Approach

There are at least two different ways of calculating the accurate nonadiabatic energies for molecules. The first is a straightforward variational calculation in which the complete wave function is expanded in terms of some basis functions which form a complete set in the space of $\mathbf{r}$ and $\mathbf{R}$. By using the complete Hamiltonian (8) and a sufficiently large number of terms one can get, in principle, the results of any desired accuracy, although in practical applications the convergence may be slow. Alternatively, the approach can be based on the set of coupled differential equations (21). In this case one may expect a rapid convergence of the expansion (16); however, several accurate wave functions for excited electronic states are still needed to calculate the C_{nm} matrix elements. Both approaches have been employed to three-particle systems such as the H_2^+ ion, and the former also to the hydrogen molecule. The results will be discussed in Section V.

B. Perturbation Theory Approach

Possible improvements of the adiabatic approximation within the framework of the perturbation theory have been discussed by Van Vleck (1936) and by several other authors (Fisk and Kirtman, 1964; Herman and Asgharian, 1966; Pack, 1966; Karl and Poll, 1967). Let us consider the rigorous set of equations (21). The adiabatic energy levels, as obtained from Eq. (22), can be improved by calculating the nondiagonal matrix elements C_{nm} of the nuclear motion corrections appearing in the right-hand side of Eqs. (21). It is seen from Eq. (12) that the matrix elements C_{nm} are different from zero only if for the two states, labeled by n and m, $\Delta\Lambda = 0$ or $\Delta\Lambda = \pm 1$. Obviously, the selection rule $\Delta K = 0$ must hold in either case. Interaction between states of equal Λ, and between states differing by one unit in Λ, gives rise to the well-known homogeneous and heterogeneous perturbations in molecular spectra (Mulliken, 1937).

Both kinds of corrections can be calculated by using the second order perturbation theory. Let us start with the complete Hamiltonian (8) and assume H', as defined by (10), to be a small perturbation. The eigenfunctions $\psi_n(\mathbf{r}; R)$ of the H^0 Hamiltonian [cf. Eq. (14)] and the functions $\chi_n(\mathbf{R})$, defined by Eq. (22), are assumed to be known. Their products represent the adiabatic wavefunctions for vibronic states of the molecule. Explicitly [cf. Eq. (27)] the adiabatic wave function is

$$\Psi_{\mathrm{ad}} = \psi_n(\mathbf{r}; R)\chi_{nvKM}(\mathbf{R}). \tag{40}$$

If the function (40) is chosen to be the zero-order wave function, the corresponding expectation value of the complete Hamiltonian, which represents the energy accurate up to the first order, is identical with the adiabatic energy [cf. Eqs. (27)–(29)].

The first-order correction to the wave function can be expanded in terms of the adiabatic wave functions, and by the standard perturbation theory the second-order energy correction for the nv vibronic state is

$$E_{nv}^{(2)} = \sum_{mu \neq nv} H'_{nv,mu} H'_{mu,nv} / (E_{nv}^{(0)} - E_{mu}^{(0)}), \tag{41}$$

where

$$\begin{aligned} H'_{nv,mu} &= \int \psi_n \chi_{nv} H' \psi_m \chi_{mu} \, d\mathbf{r} \, d\mathbf{R} \\ &= \int \chi_{nv} C_{nm} \chi_{mu} \, d\mathbf{R} \end{aligned} \tag{42}$$

and C_{nm} is defined by Eq. (20). The indices K, M have been omitted since H' is diagonal in K and M.

Depending on the choice of the basis functions labeled by the indices m and u one can use Eq. (41) to account for the interaction between states of equal Λ, or between states for which $\Delta\Lambda = \pm 1$, or between both kinds of states.

Perturbation theory approach can also be employed to calculate the nonadiabatic corrections for other properties of molecules. Let Q denote an operator whose expectation value has already been calculated in the adiabatic approximation. The nonadiabatic correction to this expectation value resulting from the perturbation theory is

$$\Delta Q_{nv} = 2 \sum_{mu \neq nv} Q_{nv,\,mu} H'_{mu,\,nv} / (E^{(0)}_{nv} - E^{(0)}_{mu}), \tag{43}$$

where the meaning of symbols is obvious from Eq. (42). The diagonal terms are not included in the summation in (43). Hence ΔQ_{nv} is different from zero only if the operator Q has nonvanishing off diagonal matrix elements in the electronic quantum number n.

1. Interaction of States with Different Λ

Let us consider the interaction between two states differing by one unit in Λ. It follows from Eq. (13) that, for example, a rotational ($K \neq 0$) Σ state is mainly perturbed by states of the Π symmetry. Thus the first-order correction to the adiabatic wave function should be expanded in terms of a basis set which includes functions of both the Σ and the Π symmetry. If for a Σ level under consideration, defined by *nv*, and for the nearest Π level, defined by *mu* (and having the same rotational quantum number), the energy difference $E^{(0)}_{mu} - E^{(0)}_{nv}$ is not very large, one may expect this particular Π level to give an important contribution to the second-order energy correction and to be primarily responsible for the heterogeneous perturbation of the Σ level. Conversely the same *nv* Σ level may be expected to be primarily responsible for the heterogeneous perturbation of the *mu* Π level. However, in the case of the Π states, there always exist the $\Pi^{\pm}$ doublets, and only one component of the doublet interacts with the Σ state which can have either the Σ^{+} or the Σ^{-} symmetry. Therefore the interaction results in a splitting of the doublet which is well known as the Λ doubling.

It is difficult to estimate the magnitude of the above perturbations. Being essentially due to the nonadiabatic effects they should be of the order of μ^{-2}. However, they critically depend on the magnitude of the energy difference between the interacting states, and therefore they are of practical importance only if the two interacting states have nearly equal values of the energy. In particular, if $E_{mu}^{(0)} - E_{nv}^{(0)} = 0$, or has a small value, the perturbation theory for degenerate states must be used and the resulting energy correction is of the order of μ^{-1}. Equations (12) also show that the heterogeneous perturbation increases with increasing K. Thus for large values of K the heterogeneous perturbations may not be negligible, even if the differences of energies between the interacting states are not very small. The coupling of states with different Λ may also play an important role in some scattering problems (see, for example, Bates, 1962).

It may also be noted that the higher-than-second-order corrections may lead, in principle, to still different effects. It has been shown above that for a state with a given value of Λ the energy correction due to perturbation by the $\Lambda + 1$ and $\Lambda - 1$ states may be obtained in the second order of the perturbation theory. The $\Lambda + 1$ state, in turn, may be perturbed by the Λ and $\Lambda + 2$ states. Hence in the fourth order of the perturbation theory the Λ state may be perturbed by the $\Lambda + 2$ and $\Lambda - 2$ states, if this does not violate the $\Delta K = 0$ selection rule. However, the corrections, being essentially of the order of μ^{-4}, do not seem to be of any practical importance.

2. *Interaction of States with the Same* Λ

Let us now consider the $\Delta\Lambda = 0$ case. For the nonrotational Σ states Eq. (41) represents the complete energy shift due to the nonadiabatic effects. If the differences between the vibrational energies in the denominators in Eq. (41) are small in comparison with the difference between the electronic energies, and may be neglected, one gets

$$E_{nv}^{(0)} = \sum_{m \neq n} (E_n^{(0)} - E_m^{(0)})^{-1} \int \chi_{nv} C_{nm} C_{mn} \chi_{nv} \, d\mathbf{R}. \tag{44}$$

Van Vleck (1936) has shown that for estimation of orders of magnitude the above formula may still be simplified. The term C_{nm}, as defined by Eq. (20), is composed of two terms: the first one, H'_{nm}, contains the derivative of the electronic wave function ψ_n with respect to R, whereas the second one, involving B_{nm}, gives in Eq. (44) the derivative of χ_{nv} with respect to R. Since the latter may be expected to be much larger in absolute value than the former, one may neglect H'_{nm} in C_{nm}. Thus one gets

$$C_{nm}(R) = \mathbf{B}_{nm}(R) \, \nabla_R, \tag{45}$$

where, for a symmetric molecule,

$$\mathbf{B}_{nm}(R) = -\frac{1}{\mu} \int \psi_n \nabla_R \psi_m \, d\mathbf{r}. \tag{46}$$

For small amplitudes of vibration it is also justified to expand B_{nm} about the equilibrium position for the nth state, and to take only the first term of the expansion, i.e., the constant value for $R = R_e$. If, in addition, use is made of the Unsöld (1927) approximation, and an average value of the excitation energy $\bar{E}$ is assumed, one gets from Eq. (44)

$$E_{nv}^{(2)} = (4/\bar{E})T_n(R_e)T_{nv}, \tag{47}$$

where

$$T_n(R) = -\frac{1}{2\mu}\int \psi_n \Delta_R \psi_n \, d\mathbf{r} \tag{48}$$

$$T_{nv} = -\frac{1}{2\mu}\int \chi_{nv} \Delta_R \chi_{nv} \, d\mathbf{R} \tag{49}$$

and in Eq. (47) T_n is taken for $R = R_e$. The above approach has been employed by Poll and Karl (1966) to estimate the nonadiabatic corrections for the electronic ground state of H_2 and D_2.

The above approach is, however, not applicable if there are two nearby states of the same Λ, i.e., if for any nv state under consideration there is an mu state such that $E_{mu}^{(0)} - E_{nv}^{(0)}$ is small. In this case strong interaction between the two states may be expected resulting in strong homogeneous perturbations. However, Eqs. (41) and (42) show the energy correction to depend on the matrix element of C_{nm} between the functions χ_{nv}. Thus, if there is little overlap between χ_{nv} and χ_{mu} the energy correction due to the interaction of the two states will be small even if the energy denominator is small. This may happen, for example, if in a low approximation a crossing of two potential energy curves of the same symmetry occurs. If the two potential curves have minima at significantly different values of the internuclear distance, the overlap between the vibrational wave functions may be negligible, and in this case the mutual perturbation of the two states is very small. It should be pointed out, however, that the above perturbation appears only if the two minima are treated separately as belonging to two different potentials, which is justified if the corresponding interaction matrix element [H_{12} in Eq. (50) below] is small (Mulliken, 1966). If the total double-minimum potential resulting from avoided crossing of the potential energy curves is considered, the above interaction can be accounted for within the framework of the adiabatic theory and irregularly spaced vibrational levels would result from Eq. (25). In this case the nonadiabatic effects and homogeneous perturbations become important only for those vibrational states which are located close or above the potential maximum. In Section V,D this will be illustrated by numerical results for the E, F, ${}^1\Sigma_g^+$ state of the hydrogen molecule.

At this place a comment may be in order with regard to the noncrossing rule and its relation to the adiabatic approximation. It has been first shown by von Neumann and Wigner (1921) that for an infinitely slow change of the internuclear distance two electronic states of the same species cannot cross each other.

Let us consider (Teller, 1937) the Hamiltonian $H(R)$ which depends on some parameter R. Suppose we know all the eigenfunctions ψ_i of $H(R)$ except two. Let us take two wave functions φ_1 and φ_2 which are orthogonal to all the known eigenfunctions ψ_i. If this is the case, the two unknown eigenfunctions, which are assumed to be mutually orthogonal, must be linear combinations of φ_1 and φ_2, and the corresponding eigenvalues can be obtained by solving the standard secular equation. This results in

$$E_{1,2} = \frac{H_{11} + H_{22}}{2} \pm \left[\left(\frac{H_{11} - H_{22}}{2}\right)^2 + H_{12}\right]^{1/2}. \tag{50}$$

In general H_{11} and H_{22} are not equal and $H_{12} \neq 0$. Hence the energies E_1 and E_2 are different. If in a low approximation a crossing occurs, i.e., $H_{11} = H_{22}$, it disappears in a more refined treatment which gives $E_1 \neq E_2$. Degeneracy (crossing) would require $H_{11} = H_{22}$ and $H_{12} = 0$. By varying only one parameter, R, one may satisfy either $H_{11} = H_{22}$ or $H_{12} = 0$ but not both these conditions. Degeneracy may only occur if more than one parameter can be varied.

The above argument applies obviously to any two curves, H_{11} and H_{22}, which represent the dependence of the two energies on one parameter. Since there is no such Hamiltonian $H(R)$ whose eigenvalue is represented by the adiabatic potential energy curves as defined by Eq. (23), the above reasoning applies, strictly speaking, only to the Born–Oppenheimer potential curves and not to those calculated in the adiabatic approximation. However, if in a certain region of R two adiabatic potential curves approach each other the adiabatic approximation breaks down anyway and strong nonadiabatic effects may be expected.

V. Accuracy of the Adiabatic Approximation

The one- and two-electron molecules are the only real systems for which adiabatic calculations have been carried out. Results of these calculations may be exploited to get insight into the adiabatic approximation and its accuracy.

For the H_2^+ ion accurate nonadiabatic calculations have been performed, and by comparing these results with those obtained in the adiabatic approach one gets directly the magnitude of the nonadiabatic effects. For the H_2 molecule the nonadiabatic calculations are significantly more difficult and at present no very accurate results are available. However, in this case, accurate experimental data exist. Since the relativistic corrections, which are usually neglected, are known to be very small, one may get insight into the magnitude of the nonadiabatic effects by comparing the adiabatic results with the experimental ones.

The adiabatic results can also be discussed from a different point of view. Since most molecular computations are carried out in the Born–Oppenheimer approximation, it is important to know how accurately it describes the vibronic states of molecules, and how much different are the results obtained in the Born–Oppenheimer approximation from those resulting from the more consistent adiabatic theory.

The above problems will be discussed in the following sections of the present article.

A. The Diagonal Corrections for Nuclear Motion

The diagonal corrections for nuclear motion, H'_{nn}, are defined by Eq. (18), with H' given by Eq. (10). They have been calculated for two states of the H_2^+ ion: the lowest ${}^2\Sigma_g^+$ state (ground state) and the lowest ${}^2\Sigma_u^+$ state, both dissociating into H^+ and a ground state hydrogen atom. For the ground state the corrections were first obtained by Johnson (1941) and for both states by Dalgarno and McCarroll (1956) and Cohen *et al.* (1959). Recently more accurate calculations for the ground state have been carried out (Kołos, 1969). Using a somewhat different formalism Hunter *et al.* (1966) have calculated the corrections for several states of the system.

For the ground state of the hydrogen molecule an approximate calculation of the diagonal nuclear motion corrections has been made by Van Vleck (1936) for the equilibrium internuclear distance, and by Dalgarno and McCarroll (1956) who also calculated the corrections for the lowest ${}^3\Sigma_u^+$ state. More accurate and more extensive computations for the ground state and for several excited states of the molecule have also been carried out (Kołos and Wolniewicz, 1964a, 1966a, 1968b, 1969a).

The diagonal corrections for nuclear motion for several states of H_2^+ and H_2 are shown graphically in Fig. 1. Since they represent essentially the expectation value of a kinetic energy operator, they are always positive and raise the total energy of the molecule. However, for most of the bound states under consideration ($X\,{}^1\Sigma_g^+$, $a\,{}^3\Sigma_g^+$, ${}^2\Sigma_g^+$) their value at $R = R_e$ is

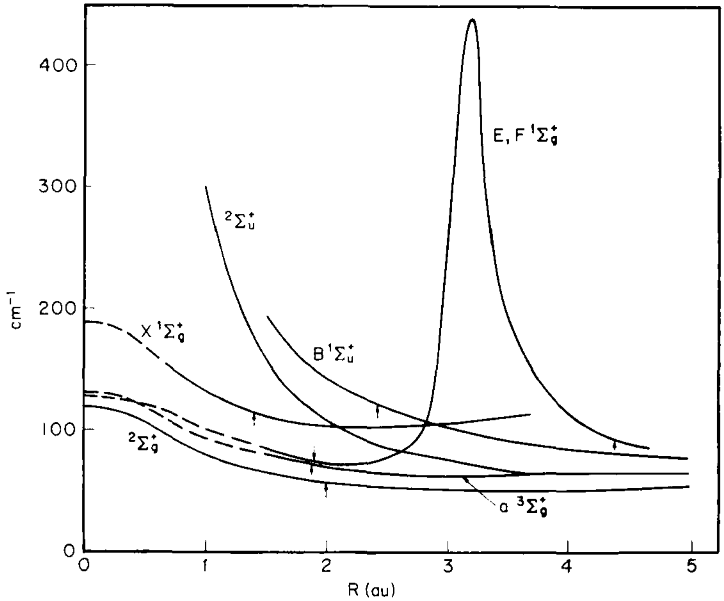

Fig. 1. Diagonal nuclear motion corrections (in cm^{-1}) for the $^2\Sigma_g^+$ and $^2\Sigma_u^+$ states of H_2^+ and for the $X\,^1\Sigma_g^+$, E, $F\,^1\Sigma_g^+$, $B\,^1\Sigma_u^+$, and $a\,^3\Sigma_g^+$ states of H_2. The arrows indicate the equilibrium internuclear distances.

smaller than for the separated atoms and therefore they increase the binding energy D_e. For the $B\,^1\Sigma_u^+$ state of H_2 and for the $^2\Sigma_u^+$ state of H_2^+ they tend to infinity for $R \rightarrow 0$. This is due to the fact that for both states the resulting united atom has a nonzero angular momentum. As discussed in Section III the last term in C_{nn}, defined by Eq. (30), becomes infinite at $R = 0$, which is due to the failure of the perturbation treatment at this limiting R value. At small R it gives the dominant, and rapidly varying with R, contribution to H'_{nn}. Therefore, if in such cases H'_{nn} is neglected, it may cause significant errors in the calculated vibrational energies.

In Fig. 2 we show again the H'_{nn} curves for the $^1\Sigma_u^+$ and $^2\Sigma_u^+$ states (solid lines) and also the curves obtained from the former by subtracting off the term which becomes infinite at $R = 0$, i.e., $[L(L+1) - 2\Lambda^2]/(2\mu R^2)$. The resulting curves (broken lines) are much more constant in the whole region of R values. It seems, therefore, that if for a particular state the diagonal nuclear motion corrections are not available, better results may be obtained if the singular term is added to the calculated potential energy curve. This is likely to give an almost constant value for the neglected

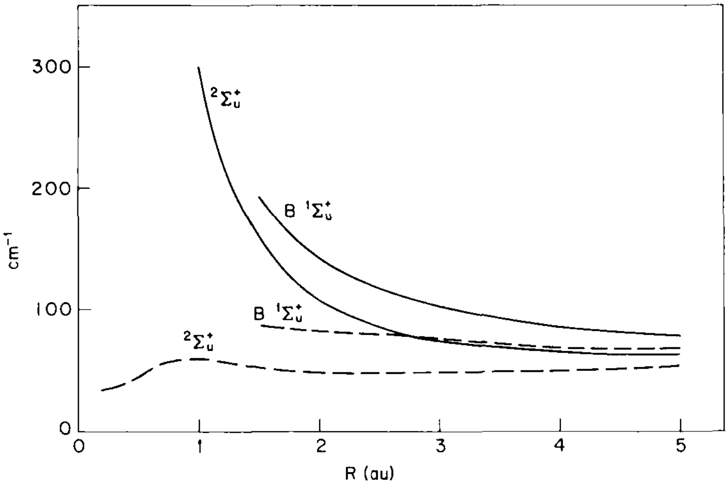

Fig. 2. Diagonal nuclear motion corrections (solid lines) for the $^2\Sigma_u^+$ state of H_2^+ and for the $B\,^1\Sigma_u^+$ state of H_2. The broken lines show that part of the corrections which remains finite at $R = 0$.

part of the corrections, i.e., for $D_{nn} + S_{nr}$ in Eq. (30). Hence the remaining error in the calculated vibrational quanta may be quite small.

The first excited $^1\Sigma_g^+$ state, i.e., the E, F state, will be discussed in more detail in Section V,D. The potential energy curve for this state has a double minimum, and at the potential maximum, which appears at $R = 3.12$ au, the electronic wave function changes drastically its character. This seems to be the reason for $-(1/2\mu)\langle n|\,\Delta_R\,|n\rangle$ having a very large value in this particular region.

B. Hydrogen Molecular Ion and Other Three-Particle Systems

The electronic Schrödinger equation for the H_2^+ ion is known to be separable (see, for example, Buckingham, 1962) in elliptic coordinates, and the resulting ordinary differential equations can readily be solved to any desired accuracy. The first extensive calculations have been carried out for several states of the molecule by Bates *et al.* (1953). For the lowest $^2\Sigma_g^+$ and $^2\Sigma_u^+$ states more accurate and more extensive calculations in the Born–Oppenheimer approximation have been performed by Wind (1965) and Peek (1965).

Using accurate values of the diagonal nuclear motion corrections, discussed in the preceding section, the vibrational equation (25) has been solved (Kołos, 1969) for several vibrational and rotational states, yielding accurate adiabatic energies.

As mentioned in Section IV,A, the nonadiabatic calculations can be carried out either in a straightforward variational approach or by solving the set of coupled differential equations (21). For a three-particle system, such as H_2^+ both approaches are feasible.

In the Ritz variational method, with an arbitrarily chosen basis set, the convergence is slow. However, the calculations can be easily extended to a large number of terms. For the H_2^+ ion the variational method has been employed by several authors (Kołos *et al.*, 1960; Diehl and Flügge, 1961; Fröman and Kinsey, 1961). The most accurate calculations have been carried out recently (Kołos 1969). For the lowest vibrational state the resulting energy obtained with a 57-term expansion was $E = -0.5971387$ au and seems to be accurate to seven significant figures. However, from the slow convergence it is quite clear that for more complex molecules the number of terms needed to achieve convergence would be prohibitively large.

Hunter *et al.* (1966, 1967) in their nonadiabatic calculation for the H_2^+ ion have solved the electronic Schrödinger equation for several states and employed the finite difference method to deal with the set of equations (21). In this approach the convergence of the energy was amazingly fast, and only three terms were needed to get the energy accurate for seven significant figures. It should be mentioned, however, that even for the hydrogen molecule it would be at present very difficult to calculate the C_{nm} functions, and therefore this approach has not been extended to systems composed of more than three particles. In Table I the nonadiabatic energies (Hunter and Pritchard, 1967) for a few lowest vibrational states of H_2^+ are compared with the corresponding adiabatic values (Kołos, 1969). In the last column their differences ΔE are shown in cm^{-1}. The nonadiabatic effects for H_2^+ are very small and are seen to be roughly a linear function of the

TABLE I

NONADIABATIC AND ADIABATIC ENERGIES FOR A FEW LOWEST VIBRATIONAL STATES OF H_2^+

v	E_{nonad} (au)	E_{ad} (au)	ΔE (cm^{-1})
0	−0.5971387	−0.5971382	−0.11
1	−0.5871548	−0.5871538	−0.22
2	−0.5777508	−0.5777492	−0.35
3	−0.5689070	−0.5689050	−0.44

TABLE II

NONADIABATIC AND ADIABATIC ENERGIES FOR SOME THREE-PARTICLE SYSTEMS

Molecule $M_aM_b/(M_a+M_b)m$		$p\mu p$ 4.4400	$p\mu d$ 5.9185	$d\mu d$ 8.8732	$d\mu t$ 10.6422	H_2^+ 918.06
$v=0$	E_{ad}	−0.488507	−0.508017	−0.529451	−0.537262	−0.5971382
	E_{nonad}	−0.49437	−0.51266	−0.53097	−0.53840	−0.5971387
	ΔE	−0.00586	−0.00464	−0.00152	−0.00114	−0.0000005
$v=1$	E_{ad}			−0.477714	−0.486021	−0.5871538
	E_{nonad}				−0.48773	−0.5871548
	ΔE				−0.00171	−0.0000010

vibrational excitation. The increased nonadiabatic effects for the higher vibrational levels are clearly due to their increased interaction with the excited ${}^2\Sigma_g^+$ states.

Similarly as for H_2^+, accurate adiabatic and nonadiabatic calculations are also feasible for other three-particle systems, such as the muonic molecules in which two singly charged nuclei (proton, p; deuteron, d; triton, t) are bound by a negative muon μ. One might even employ a nonadiabatic-type theory to the He-like systems (Kołos *et al.*, 1960; Frost *et al.*, 1964) for which the finer effects of the coupling between electronic and nuclear motion are usually neglected, and the electronic wave function is computed assuming the nucleus to be infinitely heavy. They represent, however, a completely different one-center case to which the theory presented above is not applicable.

The Born–Oppenheimer potential energy curve with diagonal corrections for nuclear motion, computed for the H_2^+ ion, can be directly employed, by changing only the mass ratio, to calculate the adiabatic energies for the muonic molecules. Some results obtained by this method (Kołos, 1969) are listed in Table II where they are compared with the nonadiabatic energies calculated recently by Carter (1968) using the Ritz variational method. For comparison the adiabatic (Kołos, 1969) and nonadiabatic (Hunter and Pritchard, 1967) results for the H_2^+ ion are also given. Convergence of the energy in the nonadiabatic approach becomes slower with decreasing ratio of m/μ, where μ denotes the reduced mass of the two nuclei and m is the mass of the muon. Inspection of Carter's (1968) results shows that they have converged to roughly four figures. Therefore, even the second significant figure in the nonadiabatic energy correction $\Delta E = E_{\text{nonad}} - E_{\text{ad}}$ is not quite certain. Nevertheless the correction is of the expected order of magnitude, i.e., of the order of $(m/\mu)^2$, and, in agreement with our previous conclusions, increases with increasing vibrational excitation, thus making the adiabatic vibration quanta larger than the adiabatic ones.

A direct comparison of the nonadiabatic and adiabatic wave functions is also possible. Thus, the adiabatic vibrational wave function f_{nvK} obtained by solving Eq. (25) can be compared with the nonadiabatic pseudo-wave function defined as

$$f_{\text{nonad}}(R) = R\left[\int |\psi(\mathbf{r}; R)|^2 \, d\mathbf{r}\right]^{1/2}, \tag{51}$$

where the integration is to be carried out only over the electronic coordinates $\mathbf{r}$. For a system sych as H_2^+ the nonadiabatic effects are very small and are not easily detectable. However, much larger and therefore much more reliable effects in the wave function may be expected for the muonic molecules. A fairly accurate nonadiabatic calculation has recently been made (Kołos; 1968) for the pμd system. From the resulting wave function, f_{nonad} was calculated using Eq. (51) and the result was compared with the adiabatic vibrational wave function (Kołos, 1969). The weighted difference

$$\bar{\Delta} = (f_{\text{nonad}} - f_{nvK})f_{nvK}^2 \tag{52}$$

is shown in Fig. 3, where the adiabatic wave function is also displayed. The negative values of $\bar{\Delta}$ for small R and positive values for large R indicate that the nonadiabatic effects increase the mean value of the internuclear distance in spite of the accompanying increase of the dissociation energy. The above conclusion gets support from the estimation made by Tipping and Herman (1966) who found that the nonadiabatic effects decrease the rotational constant of H_2 (see Section V,C).

C. Ground State of the Hydrogen Molecule

For the hydrogen molecule no accurate nonadiabatic results are available. The 147-term wave function employed in the only nonadiabatic calculation (Kołos and Wolniewicz, 1964b) was not flexible enough to yield

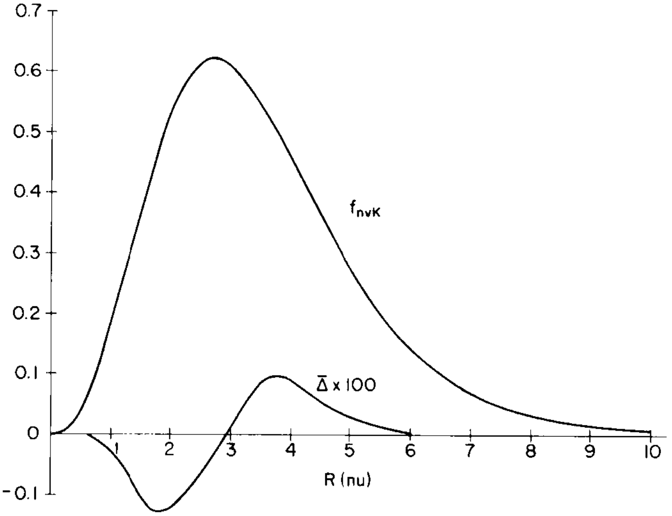

Fig. 3. Adiabatic vibrational wave function f_{nvK} for the muonic molecule pμd, and the weighted difference $\bar{\Delta}$ between the nonadiabatic vibrational pseudo-wave function and f_{nvK}.

a very accurate value of the energy. This is evident from the fact that the calculated nonadiabatic energy is somewhat higher than the adiabatic result, whereas the latter is known to represent an upper bound. Therefore a different approach should be adopted to get some insight into the accuracy of the adiabatic approximation.

It has already been indicated that in the case of H_2 the adiabatic results can be compared with the experimental values. However, from this point of view the present situation for the ground state is very unclear. The calculated adiabatic dissociation energy $D_0 = 36117.4$ cm^{-1} (Kołos and Wolniewicz, 1964, 1968a), which includes the relativistic (Kołos and Wolniewicz, 1964) and radiative corrections (Garcia, 1966), is larger than the experimental value $D_0 = 36113.6 \pm 0.3$ cm^{-1} (Herzberg and Monfils, 1960), which implies that the theoretical total energy is lower than the experimental one. Only a more accurate calculation of the radiative corrections can raise the theoretical energy. However, an upper bound for these corrections has also been found (Wolniewicz, 1966), and it shows that any raising cannot exceed a fraction of a cm^{-1}. Since the remaining energy represents an upper bound, any improvement of the theoretical energy which could be achieved by making the adiabatic wave function more flexible, or by including the nonadiabatic effects, can only result in an additional lowering of the energy and an increased discrepancy between the theoretical and experimental values. The theoretical result has recently been confirmed (Kołos and Wolniewicz, 1968a) in a more accurate calculation carried out in double precision, and the reason for the disagreement is not known.[1]

Let us now discuss the higher vibrational levels and the vibrational quanta for the ground electronic state of the hydrogen molecule. The vibrational quanta for H_2 calculated in the adiabatic approximation (Kołos and Wolniewicz, 1968a) are larger than the experimental ones (Herzberg and Howe, 1959), and the difference of the vibrational energies $\Delta E_v = E_{\text{exper}} - E_{\text{ad}}$ is an almost linear function of the vibrational excitation, as shown in Fig. 4. Qualitatively a similar discrepancy has been found between the nonadiabatic and adiabatic energies of H_2^+. Therefore, in the case of H_2, one may try to attribute the above discrepancy to the nonadiabatic effects and to estimate the magnitude of the latter by using the perturbation theory. This has already been done by Poll and Karl (1966) who employed Eq. (47) for the nonadiabatic energy shifts and, using the

[1] *Note added in proof.* Recent more accurate experimental values of the dissociation energies obtained by Dr. G. Herzberg (private communication) are in agreement with the theoretical results.

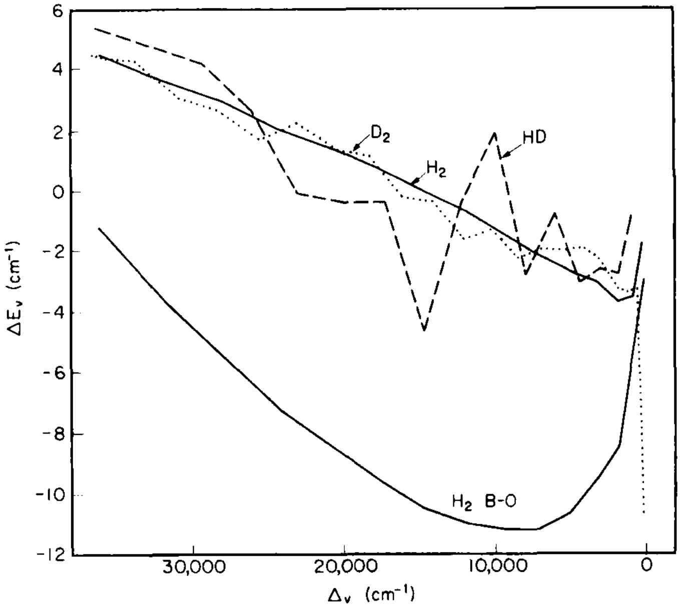

Fig. 4. Errors in the energies of the vibrational levels calculated in the adiabatic approximation, $\Delta E_v = E_{\text{exper}} - E_{\text{ad}}$, for H_2 (solid line), HD (broken line), and D_2 (dotted line). The solid line labeled H_2 B–O shows the errors for H_2 resulting from the Born–Oppenheimer potential energy curve.

Van Vleck (1936) values $(4/\bar{E})T_n(R_e) = 6 \cdot 10^{-4}$ and $3 \cdot 10^{-4}$ for H_2 and D_2, respectively, obtained a good agreement between $E^{(2)}$ and the discrepancies ΔE_v, for a few lowest vibrational states. For higher states Eq. (47) is certainly not applicable.

Recently, however, more sophisticated experiments have been carried out for HD and D_2 (Takezawa *et al.*, 1967). Previous determinations of the vibrational energies have been extended up to the highest levels, and for the lowest levels, which had been known before (Mie, 1934; Jeppesen, 1936), somewhat different, presumably more accurate, energies have been published. If the new vibrational energies of HD and D_2 are used, one gets the ΔE_v values which are shown graphically in Fig. 4 as functions of the vibrational excitation. It is seen that for all three isotopes (H_2, HD, and D_2) the energy shifts seem to be representable by roughly the same mass-independent function of the vibrational excitation. Hence they cannot be due to the nonadiabatic effects.

In view of these results one may suppose that for the ground state of

H_2, similarly as for H_2^+, the nonadiabatic energy corrections are quite small and account for only a small part of the discrepancy between the adiabatic and experimental energies. This differs from the previous opinion of the present author (Kołos, 1968b), which was based on the old experimental data.

The results shown in Fig. 4 strongly suggest that the experimental errors are in the case of D_2, and especially HD, much larger than in the case of H_2. They also suggest that the energy shifts ΔE_v, depend mainly on the location of the levels with respect to the minimum of the adiabatic potential energy curve. Thus, it is tempting to suppose that the calculated potential energy curve for $R > R_e$ (perhaps also for $R < R_e$) is not as accurate as for $R = R_e$. If this were the case, the potential energy curve in those regions could be lowered by using a more flexible wave function, and this would decrease the calculated vibrational quanta. However, the energy improvement obtained recently (Kołos and Wolniewicz, 1968a) by extending the number of terms in the electronic wave function from 80 to 100 was almost negligibly small (0.01 and 0.08 cm^{-1} for the lowest and second lowest vibrational quantum, respectively), and therefore it does not seem very likely that the lack of convergence of the electronic energy is responsible for the discrepancy, at least for the lowest vibrational states. On the other hand, if the potential energy curve could somehow be raised in the vicinity of the equilibrium internuclear distance, this could remove the disagreement with experiment of the vibrational quanta as well as of the dissociation energy. However, no physical effect is known which might produce the above result.

In Fig. 4 the "H_2 B–O" curve shows the errors in the vibrational energies of H_2 which result if the Born–Oppenheimer potential energy curve is used in the calculation. In general the errors both in the vibrational energies and in the vibrational quanta are seen to be larger than those resulting in the adiabatic approach.

The differences between the Born–Oppenheimer and the adiabatic energies can be represented by a curve similar to the "H_2 B–O" curve in Fig. 4. Their absolute value is largest for $v = 6$ and decreases for smaller or larger vibrational quantum numbers. For H_2^+ they also have a maximum which appears for $v = 8$ (Kołos, 1969). The above maxima can easily be accounted for by the form of the diagonal nuclear motion corrections (Fig. 1) which have minima at $R = 2.3$ and $R = 3.4$ au for the electronic ground states of H_2 and H_2^+, respectively. The expectation value of the internuclear distance for the $v = 6$ state of H_2 is $\langle R \rangle = 2.112$, and for the $v = 8$ state of H_2^+ $\langle R \rangle = 3.362$ au which is quite near to the location of the minima of the nuclear motion corrections. Therefore it is not surprising that for these vibrational states one gets the largest discrepancy between the Born–Oppenheimer and the adiabatic approximations.

A perturbation theory approach has also been employed to calculate nonadiabatic corrections to other properties of the hydrogen molecule. Karl and Poll (1967) used Eq. (45) with a constant effective denominator and the Wang wave function to calculate the nonadiabatic corrections to $\langle z^2 \rangle$ and $\langle r^2 \rangle$, where z and r are sums of the corresponding coordinates for the two electrons, the z coordinate being measured along the internuclear axis. Both corrections are of the expected order of magnitude, i.e., of the order of m/M, and both have been found to be negative. The results of direct nonadiabatic (Kołos and Wolniewicz, 1964b) and adiabatic (Wolniewicz, 1965) calculations agree with their result for Δz^2; however, for Δr^2 they differ in sign. The decrease of $\langle z^2 \rangle$ caused by the nonadiabatic effects is consistent with the general conclusion with regard to the nonadiabatic energy, which is lower than the adiabatic value. A smaller value of $\langle z^2 \rangle$ indicates a larger accumulation of the electronic charge between the nuclei which results in the increased binding of the molecule.

Karl and Poll (1967) also concluded that there is no nonadiabatic correction of the order of m/M to any function of the internuclear distance. If Q in Eq. (45) is a function of R only, all matrix elements of Q which are off diagonal in n vanish upon integration over the electronic coordinates. This agrees with the direct computation of $\langle R \rangle$ and $\langle R^{-2} \rangle$ for which in the nonadiabatic (Kołos and Wolniewicz, 1964b) and adiabatic (Wolniewicz, 1965) calculations identical values, up to five significant figures, were obtained. Tipping and Herman (1966) have also employed the perturbation theory to calculate the adiabatic and nonadiabatic corrections to the clamped nuclei value of B_e and hence to R_e. The values of R_e resulting from their calculation are $R_e(\text{cl. n.}) = 1.40107$, $R_e(\text{ad.}) = 1.40146$, and $R_e(\text{nonad.}) = 1.40150$ au, and it is seen that the nonadiabatic correction indeed does not change the fifth significant figure of R_e. Tipping and Herman included also the relativstic corrections in their calculation of B_e. They changed the nonadiabatic value of R_e to $R_e(\text{rel.}) = 1.40148$ au, which is in fair agreement with the value $R_e(\text{exper.}) = 1.40135$ au, obtained from the experimental data (Fink *et al.*, 1965) through the Dunham (1932) theory.

There is still another property of the hydrogen molecule which should be included in the present discussion. For a nonsymmetric molecule, such as HD, the complete Hamiltonian (8) is not invariant under inversion of R. This introduces a slight asymmetry into the electron density distribution along the internuclear axis and results in a net dipole moment of the molecule. It is the last term in (10) which is responsible for this effect. In the adiabatic approximation the electronic wave function is an eigenfunction of H^0 which is symmetric under inversion and therefore the wave function must have either the g or the u symmetry. In this approximation the expectation value of the last term in (10) vanishes, and no asymmetry of the charge distribution appears. If, however, a correction to the wavefunction due to the last term in (10) is calculated it must have the g or u symmetry different from that of the unperturbed wave function. The perturbed wave function thus gives a nonvanishing dipole moment which represents a purely nonadiabatic effect.

The existence of the dipole moment of HD has been established experimentally by Herzberg (1950) and Durie and Herzberg (1960). An extensive theoretical study of this problem has been carried out by Blinder (1960, 1961) who obtained for the dipole moment the value $\mu = 0.567 \times 10^{-3}$ D. More recently a more elaborate calculation has been performed (Kołos and Wolniewicz, 1966b) which resulted in $\mu = 1.54 \times 10^{-3}$ D. A value closely related to the dipole moment has also been measured experimentally. Trefler and Gush (1968) determined the dipole moment matrix elements for pure rotational transitions. The average for several transitions with different initial J values was $\mu = 0.585 \times 10^{-3}$ D, which seems to agree with the theoretical value of Blinder (1960, 1961). However, the problem is not quite so simple. The measured property was essentially a matrix element between different rotational states. Karl (1968) estimated that, for example, a $J = 0 \rightarrow 1$ matrix element should be only negligibly larger than the dipole moment. On the other hand, for HD$^+$ the dipole moment has been found (Hunter and Pritchard, 1967) to be almost twice as large as its matrix element for the $J = 0 \rightarrow 1$ transition. In addition the measurements involved rotational states which are coupled through Eqs. (13) with the electronic Π states and the effect of coupling may be of the same order of magnitude as the dipole moment itself. Since all calculations for HD were carried out for rotationless states and did not involve coupling with the $\Lambda = \pm 1$ states, they are not directly comparable with the existing experimental data.

D. Excited States of the Hydrogen Molecule

Fairly accurate calculations in the adiabatic approximation have also been carried out for a few excited states of the hydrogen molecule, viz., for the $C\,^1\Pi_u$, $B\,^1\Sigma_u^+$, $a\,^3\Sigma_g^+$, and $E, F\,^1\Sigma_g^+$ states (Kołos and Wolniewicz, 1965, 1966a, 1968b, 1969a). Except for the $C\,^1\Pi_u$ state the diagonal nuclear motion corrections for the above states have been calculated, and they were discussed in Section V,A. For the $C\,^1\Pi_u$ state the vibrational energies have been calculated by solving both Eq. (26) and Eq. (36). In the first case the neglected corrections for nuclear motion are infinite at $R = 0$, whereas in the second case the neglected corrections are finite for all value of R. The second case will be referred to as the approximate adiabatic approach.

The errors in the vibrational energies are shown in Fig. 5 as functions of the vibrational excitation. In general the adiabatic results (solid lines) are better than those resulting in the Born–Oppenheimer approximation (broken lines). This applies both to the vibrational energies and to the vibrational quanta. For all states the adiabatic total energies are higher than the corresponding experimental values.

The diagonal nuclear motion corrections for the $a\,^3\Sigma_g^+$ state have a minimum at $R \approx 3$ au, and $\langle R \rangle$ reaches this value in the $v = 7$ vibrational state, for which $D_v \approx 8400\ \mathrm{cm}^{-1}$. Therefore one may expect that if experi-

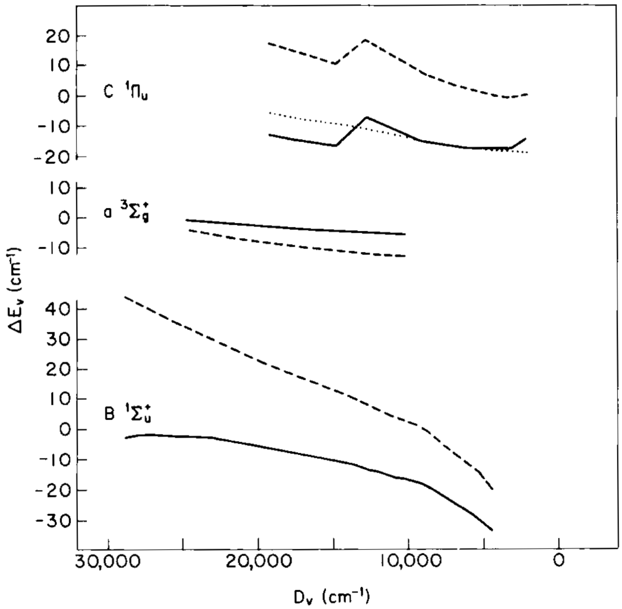

Fig. 5. Errors in the energies of the vibrational levels for various electronic states of H_2, resulting in the Born–Oppenheimer (broken lines) and in the adiabatic (solid lines) approximation; the dotted line for the $C\,^1\Pi_u$ state refers to results extrapolated to $K = 0$.

mental results (Dieke, 1958) were available for the higher vibrational levels, and the broken curve could be extended, it would have a minimum in the vicinity of $D_v = 8000 \text{ cm}^{-1}$.

The $B\,^1\Sigma_u^+$ and $C\,^1\Pi_u$ states provide an example of interaction between states with different Λ values, which gives rise to strong heterogeneous perturbations in some vibrational states. No ab initio calculations of the interaction have been carried out. In the case of the $C\,^1\Pi_u$ state each unperturbed line represents a $\Pi^\pm$ doublet and only Π^+ interacts with the $B\,^1\Sigma_u^+$ state. Thus the magnitude of splitting into two Π sublevels, i.e., the Λ doubling, determines directly the magnitude of the perturbation. In Fig. 5 the experimental results (Dieke 1958, Namioka, 1964) for the unperturbed Π^- sublevel are compared with the theoretical values. The Born–Oppenheimer energies, and especially the vibrational quanta, are seen to be somewhat inferior to those resulting in the adiabatic calculation. The inconsistency of the error for $v = 3$ is due either to an error or to a misprint in the published experimental data (Dieke, 1958). The discrepancy between the theoretical energies (Kołos and Wolniewicz, 1968b) for $K = \Lambda = 0$ and the experimental values extrapolated to $K = 0$ (Namioka, 1965), shown by the dotted line in Fig. 5, is seen to be a smooth function of the vibrational excitation.

In the case of the $B\,^1\Sigma_u^+$ state a semiempirical procedure can be employed to "deperturb" the observed lines, and in Fig. 5 the deperturbed wave numbers (Namioka, 1964) are compared with the theoretical values (Kołos and Wolniewicz, 1968b). The adiabatic results are in this case significantly better than those obtained in the Born–Oppenheimer approximation. The increase of the error for higher vibrational states will be discussed below.

The first excited $^1\Sigma_g^+$ state of the hydrogen molecule is known to have a double minimum (Davidson, 1960, 1961) resulting from the avoided crossing of the potential energy curves for the $1\sigma_g 2s$ and $(1\sigma_u)^2$ configurations. A detailed theoretical study for this state has recently been made (Kołos and Wolniewicz, 1969a) and the results can be compared with the available experimental data for the symmetric molecules H_2, D_2, and T_2 (Dieke 1936, 1949, 1958; Dieke and Cunningham, 1965). The maximum of the potential occurs at $R = 3.12$ au, and is located about 6250 cm^{-1} above the lower (inner) minimum. At almost the same values of R the diagonal nuclear motion corrections have a very sharp maximum (Fig. 1), resulting probably from a drastic change which occurs in the character of the electronic wave function in the vicinity of the point of the avoided crossing. The improvement of the vibrational quanta obtained by introduc-

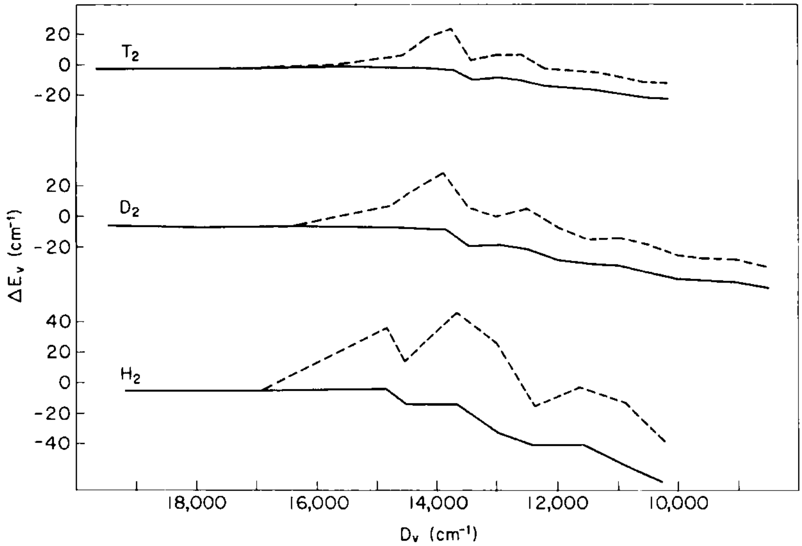

Fig. 6. Errors in the energies of the vibrational levels for the *E*, *F* $^1\Sigma_g^+$ state of H_2, D_2, and T_2, resulting in the Born–Oppenheimer (broken lines) and in the adiabatic (solid lines) approximation.

ing the diagonal corrections for nuclear motion is very striking. The errors for H_2, D_2, and T_2 are shown in Fig. 6, and it should be remembered that a horizontal line would indicate a perfect agreement between the theoretical and experimental vibrational quanta.

The question again arises, what is responsible for the remaining discrepancies between the adiabatic and experimental energies for the *E*, *F*, $^1\Sigma_g^+$ state. The computed total energies are higher than the experimental values; hence, the discrepancies may be due partly to an insufficient flexibility of the variational wave function, to not very accurate diagonal nuclear motion corrections, and also partly to the nonadiabatic effects. The almost constant errors for the few lowest vibrational levels in the excited $^1\Sigma_g^+$ state give the impression that the nonadiabatic effects for these levels are probably quite small. On the other hand the different slopes of the curves in Fig. 6 for higher vibrational levels of different isotopes suggest that in this region a significant part of the errors is due to the nonadiabatic effects. This seems to be a plausible conjecture in view of the fact that the maximum of the potential energy curve, resulting from the avoided crossing of the curves for the *E* and *F* states, occurs at $D \approx 14{,}000$ cm^{-1}. It is likely that for the vibrational levels located in the vicinity and above the potential maximum the nonadiabatic effects are quite strong.

Also for the $B\,^1\Sigma_u^+$ state the errors may be partly attributed to the nonadiabatic effects. It is seen from Fig. 5 that the errors increase more rapidly for $D < 10{,}000$, cm^{-1}. This is not very surprising if one realises that the second lowest electronic state of the same symmetry, i.e., the $B'\,^1\Sigma_u^+$ state, has the minimum of the potential energy curve located about 20,000 cm^{-1} above that for the B state (Namioka, 1965). Hence for $D < 8900$ cm^{-1} there may be vibrational levels of these states which lie very near to each other, and strong nonadiabatic effects are likely to appear, as discussed in Section IV,B,2. It is, of course, also possible that the potential energy curve for the B state is for large R somewhat less accurate than in the vicinity of the equilibrium and this would obviously raise the energy of the higher vibrational levels.

One might also speculate that the nonadiabatic effects are responsible for the discrepancy which has been found between the adiabatic (Kołos and Wolniewicz, 1966a) and the Rydberg-Klein-Rees (Namioka, 1965) potential energy curves for the $B\,^1\Sigma_u^+$ state. This interpretation may raise objections, since the respective discrepancy between the two curves for the $C\,^1\Pi_u$ state is much smaller (Kołos and Wolniewicz, 1965; Namioka, 1965), in spite of the possible interaction with the $D\,^1\Pi_u$ state. However, for the two $^1\Sigma_u^+$ states the dissociation limits are the same and therefore they represent a somewhat different case than the C and D states for which they are different.

ACKNOWLEDGMENTS

The main part of the article represents the contents of two lectures given by the author in August 1968 at the Summer Institute in Quantum Chemistry, Solid State Physics and Quantum Biology in Uppsala and Beitostølen. The author is very grateful to Professor Per-Olov Löwdin for making it possible for him to visit the Institute and to benefit from its stimulating atmosphere. He is also very indebted to Dr. L. Wolniewicz whose numerous comments substantially contributed to the contents of the article.

REFERENCES

BATES, D. R. (1962). *in* "Atomic and Molecular Processes" (D. R. Bates, ed.), p. 597. Academic Press, New York.

BATES, D. R., LEDSHAM, K., and STEWART, A. L. (1953). *Phil. Trans. Roy. Soc.* **A246**, 215.

BETHE, H., and SALPETER, E. E. (1957). "Quantum Mechanics of One- and Two-Electron Atoms." Academic Press, New York.

BLINDER, S. M. (1960). *J. Chem. Phys.* **32**, 102, 582.

BLINDER, S. M. (1961). *J. Chem. Phys.* **35**, 974.

BORN, M. (1951). *Nachr. Akad. Wiss. Göttingen* **1**.

BORN, M., and OPPENHEIMER, R. (1927). *Ann. Phys.* **84**, 457.

BORN, M., and HUANG, K. (1956). "Dynamical Theory of Crystal Lattices," Oxford Univ. Press, New York.

BRATTSEV, V. F. (1965). *Dokl. Akad. Nauk SSSR.* **160**, 570.

BUCKINGHAM, R. A. (1962). In "Quantum Theory" (D. R. Bates, ed.), Vol. 1, p. 121. Academic Press, New York.

CARTER, B. P. (1968). *Phys. Rev.* **165**, 139.

COHEN, S., JUDD, D. L., and RIDDELL, R. J. (1959). Report No UCRL-8802, Lawrence Radiation Lab., Univ. of California.

DALGARNO, A., and MCCARROLL, R. (1956). *Proc. Roy. Soc. (London)* **A237**, 383.

DALGARNO, A., and MCCARROLL, R. (1957). *Proc. Roy. Soc. (London)* **A239**, 413.

DAVIDSON, E. R. (1960). *J. Chem. Phys.* **33**, 1577.

DAVIDSON, E. R. (1961). *J. Chem. Phys.* **35**, 1189.

DIEHL, H., and FLÜGGE, S. (1961). *Z. Physik* **162**, 21.

DIEKE, G. H. (1936). *Phys. Rev.* **50**, 797.

DIEKE, G. H. (1949). *Phys. Rev.* **76**, 50.

DIEKE, G. H. (1958). *J. Mol. Spectr.* **2**, 494.

DIEKE, G. H., and CUNNINGHAM, S. P. (1965). *J. Mol. Spectr.* **18**, 288.

DUNHAM, J. L. (1932). *Phys. Rev.* **41**, 721.

DURIE, R. A., and HERZBERG, G. (1960). *Can. J. Phys.* **38**, 806.

EPSTEIN, S. T. (1966). *J. Chem. Phys.* **44**, 836, 4062.

FINK, U., WIGGINS, T. A., and RANK, D. H. (1965). *J. Mol. Spectr.* **18**, 384.

FISK, G. A., and KIRTMAN, B. (1964). *J. Chem. Phys.* **41**, 3516.

FRÖMAN, A., and KINSEY, J. L. (1961). *Phys. Rev.* **123**, 2077.

FROST, A. A., INOKUTI, M., and LOWE, J. P. (1964). *J. Chem. Phys.* **41**, 482.

GARCIA, J. D. (1966). *Phys. Rev.* **147**, 66.

HERMAN, R. M., and ASGHARIAN, A. (1966). *J. Mol. Spectry.* **19**, 305.

HERZBERG, G. (1950). *Nature* **166**, 563.

HERZBERG, G., and HOWE, L. L. (1959). *Can. J. Phys.* **37**, 636.

HERZBERG, G., and MONFILS, A. (1960). *J. Mol. Spectr.* **5**, 482.

HIRSCHFELDER, J. O., and WIGNER, E. P. (1935). *Proc. Natl. Acad. Sci.* **21**, 113.

HUNTER, G. (1966). *J. Chem. Phys.* **45**, 3022.

HUNTER, G., and PRITCHARD, H. O. (1967). *J. Chem. Phys.* **46**, 2146, 2153.

HUNTER, G., GRAY, B. F., and PRITCHARD, H. O. (1966). *J. Chem. Phys.* **45**, 3806.

JEPPESEN, C. R. (1936). *Phys. Rev.* **49**, 797.

JEPSEN, D. W., and HIRSCHFELDER, J. O. (1960). *J. Chem. Phys.* **32**, 1323.

JOHNSON, V. A. (1941). *Phys. Rev.* **60**, 373.

KARL, G. (1968). (To be published).

KARL, G., and POLL, J. D. (1967). *J. Chem. Phys.* **46**, 2944.

KOŁOS, W. (1968a). *Phys. Rev.* **165**, 165.

KOŁOS, W. (1968b). *Intern. J. Quantum Chem.* **2**, 471.

KOŁOS, W. (1969). *Acta Phys. Acad. Sci. Hung.* **27**, 241.

KOŁOS, W., and WOLNIEWICZ, L. (1963). *Rev. Mod. Phys.* **35**, 473.

KOŁOS, W., and WOLNIEWICZ, L. (1964a). *J. Chem. Phys.* **41**, 3663.

KOŁOS, W., and WOLNIEWICZ, L. (1964b). *J. Chem. Phys.* **41**, 3674.

KOŁOS, W., and WOLNIEWICZ, L. (1965). *J. Chem. Phys.* **43**, 2429.

KOŁOS, W., and WOLNIEWICZ, L. (1966a). *J. Chem. Phys.* **45**, 509.

KOŁOS, W., and WOLNIEWICZ, L. (1966b). *J. Chem. Phys.* **45**, 944.

KOŁOS, W., and WOLNIEWICZ, L. (1968a). *Phys. Rev. Letters* **20**, 243; *J. Chem. Phys.* **49**, 404.

KOŁOS, W., and WOLNIEWICZ, L. (1968b). *J. Chem. Phys.* **48**, 3672.

KOŁOS, W., and WOLNIEWICZ, L. (1969a). *J. Chem. Phys.* **50**, 3228.

KOŁOS, W., and WOLNIEWICZ, L. (1969b). *J. Chem. Phys.* **51**, 1417.

KOŁOS, W., ROOTHAAN, C. C. J., and SACK, R. A., (1960). *Rev. Mod. Phys.* **32**, 178.

LAUE, H. (1967). *J. Chem. Phys.* **46**, 3034.

MIE, K. (1934). *Z. Physik* **91**, 475.

MULLIKEN, R. S. (1937). *J. Phys. Chem.* **41**, 5.

MULLIKEN, R. S. (1966). *J. Am. Chem. Soc.* **88**, 1849.

NAMIOKA, T. (1964). *J. Chem. Phys.* **40**, 3154.

NAMIOKA, T. (1965). *J. Chem. Phys.* **43**, 1636.

NEUMANN, J. von, and WIGNER E. P. (1929). *Physik. Z.* **30**, 467.

PACK, R. T. (1966). Ph. D. Disssertation, Univ. of Wisconsin, Theoretical Chemistry Inst. Rept. No. WIS-TCI-197.

PEEK, J. M. (1965). Sandia Corp. Rept. No. SC-RR-65-77; *J. Chem. Phys.* **43**, 3004.

POLL, J. D., and KARL, G. (1966). *Can. J. Phys.* **44**, 1467.

TAKEZAWA, S., INNES, F. R., and TANAKA, Y. (1967). *J. Chem. Phys.* **46**, 4555.

TELLER, E. (1937). *J. Phys. Chem.* **41**, 109.

TIPPING, R., and HERMAN, R. M. (1966). *J. Chem. Phys.* **44**, 3112.

TREFLER, M., and GUSH, H. P. (1968). *Phys. Rev. Letters* **20**, 703.

UNSÖLD, A. (1927). *Z. Physik* **43**, 563.

VALATIN, J. G. (1947). *Hung. Acta Phys.* **1**, 23.

VAN VLECK, J. H. (1936). *J. Chem. Phys.* **4**, 327.

WIGNER, E. (1959). "Group Theory and Its Application to the Quantum Mechanics of Atomic Spectra." Academic Press, New York.

WIND, H. (1965). Thesis, Univ. of Utrecht; *J. Chem. Phys.* **42**, 2371.

WOLNIEWICZ, L. (1966). *J. Chem. Phys.* **45**, 515.

The Theory of Nonadiabatic Transitions: Recent Development with Exponential Models

E. E. NIKITIN

Institute of Chemical Physics
Academy of Sciences
Moscow

I. An Exponential Model of Nonadiabatic Coupling of Two Electronic States

The rapid development of computational methods in recent years has provided important information about electronic wave functions and electronic terms of some simple molecular systems. The approximation commonly used is the adiabatic one implying fixed nuclear positions. The next step in calculations desirable for the evaluation of vibronic eigenvalues, and indispensable for studying kinetic problems, consists in taking into account the interaction of electrons and nuclei induced by their motion. Mathematically, this problem reduces to solution of coupled equations for nuclear functions; general features of such equations are discussed in books on the collision theory (see, for example, Mott and Massey, 1965). At present there is a real possibility of solving these equations by means of electronic computers. Nevertheless, due to the rather special behavior of the solutions (very rapid oscillations of nuclear wave functions under quasiclassical conditions of collisions) some very simple models which allow finding an analytical solution still play an important part in understanding the physical picture of kinematic interaction between electrons and nuclei. The most widely applied type of model is that which takes into account only two nonadiabatically coupled electronic terms. For bound states of a molecular system (eigenvalue problem) this model has been extensively discussed by Longuet-Higgins (Longuet-Higgins, 1961) in connection with the Renner effect, and the dynamic Jahn-Teller effect. For unbounded states (scattering problem) two-state models have been applied for interpretation of excitation transfer, charge transfer, and electronic-translation energy exchange (Bates, 1962). In particular a recent review article (Nikitin, 1968) deals with the so-called linear model firts investigated by Landau (Landau, 1932a, 1932b) and Zenar (Zener, 1932). This model can be used to describe nonadiabatic transitions provided two conditions are satisfied:

$$\eta = \Delta U_p/\Delta\varepsilon \ll 1, \qquad \xi = \Delta\varepsilon/\alpha\hbar v \gg 1. \tag{1}$$

Here ΔU_p stands for the splitting of two adiabatic electronic terms in the nonadiabaticity region, $\Delta\varepsilon$ is the asymptotic splitting of these terms far from this region, and $1/\alpha$ is a characteristic length over which a term splitting ΔU changes significantly. Usually, α can be identified with the exponent of a resonance or exchange integral of the system considered.

This paper will deal with another model for which there will be no restrictions of type (1) on the relative term splitting η, and the Massey parameter ξ. However, unlike the linear model case, a special type of interaction will be considered in the region of nonadiabatic coupling. We choose the exponential function $\exp(-\alpha R)$ as an approximation to true interaction, thus confining ourselves to studying an exponential model of nonadiabatic coupling of two electronic states.[1] Such a choice is prompted by two reasons.

First, the exponential function is characteristic of the splitting of molecular terms (emerging from quasi-degenerate atomic states) at large

---

[1] The two states in equation need not always be electronic states. They may as well be two vibrational states (see Section V). In this case the model would describe nonadiabatic coupling between two kinds of nuclear motion: vibrational and translational.

interatomic distances if the main contribution is due to exchange interaction. After the pioneering work of Herring (1962) and Gor'kov and Pitaevski (1963) several authors (Herring, and Flicker, 1964; Smirnov, 1964; Ovchinnikova, 1965; Smirnov and Chibisov, 1965; Smirnov, 1966; Roueff, 1967) have calculated the asymptotic splitting of molecular terms under the assumption that $R\alpha \gg 1$. The general expression for the interaction matrix elements is of the form

$$H_{ik}(R) = CR^m \exp(-\alpha R). \tag{2}$$

When the nonadiabatic region is centered at $R = R_p$, a function of the type (2) under condition $\alpha R_p \gg 1$ can be approximated by the pure exponential

$$\begin{aligned} H_{ik}(R_p + \Delta R) &= CR_p{}^m \exp(-\alpha R_p)\exp\left[-\alpha\,\Delta R + m \ln \frac{R_p + \Delta R}{R_p}\right] \\ &= CR_p{}^m \exp(-\alpha R_p)\exp\left[-\left(\alpha - \frac{m}{R_p}\right)\Delta R - m\frac{(\Delta R)^2}{2R_p{}^2} + \cdots\right]. \end{aligned} \tag{3}$$

Here ΔR means a small variation of R near R_p ($\Delta R/R_p \ll 1$). The characteristic length of the nonadiabaticity region being $1/\alpha$ (*vide infra*), all except the first term of the second exponential may be neglected provided the following condition is satisfied:

$$\alpha R_p \gg \sqrt{m}. \tag{4}$$

This inequality is fulfilled for many problems connected with atomic and molecular collisions. The first term in the exponential contains a correction for the preexponential factor in (2). This correction is usually very small, but if needed it may be retained. Hereafter α will denote a corrected value. As to the expression of α in terms of orbital exponents of bound electrons and the calculation of m, this is discussed in the papers cited above.

The second argument for choosing an exponential model is that such a function is very often used in semiempirical approximations of intermolecular potentials. For example, this approximation is widely adopted in the theory of vibrational energy transfer in molecular collisions (Herzfeld and Litovitz, 1959; Takayanagi, 1963, 1965).

Thus the exponential model can be considered as applicable to many elementary processes and also as a basic unit for matching electronic adiabatic functions when the nuclear coordinate R passes the nonadiabaticity region at R_p. The exponential model will be discussed, as closely as possible, in anaology with the linear model (Nikitin, 1968) in order to facilitate comparison.

In constructing the exponential model we consider the one-dimensional case taking, for definiteness, the interaction of two atoms. In accordance with the idea of a crude adiabatic approximation (Longuet-Higgins, 1961) let us assume that the molecular adiabatic wave functions φ_1 and φ_2 do not depend on R on both sides of the nonadiabaticity region, but that the coefficients of the linear combinations expressing the expansion φ_i in terms of a basic set $\varphi_i{}^0$ of the crude adiabatic approximation do depend on R within the region of nonadiabatic coupling. Thus, close to $R \sim R_p$ we can write

$$\begin{aligned} \varphi_1 &= \varphi_1{}^0 \cos \chi/2 + \varphi_2{}^0 \sin \chi/2 \\ \varphi_2 &= -\varphi_1{}^0 \sin \chi/2 + \varphi_2{}^0 \cos \chi/2, \end{aligned} \tag{5}$$

where χ is a function of R. A new requirement is now imposed on $\chi(R)$ demanding that at $R \gg R_p$ and $R \ll R_p$ the χ function tends to constant values:

$$\begin{aligned} \chi(R) &\to 0 \quad \text{at} \quad R \gg R_p \\ \chi(R) &\to \theta \quad \text{at} \quad R \ll R_p, \end{aligned} \tag{6}$$

where θ is a parameter of our model. In the basic set $\varphi_i{}^0$ the Hamiltonian matrix H is nondiagonal. Its general form under restriction (6) and using only exponential functions as an approximation to all matrix elements will be

$$H = \left|\begin{array}{c:c} B\exp(-\alpha R) + \dfrac{\Delta\varepsilon}{2} & -\dfrac{A}{2}\sin\theta\exp(-\alpha R) \\ \quad -\dfrac{A}{2}\cos\theta\exp(-\alpha R) & \\ \hdashline & B\exp(-\alpha R) - \dfrac{\Delta\varepsilon}{2} \\ -\dfrac{A}{2}\sin\theta\exp(-\alpha R) & \quad +\dfrac{A}{2}\cos\theta\exp(-\alpha R) \end{array}\right|. \tag{7}$$

Diagonalizing this matrix we obtain

$$\chi = \arctan\frac{-A\sin\theta\exp(-\alpha R)}{\Delta\varepsilon - A\cos\theta\exp(-\alpha R)}. \tag{8}$$

The condition (6) follows of course from (8), and asymptotic values of χ are attained when $|Ae^{-\alpha R}| \gg \Delta\varepsilon$ and $|Ae^{-\alpha R}| \ll \Delta\varepsilon$. The coefficient A in this model depends on R_p but it is still not fixed. We define now the center of the nonadiabaticity region making use of equation

$$A(R_p)\exp(-\alpha R_p) = \Delta\varepsilon. \tag{9}$$

Thus the following parameters specify the adiabatic Hamiltonian (7): $B(R_p)$, $A(R_p)$ (or R_p as usual), $\Delta\varepsilon$, and α. Taking into account (9) the eigenvalues of (7) can be written as

$$\begin{aligned} U_{1,2} &= U(R) \pm \Delta U(R) = B\exp(-\alpha R) \\ &\quad \pm \frac{\Delta\varepsilon}{2}[1 - 2\cos\theta\exp(-\alpha\Delta R) + \exp(-2\alpha\Delta R)]^{1/2} \end{aligned} \tag{10}$$

At $R = R_p$, at the center of the nonadiabaticity region, the splitting $\Delta U(R_p)$ is

$$\Delta U(R_p) = \Delta U_p = 2\Delta\varepsilon\sin\theta/2. \tag{11}$$

Thus the parameter η given in Eq. (1) will for the exponential model be

$$\eta = 2\sin\theta/2. \tag{12}$$

This completes the specification of the model in terms of adiabatic parameters of the Hamiltonian (7) (see Fig. 1).

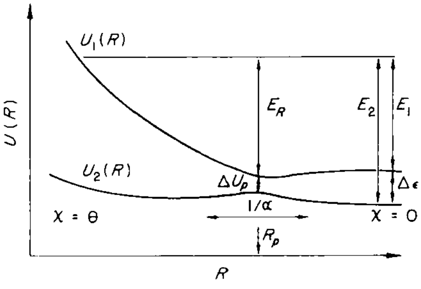

Fig. 1. Adiabatic characteristics of the Hamiltonian (7). The nonadiabaticity region is far from the turning points.

II. Semiclassical Description of Nonadiabatic Coupling in the Constant Velocity Approximation

Within the framework of the semiclassical approximation, the nuclear motion is described by a trajectory $R = R(t)$. This approximation is valid only if two conditions are satisfied: The de Broglie wavelength must be small compared to the length $1/\alpha$ and the term splitting ΔU_p must be small compared to the kinetic energy of nuclei E_R in the region near $R \sim R_p$. Taking two conditions

$$\mu v_R/\hbar\alpha \quad \gg 1 \tag{13a}$$

$$\mu {v_R}^2/2\,\Delta\varepsilon \gg 1 \tag{13b}$$

and defining ξ according to (1), we obtain the following range of variation for the Massey parameter:

$$\Delta\varepsilon/\mu {v_R}^2 \ll (\xi = \Delta\varepsilon/\hbar\alpha v_R) \ll \mu v_R/2\hbar\alpha. \tag{14}$$

The upper limit in (14) is far above unity, and the lower is far below it. Thus the allowed region for ξ includes the value $\xi \sim 1$. Moreover, the case $\eta \ll 1$ and $\xi \gg 1$ is also described to this approximation, so that under these conditions the exponential model will yield results identical to those for the linear model.

As a simple approximation for a trajectory in the coupling region we take the constant velocity approximation

$$\Delta R = v_R\, t, \tag{15}$$

where the velocity v_R is referred to some point in the nonadiabaticity region.

We now look for the nonadiabatic electronic wave function $\Psi(t)$ following the trajectory (15). The function $\Psi(t)$ satisfies the nonstationary state Schrödinger equation with the Hamiltonian depending on $R(t)$ and can be represented as a superposition of functions φ_i or ${\varphi_i}^0$. Taking

$$\Psi(t) = b_1(t){\varphi_1}^0 + b_2(t){\varphi_2}^0 \tag{16}$$

we obtain for $b_i(t)$ the following system of equations:

$$i\hbar\begin{pmatrix} b_1 \\ b_2 \end{pmatrix} = \begin{pmatrix} H_{11}(t) & H_{12}(t) \\ H_{21}(t) & H_{22}(t) \end{pmatrix}\begin{pmatrix} b_1 \\ b_2 \end{pmatrix}, \tag{17}$$

where the matrix elements $H_{ik}(t)$ are given by (7) taking into account (15). It can readily be seen that solutions of (17) depend only on difference $H_{11}(t) - H_{22}(t)$, but not on H_{ii} as such, This means that all essential features of the problem are determined by two functions of time: $H_{11} - H_{22}$ and H_{12}. For the matrix (17) these two functions are

$$\begin{aligned} H_{11} - H_{22} &= \Delta\varepsilon[1 - \cos\theta \exp(-\tau)] \\ H_{12} &= -\tfrac{1}{2}\Delta\varepsilon \sin\theta \exp(-\tau), \end{aligned} \tag{18}$$

where a dimensionless time parameter $\tau = t\alpha v_R$ is introduced.

The probability of transition between adiabatic terms as a result of passing the nonadiabaticity region from $\tau = \infty$ to $\tau = -\infty$ is obtained by projection of the function $\Psi(t)$ at $t \to -\infty$ on the adiabatic state in question. Thus we obtain

$$P_{12} = \lim_{t \to -\infty} |\langle \varphi_2 \Psi(t) \rangle|^2 = \lim_{t \to -\infty} \left| -b_1(t) \sin\frac{\theta}{2} + b_2(t) \cos\frac{\theta}{2} \right|^2 \tag{19}$$

under the following initial conditions:

$$\begin{matrix} b_1(t) \to 1 \\ b_2(t) \to 0 \end{matrix} \quad \text{at} \quad t \to \infty. \tag{20}$$

If another basic set is adopted and $\Psi(t)$ is expressed by the equation

$$\Psi(t) = a_1(t)\varphi_1 + a_2(t)\varphi_2, \tag{21}$$

the set of equations for $a_i(t)$ will be

$$i\hbar \begin{pmatrix} \dot{a}_1 \\ \dot{a}_2 \end{pmatrix} = \begin{pmatrix} U_1(t) & i\dot{\chi}/2 \\ -i\dot{\chi}/2 & U_2(t) \end{pmatrix} \begin{pmatrix} a_1 \\ a_2 \end{pmatrix}$$

$$U_1(t) - U_2(t) = \Delta\varepsilon[1 - 2\cos\theta \exp(-\tau) - \exp(-2\tau)]^{1/2} \tag{22}$$

$$\dot{\chi} = \alpha v_R \frac{d}{d\tau} \arctan\left[\frac{-\sin\theta \exp(-\tau)}{1 - \cos\theta \exp(-\tau)}\right].$$

The transition probability for this representation is

$$P_{12} = \lim_{t \to -\infty} |a_2(t)|^2, \tag{23}$$

the initial conditions being

$$\begin{matrix} a_1(t) \to 1 \\ a_2(t) \to 0 \end{matrix} \quad \text{at} \quad t \to \infty. \tag{24}$$

Representation (16) is convenient for approximate calculation of P_{12} for low values of H_{12}. Representation (21) is appropriate in the calculation of the transition probability at the adiabatic limit, where $\dot{\chi}$ is considered to be small. It is now known (Pokrovskii and Khalatnikov, 1961; Dykhne, 1961) that the perturbation treatment with respect to $\dot{\chi}$, performed to the first order only, gives an incorrect preexponential factor in the expression for the transition probability (even at the limit of vanishing $\dot{\chi}$). The main idea of correct perturbation treatment in the adiabatic case is integration of the system (22) along a path connecting limiting points $t = -\infty$ and $t = +\infty$, but otherwise shifted from the real axis. Under condition $\chi \to 0$ the integration path can be chosen such that a drastic simplification of $\Delta U(t)$ and χ functions can be achieved on this path. An exact solution can be found for this simplified problem, and the transition probability which will always be exponentially small, will represent a good approximation to that for the initial problem. The probability amplitude will be a superposition of terms such as

$$J_k \sim \exp\left[-\frac{1}{\hbar}\,\mathrm{Im}\int^{t_k^*} \Delta U(t)\,dt\right], \tag{25}$$

where t_k^* are singularity points of the function $\Delta U(t)$ (Landau and Lifshitz, 1963); e.g., poles or branching points. To the approximation considered here, only the leading term (among all possible J_k) should be retained. We shall discuss this and related topics in Section IV.

If exact solution of the problem is attempted, there will be no difference in representation. For this model $b_i(t)$ or $a_i(t)$ can be expressed by confluent hypergeometric functions (Nikitin, 1962a, 1962b; Ellison and Borovitz, 1964). The transition probability is given by

$$P_{12} = \exp\left[-\frac{\pi}{2}\,\xi(1-\cos\theta)\right]\frac{\sinh[(\pi/2)\xi(1+\cos\theta)]}{\sinh \pi\xi} \tag{26}$$

so that both parameters (1) enter this formula.

In case of atomic collisions a particle usually crosses the coupling region twice (Fig. 2, trajectory 1). The transition probability for repeated crossings of the coupling regions can be found by a matching procedure. We consider first the time evolution of coefficients $a_k(t)$, referring $t = 0$ to the distance of the closest approach. Thus we write

$$\begin{pmatrix} a_1(t') \\ a_2(t') \end{pmatrix} = \mathrm{S}_a(t', -t_p)\mathrm{S}_p(-t_p)\mathrm{S}_a(-t_p, -\infty)\begin{pmatrix} a_1(-\infty) \\ a_2(-\infty) \end{pmatrix}, \tag{27}$$

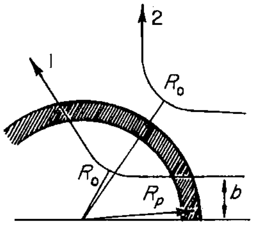

Fig. 2. Nonadiabaticity region and different kinds of classical trajectories in collisions.

with

$$\mathrm{S}_a(t_1, t_2) = \begin{pmatrix} \exp\left(-\frac{i}{\hbar}\int_{t_2}^{t_1} U_1\, dt\right) & 0 \\ 0 & \exp\left(-\frac{i}{\hbar}\int_{t_2}^{t_1} U_2\, dt\right) \end{pmatrix} \tag{28}$$

$$\mathrm{S}_p(-t_p) = \begin{pmatrix} (1 - P_{12})^{1/2}\exp(i\omega_1) & \sqrt{P_{12}}\exp(i\omega_2) \\ -\sqrt{P_{12}}\exp(-i\omega_2) & (1 - P_{12})^{1/2}\exp(-i\omega_1) \end{pmatrix} \times \exp(i\omega_0).$$

Here the matrix $\mathrm{S}_a(t_1, t_2)$ describes the adiabatic evolution of the system and $\mathrm{S}_p(-t_p)$ is a unitary matrix which characterizes the general solution of Eqs. (22) (to be called "transition matrix"). In Eq. (27) it is understood that $-t_p$ corresponds to R_p at the first crossing, and $t' - (-t_p)$ is sufficiently large for the nonadiabatic coupling to be negligible. The P_{12} in (28) is given by Eq. (22). Following trajectory 1 we find for the second crossing

$$\begin{pmatrix} a_1(+\infty) \\ a_2(+\infty) \end{pmatrix} = \mathrm{S}_a(\infty, t_p)\mathrm{S}_p(t_p)\mathrm{S}_a(t_p, t')\begin{pmatrix} a_1(t') \\ a_2(t') \end{pmatrix}. \tag{29}$$

The important step now is to establish connection between $\mathrm{S}_p(-t_p)$ and $\mathrm{S}_p(t_p)$. Equations describing the second crossing can be obtained from the equations for the first crossing by two operations: by replacing t by $-t$ and by taking the complex conjugate. Thus we have

$$\mathrm{S}_p(t_p) = \{[\mathrm{S}_p(-t_p)]^{-1}\}^* = \mathrm{S}_p^{\mathrm{tr}}(-t_p), \tag{30}$$

where $\mathrm{S}_p^{\mathrm{tr}}$ means the transposed matrix [the last step in (30) follows from the unitary of S_p]. Matching Eqs. (28) and (29) we obtain

$$\mathscr{P}_{12} = 4\sin^2(\phi + \tau)P_{12}(1 - P_{12}); \qquad \phi = \int_{-t_p}^{t_p} \frac{\Delta U}{2\hbar}\, dt, \qquad \tau = \omega_2 - \omega_1. \tag{31}$$

Note that ϕ depends on the model only through the integration limits and thus constitutes essentially a new parameter which characterizes the system in the internal region $R < R_p$. In this region there are no special restrictions imposed either on the approximation of the splitting $\Delta U(t)$ or on the kind of trajectory: in particular, it might not be rectilinear (as it is in Fig. 2). The only limitation on ϕ is that the region where $\Delta U(t) \gg \Delta\varepsilon$ the motion on *two* adiabatic electronic terms is still represented by *one* trajectory. But even this limitation can be lifted if ϕ is represented in the form

$$\phi = -\int_{R_0^{(1)}}^{R'} p_1\, dR/\hbar + \int_{R_0^{(2)}}^{R'} p_2\, dR/\hbar + \int_{R'}^{R_p} \Delta U(R)\, dR/\hbar v(R). \tag{32}$$

Here $p_k(R)$ is the momentum of a particle moving on the corresponding electronic adiabatic term, $R_0^{(k)}$ is the turning point, and R' is the joining distance at which the difference of WKB and semiclassical phases match. The approximation (31) is valid so far as ϕ does not depend on R'. As far as τ is concerned it is completely defined by the model of the nonadiabatic coupling itself.

In what follows we shall use the approximation $\tau = 0$, which is sufficient for our purposes. Explicit expressions for τ have, however, been obtained for the particular cases $\theta \ll 1$ (Kotova, 1968) and $\theta = \pi/2$ (Rosen and Zener 1932, Demkov 1963); corresponding formulas for $\bar{\mathscr{P}}_{12}$ are given by Eqs. (38) and (44). Thus, to this approximation, we obtain the following final expression for $\mathscr{P}_{12}$:

$$\mathscr{P}_{12} = 4 \sin^2 \phi \exp(\pi\xi \cos\theta) \frac{\sinh\left[\frac{\pi}{2}\xi(1-\cos\theta)\right] \sinh\left[\frac{\pi}{2}\xi(1+\cos\theta)\right]}{\sinh^2[\pi\xi]}. \tag{33}$$

To estimate the importance of the interference, given by the $\sin\phi$ in Eq. (33), we put

$$\phi \sim \frac{\Delta U_{\max} R_p}{\hbar v_R} \sim \frac{\Delta U_{\max}}{\Delta\varepsilon} \cdot \alpha R_p \xi. \tag{34}$$

For the model considered, two inequalities hold: $\Delta U_{\max} \gg \Delta\varepsilon$ and $\alpha R_p \gg 1$. If $\xi \geq 1$ then $\phi \gg 1$, and oscillations of $\sin^2\phi$ with variations of the velocity are so rapid that in any averaging procedure which is always performed for real cases it is possible to replace this factor by its mean value $\frac{1}{2}$. Moreover, under the condition $\phi \gg 1$, this replacement must always be made, as the one-trajectory approximation (*vide supra*) is not very good in this case. The probability $\bar{\mathscr{P}}_{12}$ averaged in this way is

$$\bar{\mathscr{P}}_{12} = 2 \exp[\pi\xi\cos\theta] \frac{\sinh\left[\frac{\pi}{2}\xi(1+\cos\theta)\right] \sinh\left[\frac{\pi}{2}\xi(1-\cos\theta)\right]}{\sinh^2 \pi\xi} \tag{35}$$

$$(\phi \gg 1).$$

If $\xi \ll 1$, then ϕ may be of the order of unity. It is under these conditions that the interference markedly influences the net result. Keeping the oscillating factor, but taking advantage of ξ being small, we find from (33)

$$\mathscr{P}_{12} = \sin^2 \phi \sin^2 \theta. \tag{36}$$

This equation is valid at $\phi \lesssim 1$ and goes over into (35) at $\phi \gg 1$ with replacement $\sin^2 \phi \to \frac{1}{2}$.

Thus the matching method allows one to obtain a convenient interpolation formula for the transition probability $\mathscr{P}_{12}$. It will be valid for various limiting cases.

III. General Formula for the Transition Probability and the Analytical Behavior of the Adiabatic Term Splitting

The contour map of the transition probability $\overline{\mathscr{P}}_{12}$ is shown in Fig. 3 as a function of $2/\pi\xi$ (dimensionless velocity) and η (dimensionless splitting in the coupling region). The region of very small velocities is not covered in Fig. 3 because conditions (13a) and (13b) do not hold there. The probability $\overline{\mathscr{P}}_{12}$ reaches its maximum value $\frac{1}{2}$ on the curve

$$\exp(\pi\xi \cos \theta) = \cosh(\pi\xi). \tag{37}$$

The two sides of the "watershed" lead to regions where one of the two perturbation treatments is applicable: perturbation with respect either to η or to $1/\xi$; both of these cases will be discussed later.

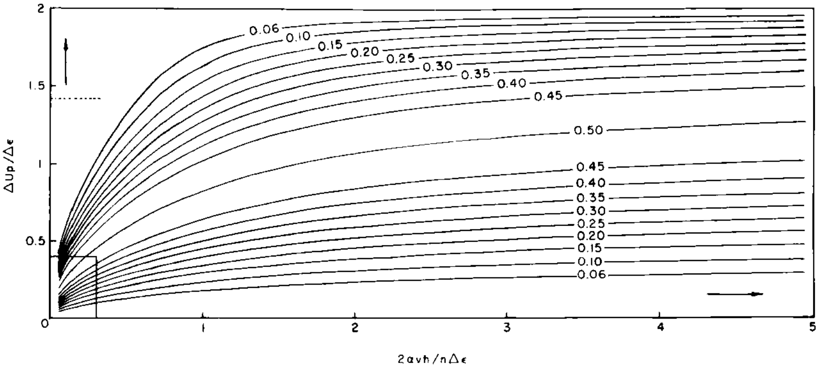

Fig. 3 Contour map of the transition probability $\overline{\mathscr{P}}_{12}$ as a function of η and $1/\xi$. The lower left corner corresponds to the region of the linear model validity. The curves are labeled with $\overline{\mathscr{P}}_{12}$ values.

Let us now consider some special cases which reduce to already-known results.

1. At the limit $\xi \gg 1$, $\eta \ll 1$, Eq. (35) will be

$$\bar{\mathscr{P}}_{12} = 2\exp\left(-\frac{\pi}{2}\xi\eta^2\right)\left[1 - \exp\left(-\frac{\pi}{2}\xi\eta^2\right)\right]. \tag{38}$$

Expressing ξ and η by physical parameters we find

$$\frac{\pi}{2}\xi\eta^2 = \frac{\pi}{2}\frac{\Delta U_p{}^2}{\hbar\alpha\Delta F}, \tag{39}$$

where ΔF stands for difference in slopes of diagonal terms at $R = R_p : \Delta F = \alpha\Delta\varepsilon$. After this identification it may be seen that (38) is just the Landau–Zener formula (Landau and Lifshitz, 1963). This formula refers to the linear model, if only two of the total four branching points τ_c of $U(t)$ are taken into account (Nikitin, 1968). These branching points are found from equation

$$\begin{aligned} \Delta U(\tau) &= [(\Delta F \Delta R)^2 + \Delta U_p{}^2]^{1/2} = 0 \\ \Delta R &= v_R\, t = \tau/\alpha, \end{aligned} \tag{40}$$

which gives

$$\tau_c = \pm i\frac{\alpha\Delta U_p}{\Delta F} = \pm i\theta. \tag{41}$$

All branching points for the exponential model are defined by the equation that follows from (10):

$$\Delta U(\tau) = \Delta\varepsilon[1 - 2\cos\theta\exp(-\tau) + \exp(-2\tau)]^{1/2} = 0. \tag{42}$$

From this we find (Fig. 4)

$$\tau_c = \pm i\theta \pm i\pi. \tag{43}$$

As the nonadiabatic transition probability depends on the analytical behavior of the adiabatic term splitting $\Delta U(\tau)$, it is not difficult to understand when the exponential model yields the same result as does the linear model. First, the branching points nearest to the real axis of τ should be the same for two models. Second, contribution from all other branching points of $\Delta U(\tau)$ for the exponential model have to be negligible. These two conditions are met at $\xi \to \infty, \eta \to 0$; and $\xi\eta^2$ is bound as stated above.

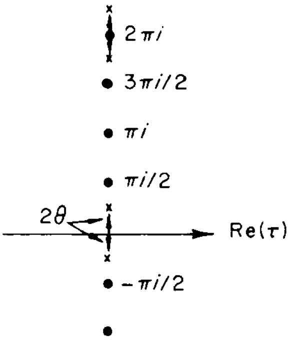

Fig. 4. Location of branching points (marked with ×) of the function $\Delta U(\tau)$ for the exponential model in the constant velocity approximation.

This smooth matching of two models at $\xi \gg 1$ and $\eta \ll 1$ allows application of the wave-mechanical theory of nonadiabatic coupling to the region shown in Fig. 3 (lower left corner), as this theory is available for the linear model (Nikitin, 1968). Thus, if conditions (13a) and (13b) are not satisfied, but still $\xi \gg 1$ and $\eta \ll 1$, the wave-mechanical version of the linear model must be used.

2. An interesting example corresponds to the particular value $\theta = \pi/2$. For this case the transition probability is

$$\bar{\mathscr{P}}_{12} = \tfrac{1}{2}\,\mathrm{ch}^{-2}(\pi\xi/2). \tag{44}$$

This equation may be derived from the results obtained by Rosen and Zener (Rosen and Zener, 1932) and by Demkov (Demkov, 1963), if the oscillating factor in their equations is replaced by its mean value. For this particular case Eq. (18) becomes

$$\begin{aligned} H_{11} - H_{22} &= \Delta\varepsilon \\ H_{12} &= \tfrac{1}{2}\,\Delta\varepsilon\exp(-\tau). \end{aligned} \tag{45}$$

Let us turn now to the perturbation approach for calculating $\mathscr{P}_{12}$. Brief comments will be sufficient here, because detailed analysis is given in Section IV in connection with more sophisticated models.

(*a*) *Weak interaction between zero-order terms.* Taking θ in (26) as being close to zero or π, we find

$$\bar{\mathscr{P}}_{12} = \sin^2\phi\cdot\theta^2\,\frac{\pi\xi\exp(\pi\xi)}{\sinh(\pi\xi)}, \qquad \theta \ll 1 \tag{46}$$

$$\mathscr{P}_{12} = \sin^2\phi\cdot\bar{\theta}^2\,\frac{\pi\xi\exp(-\pi\xi)}{\sinh(\pi\xi)}, \qquad \bar{\theta} = |\pi - \theta| \ll 1. \tag{47}$$

(*b*) *Almost adiabatic condition of coupling.* Taking $\pi\xi(1 - \cos\theta) \gg 1$ we find from (26)

$$\mathscr{P}_{12} = 4\sin^2\phi \frac{2\,\mathrm{sh}\left[\frac{\pi\xi}{2}(1 + \cos\theta)\right]}{\exp\left[\frac{\pi\xi}{2}(1 + \cos\theta)\right]} \exp[-\pi\xi(1 - \cos\theta)]. \tag{48}$$

The main velocity dependence of $\mathscr{P}_{12}$ comes from the last factor, so that under adiabatic conditions $\mathscr{P}_{12}$ depends exponentially on the velocity. If $\pi\xi(1 + \cos\theta) \gg 1$ also, then (48) becomes simplified to

$$\bar{\mathscr{P}}_{12} = 4\sin^2\phi \exp[-\pi\xi(1 - \cos\theta)]. \tag{49}$$

This result coincides with the formula that can be obtained in the framework of adiabatic perturbation theory if only one branching point of $\Delta U(\tau)$ is taken into account. The approximation to $\Delta U(\tau)$ that has to be put in (22) when integrating along the contour passing near the point $\tau_c = i\theta$ is

$$\Delta U(\tau) \simeq \Delta\varepsilon[(1 - e^{-2i\theta})(\tau - i\theta)]^{1/2}. \tag{50}$$

It is known that, if only one branching point is taken into account, the preexponential factor will be unity (Landau and Lifshitz, 1963; Dykhne, 1961). This is consistent with (49) where the preexponential factor is entirely due to the interference effect arising from two crossings.

If $\pi\xi(1 + \cos\theta) \lesssim 1$ then, taking into account the condition $\xi \gg 1$, this means that $\bar{\theta} = \pi - \theta \ll 1$. Then (48) can be presented as

$$\mathscr{P}_{12} = 4\sin^2\phi\left[1 - \exp\left(-\frac{\pi}{2}\xi\bar{\theta}^2\right)\right]\exp\left[-2\pi\xi + \frac{\pi\xi\bar{\theta}^2}{2}\right]. \tag{51}$$

This result can be obtained within the adiabatic perturbation treatment if two branching points $\tau_c = i\pi \pm i\theta$ are taken into account, and if the adiabatic splitting on the integration path is approximated by

$$\Delta U(\tau) \simeq \Delta\varepsilon[\bar{\theta}^2 + (\tau - i\pi)^2]^{1/2}. \tag{52}$$

The second factor in (51) is similar to that in the Landau–Zener formula. It is known to give the probability $1 - P_{12}$ of staying on the same initial adiabatic term. This coincidence is not accidental: The linear model takes into account only two branching points $\tau_c = \pm i\theta$ and the integration path is just the real axis of τ. In comparing these two integration paths (Fig. 5) the following interpretation can be given to the three factors in (51). Shifting of the integration path into the upper half-plane of τ up to the point

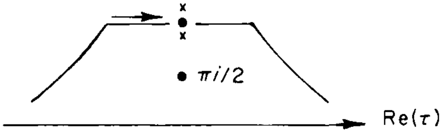

Fig. 5. Integration path for the system (32) in the adiabatic case.

$\tau_c = i\pi - i\theta$ yields the last (exponential) factor. Integration along the rectilinear part of the path gives the second factor, and double repetition of this procedure yields the first oscillating factor. It might be of interest to mention that the preexponential factor in (49) also can be related to the preexponential factor of $\mathscr{P}_{12}$ for the linear model at the limit, when nonadiabatic tunneling is essential (Nikitin, 1965a). We shall not discuss this question here.

It is seen that (51) goes over to (49) when conditions $\pi\xi\bar{\theta}^2/2 \gg 1$, $\bar{\theta} \ll 1$, are satisfied.

IV. Effect of the Turning Point

The general wave-mechanical problem related to the Hamiltonian (7) takes into account the effect of the turning point, i.e., the change of the velocity in the coupling region, on the transition probability. It is rather difficult to differentiate this effect from those related to breakdown of the quasi-classical approximation near turning points R_1 and R_2 on adiabatic terms U_1 and U_2 (Fig. 6). Thus, it is instructive to consider first the semiclassical approximation, but allowing for the only time dependence of v_R. However, an analytical solution for this case can only be obtained for two limiting cases: either to the first order with respect to H_{12} or for the almost adiabatic case.

The main question now is the selection of the trajectory. The choice of any function $R = R(t)$ different from (15) changes the time dependence of

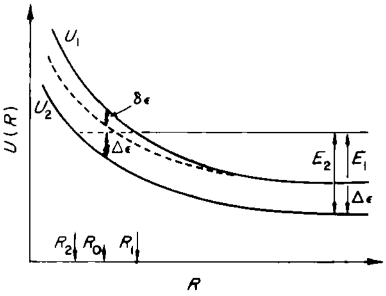

Fig. 6. Adiabatic characteristics of the Hamiltonian (7). The nonadiabaticity region is close to the turning points.

ΔU as given in (22) and introduces some new Hamiltonian $\bar{H}(t)$. Surely this choice is bound to be such that at $R \to \infty$, when the system moves far from the turning point, the matrix $\bar{H}(t)$ must go over to $H(t)$ Thus the mathematical result for the turning point consists of replacing $H(t)$ from (18) by another function $\bar{H}(t)$ that describes the evolution of the system during the time interval including the moment of the particle turning. The moment $t = 0$ will be referred to as the turning point.

The model put forward by Rosen and Zener (Rosen and Zener, 1932) can be thought to represent a simple extension of the exponential model in this sense. The Hamiltonian they considered was of the form

$$\begin{aligned} \bar{H}_{11} - \bar{H}_{22} &= \Delta\varepsilon \\ \bar{H}_{12} &= \frac{A}{4}\cosh^{-1}(\tau). \end{aligned} \tag{53}$$

The relation of (53) to (18) is quite clear: In the latter $\cos\theta = 0$ and $\exp(-\tau)$ is replaced by $\frac{1}{2}\,\mathrm{ch}^{-1}(\tau)$. The analytical behavior of the splitting $\Delta\bar{U}(\tau)$ calculated by making use of (53) is shown in Fig. 7. Besides branching points with imaginary parts which are the same as in (43) with $\theta = \pi/2$, there are poles $\tau_p = \pm i\pi/2 \pm i\pi n$. For large A, regions of location of branching points and poles are far apart, and this corresponds, in fact, to a weak effect of the turning points on the nonadiabatic coupling. When A diminishes, the branching points come closer to each other and to the poles.

The transition probability calculated by Rosen and Zener is

$$\mathscr{P}_{12} = \sin^2\left(\frac{A\pi}{4\alpha\hbar v}\right)\cosh^{-2}\left(\frac{\pi\Delta\varepsilon}{2\alpha\hbar v}\right) = \sin^2\left(\frac{\pi}{4}\frac{A}{\Delta\varepsilon}\,\xi\right)\cosh^{-2}\left(\frac{\pi}{2}\,\xi\right). \tag{54}$$

Comparing (54) with (33) under condition $\theta = \pi/2$ the difference between them can be ascribed only to the phase factor. Namely, in the Rosen–Zener formula the phase ϕ is given by

$$\phi = \int_{-\infty}^{\infty} \bar{H}_{12}(t)\,\frac{dt}{\hbar} \tag{55}$$

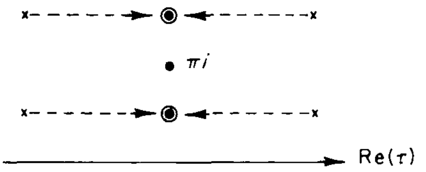

Fig. 7. Motion of the branching points (×) of $\Delta\bar{U}(\tau)$ for the model (53) with diminishing A. Poles of $\Delta U(\tau)$ are marked with O.

and is different from ϕ as defined by (31). But the real difference, as anticipated, is revealed only at $\xi \gg 1$ At $A/\Delta\varepsilon \gg 1$ this is again immaterial, as the oscillating factor is well represented by its mean value. Only at $A/\Delta\varepsilon \ll 1$ will the effect of the turning point be quite pronounced, and the interference cannot be accounted for by the simple matching procedure. Thus, in what follows we concentrate mainly on the case $A/\hbar\alpha v \ll 1$ and will use this ratio as a small parameter in the perturbation treatment.

Now the question arises as to the potential $U(R)$ for which the trajectory gives the Hamiltonian (53). Rapp and Sharp (1963) have found that this potential is not an exponential function of R, although it is quite close to it in the region $\Delta R \sim 1/\alpha$ near the turning point. As we are interested in the exponential model, we take as an average potential $U(R)$, which governs the classical motion of nuclei, the mean adiabatic electronic energy $U(R) = \frac{1}{2}[U_1(R) + U_2(R)]$, i.e.,

$$U(R) = B \exp(-\alpha R). \tag{56}$$

The trajectory for this potential is given by the equation

$$\exp(-\alpha R) = (E/B)\,\mathrm{ch}^{-2}(\alpha v t/2), \qquad E = \mu v^2/2, \tag{57}$$

where energy is now referred to $U(R)$ at infinity. Introducing (57) into (7) we find

$$\begin{aligned} \bar{H}_{11} - \bar{H}_{22} &= \Delta\varepsilon - \bar{A}\cos\theta[2\,\mathrm{ch}(\tau/2)]^{-2} \\ \bar{H}_{12} &= -(\bar{A}/2)\sin\theta[2\,\mathrm{ch}(\tau/2)]^{-2}, \end{aligned} \tag{58}$$

where

$$\bar{A} = (A/B)E.$$

The motion of the branching points τ_c with variations in $\bar{A}$ and the position of the poles τ_p of $\Delta\bar{U}(\tau)$ are shown in Fig. 8 for the case $\theta = \pi/2$. Here again the branching points τ_c come nearer to each other if $\bar{A}$ diminishes. But by taking θ to be small enough, we may reach a situation such that

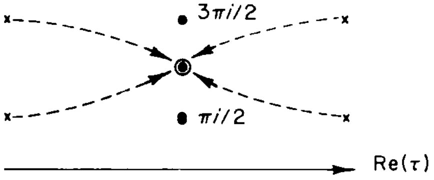

Fig. 8. Motion of the branching points (×) of $\Delta\bar{U}(\tau)$ for the model of Eq. (61) with diminishing $\bar{A}$; $\cos\theta = 0$.

two of the branching points will be far more important than the poles or other branching points. This again will be the linear model which was briefly mentioned in the preceding section.

The first calculation for the model of Eq. (58) has been made by Landau and Teller (Landau and Teller, 1936). These authors considered the case $\theta = \pi/2$, $\xi \gg 1$, $\bar{A}$ being small.

It proved to be of interest for many applications to consider the case of ξ having any value and also to take into account that the diagonal terms are not strictly parallel. For this rather general case the first-order perturbation treatment gives

$$\mathcal{P}_{12} = \left(\frac{a}{\hbar\alpha v}\right)^2 \left| \int_{-\infty}^{\infty} \cosh^{-2}\left(\frac{\tau}{2}\right) \exp\left[i\xi\tau + i\delta\xi \int^{\tau} \cosh^{-2}\left(\frac{\tau}{2}\right) d\tau \right] d\tau \right|^2 \tag{59}$$

$$\xi = \Delta\varepsilon/\alpha v\hbar, \qquad \delta\xi = \delta\varepsilon/\alpha v\hbar,$$

where

$$\begin{aligned} a &= -\tfrac{1}{8}\bar{A}\sin\theta = -\tfrac{1}{8}A(E/B)\sin\theta \\ \delta\varepsilon &= \tfrac{1}{4}\bar{A}\cos\theta = \tfrac{1}{4}A(E/B)\cos\theta. \end{aligned} \tag{60}$$

It is seen that a and $\delta\varepsilon$ are the respectively, the nondiagonal matrix element H_{12} and an additional shift of the energy difference $H_{11} - H_{22}$ referred to the turning point (Fig. 6). The integral in (59) is expressed by the confluent hypergeometric function (Nikitin, 1962b; Mies, 1964b)

$$\mathcal{P}_{12} = \left(\frac{4a^2}{\hbar\alpha v}\right)^2 \left(\frac{\pi\xi}{\sinh \pi\xi}\right)^2 |\Phi(1 + i\xi, 2, 4i\,\delta\xi)|^2. \tag{61}$$

To find the relation of this expression to that derived earlier [Eqs. (46) and (47)] and thus to make clear the effect of the turning point, two limiting procedures have to be applied to (58). First, θ or $\bar{\theta}$ must be very small and $\bar{A}$ (or $\delta\varepsilon$) must tend to infinity. Using parameters from expressions (58), Eq. (61) can be rewritten as

$$\mathcal{P}_{12} = \left(\frac{\bar{A}}{\Delta\varepsilon}\right)^2 \frac{\theta^2}{4}\xi^2 \left(\frac{\pi\xi}{\sinh \pi\xi}\right)^2 \left|\Phi\left(1 + i\xi, 2, -i\frac{\bar{A}}{\Delta\epsilon}\xi\right)\right|^2. \tag{62}$$

A similar expression is valid for $\bar{\theta}$: Only the sign of the argument in Φ must be reversed. To consider the case $\bar{A}/\Delta\varepsilon \gg 1$ we use asymptotic expansions for Φ (Erdelyi, 1953).

$$\lim_{\bar{A}/\Delta\epsilon\to\infty} \left|\Phi\left(1 + i\xi, 2, \pm i\frac{\bar{A}}{\Delta\varepsilon}\xi\right)\right|^2 = 4\sin^2\phi\, \frac{\sinh \pi\xi}{\pi\xi} \exp(\mp\pi\xi)\left(\frac{\bar{A}}{\Delta\epsilon}\xi\right)^{-2}. \tag{63}$$

The explicit expression for the phase will not be given here; if needed, it can be readily found from asymptotic formulas (Erdelyi, 1953). Now, introducing (63) into (62) we obtain Eqs. (46) and (47).

For vibrational energy transfer in molecular collisions, the $\delta\varepsilon/\Delta\varepsilon$ value is usually rather low. If there is no extra splitting, Φ is unity and (62) gives

$$\mathscr{P}_{12} = \left(\frac{A}{2B}\right)^2 4\left(\frac{\mu v}{\hbar\alpha}\right)^2 \left(\frac{\pi\xi}{\sinh \pi\xi}\right)^2 . \tag{64}$$

For the $n \rightarrow n+1$ vibrational transition the ratio $(A/2B)$ is identified with the dimensionless vibrational matrix element of an interaction, and the last factor can usually be presented in its asymptotic form:

$$\begin{aligned} \mathscr{P}_{n+1,n} &= Z^{\text{vib}}_{n+1,n} \cdot Z^{\text{tr}} \\ Z^{\text{vib}}_{n+1,n} &= (A/2B)^2 \\ Z^{\text{tr}} &= 4(\pi\Delta\varepsilon/\varepsilon_0)^2 \exp(-2\pi\xi), \end{aligned} \tag{65}$$

where

$$\varepsilon_0 = \hbar^2\alpha^2/2\mu.$$

This is the well-known Landau–Teller formula. If the extra splitting is small, but the Massey parameter is large, the following relation can be used:

$$\lim |\Phi(1 + i\xi, 2, 4i\delta\xi)|^2 = \frac{1}{y} J_1{}^2(2\sqrt{y}) \tag{66}$$

$$y = 4\xi\delta\xi, \qquad \xi \rightarrow \infty, \qquad |\delta\xi/\xi| \ll 1.$$

When expressed by parameters of the Hamiltonian (7), y does not depend on velocity:

$$y = -\frac{\Delta\varepsilon}{\varepsilon_0}\frac{1}{4}\frac{A}{B}\cos\theta. \tag{67}$$

Thus, under condition 1, $y \ll \xi$ the transitions probability can be written as

$$\mathscr{P}_{12} = (\lambda \sin\theta)^2 \frac{1}{\lambda\cos\theta} J_1{}^2(2(\lambda\cos\theta)^{1/2})\pi^2 \exp(-2\pi\xi) \tag{68}$$

$$\lambda = \tfrac{1}{4}(\Delta\varepsilon/\varepsilon_0)(A/B).$$

This equation clearly illustrates the dependence of the transition probability not only on velocity but on the relative position of the terms as well. The first factor in (68) is trivial, since it comes as a result of the perturbation treatment. The second factor represents the effect of small extra

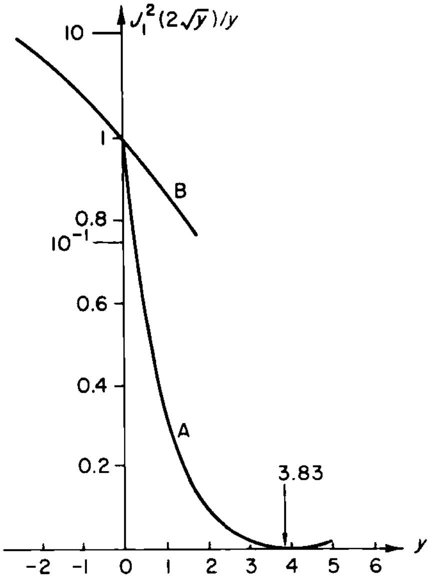

Fig. 9. Effect of the difference in diagaonal matrix elements on the transition probability under adiabatic condition for the model (58). Curve *A*, linear scale; curve *B*, logarithmic scale; $y = \lambda \cos \theta$.

splitting on the transition probability (Fig. 9). Two features should be mentioned: the oscillatory character of this factor at $\lambda \cos \theta > 0$ and its steep rise at $\lambda \cos \theta < 0$. This can be explained in the following way. As the difference $\bar{H}_{11} - \bar{H}_{22} \sim \lambda \cos \theta$ increases, the region of nonadiabatic coupling at $R \sim R_p$ shifts from the turning point R_0 towards a larger value of R. The phase difference ϕ in the internal region $R_0 < R < R_p$ becomes greater and this gives rise to oscillations. In limiting case corresponding to Eq. (63) this oscillatory factor appears to be $\sin^2 \phi$. When $\lambda \cos \theta < 0$ the diagonal elements of the Hamiltonian (7) cross at some point R_c. Two possibilities will arise here: The nonadiabaticity region is located either near R_c or near R_0. At small negative values of parameter $\lambda \cos \theta$ the main contribution to the nonadiabatic transition comes from the region near R_0, and the additional increase in $\mathscr{P}_{12}$ is due only to very small splitting of terms at R_0, as compared to $\Delta\varepsilon$. There are no oscillations in this case because there is no internal region (see Fig. 2, trajectory 2). At rather large negative values of $\lambda \cos \theta$ a situation will arise when R_c coincides with R_0 and even moves beyond it. Being located then in the classically accessible region and defining the position of the nonadiabaticity region, the point R_c

will represent the external boundary of the internal region $R_0 < R < R_c$. There again an oscillating factor will appear, as may actually be seen from (63), where the argument in Φ is $-(iA/\Delta\varepsilon)\xi$.

V. Quantum Corrections to the Semiclassical Formula

Consider now the exact quantum-mechanical problem of nonadiabatic coupling with the Hamiltonian (7). Nuclear motion is described by two coupled wave equations, the matrix H from (7) playing the part of the potential energy. Thus we have

$$\begin{aligned} -\frac{\hbar^2}{2\mu}\frac{d^2\psi_1}{dR^2} + \left[E + \frac{\Delta\varepsilon}{2} + \left(B - \frac{A}{2}\cos\theta\right)\exp(-\alpha R)\right]\psi_1 &= \frac{A}{2}\sin\theta\psi_2 \\ -\frac{\hbar^2}{2\mu}\frac{d^2\psi_2}{dR^2} + \left[E - \frac{\Delta\varepsilon}{2} + \left(B + \frac{A}{2}\cos\theta\right)\exp(-\alpha R)\right]\psi_2 &= \frac{A}{2}\sin\theta\psi_1. \end{aligned} \tag{69}$$

Here $E + \Delta\varepsilon/2 = k_1{}^2\hbar^2/2\mu$ and $E - \Delta\varepsilon/2 = k_2{}^2\hbar^2/2\mu$ are kinetic energies of nuciei referred to the first and the second electronic states, respectively. Boundary conditions for the scattering problem corresponding to an ingoing wave with unit amplitude and an outgoing wave with amplitude X in the first electronic state and to an outgoing wave with amplitude Y in the second electronic state are

$$\begin{aligned} \psi_1 &\sim \exp(-ik_1R) + X\exp(ik_1R) \\ \psi_2 &\sim Y\exp(ik_2R). \end{aligned} \qquad (R \to \infty) \tag{70}$$

In the classically inaccessible region wave functions ψ_1 and ψ_2 must tend to zero. This can be achieved by putting the functions as zero either at $R = 0$ (three-dimensional problem) or at $R = -\infty$ (one dimensional problem). When $E \ll B$ this difference in boundary conditions scarcely influences the net result. Corresponding numerical estimations have been made by Takayanagi (1959). Besides, for the three-dimensional case, the centrifugal potential $\hbar^2l(l+1)/2\mu R^2$ taken at some distance R_0 (*vide infra*) can be incorporated in E, thus reducing the three-dimensional problem to one-dimensional (the so-called modified wave number method) (see Section VI). The transition probability $\mathscr{P}_{12}$ related to system (69) is given by

$$\mathscr{P}_{12} = (k_2/k_1)|Y|^2 \tag{71}$$

The system (69) has been solved first by Jackson and Mott (1932) for a particular case $\cos\theta = 0$, making use of the distorted wave method which is a perturbation treatment of the nondiagonal interaction. As compared to the semiclassical approximation, the quantum formula for $\mathcal{P}_{12}$ depends not only on the difference in diagonal elements $H_{11} - H_{22}$, but also on the elements as such. To the first approximation with respect to the (A/B) ration the transition probability is given by

$$\mathcal{P}_{12} = \frac{\pi^2}{4}\left(\frac{A}{2B}\right)^2 [\Delta q^2]^2 \frac{\sinh \pi q_1 \sinh \pi q_2}{(\cosh \pi q_1 - \cosh \pi q_2)^2}, \tag{72}$$

where

$$q_1 = 2k_1/\alpha, \qquad q_2 = 2k_2/\alpha,$$
$$\Delta q^2 = q_2{}^2 - q_1{}^2 = 8\mu\, \Delta\varepsilon/\hbar^2\alpha^2 = 4\Delta\varepsilon/\varepsilon_0 . \tag{73}$$

Under quasi-classical conditions of motion the wave numbers k_1 and k_2 are usually large compared to $1/\alpha$. If this is the case, the last factor in (72) takes the simpler form

$$\frac{\sinh \pi q_1 \sinh \pi q_2}{(\cosh \pi q_1 - \cosh \pi q_2)^2} \to \tfrac{1}{4} \sinh^{-2}\left[\frac{\pi}{2}(q_1 - q_2)\right]. \tag{74}$$

Transition to the semiclassical approximation is accomplished as a result of the further reduction

$$\sinh\left[\frac{\pi}{2}(q_1 - q_2)\right] \to \sinh(\pi\xi), \tag{75}$$

which is valid under condition (30).

Putting Eq. (75) into Eq. (72), we obtain again (67). In case of an arbitrary θ, an extra factor (Mies, 1964a)

$$\Phi^2\left[1 + \frac{i}{2}(q_1 + q_2), 1 + \frac{i}{2}(q_2 - q_1), 2, \frac{\delta\varepsilon}{\Delta\epsilon}\right] \tag{76}$$

should be introduced in (72). This factor is similar to the extra factor Φ^2 in (61). The semiclassical result is obtained when the hypergeometric function (76) becomes the confluent hypergeometric function at the limit $(q_1 + q_2) \gg 1$. This is just the condition (13a).

Passing now beyond the limits of the first-order perturbation treatment let us note that, in the adiabatic case with $\xi \gg 1$, the transition probability varies quite considerably with very small changes of v. Thus the uncertainty $\Delta\varepsilon$ in the energy $\mu v^2/2$ of the semiclassical description, which takes the initial and final velocities as equal, should be accounted for. The most simple way to improve the semiclassical approximation is the following. At the limit of small velocities the exponential factor can be calculated by the Landau method (Landau and Lifshitz, 1963) without resorting to the semiclassical approximation. The preexponential factor can be found only as a result of integration of the coupled equation, so that it can be calculated with relative ease only in the semiclassical approximation. At $\xi \lesssim 1$, the semiclassical and wave-mechanical methods give practically the same result, At $\xi \geq 1$, when the results obtained by using the two methods differ, the exponential factor in $\mathscr{P}_{12}$ of the semiclassical formula should be replaced by the exponential wave-mechanical factor, but the semiclassical preexponential factor should be retained.

Let us now calculate the correct exponential factor for the nonadiabatic transition probability by the Landau method (Landau and Lifshitz, 1963). The basic formula is

$$\mathscr{P}_{12} \sim \exp\left[-2\frac{(2\mu)^{1/2}}{\hbar}\operatorname{Im}\left\{\int^{R_s}(E-U_2)^{1/2}\,dR-\int^{R_s}(E-U_1)^{1/2}\,dR\right\}\right], \tag{77}$$

Here the upper limit for integrals is a point of the stationary phase in the upper half-plane of the complex variable R closest to the real axis. The lower limit is any point on the real axis in the classically accessible region. All possible points R_s can be found from equations

$$\Delta U(R_s) = 0 \tag{78a}$$

$$U(R_s) = \infty. \tag{78b}$$

For the model considered these equations yield correspondingly

$$R_s = \ln(A/\Delta\varepsilon) + i\theta/\alpha = R_p + i\theta/\alpha \tag{79a}$$

$$R_s = -\infty. \tag{79b}$$

Contributions to $\mathscr{P}_{12}$ due to various stationary phase points are additive. As $\mathscr{P}_{12}$ is exponentially small, these contributions in general differ considerably, so that it is usually sufficient to take only one of them.

Consider first the contribution due to point (79a). The point R_s from (79a) coincides (trivial scaling being introduced) with τ_c from (43). Thus it is clear that the exponent in (77) can be presented as a series, the first term of which will be identical to the semiclassical approximation term. Take now the point R_p as the lower integration limit in (77) and expand radicals in power series to $\Delta U(R)/[E - U(R_p)]$ and $[U(R) - U(R_p)]/[E - U(R_p)]$. Putting $E - U(R_p) = E_R$ we find

$$\mathscr{P}_{12} \sim \exp\left[-\frac{2\,\Delta\varepsilon}{\hbar\alpha v_R} \operatorname{Im}\left\{ \int_{R_p}^{R_s} \frac{\Delta U(R)}{\Delta\varepsilon}\,dR + \int_{R_p}^{R_s} \frac{[U(R) - U(R_p)]\Delta U(R)}{2E_R\Delta\varepsilon}\,dR + \cdots \right\}\right], \tag{80}$$

where all higher-order terms are neglected. The energy E_R is now identified as the kinetic energy referred to the point R_p (compare Section II). It will be shown in the next section that the approximation (80) is sufficient for making two important corrections in the mean transition probability.

The integrals in (80) are

$$\operatorname{Im}\left[\int_{R_p}^{R_s} \frac{\Delta U}{\Delta\varepsilon}\,dR + \int_{R_p}^{R_s} \frac{(U - U_p)\Delta U}{2E_R\Delta\varepsilon}\,dR\right] = \frac{\pi}{2}(1 - \cos\theta) - \left(\frac{B\Delta\varepsilon}{2AE_R}\right)\frac{\pi}{4}(1 - \cos\theta)^2. \tag{81}$$

Introducing this expression into (80) we, at the same time, take into account that v_R is connected with $v_{R,1}$ or $v_{R,2}$ by the relation $v_R = v_{R,1,2}(1 \mp \Delta\varepsilon/4E_{R,1,2})$, where the second term is considered to be a small correction to unity. This correction must be kept only in the leading term; in the second term in (80) E_R can be replaced safely by $E_{R,1}$. Thus (80) becomes

$$\mathscr{P}_{12} \sim \exp\left[-\frac{\pi\Delta\varepsilon}{\hbar\alpha v_{R,1}}(1 - \cos\theta)\left\{1 - \frac{B\Delta\varepsilon}{4AE_{R,1}}(1 - \cos\theta) - \frac{\Delta\varepsilon}{4E_{R,1}}\right\}\right]. \tag{82}$$

The transition probability for the reverse process (according to Figs. 1 and 6 this is an activation process) is given by Eq. (82)), with $v_{R,1}$ and $E_{R,1}$ replaced by $v_{R,2}$ and $E_{R,2}$, and the sign before the last term reversed. The two correction terms in braces are supposed to be small compared to unity. Nevertheless their absolute contribution to $\mathscr{P}_{12}$ may be quite considerable, as they are multiplied by a large number, i.e., the Massey parameter for adiabatic collisions. The next correction terms that are not written here are of the order of $(\Delta\varepsilon/E_R)^2$ and $(\Delta\varepsilon/E_R)^2(B/A)^2$.

We concentrate now on the second term in braces, taking into account that $v_{R,1}$ depends on B:

$$v_{R,1} = \left(\frac{2}{\mu}(E_1 - U_p)\right)^{1/2} = \left(\frac{2}{\mu}\left(E_1 - \frac{B\Delta\varepsilon}{A}\right)\right)^{1/2}. \tag{83}$$

If the first factor in the exponent of Eq. (82) is fixed, then taking the second factor into account will increase the transition probability. This increase is due to the contribution of tunneling which is completely neglected for the constant velocity approximation. The same qualitative effect is known for the linear model (Nikitin, 1968). To compare the two models, we consider the case $\xi \to \infty$, $\theta \to 0$, $\xi\theta^2$ is bound. A parameter which describes tunneling corrections for the linear model is $\varepsilon = (E_R/\Delta U_p)(\Delta F/F)$, where $\Delta F = |F_1 - F_2|$, $F = (F_1F_2)^{1/2}$, and $F_1 = (d/dR)H_{11}$, $F_2 = -(d/dR)H_{22}$, calculated at $R = R_p$ (Nikitin, 1968). If this parameter is used to represent the first correction in Eq. (82), we find

$$\frac{B}{4A}\frac{\Delta\varepsilon}{E_R}(1-\cos\theta) = \frac{B}{4A}\frac{\Delta\varepsilon}{E_R}\frac{\theta^2}{2} = \left[\frac{F_1+F_2}{(F_1F_2)^{1/2}}\right]\frac{\theta}{8}\cdot\frac{1}{\varepsilon}, \tag{84}$$

with

$$\varepsilon = \left(\frac{E_R}{\Delta\varepsilon\theta}\right)\frac{|F_1 - F_2|}{F}.$$

At $\xi\theta^2$ and ε fixed and with θ tending to zero, this correction vanishes. This is consistent with the results found within the linear model for which the first correction is proportional to $1/\varepsilon^2$. Moreover, there is no such parameter in the linear model as the first factor in Eq. (84), so that correction in Eq. (82) is essentially due to the nonlinear character of the model.

To obtain a correction that does not vanish for the linear model, the higher-order terms in the expansion (80) should be retained.

Consider now the effect of $U(R_p)$ as such on the transition probability, taking the ratio $B\Delta\varepsilon/AE$ to be small. Expanding Eq. (83) in powers of $B\Delta\varepsilon/AE$ and summing up the contributions to the second correction term, we obtain

$$\mathscr{P}_{12} \sim \exp\left[-\frac{\pi\Delta\varepsilon}{\hbar\alpha v_1}(1-\cos\theta)\left\{1 + \frac{B\Delta\varepsilon}{4AE_1}(1+\cos\theta) - \frac{\Delta\varepsilon}{4E_1}\right\}\right], \tag{85}$$

where the velocity and the kinetic energy refer to infinite separation. The effect of the turning point becomes more and more pronounced as the ratio $B\Delta\varepsilon/AE_1$ increases, and the nonadiabaticity region comes closer to the turning point. When the correction is of the order of unity, the expansion (80) is not valid, and it is expected that under these conditions the contribution from point (79b) will be predominant.

In calculating this contribution we confine ourselves to the case $\Delta\varepsilon \gg A\exp(-\alpha R_k)$, which means, in terms of parameters introduced in Section

IV, that the extra shifting $\delta\varepsilon$ of the terms is small compared to $\Delta\varepsilon$. Then making use of the simplification $\Delta U = \Delta\varepsilon$, Eq. (77) can be rewritten as

$$\mathscr{P}_{12} \sim \exp\left[-2\frac{(2\mu)^{1/2}}{\hbar}\,\mathrm{Im}\left\{\int_{R_2}^{-\infty}\left(E+\frac{\Delta\varepsilon}{2}-U\right)^{1/2}dR - \int_{R_1}^{-\infty}\left(E-\frac{\Delta\varepsilon}{2}-U\right)^{1/2}dR\right\}\right]. \tag{86}$$

Calculation of these integrals gives (Landau and Lifshitz, 1963)

$$\mathscr{P}_{12} \sim \exp\left[-\frac{2\pi}{\hbar\alpha}((2\mu E_2)^{1/2} - (2\mu E_1)^{1/2})\right]. \tag{87}$$

Further expansion then gives

$$\mathscr{P}_{12} \sim \exp\left[-\frac{2\pi\Delta\varepsilon}{\hbar\alpha v_1}\left(1-\frac{\Delta\varepsilon}{4E_1}\right)\right]. \tag{88}$$

This expression has to be compared with Eq. (85). Of particular interest is the fact that when the correction term in (85) becomes large and the expansion, as such, is invalid, then Eq. (88) gives the correct result. Thus the following simple interpolation formula, which takes into account the effect of the turning point, can be suggested:

$$\mathscr{P}_{12} = \begin{cases} \mathscr{A}_1 \exp\left[-\dfrac{\pi\Delta\varepsilon}{\hbar\alpha v_{R,1}}(1-\cos\theta)\left\{1-\dfrac{B\Delta\varepsilon}{4AE_{R,1}}(1-\cos\theta)-\dfrac{\Delta\varepsilon}{4E_{R,1}}\right\}\right] & \\ \qquad (B\Delta\varepsilon(1-\cos\theta)\,4AE_{R,1} \ll 1) & \text{(89a)} \\ \mathscr{A}_2 \exp\left[-\dfrac{2\pi\Delta\varepsilon}{\hbar\alpha v_1}\left\{1-\dfrac{\Delta\varepsilon}{4E_1}\right\}\right] & \text{(89b)} \\ \qquad (\delta\varepsilon/\Delta\varepsilon \ll 1). & \end{cases}$$

Here the preexponential factors can be found by comparing these expressions with the corresponding semiclassical asymptotic expansions. The main terms in the exponents of Eqs. (89a) and (89b) coincide with those of Eqs. (48) and (68).

The first correction to the semiclassical approximation could also be found by making use of the following arguments which are valid for any interaction potential (Nikitin, 1962).

The semiclassical result comes at the limit of the wave-mechanical formula for $\mathscr{P}_{12}$, provided that $|v_1 - v_2|$ is small. The parameter v of the semiclassical expression is some symmetrical function of v_1 and v_2. For small $\Delta v = |v_2 - v_1|$ we can write

$$v(v_1, v_2) = v(v_1, v_1) + \left.\frac{\partial v(v_1, v_2)}{\partial v_2}\right|_{v_2=v_1} \Delta v_2 + \cdots. \tag{90}$$

But for any symmetrical function we have

$$\left.\frac{\partial}{\partial v_2} v(v_1, v_2)\right|_{v_2=v_1} = \frac{1}{2}\frac{d}{dv_1} v(v_1, v_1) = \tfrac{1}{2}. \tag{91}$$

Thus we obtain

$$v = v_1\left(1 - \frac{\Delta\varepsilon}{4E_1} + \cdots\right). \tag{92}$$

Higher-order terms do depend on the explicit form of the function $v(v_1, v_2)$ but the first (v) and the second ($\partial v/\partial v_1$) do not.

VI. Mean Transition Probability, Cross Section, and Rate Constant for a Nonadiabatic Process

The mean transition probability $\langle\mathscr{P}_{12}\rangle$ corresponding to the thermal velocity distribution is of interest for many applications. For the one-dimensional model considered, averaging should be performed with a normalized one-dimensional flux taken as the distribution function

$$f(E)\,dE = \exp(-\beta E)\,d(\beta E). \tag{93}$$

Let us consider first the calculation of $\langle\mathscr{P}_{12}\rangle$ in the case of an exponentially small transition probability. Representing $\mathscr{P}_{12}$ in a more general form, we have

$$\langle\mathscr{P}_{12}\rangle \sim \int \exp\left[-\Xi(\varepsilon)\left(1 - \frac{E_0}{2\varepsilon} - \frac{\Delta\varepsilon}{4\varepsilon}\right)\right]\exp(-\beta\varepsilon)\beta\,d\varepsilon \tag{94}$$

$$\Xi(\varepsilon) = \begin{cases} \dfrac{\pi\Delta\varepsilon}{\hbar\alpha(2\varepsilon/\mu)^{1/2}}(1 - \cos\theta) & \text{for (89a)} \\[2ex] \dfrac{2\pi\Delta\varepsilon}{\hbar\alpha(2\varepsilon/\mu)^{1/2}} & \text{for (89b)} \end{cases}$$

$$E_0 = \begin{cases} \dfrac{B\Delta\varepsilon}{4A}(1 - \cos\theta) & \text{for (89a)} \\[2ex] 0 & \text{for (89b)} \end{cases}$$

$$\varepsilon = \begin{cases} E_{R,1} & \text{for (89a)} \\ E_1 & \text{for (89b).} \end{cases}$$

Here the first factor in the integrand is meant to represent the exponential functions from Eqs. (89). In general, the integration over $E_{R,1}$ should begin from the level $E_{R,1} = U_p$, which represents the activation barrier. Shifting the energy scale we find

$$\langle \mathscr{P}_{12} \rangle \sim \exp(-\beta U_p) \int_0^\infty \exp\left[-\Xi(\varepsilon)\left(1 - \frac{E_0}{2\varepsilon} - \frac{\Delta\varepsilon}{4\varepsilon}\right)\right] \exp(-\beta\varepsilon)\beta \, d\varepsilon. \tag{95}$$

The asymptotic expression for $\mathscr{P}_{12}$ can be used as the integrand only if the main contribution to the integral comes from a region near a value ε^* for which $\Xi(\varepsilon^*) \gg 1$. This point is found from the steepest descent procedure

$$\Xi(\varepsilon^*) - \beta\varepsilon^* = \min. \tag{96}$$

Near $\varepsilon = \varepsilon^*$ the integrand is approximated by the Gaussian function, two correction terms being taken at this point. Straightforward integration then gives

$$\begin{aligned} \langle \mathscr{P}_{12} \rangle &\sim 2\left(\frac{\pi}{2}(\beta\varepsilon^*)\right)^{1/2} \exp(-\beta U_p^*) \\ &\quad \times \exp\left[-\Xi(\varepsilon^*) + E_0\beta + \frac{\Delta\varepsilon}{2}\beta\right] \exp(-\beta\varepsilon^*) \end{aligned} \tag{97}$$

$$U_p^* = \begin{cases} U(R_p) & \text{for (89a)} \\ 0 & \text{for (89b).} \end{cases}$$

Rearranging the terms we can present Eq. (97) in the form

$$\langle \mathscr{P}_{12} \rangle \sim 2\left(\frac{\pi}{3}\right)^{1/2} (\Gamma)^{1/3} \exp(-3\Gamma^{2/3}) \times \exp(-\beta E_a) \times \exp\left(\frac{\Delta\varepsilon}{2}\beta\right) \tag{98}$$

$$\begin{aligned} \Gamma = (\beta\varepsilon^*)^{3/2} &= \begin{cases} \dfrac{\pi}{2} \dfrac{\Delta\varepsilon}{\hbar\alpha} \left(\dfrac{\mu}{2kT}\right)^{1/2} (1 - \cos\theta) & \text{for (89a)} \\ \pi(\Delta\varepsilon/\hbar\alpha)(\mu/2kT)^{1/2} & \text{for (89b)} \end{cases} \\ E_a &= \begin{cases} U_p - E_0 = \dfrac{B\Delta\varepsilon}{2A}(1 + \cos\theta) & \text{for (89a)} \\ 0 & \text{for (89b).} \end{cases} \end{aligned} \tag{99}$$

The first factor here is due to the mean semiclassical transition probability. The second (Arrhenius) factor is due to the existence of an effective activation energy E_a. This is the sum of the height $U(R_p)$ of the nonadiabaticity region and the first quantum correction that arises from the second term in Eq. (80). The last factor in Eq. (98), which is due to the last correction term in Eqs. (89a) and (89b) ensures detailed balancing for the direct and reverse processes

$$\langle \mathscr{P}_{12} \rangle / \langle \mathscr{P}_{21} \rangle = \exp(\beta \Delta\varepsilon). \tag{100}$$

The conditions under which higher-order terms in the expansion (80) can be neglected in calculating the mean transition probability according to Eq. (94) can now be formulated as

$$2(\Gamma)^{2/3} = \Xi(\varepsilon^*) \gg 1 \tag{101a}$$

$$2(\Gamma)^{2/3} \gg \beta \Delta\varepsilon \tag{101b}$$

$$2(\Gamma)^{2/3} \gg \beta E_0 . \tag{101c}$$

Consider now the case of $E_a = 0$ in more detail. If $\beta \Delta\varepsilon \ll 1$, then the last factor in (98) can be approximately replaced by unity. At the same time Eq. (100) can be considered to be satisfied, as a very slight change in $\langle \mathscr{P}_{12} \rangle$ and $\langle \mathscr{P}_{21} \rangle$ will be sufficient for consistency with Eq. (100) [e.g., multiplying uncorrected and, consequently, equal values $\langle \mathscr{P} \rangle$ by $(1 + \Delta\varepsilon\beta/2)$ and $(1 - \beta\Delta\varepsilon/2)$, respectively]. This "trimming" of the semiclassical approximation is widely used in kinetic problems including systems with small separations between energy levels. If $\Delta\varepsilon\beta \gg 1$, then the last factor in Eq. (98) is important. Higher-order terms, which would come as extra factors, are of the order $\exp[\simeq \Xi(\varepsilon^*)(\Delta\varepsilon/2\beta)^2]$. They can be neglected only under condition (101b). This condition (when $\beta\Delta\varepsilon > 1$) is more restrictive than that for the adiabatic semiclassical approximation (101a). Nevertheless condition (101b) is fulfilled for many practical applications, so that $\langle \mathscr{P}_{12} \rangle$ can be represented by equation (99).

When averaging and calculating Eq. (97) we explicitly considered only the exponential factor in $\overline{\mathscr{P}}_{12}$. Any preexponential factor which may be eventually present in $\overline{\mathscr{P}}_{12}$ can be simply carried out through the integral sign in Eq. (94) or (95) with the energy ε substituted by $\varepsilon^* = (\Gamma)^{2/3} kT$. In particular, for the Landau–Teller formula (65) we find

$$\langle \mathscr{P}_{n+1,n} \rangle = Z^{\text{vib}}_{n+1,n} 8(\pi\Delta\varepsilon/\varepsilon_0)^2 (\pi/3)^{1/2} \chi^{1/2} \exp[-3\chi + \beta\Delta\varepsilon/2] \tag{102}$$

$$\chi = (\beta\pi^2\Delta\varepsilon^2/4\varepsilon_0)^{1/3}.$$

Consider now the general case of the semiclassical approximation making use of formula (21). The average transition probability $\langle \mathscr{P}_{12} \rangle$ is given by

$$\langle \mathscr{P}_{12} \rangle = \exp[-\beta E_a] \int_0^\infty 2 \exp(\pi\xi \cos\theta) \times \frac{\sinh\left(\frac{\pi}{2}\,\xi(1-\cos\theta)\right)\sinh\left[\frac{\pi}{2}\,\xi(1+\cos\theta)\right]}{\sinh^2(\pi\xi)} \exp(-\beta E)\beta\, dE. \qquad (103)$$

The specific case $\theta \ll 1$ has been discussed earlier in connection with the linear model (Nikitin, 1968). For $\bar{\theta} \ll 1$ and $\Gamma \gg 1$ the mean transition probability is exponentially small, so that it can be calculated according to Eq. (98). For intermediate values of θ the results of some numerical calculations are presented in Fig. 10. For large values of the argument $\gamma = (\Delta\varepsilon/\hbar\alpha)(\mu/2kT)^{1/2}$, the curves presented are described by Eq. (98) where an additional factor of 2 should be introduced to take into account the double crossing of the nonadiabaticity region.

Now let us consider the mean value of $\mathscr{P}_{12}$ in Eq. (64) which is of interest for the theory of vibrational relaxation. The function $f(\gamma)$ defined by

$$f(\gamma) = \int_0^\infty (\pi\xi/\sinh \pi\xi)^2(\beta E)\exp(-\beta E)\, d(\beta E) \qquad (104)$$

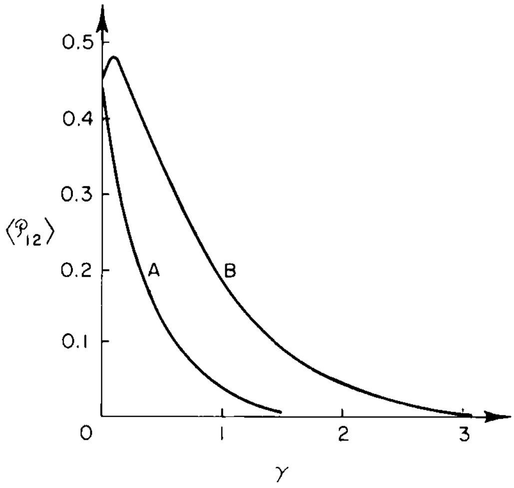

Fig. 10. Mean transition probability (27) as a function of $\gamma = (\pi\Delta\varepsilon/\alpha\hbar)(\mu\beta/2)^{1/2}$. Curves A and B correspond to $\cos\theta = -\frac{1}{3}, \frac{1}{3}$.

has the following asymptotic behavior:

$$f(\gamma) \approx 8\left(\frac{\pi}{3}\right)^{1/2} \gamma^{7/3} \exp(-3\gamma^{2/3}), \qquad \gamma = \frac{\pi\Delta\varepsilon}{\hbar\alpha}\left(\frac{\mu\beta}{2}\right)^{1/2}. \tag{105}$$

Crude estimation of $f(\gamma)$ (discrepancy ~20%) in the range $0 < \gamma < 20$ can be made by means of the interpolation formula (Keck and Carrier, 1965)

$$f(\gamma) \approx \tfrac{1}{2}[3 - \exp(-2\gamma/3)]\exp(-2\gamma/3). \tag{106}$$

If the conditions are such that Eq. (101b) is not fulfilled, the mean transition probability can be found by direct averaging of the wave-mechanical expression (72) with possible use of Eq. (74). Corresponding numerical calculations have been performed by Takayanagi and Miyamoto (1959). The dependence of $\langle \mathscr{P}_{12} \rangle$ on two parameters, i.e., the reduced temperature $T^* = 2/\beta\varepsilon_0$ and the reduced transferred energy $\Delta(q^2) = 4\Delta\varepsilon/\varepsilon_0$, is shown in Fig. 11, which is taken from the paper by the above authors.

The cross-section σ_{12} for a nonadiabatic process with a spherically symmetrical interaction is defined by the following semiclassical expression:

$$\sigma_{12}(\theta, E) = 2\pi \int_0^\infty \mathscr{P}_{12}(\theta, v, b) b\, db. \tag{107}$$

Here $\mathscr{P}_{12}$ depends on the impact parameter b, as v_R and ϕ depend on b. With respect to v_R, this dependence can be expressed as

$$v_R = \{(2/\mu)^{1/2}[E - E(b^2/R_p{}^2) - E_a]\}^{1/2}. \tag{108}$$

The probability $\mathscr{P}_{12}$ becomes lower as ξ increases and ϕ decreases. Practically, the upper limit in the integral (107) depends on one of these parameters, so that the two different cases may be discussed separately.

Let us suppose that in the same region of impact parameters the following two conditions are satisfied:

$$\xi(b) > 1 \tag{109a}$$

$$\phi(b) \gg 1. \tag{109b}$$

Then $\mathscr{P}_{12}$ in Eq. (107) can be replaced by $\overline{\mathscr{P}}_{12}$ and the upper limit taken as equal to R_p. Considering for simplicity, the case $E_a = 0$, we put $E_R = E(1 - b^2/R_p{}^2)$ and represent Eq. (107) as

$$\sigma_{12}(\theta, E) = \pi R_0{}^2 \times \frac{1}{E}\int_0^E \overline{\mathscr{P}}_{12}(\theta, E_R)\, dE_R. \tag{110}$$

This approximation is known as the MWN method (modified wave number method) (Takayanagi, 1959). An illustrative example of the function $\sigma_{12} = \sigma_{12}(E)$ together with corresponding values of $\langle \mathscr{P}_{12} \rangle$ are given in Table I for $\cos\theta = 0$. These functions are of interest for the theory of charge transfer in collisions.

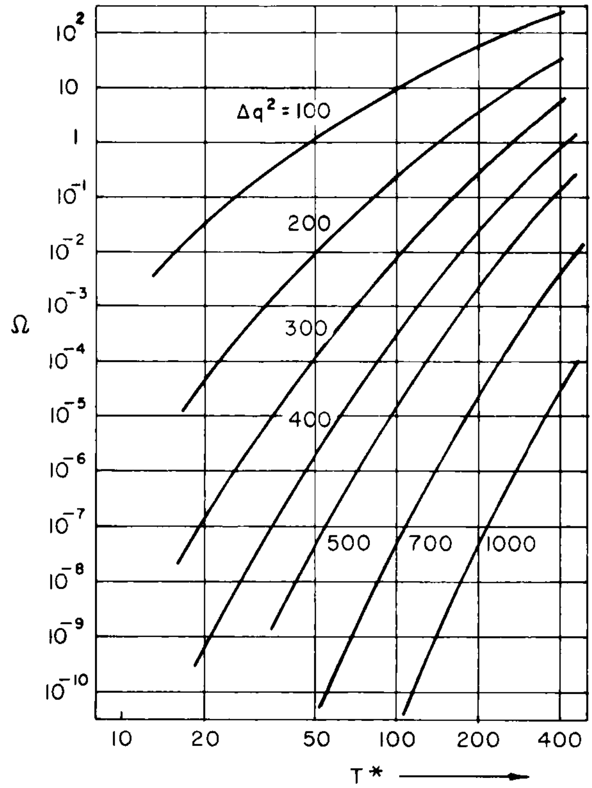

Fig. 11. Mean reduced transition probability Ω for the quantum case [Eq. (72)] as a function of reduced temperature $T^* = 2kT/\varepsilon_0$ and reduced transferred energy $\Delta q^2 = 4\Delta\varepsilon/\varepsilon_0$. Ω is defined by

$$\Omega = \int_0^\infty \frac{(\Delta q^2)^2 \sinh(\pi q_1)\sinh(\pi q_2)}{[\cosh(\pi q_1) - \cos(\pi q_2)]^2} \exp(-q_1{}^2/2T^*) \frac{q_1 dq_1}{T^*}$$

and related to $\mathscr{P}_{12}$ by $\langle \mathscr{P}_{12} \rangle = (A/2B)^2 \Omega(T^*, \Delta q^2)$.

TABLE I

A SHORT TABLE USEFUL IN CALCULATION OF CROSS SECTIONS AND RATE CONSTANTS FOR THE NONRESONANCE CHARGE TRANSFER AND SIMILAR PROCESSES

y	$f_1 = \int_0^\infty \frac{\exp(-x^2)2x\,dx}{\cosh^2(y/x)}$	$f_2 = \int_0^1 \frac{2x\,dx}{\cosh^2(y/x)}$
0.0	1.000	1.000
0.2	0.879	0.859
0.4	0.706	0.647
0.6	0.549	0.456
0.8	0.422	0.308
1.0	0.322	0.203
1.2	0.245	0.131
1.4	0.186	0.084
1.6	0.142	0.054
1.8	0.109	0.034
2.0	0.083	0.022
2.2	0.064	0.14
2.4	0.049	0.009
2.6	0.038	0.0055
2.8	0.030	0.0035
3.0	0.023	0.0027
3.2	0.018	0.0014
3.4	0.014	0.0009
3.6	0.011	0.0006
3.8	0.009	0.0004
4.0	0.007	0.0002
$y > 4$	$f_1 = 8y^{1/3}\left(\frac{\pi}{3}\right)^{1/2} \exp[-3y^{2/3}]$	$f_2 = (4/y)\exp(-2y)$
	$\sigma_{12} = \frac{1}{2}\pi R_p^2 f_2(y),$	$y = \pi\Delta\varepsilon/2\hbar\alpha v$
	$k_{12} = \frac{1}{2}\pi R_p^2 \left(\frac{8kT}{\pi\mu}\right)^{1/2} f_1(y),$	$y = \frac{\pi\Delta\varepsilon}{2\hbar a}\left(\frac{\mu}{2kT}\right)^{1/2}$

If two alternative conditions

$$\xi(b) \ll 1 \tag{111a}$$

$$\phi(b) < 1 \tag{111b}$$

are satisfied, Eq. (107) can be presented as

$$\sigma_{12}(\theta, E) = 2\pi \int_0^\infty \sin^2 \phi(b, E) \sin^2 \theta b \, db. \tag{112}$$

The value of the integral (112) depends on the critical value of b_c at which $\phi(b, E) \sim 1$. To calculate ϕ in this region we can use Eq. (55) together with adiabatic splitting $\Delta U(R)$ corresponding to the Hamiltonian (7). Here A must be considered as a function of R corresponding to the asymptotic form (2) of matrix elements. If a trajectory is represented by a straight path, Eq. (55) will be

$$\phi(b, E) = \tfrac{1}{2} \int \Delta U[(b^2 + v^2 t^2)^{1/2}](dt/\hbar) \tag{113}$$

$$(b^2 + v^2 t^2)^{1/2} < R_p.$$

Now, under condition (111a), $\Delta U(R)$ as integrand can be simplified as

$$\begin{aligned} \Delta U(R) &= \{\Delta\varepsilon^2 - 2\Delta\varepsilon A(R) \cos\theta \exp(-\alpha R) + A^2(R) \exp(-2\alpha R)\}^{1/2} \\ &\approx A(R) \exp(-\alpha R). \end{aligned} \tag{114}$$

Then the limits of integration can be extended to $\pm\infty$ and integration as such can be performed in line with the main idea of the exponential model, considering $A(R)$ as a constant $A(b)$. Thus we obtain

$$\phi(b, E) = [A(b)/\hbar v] \exp(-\alpha b)(2\pi b/\alpha)^{1/2}. \tag{115}$$

This value of ϕ can now be introduced into Eq. (112) for actual calculation. Detailed analysis shows (Smirnow, 1964a) that the cross section can be written as

$$\sigma_{12} = \sin^2\theta \, \pi b_c{}^2(E)[1 + O(1/\alpha\beta_c)], \tag{116}$$

where $b_c(E)$ is given by equation

$$\phi(b_c, E) = 0.28. \tag{117}$$

Cross sections (110) and (116) could be matched in the energy region $b_c(E) \sim R_p$. We shall not discuss this here, but refer to the paper by Smirnov (1966b).

The rate constant k_{12} for some nonadiabatic process in thermal collision is defined in terms of the corresponding cross section σ_{12} by

$$k_{12} = \int \sigma_{12}(v) v F(v) \, d^3 v, \tag{118}$$

where $F(v)$ represents the Maxwell–Boltzmann distribution function. Expressed in terms of kinetic energy (118) will be

$$k_{12} = \left(\frac{8}{\pi\beta\mu}\right)^{1/2} \int_0^\infty \sigma_{12}(E)(\beta E)\exp(-\beta E)\, d(\beta E). \tag{119}$$

Introducing Eq. (110) into Eq. (119) and integrating by parts we find

$$k_{12} = (8/\pi\beta\mu)^{1/2} \times \pi R_p{}^2 \times \langle \mathscr{P}_{12} \rangle. \tag{120}$$

Thus for this case the three-dimensional problem reduces to the one-dimensional problem; i.e., the average transition probability is multiplied by the "hard-sphere" collision number. Equation (94) is easily extended to more complex systems if the idea of the transition state method is adopted (Glasstone, *et al.*, 1941). The transition probability is then referred to the motion along the reaction coordinate, and all other degrees of freedom contribute only to the partition functions. The transition state is defined by $R = R_p$ (or, more exactly, by $R = R_s$; see Section V), and a generalization of (94) would be

$$k_{12} = (kT/2\pi\hbar)(F^{\neq}/F)\langle \mathscr{P}_{12} \rangle, \tag{121}$$

where $F^{\neq}$ and F are the partition functions of the transition state and the initial system respectively. Here $\langle \mathscr{P}_{12} \rangle$ includes the Arrhenius factor which is due to the activation energy corresponding to the nonadiabaticity region.

VII. Extensions of the Exponential Model to Nonexponential Interactions

Applications of the exponential model are not confined to those processes in which energy matrix is really of an exponential form. In previous sections we discussed various approximate solutions for a nonadiabatic process provided that the Hamiltonian is given by Eq. (7). We shall now consider some problems which arise if the matrix elements are not written as a simple exponential function. The basic question to answer is how the transition probability depends on approximations made in the adiabatic part of a problem.

A. Relation between the Exponential and the Morse Interaction

One possible extension of the exponential model consists in approximating the matrix elements H_{ik} by a sum of exponentials with different exponents. The simplest way would be to use the Morse function in approximating H_{11} and H_{22} instead of a repulsive exponential. This kind of approach was used by several authors in connection with studies of the vibrational excitation of molecules in collisions (Zener, 1932; Devonshire, 1937; Cottrell and Ream, 1955; Takayanagi and Miamoto, 1959; Allen and Feuer, 1964; Calvert and Amme, 1966). In processes like these the nondiagonal matrix element H_{12} is related to H_{11} and H_{22} by the interaction assumed. Thus, following papers cited above we consider now the Hamiltonian

$$H = \begin{pmatrix} B\exp(-\alpha R) - 2B\exp(-\alpha R/2) + \Delta\varepsilon/2 & -\frac{A}{2}\exp(-\alpha R) - \frac{A}{2}\exp(-\alpha R/2) \\ -\frac{A}{2}\exp(-\alpha R) - \frac{A}{2}\exp(-\alpha R/2) & B\exp(-\alpha R) - 2B\exp(-\alpha R/2) - \Delta\varepsilon/2 \end{pmatrix} \tag{122}$$

written in a form closely related to the Hamiltonian given by Eq. (7). The solution of the corresponding coupled wave mechanical equations similar to that in Eq. (69) gives the following expression for the transition probability:

$$\mathscr{P}_{12} = \frac{\pi^2}{4}\left(\frac{A}{2B}\right)^2 (\Delta q)^2 \frac{\sinh(2\pi q_1)\sinh(2\pi q_2)}{(\cosh(2\pi q_1) - \cosh(2\pi q_2))^2} W(q_0, q_1, q_2), \tag{123}$$

where q_1, q_2, and Δq are defined by Eq. (73) and

$$W(q_0, q_1, q_2) = \frac{[|\Gamma(-q_0 + \frac{1}{2} + iq_1)|^2 + |\Gamma(-q_0 + \frac{1}{2} + iq_2)|^2]^2}{|\Gamma(-q_0 + \frac{1}{2} + iq_1)|^2\,|\Gamma(-q_0 + \frac{1}{2} + iq_2)|^2} \tag{124}$$
$$q_0 = 2(2\mu B)^{1/2}/\alpha\hbar.$$

Now, transition to a semiclassical approximation, analogous to Eqs. (74) and (75), is given by the following reduction ($\pi q_1, \pi q_2 \gg 1$; $\Delta\varepsilon \ll E$):

$$\frac{\sinh(2\pi q_1)\sinh(2\pi q_2)}{[\cosh(2\pi q_1) - \cosh(2\pi q_2)]^2} W(q_0, q_1, q_2) \to \sinh^{-2}(2\pi\xi)\cosh^2[\xi(\pi + 2\phi_0)] \tag{125}$$
$$\phi_0 = \arctan(B/E)^{1/2} = \arctan(q_0/q_1).$$

Equations (123) and (125) should be compared with Eqs. (72) and (75), valid for pure repulsive exponential interaction. It can be expected that for energies much higher than the depth B of the Morse potential well, $E \gg B$, the effect of the attractive interaction will be comparatively small. Considering a near adiabatic situation ($\xi \gg 1$) we have

$$\sinh^{-2}(2\pi\xi)\cosh^2[\xi(\pi + 2\phi_0)] \to \exp(-\pi\xi)\exp[(2/\pi)(B/E)^{1/2}]. \tag{126}$$

The exponential factor in the right-hand side of Eq. (126) replaces now the exponential in Eq. (65). The effect of the attraction is seen to be an increase in the transition probability over that for a pure exponential repulsion $\mathscr{P}_{n+1,n}$, as given by (65), by the last factor in Eq. (126). After averaging over thermal distribution, this factor will take the form

$$\exp[(4/\pi)(\chi\beta B)^{1/2}], \tag{127}$$

where χ is defined in Eq. (102). All these semiclassical results can be obtained directly by the time-dependent perturbation method, provided only the first term in nondiagonal matrix elements [matrix H given by Eq. (122)] is retained and ξ is supposed to be large.

B. Application of the Exponential Model to Inverse-Power Interaction

In a sense an exponential function can be considered as a limiting case of a power function with the very high value of the exponent. Approximations of this kind have already been used in reducing Eq. (2) to Eq. (3), but with the main contribution supposed to come from the exponential. Now we consider inverse-power representation of the matrix elements H_{ik} proportional to R^{-s}. There are some problems where s will be different for nondiagonal and diagonal matrix elements, but it will be supposed here that s is the same as are exponentials in (7). More recent investigations of a problem of nonadiabatic coupling for interaction with different s values is due to Callaway and Bartling (1966). These authors used an approach originally suggested by Callaway and Bauer (1965) who wrote the evolution operator in the simple exponential form. Corrections to this approximation are known (Pechukas and Light, 1966) to depend basically on the commutators of perturbations at different moments, and they will be large under almost adiabatic conditions.

We begin now with the simple Hamiltonian

$$\begin{aligned} H_{11} - H_{22} &= \Delta\varepsilon \\ H_{12} &= CR^{-s}, \end{aligned} \tag{128}$$

which now replaces Eq. (45) and in which R is supposed to be the interatomic distance. Under almost adiabatic conditions the transition probability is given by Eq. (80) which is rewritten now with an oscillating preexponential factor and with the leading term in exponent:

$$\mathscr{P}_{12} = 4\sin^2\phi\,\exp\left[-\frac{1}{\hbar}\,\mathrm{Im}\int_{R_s^*}^{R_s}\frac{\Delta U(R)\,dR}{v(R)}\right]. \tag{129}$$

Here ΔU is the adiabatic splitting of terms obtained from (128),

$$\Delta U(R) = [\Delta\varepsilon^2 + 4C^2/R^{-2s}]^{1/2}, \tag{130}$$

and $v(R)$ is a relative radial velocity. We cannot expect a priori that the constant velocity approximation, which is a good one for the exponential model with large value of αR_p, will still hold for a model with a softer inverse-power interaction. Thus R dependence of v is accounted for in (129). Consider now a straight-path trajectory for which $v(R) = v(1 - b^2/R^2)^{1/2}$. The geometry of a collision is depicted in Fig. 12a. Singular points of $\Delta U(R)$, as they can be easily found from (130) are

$$R_s = \left[\frac{2C}{\Delta\varepsilon}\exp\left(\pm i\,\frac{\pi}{2} + 2k\pi i\right)\right]^{1/s} \equiv R_c\exp\left[\pm i\,\frac{\pi}{2s} + 2k\pi i/s\right]. \tag{131a}$$

$$R_s = 0. \tag{131b}$$

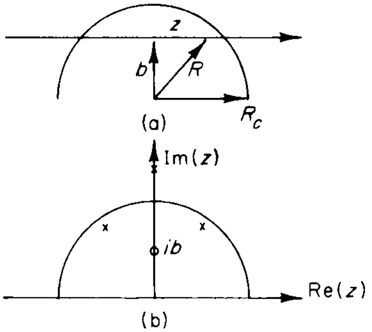

Fig. 12. (a) Geometry of a collision adopting a straight-path trajectory. (b) Location of singular points of $\Delta U(z)$ from Eq. (130) with $s = 3$: branching points (×) and poles (O).

In terms of the complex variable $z = vt$, which will be used now to establish closer correspondence with previous results, these singular points are shown in Fig. 12b, where again branching points and poles are shown for representative case $b < R_c$. [R_c as defined by (131) is $R_c = (2C/\Delta\varepsilon)^{1/s}$.] No significance should be attached to poles $x = ib$ for small b values because at short interatomic distances the interaction certainly cannot be presented in the form (128). To calculate the exponent in (129), we develop $1/v(R)$ in terms of b^2/R^2, taking advantage of the fact that for collisions with small impact parameters b is less than R_c. Introducing a new variable $y = (R_c/R)^s$ we have

$$\operatorname{Im} \int_{R_s^*}^{R_s} \frac{\Delta U(R)\,dR}{\hbar v(R)} = \frac{\Delta\varepsilon R_c}{\hbar v s}\left\{M(s) + \frac{1}{2}\frac{b^2}{R_c{}^2}\,M(-s) + \cdots\right\}. \tag{132}$$

where

$$M(s) = i \int_{-i}^{i} y^{-1-1/s}(1 + y^2)^{1/2}\,dy = s\sin(\pi/2s)\,\frac{\Gamma(1 - 1/2s)\Gamma(\frac{1}{2})}{\Gamma(\frac{3}{2} - 1/2s)} \tag{133}$$

and Γ being the Γ function. Now the exponential approximation to H_{12} near the point $R = R_c$ is obtained in the usual way:

$$\begin{aligned} H_{12}(R) = CR^{-s} &= \frac{\Delta\varepsilon}{2}\left(\frac{R}{R_c}\right)^{-s} = \frac{\Delta\varepsilon}{2}\left[1 - \frac{R - R_c}{R_c}\right]^{-s} \\ &= \frac{\Delta\varepsilon}{2}\exp\left[-s\,\frac{R - R_c}{R_c}\right] \end{aligned} \tag{134}$$

in the limit of large s. Thus R_c/s in (132) is immediately identified as $1/\alpha$ of the exponential model. The only difference thus left in (132) between inverse-power law and exponential model is due to coefficients $M(s)$ and $M(-s)$. If the right-hand side of Eq. (133) is developed in series of $1/s$ and only the first two terms are retained we obtain

$$M(s) = \pi[1 - (1 - \ln 2)/s] = \pi[1 + 0.307/s]. \tag{135}$$

In the limit $s \gg 1$ we have $M(s)$, $M(-s) \to \pi$ as it should be for the exponential model. Now the striking result, contained in Eq. (135) is, that even for very soft interactions the exponential model gives very good results provided the " natural " approximation (134) is used. For a R^{-3} interaction, responsible for the dipole–dipole nonresonance excitation transfer, $M(3)$ and $M(-3)$ are 1.1π and 0.9π, with only 10% difference from the value π, valid for the exponential model. This small difference suggests that the same type of approximation can be used for calculation of $\mathscr{P}_{12}$ for more general Hamiltonians with both nondiagonal and diagonal inverse law interactions. The corresponding R_c value is found from the equations

$$\Delta U(R_s) = 0, \qquad R_c = |R_s| \tag{136}$$

and inverse law matrix elements H_{ik} are approximated according to (134). Thus the problem reduces again to the exponential model with R_c/s as $1/\alpha$, and the general expression (33) to be used in the case of strong coupling. It is seen from Eqs. (131) and (132) that under near-adiabatic conditions

($\Delta\varepsilon R_c/\hbar v \gg 1$) the main contribution to the cross section comes from the close collisions (small b). However, it is instructive to see when distant collisions can be treated by the perturbation approach. With increasing impact parameter b the branching points of $\Delta U(z)$ move farther from the real axis thus making $\mathscr{P}_{12}$ smaller. Equation (129) is based on a matching procedure discussed in Section III and it will stay valid until there exists an internal adiabatic region at $R < R_c$ where the evaluation is described by S_a [Eq. (28)]. This region does exist if ϕ, defined by Eq. (32) with R_p replaced by R_c, is much greater than unity. A simple estimation will give (for $s = 3$)

$$\phi \approx \left(\frac{\Delta\varepsilon R_c}{3\hbar v}\right)\frac{{R_c}^2}{b^2}. \tag{137}$$

The perturbation solution of Eqs. (17) with the Hamiltonian (128) will give essentially

$$\mathscr{P}_{12} \sim \phi^2(b)\exp[-2\Delta\varepsilon b/\hbar v]. \tag{138}$$

Compare now Eq. (138) with Eqs. (129) and (132). Exponential factors can be approximately matched at $b \sim R_c$, if it is realized that the total series in parentheses in Eq. (132) will contribute a number of the order of π. At $b \sim R_c$ the phase difference ϕ will be a large number, so that the correct preexponential factor must be a rapidly oscillating function around its mean value 2, rather than a large value $\phi^2(b)$. Thus the perturbation treatment, leading to Eq. (138), gives an incorrect result, although the transition probability itself is very low because of the very small exponential. The situation here is similar to that discussed earlier in connection with Eq. (94). Referring to Figs. 5, 7, and 8, showing the motion of branching points, it will ge immediately seen that perturbation treatment is valid if the phase differences between branching points is small. Under adiabatic conditions it can be achieved only if b exceeds R_c, as shown in Fig. 13.

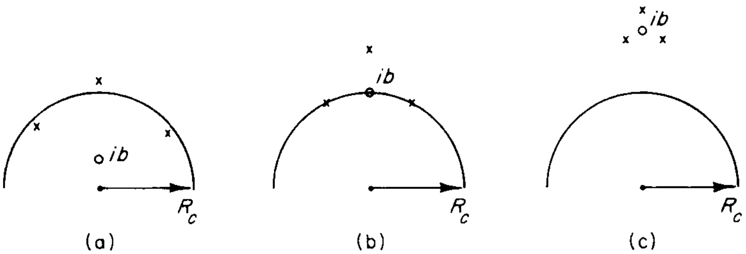

Fig. 13. Motion of branching points (×) and poles (O) of $\Delta U(z)$ from Eq. (130) with increasing impact parameter b: (a) $b < R_c$, (b) $b = R_c$, (c) $b > R_c$.

The essential result, obtained here for near-adiabatic collision, can be stated as follows:

(1) If $b \leq R_c$, the main contribution to the transition probability does not come from the region of the closest approach, but from rather larger distances $R \sim R_c$.

(2) If $b \gg R_c$ and $\phi(b) \ll 1$ the main contribution to $\mathscr{P}_{12}$ comes from the region of the closest approach, but the value of $\mathscr{P}_{12}$ is much less than in the previous case.

(3) Under no circumstances can the preexponential factor in $\mathscr{P}_{12}$ be much larger than its "amplitude" value 4.

In the earlier study of nonadiabatic phenomenon Stueckelberg (1932) used an approximation similar to (138) with $\phi(b) \gg 1$ to calculate a cross section for excitation transfer (see also Mott and Massey, 1965). It is now concluded that this method is not correct, because it is at variance with point 3 above. Bates (1962) corrected this mistake, but the method of solution used at his study assumes that the main contribution comes from the region of the closest approach. It was then necessary to introduce a cutoff parameter a, and represent the interaction in the form $C(R^2 + a^2)^{-s/2}$. This is at variance with point 1 above.

As far as the total cross section is concerned, the proper conclusion seems to be that the main contribution to the cross section comes from large interatomic distances ($R \sim R_c$) (where the power law representation of the interaction might be good) but from small impact parameters $b < R_c(s\hbar v/\Delta\varepsilon R_c)^{1/2}$ (Nikitin, 1968).

Consider now a more general Hamiltonian with inverse law interaction:

$$H = \begin{pmatrix} \Delta\varepsilon/2 - q_2 R^{-s} & q_1 R^{-s} \\ q_1 R^{-s} & -\Delta\varepsilon/2 + q_2 R^{-s} \end{pmatrix}, \tag{139}$$

where R is understood to be the interatomic distance. The nonadiabatic coupling for this Hamiltonian along straight-path trajectories has been discussed by Callaway and Bartling (1966). These authors compared numerical solutions of Eqs. (17) with that obtained by the approximation suggested earlier (Callaway and Bauer, 1965). It was found that this approximation does not discriminate the two cases with $q_1 q_2 > 0$ and $q_1 q_2 < 0$. This implies that if H given by Eq. (139) is simulated by the exponential model, then the Callaway–Bauer approximate solution gives identical transition probabilities $\mathscr{P}_{12}$ for adiabatic terms characterized by θ and $\pi - \theta$. If approximation (134) is now adopted to approximate diagonal and nondiagonal elements of H given by Eq. (139) we arrive at a simple connection between the two model Hamiltonians given by Eqs. (128) and (139). This connection is shown in Table II where a new parameter x, due to Callaway and Bartling (1966), has been introduced. It would be very interesting to compare numerical results obtained by these authors with values of $\mathcal{P}_{12}$ given by Eq. (33). The comparison made for $\bar{\mathcal{P}}_{12}$ with parameters $x = 1$ and $q_1 q_2 = \pm 1$ reveals very good agreement between exact values of $\bar{\mathcal{P}}_{12}$, obtained by numerical integration of Eqs. (17) for the Hamiltonian (139) with $s = 3$ (Callaway and Bartling, 1966) and analytical solution (33) for the exponential model.[2]

TABLE II

CORRESPONDENCE BETWEEN THE EXPONENTIAL AND THE POWER-LAW MODELS OF NONADIABATIC COUPLING

Parameters of the exponential model [Eq. (7)]	Parameters of the power-law model [Eq. 139)]
$\Delta\varepsilon$	$\Delta\varepsilon = \hbar\omega$
$\cos\theta$	$q_1/(q_1{}^2 + q_2{}^2)^{1/2}$
α	s/R_c
$R_p = \ln(A/\Delta\varepsilon)$	$R_c = [2(q_1{}^2 + q_2{}^2)^{1/2}/\Delta\varepsilon]^{1/s}$
$\xi = \Delta\varepsilon/\hbar\alpha v$	$(1/s)x^{(s-1)/s}\lvert (q_1{}^2 + 2q_2{}^2)^{1/2}/q_1 \rvert^{1/s}$ where $x = (\omega/v)(q_1/\hbar v)^{1/(s-1)}$

A problem of matching an inverse-power potential or any nonexponential potential by exponential was extensively discussed in a number of papers (Nikitin 1959; Shin 1964, 1965, 1968a, and 1968b) in connection with the study of the vibrational energy transfer. However, these discussions were limited to the case when the perturbation treatment is applicable. In those cases the main contribution to the transition probability comes from the singular point $R = 0$, and $\mathcal{P}_{12}$ is expressed by Eq. (65) with the correction for attraction given by Eq. (132) depending on the interaction potential. For intance, in the particular case of a repulsive potential of the form $U(R) = 4B(R_0/R)^s$ we will have

$$\xi = \frac{\Delta\varepsilon}{\hbar v \alpha^*}, \qquad \frac{1}{\alpha^*} = \frac{R_0}{\sqrt{\pi}} \frac{\Gamma(\frac{1}{2} + 1/s)}{\Gamma(1/s)} \left(\frac{B}{E}\right)^{1/s}. \tag{140}$$

---

[2] The author acknowledges fruitful cooperation with professor J. Callaway of Louisiana University in discussing the interrelation of the exponential and power-law models.

We see that α^* is slightly velocity dependent and this constitutes the principal difference between the exponential and the power-law models in cases when the effect of the turning point is essential.

C. Overlapping of Exponential and Linear Models

The linear model reviewed recently (Nikitin, 1968) and the exponential model here discussed illustrate extreme situations when matrix elements H_{ik} are approximated either by slowly varying functions, or by rapidly varying functions of R. In actual problems however, diagonal and nondiagonal matrix elements are often different in R dependence. This effect can to some extent be taken into account if a slow-varying part of H_{ik} is replaced by a constant appropriate to the coupling region. This method is satisfactory if a slow-varying part of H_{ik} constitutes a relatively small correction to a rapidly varying part all over the coupling region. If this is not the case both types of interaction should be taken into account explicitly when solving Eqs. (17) and (22).

As an illustrative example we consider now the superposition of the linear and the exponential models which is relevant to the nonresonant charge exchange with one channel giving neutral particles and another giving charged particles (Bykhovski and Nikitin, 1965). We suppose now that the diagonal elements of $H_{ii}(R)$ cross at some distance R_0 and that the variation of ΔH near this point can be accurately described by the linear functions of $(R - R_0)$ over distances longer than $1/\alpha$ (crossing of the long-range Coulomb term with a " flat " covalant term). At the same time H_{12} is supposed to vary as an exponential (exchange interaction). Thus we have

$$\Delta H = -\Delta F\ R - R_0), \qquad \Delta F = (-\partial H_{11}/\partial R + \partial H_{22}/\partial R|)_{R=R_0} \tag{141}$$
$$H_{12} = a\exp[-\alpha(R - R_0)].$$

It is convenient now to introduce the new parameters:

$$\begin{gathered} \Delta\varepsilon_0 = \Delta F R_0 \\ v = a^2/\Delta F \hbar v, \qquad \delta = (2a/\Delta\varepsilon_0)(\alpha R_0). \end{gathered} \tag{142}$$

Although formally defined by (142), $\Delta\varepsilon_0$ in case of nonresonant charge exhange will be the energy difference between two states at $R \to \infty$. This establishes a correspondence between $\Delta\varepsilon_0$ and $\Delta\varepsilon$ in Eq. (18). The parameter v is in fact the Massey parameter for the linear model, and as such it replaces ξ of the exponential model, and δ characterizes the relative contribution of nondiagonal and diagonal interactions, thus replacing θ of the exponential model. Although usually $a \ll \Delta\varepsilon_0$, (αR_0) is often so large that δ

may well be of the order of unity, or even large. The main features of the transition probability are most easily understood in terms of singular points of the adiabatic splitting ΔU, corresponding to the Hamiltonian (141). Introducing now $z = \alpha(R - R_0)$, we obtain

$$\Delta U(z) = (\Delta F/\alpha)[z^2 + \delta^2 \exp(-2z)]^{1/2}. \tag{143}$$

All branching points of $\Delta U(z)$ from Eq. (133) correspond to the intersection of curves, defined by (144a) and (144b):

$$\arg(\pm z e^z) = 0 \tag{144a}$$

$$|z e^z| = \delta. \tag{144b}$$

Equation (144a) gives a family of curves which do not depend on δ and are more or less parallel to the real axis of z. Equation (144b) gives one ($\delta > 1/e$) or two ($\delta < 1/e$) curves which run generally along the imaginary axis of z and which depend on δ. The motion of the branching points with variations of δ is shown in Fig. 14. Equations (144) can be approximately solved in the limit $\delta \ll 1$. Putting $z = x + iy$ we find two sets of solutions:

$$x_a = -\delta^2, \qquad y_a = \pm\delta \tag{145a}$$

$$x_b \approx -\ln(1/\delta), \qquad y_b = \pm\pi/2 \pm n\pi \pm \pi/2x_b. \tag{145b}$$

It is in this case, in the limit $\delta \ll 1$, when there are two separate regions of interaction; one near the crossing point R_0 (region a) and another near the region where $H_{11} - H_{22}$ is of the order of H_{12}(region b). If the mutual influence of the two regions is small (nonoverlapping linear and exponential models), then the transition probability is obtained by summing the currents (all interference effect neglected). That gives

$$\mathcal{P}_{12} = \mathcal{P}_{12}^{(a)} + \mathcal{P}_{12}^{(b)} + 2\mathcal{P}_{12}^{(a)}\mathcal{P}_{12}^{(b)}, \tag{146}$$

where $\mathcal{P}_{12}^{(a)}$ and $\mathcal{P}_{12}^{(b)}$ are calculated according to Eq. (43) and Eq. (44) (the Landau–Zener and the Rosen–Zener formulas) with proper values of parameters. Referring to (145a) and (145b) we find

$$\mathcal{P}_{12}^{(a)} = 2\exp(-\pi v)[1 - \exp(-\pi v)] \tag{147}$$

$$\mathcal{P}_{12}^{(b)} = \tfrac{1}{2}\cosh^{-2}[\pi\xi_b(\delta)/2], \tag{148}$$

where v is defined by (142) and

$$\xi_b = \frac{\Delta U(x_b)}{\hbar \alpha v}, \qquad \Delta U(x_b)\Big|_{\delta \ll 1} \approx \frac{\Delta F}{\alpha} x_b = \Delta F(R_b - R_0). \tag{149}$$

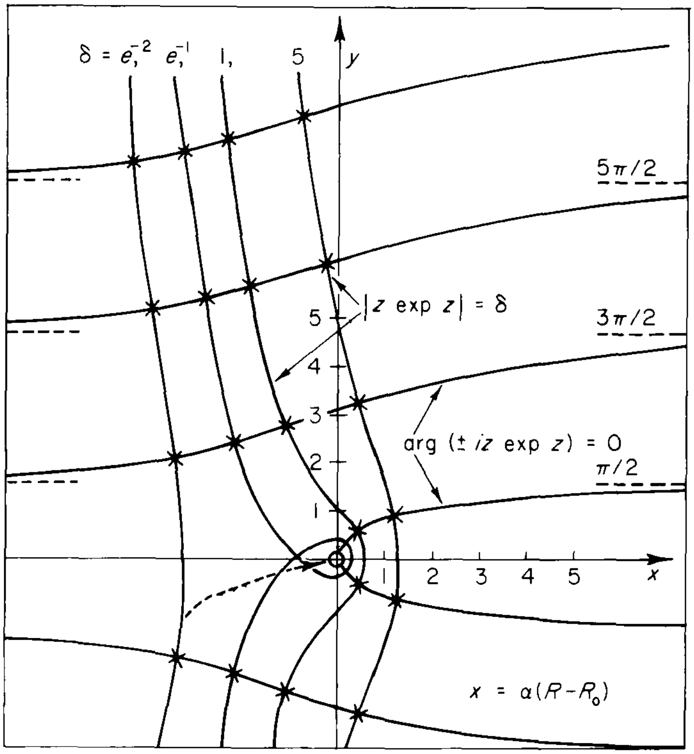

Fig. 14. Motion of branching points (×) of $\Delta U(z)$ from Eq. (143) with increasing value of δ, defined by Eqs. (144a) and (144b).

The overlapping effect will be more pronounced if δ increases. It is seen from Fig. 14 that at large values of δ ($\delta \gg 1$) the situation will be similar to that depicted in Fig. 7. Then there will be one coupling region, and branching points of $\Delta U(z)$ are given by the equation

$$x_b' = \ln \delta, \qquad y_b' = \pm\pi/2 \pm n\pi \mp \pi/2x_b'. \tag{150}$$

The transition probability for this case is given by Eq. (148) and the Hamiltonian (141) will be essentially equivalent—from the point of view of nonadiabatic coupling—to the Hamiltonian of a simple exponential model (45) with a $\Delta\varepsilon$ value defined by

$$\Delta\varepsilon = \Delta F(R_b' - R_0), \qquad R_b' = \alpha x_b'. \tag{151}$$

For intermediate values of δ, when the nonadiabatic coupling for the Hamiltonian (141) cannot be treated on the basis of nonoverlapping models, numerical calculations of $\mathscr{P}_{12}$ are available (Bykhovski and Nikitin, 1965). Figure 15 shows the dependence of transition probability on ν and δ.

Features of practical importance are:

(1) Sharper increase of $\mathscr{P}_{12}$ with velocity in the adiabatic region (small $1/\nu$) as compared to that given by the Landau–Zener formula.

(2) Occurrence of two maxima in the function $\mathscr{P}_{12}$ with increasing velocity. The first is associated with the Landau–Zener region *a*, and the second with the Rozen–Zener region *b*. The two maxima will merge if δ is of the order of 1.

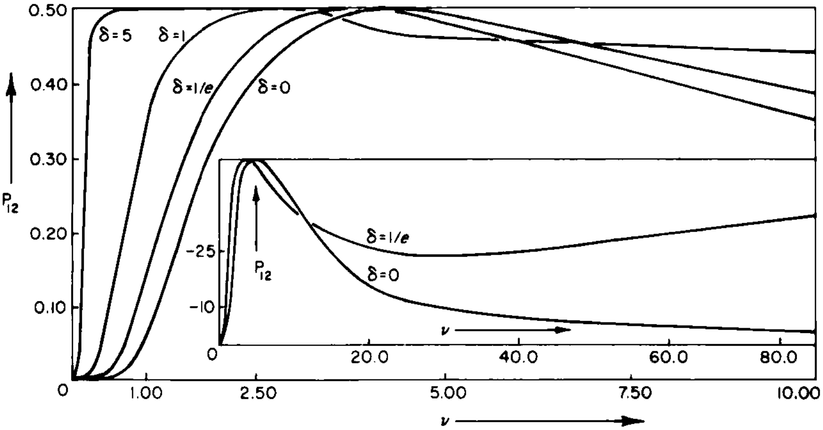

Fig. 15. Transition probability $\mathscr{P}_{12}$ for the Hamiltonian (141) as a function of two parameters ν and δ defined by Eq. (142).

VIII. Application of Exponential Models to Elementary Processes

Exponential models of nonadiabatic coupling between two electronic or vibrational states have been widely used for calculation of cross sections and rate constants for many elementary processes of energy transfer in collisions. Table III illustrates the application of the models discussed and gives specification of some parameters. Only references to books, review articles, and recent theoretical papers are given.

TABLE III

APPLICATIONS OF THE EXPONENTIAL MODEL

Process	Specification	References
Transitions between fine-structure components in atomic processes $M(^2P_{1/2}) + X(^1S_0) \to M(^2P_{3/2}) + X(^1S_0)$	Rectilinear trajectory, constant velocity approximation $\cos\theta = \frac{1}{3}$, Eqs. (97) and (103), any value of ξ	Nikitin (1965b) Nikitin (1965c) Nikitin (1967) Dashevskaya and Nikitin (1967)
Nonresonance charge transfer $A^+ + B \to A + B^+$ in slow collisions	Rectilinear trajectory, constant velocity approximation $\cos\theta = 0$, Eq. (110) and (112)	Nikitin (1963) Smirnov (1964a) Demkov (1963) Smirnov (1966b)
Non resonance charge transfer $A^+ + B^-$ or $A^+ + B^+ \to A + B^{++}$ in slow collisions	Straight-path trajectory, constant velocity approximation, two regions of nonadiabatic coupling, Eqs. (141) and (146)	Bykhovski and Nikitin (1965)
One-quantum transitions between vibrational states in a molecule, simulated by an harmonic oscillator	Effect of the turning point taken into account, $\cos\theta = 0$, Eq. (102), $\xi \gg 1$	Landau and Teller (1936) Herzfeld and Litovitz (1959) Takayanagi (1963) Takayanagi (1965) Stupochenko *et al.* (1965)
One-quantum transitions between lower vibrational states in a molecule, simulated by an anharmonic oscillator	Effect of the turning point taken into account, $\cos\theta < 0$, $\xi \gg 1$ Eqs. (102) and (66)	Mies (1964a) Mies (1964b)
One-quantum transition between lower vibrational states in a molecule simulated by an harmonic or an anharmonic oscillator	Effect of the turning point into account, $\cos\theta = 0$; the morse or Lennard-Jones interaction potentials; correction given by Eq. (126) to Eq. (102)	Calvert and Amme (1966) Shin (1968)

Notation

A	a parameter of exponential models
B	a parameter of exponential models
b	impact parameter
C	a parameter of power-law models
E, v	average energy and velocity
E_i, v_i	energy and velocity referred to an adiabatic term i
E_R, v_R	energy and velocity along reaction coordinate in the nonadiabatic region
H_{ik}	matrix elements of the model Hamiltonian
P_{12}	probability of transition 1 → 2 upon one crossing of the nonadibaticity region
$\mathscr{P}_{12}$	probability of transitions 1 → 2 upon double crossing of the nonadiabaticity region
$\bar{\mathscr{P}}_{12}$	transition probability averaged over oscillations
$\langle\mathscr{P}_{12}\rangle$	mean transition probability in a thermal process
R	reaction coordinate, interatomic distance
R_c	characteristic radius of a power-law model
R_p	center of the nonadiabaticity region
R_s	singular points
$U(R)$	average adiabatic term
$\Delta U(R)$	splitting of adiabatic terms
$U_i(R)$	adiabatic electronic terms
α	parameter of exponential models
β	$1/kT$
$\Delta\varepsilon$	parameter of exponential models, adiabatic asymptotic splitting of two terms
η	parameter of exponential models, $\eta = \Delta U_p/\Delta\varepsilon$
θ	parameter of exponential models
$\bar{\theta}$	parameter of exponential models, $\bar{\theta} = \pi - \theta$
μ	effective mass, reduced mass of colliding atoms
ξ	the Massey parameter, $\xi = \Delta\varepsilon/\alpha\hbar v$
τ	dimensionless time, $\tau = t\alpha v$
ϕ	phase difference in the internal adiabatic region $R < R_p$
φ_i	orthonormal adiabatic wave functions
φ_i^0	orthonormal adiabatic wave functions of the crude basic set

References

Allen, R. A., and Feuer, P. (1964). *J. Chem. Phys.* **40**, 2810.

Bates, D. R. (1962). *in* "Atomic and Molecular Processes." Academic Press, New York and London.

Bates, D. R. (1962). *Discussions Faraday Soc.* **33**, 7.

Bykhovski, V. K., and Nikitin, E. E. (1965). *Soviet Phys.—JETP* **48**, 1499.

Callaway, J., and Bauer E. (1965). *Phys. Rev.* **140**, A1072.

Callaway, J., and Bartling, J. Q. (1966). *Phys. Rev.* **150**, 69.

Calvert, J. B., and Amme, R. C. (1966). *J. Chem. Phys.* **45**, 4710.

Cottrell, T. L., and Ream, N. (1955). *Trans. Faraday Soc.* **51**, 1453.

Dashevskaya, E. I., and Nikitin, E. E. (1967). *Opt. Spectr. (USSR)* **22**, 866.

Demkov, Yu, N. (1963). *Soviet Phys.—JETP* **45**, 195.

Devonshire, A. F. (1937). *Proc. Roy. Soc.* **A158**, 269.

Dykhne, A. M. (1961). *Soviet Phys—JETP* **41**, 1324.

Ellison, W. D. and Borovitz, S. (1964). *in* "Atomic Collision Processes" (M. R. C. McDowell, ed.), p. 790. North Holland Publ., Amsterdam.

Erdelyi, A. (1953). "Higher Transcendental Functions," Vol. 1. McGraw-Hill, New York.

Glasstone, S., Laidler, K. J., and Eyring, H. (1941). "The Theory of Rate Processes." McGraw-Hill, New York.

Herring, C. (1962). *Rev. Mod. Phys.* **34**, 631.

Herring, C., and Flicker, M. (1964). *Phys. Rev.* **134**, 362.

Gor'kov, L. P., and Pitaevskii, L. P. (1963). *Dokl. Akad. Nauk SSSR* **151**, 822.

Herzfeld, K. F., and Litovitz, T. A. (1959). "Absorption and Dispersion of Ultrasonic Waves." Academic Press, New York and London.

Jackson, J. M., and Mott, N. F. (1932). *Proc. Roy. Soc.* **A137**, 703.

Keck, J., and Carrier, G. (1965). *J. Chem. Phys.* **43**, 2284.

Kotova, L. (1968). *Soviet Phys.—JETP* **55**, 1375.

Landau, L. (1932a). *Phys. Z. Sow.* **1**, 88.

Landau, L. (1932b). *Phys. Z. Sow.* **2**, 46.

Landau, L., and Teller, E. (1936). *Phys. Z. Sow.* **10**, 34.

Landau, L. D., and Lifshitz, E. M. (1963). "Kvantovaya Mekhanika." Fizmatgiz, Moscow.

Longuet-Higgins, H. C. (1961). *in* "Advances in Spectroscopy," Vol. 2, p. 429. Wiley (Interscience), New York.

Mies, F. H., (1964a). *J. Chem. Phys.* **40**, 523.

Mies, F. H. (1964b). *J. Chem. Phys.* **41**, 903.

Mott, N. F., and Massey, H. S. W., (1965). "The Theory of Atomic Collisions." Oxford Univ. Press (Clarendon), London and New York.

Nikitin, E. E. (1959). *Opt. Spectra. (USSR)* **6**, 141.

Nikitin, E. E. (1962a). *Opt. Spectr. (USSR)* **13**, 761.

Nikitin, E. E. (1962b). *Discussions Faraday Soc.* **33**, 14.

Nikitin, E. E. (1963). *Isv. A. N. SSSR Ser. Phys.* **27**, 996.

Nikitin, E. E. (1965a). *Opt. Spectr. (USSR)* **18**, 763.

Nikitin, E. E. (1965b). *Opt. Spectr. (USSR)* **19**, 161.

Nikitin, E. E., (1965c), *J. Chem. Phys.* **43**, 744.

Nikitin, E. E. (1967). *Opt. Spectr. (USSR)* **22**, 689.

Nikitin, E. E. (1968). *Chem. Phys. Letters* **2**, 402.

Nikitin, E. E. (1968). *in* "Chemische Elementarprozesse." Springer Verlag, Berlin, Heidelberg, New York.

Ovchinnikova, M. Ya. (1965). *Soviet Phys.—JETP* **49**, 275.

Pechukas, P., and Light, J. C. (1966). *J. Chem. Phys.* **44**, 3897.

Pokrovskii, V. L., and Khalatnikov, I. M., (1961). *Soviet Phys.—JETP* **40**, 17[illegible]3.

Rapp, D., and Sharp, T. E. (1963). *J. Chem. Phys.* **38**, 2641.

Rosen, N. and Zener, C. (1932). *Phys. Rev.* **40**, 502.

Roueff, E. (1967). *Compt. Rend. Acad. Sci.* **264**, 25.

Shin, H. K. (1964). *Can. J. Chem.* **42**, 2351.

Shin, H. K. (1965). *J. Chem. Phys.* **42**, 59.

SHIN, H. K. (1968a). *J. Chem. Phys.* **48**, 3644.

SHIN, H. K. (1968b). *J. Am. Chem. Soc.* **90**, 3025.

SMIRNOV, B. M. (1964a). *Soviet Phys.—JETP* **46**, 1017.

SMIRNOV, B. M. (1964b). *Soviet Phys.—JETP* **47**, 518.

SMIRNOV, B. M., and CHIBISOV, M. I. (1965). *Soviet Phys.—JETP* **48**, 939.

SMIRNOV, B. M. (1966a). *Soviet Phys-JETP* **51**, 446.

SMIRNOV, B. M. (1966b). *Teplofisika Vysokikh Temperatur* **4**, 429.

STUECKELBERG, E. C. G. (1932). *Helv. Phys. Acta* **5**, 369.

STUPOCHENKO, E. V. LOSEV, S. A., and OSIPOV, A. I. (1965)." Relaksationnye Protsessy v udarnykh volnakh." Nauka, Moscow.

TAKAYANAGI, K. (1959). *J. Phys. Soc. Japan* **14**, 75.

TAKAYANAGI, K. (1963). *Progr. Theoret. Phys. (Kyoto), Suppl.* **25**, 1.

TAKAYANAGI, K. (1965). *in* "Advances in Atomic and Molecular Physics," Vol. 1, p. 149. Academic Press, New York.

TAKAYANAGI, K., and MIYAMOTO, Y. (1959). *Sci. Rept. Saitama Univ. (Ser. A)* **A3**, 101.

ZENER, C. (1932). *Proc. Roy. Soc.* **A137**, 696.

ZENER, C. (1932). *Proc. Cambridge Phil. Soc.* **29**, 136.

On the Nonorthogonality Problem*

PER-OLOV LÖWDIN

Department of Quantum Chemistry
Uppsala University
Uppsala, Sweden
and
Quantum Theory Project
University of Florida
Gainesville, Florida

I. Introduction

When the author was looking for a suitable thesis problem in 1946, Professor Ivar Waller suggested to him the study of the classical question of the failure of the Cauchy relations for the elastic constants of the alkali halides. He emphasized the importance of Landshoff's work (1936) in this connection, and he also stressed that any progress towards the calculation of the cohesive and elastic properties of these solids would depend on whether one could first solve the "nonorthogonality" problem connected with the fact that the overlap integrals between the electronic orbitals of neighboring ions are not vanishing.

If the problem of the Cauchy relations dates from 1827, the nonorthogonality problem is about one hundred years younger. The overlap integrals occur for the first time in 1927 in Heitler and London's (1927) quantum-mechanical study of the physical properties of the covalent

---

* The work reported in this paper has been sponsored in part by the Swedish Natural Science Research Council, in part by the Air Force Office of Scientific Research (OSR) through the European Office of Aerospace Research (OAR), U.S. Air Force under Grant AF-EOAR 67-50 with Uppsala University, and in part by the National Science Foundation under Grant GP-5419 with the University of Florida.

chemical bond in the hydrogen molecule, and they caused no probem whatsoever in this connection. However, in Bloch's (1929) treatment of the electronic structure of solids in 1928, the numerous overlap integrals seemed to cause an undesirable mathematical complication and Bloch suggested that, in a first approximation, one should neglect them. In 1930, Slater (1930b) pointed out that, even if the overlap integrals are small, they are so numerous in a solid that the numerator and denominator in the quotient

$$\langle H \rangle = \frac{\langle \Psi | H | \Psi \rangle}{\langle \Psi | \Psi \rangle} \tag{1}$$

become divergent, i.e., they are not proportional towards the volume. In 1934, Inglis coined the word "nonorthogonality catastrophe" in connection with the theory of magnetic properties, and it had now become clear that the overlap integrals instead of being negligible were quantities of essential importance for the understanding of the physical properties of solids.

In molecular theory, Pauling (1931) and Slater (1931a) studied the properties of directed valency by means of the theory of hybridization, and, in this connection, they had also developed the principle of "maximum overlap," saying that the strength of a chemical bond increases with the overlap between the orbitals involved, measured essentially by the overlap integrals. For small molecules, it may seem easy to take all the overlap integrals into proper account, but the difficulties start as soon as one goes beyond the two-electron systems. In the valence bond method (Slater, 1930a, 1931), calculational schemes were developed by Rumer (1932) and Pauling (1933) only under rather unrealistic orthogonality assumptions.

In the molecular orbital method, the nonorthogonality between the atomic orbitals occurs essentially in the MO-LCAO-scheme, and it ought to be comparatively easy to treat the overlap integrals properly. In his treatment of the mobile electrons of the conjugated systems, Hückel (1930) included all the overlap integrals but, in the so-called "naive" Hückel scheme, they are all assumed to be identically vanishing. Even today, the overlap integrals are often neglected in studies of the charge and bond orders of large conjugated systems, and still one knows that these integrals may be key quantities in understanding the electronic structure of such systems.

In the 1930's, particular attention seems to have been given the nonorthogonality problem only in connection with studies of the cohesive and elastic properties of the alkali halides. This depends partly on the fact that, if one neglects the overlap integrals, there are no repulsive forces and the ionic crystal breaks down completely—in this model, it is hence impossible to assume that the overlap integrals are vanishing. In his treatment of lithium hydride in 1930, Hylleraas included overlap integrals through the first order, whereas, in his study of sodium chloride in 1936, Landshoff included overlap effects essentially through the second order. In both cases, the theory gave results in good agreement with the experimental experience.

Instead of the original atomic orbitals, Landshoff used linear combinations of these orbitals treated on an equivalent basis which were orthonormal essentially through the second order in the overlap integrals. Using the original atomic orbitals to construct normalized Bloch functions and carrying out a unitary transformation back to localized orbitals, Wannier could in 1937 implicitly construct "orthonormalized atomic orbitals" or "Wannier functions" and derive the first two terms in Landshoff's formula explicitly. In looking at this development and all the partial results in 1946, it seemed hence highly desirable for the author to follow Professor Waller's suggestion and try to find the complete formula for the "orthonormalized atomic orbitals" which would be exact through any order.

II. Orthonormalization Procedures

In quantum theory, a physical situation is represented by a wave function Ψ which is an element of a linear space. The superposition principle says that if Ψ_1 and Ψ_2 are wave functions representing physical states, one can also give physical significance to the wave functions $(\Psi_1 + \Psi_2)$ and $c\Psi$, where c is an arbitrary complex constant. A "scalar product" $\langle\Psi_1 | \Psi_2\rangle$ is further a complex number associated with two elements of the linear space satisfying the following four axioms:

$$\begin{array}{ll} (1) & \langle\Psi_1 | \Psi_2 + \Psi_3\rangle = \langle\Psi_1 | \Psi_2\rangle + \langle\Psi_1 | \Psi_3\rangle, \\ (2) & \langle\Psi_1 | c\Psi_2\rangle = c\langle\Psi_1 | \Psi_2\rangle, \\ (3) & \langle\Psi_1 | \Psi_2\rangle = \langle\Psi_2 | \Psi_1\rangle^*, \\ (4) & \langle\Psi | \Psi\rangle \geq 0 \quad \text{and} \quad \langle\Psi | \Psi\rangle = 0 \quad \text{only if} \quad \Psi = 0. \end{array} \tag{2}$$

In order to describe the space, it may be convenient to introduce a basis $\mathbf{\Phi} = \{\Phi_k\} = \{\Phi_1, \Phi_2, \Phi_3, \ldots, \Phi_n\}$ such that every element Ψ may be expressed in terms of the basis:

$$\Psi = \mathbf{\Phi}\mathbf{c}, \tag{3}$$

or

$$\Psi = \sum_k \Phi_k c_k, \tag{4}$$

where $\mathbf{c} = \{c_k\}$ is the column vector of the expansion coefficients c_k. The basis has a *metric matrix* $\boldsymbol{\Delta} = \langle \boldsymbol{\Phi} \mid \boldsymbol{\Phi} \rangle$ having the elements

$$\Delta_{kl} = \langle \Phi_k \mid \Phi_l \rangle, \tag{5}$$

and the *overlap matrix* $\mathbf{S}$ is introduced through the relation $\boldsymbol{\Delta} = \mathbf{1} + \mathbf{S}$, or

$$S_{kl} = \langle \Phi_k \mid \Phi_l \rangle - \delta_{kl}. \tag{6}$$

In the standard realization of the binary product (2), one has $S_{kl} = \int \Phi_k{}^* \Phi_l \, dv$ for $k \neq l$, i.e., S_{kl} is the overlap integral between the functions Φ_k and Φ_l.

It is easily shown that the basis $\boldsymbol{\Phi}$ is linearly independent, if and only if the metric matrix has an inverse matrix $\boldsymbol{\Delta}^{-1}$, and, in the following, we will assume that this is the case. Let us now consider a nonsingular linear transformation $\mathbf{A}$ of the basis $\boldsymbol{\Phi}$ leading to a new basis $\boldsymbol{\varphi}$:

$$\boldsymbol{\varphi} = \boldsymbol{\Phi}\mathbf{A}, \tag{7}$$

which is orthonormal, so that

$$\langle \boldsymbol{\varphi} \mid \boldsymbol{\varphi} \rangle = \mathbf{1}. \tag{8}$$

One has immediately the following result:

$$\begin{aligned} \langle \boldsymbol{\varphi} \mid \boldsymbol{\varphi} \rangle &= \langle \boldsymbol{\Phi}\mathbf{A} \mid \boldsymbol{\Phi}\mathbf{A} \rangle = \mathbf{A}^\dagger \langle \boldsymbol{\Phi} \mid \boldsymbol{\Phi} \rangle \mathbf{A} \\ &= \mathbf{A}^\dagger \boldsymbol{\Delta} \mathbf{A} = \mathbf{1}, \end{aligned} \tag{9}$$

and we will see that this equation has several types of solutions.

A. Successive Orthonormalization

The simplest way of orthonormalizing a finite set of functions is by the classical Schmidt procedure in which each member of the set in order is orthogonalized against all the previous members and subsequently normalized (Courant and Hilbert, 1931). The orthogonalization is based on the fact that if $\boldsymbol{\eta}$ is an orthonormal set and h is an extra function, the component $h_\perp$ of h orthogonal to the set $\boldsymbol{\eta}$ is given by the formula

$$h_\perp = h - \boldsymbol{\eta}\langle \boldsymbol{\eta} \mid h \rangle = (1 - Q)h, \tag{10}$$

where $Q = |\eta\rangle\langle\eta|$ is a projection operator associated with the subspace of η satisfying the relations $Q^2 = Q$ and $Q^\dagger = Q$. For the normalization integral, one obtains directly

$$\begin{aligned}\langle h_\perp | h_\perp\rangle &= \langle(1 - Q)h | (1 - Q)h\rangle \\ &= \langle h | 1 - Q | h\rangle = \langle h | h\rangle - \langle h | \eta\rangle\langle\eta | h\rangle.\end{aligned} \tag{11}$$

In order to apply the Schmidt procedure to a given basis $\boldsymbol{\Phi} = \{\Phi_1, \Phi_2, \ldots, \Phi_n\}$, one should hence apply a recursion formula of the following type:

$$\begin{aligned}\varphi_1 &= \Phi_1\langle\Phi_1 | \Phi_1\rangle^{-1/2}, \\ \varphi_{m+1} &= \left\{\Phi_{m+1} - \sum_{k=1}^{m} \varphi_k\langle\varphi_k | \Phi_{m+1}\rangle\right\} N_{m+1}^{-1/2}, \\ N_{m+1} &= \langle\Phi_{m+1} | \Phi_{m+1}\rangle - \sum_{k=1}^{m} |\langle\varphi_k | \Phi_{m+1}\rangle|^2.\end{aligned} \tag{12}$$

The result corresponds to a solution of Eq. (19) in which the matrix $\mathbf{A}$ is triangular.

If one wants the functions $\boldsymbol{\varphi}$ expressed directly in terms of the original functions $\boldsymbol{\Phi}$, the calculations based on (12) lead to a rather cumbersome procedure, and it is worthwhile to try a more direct approach. Let us assume that $\mathbf{g}$ is an arbitrary linearly independent set having the metric matrix $\langle\mathbf{g} | \mathbf{g}\rangle$ and that h is an extra function. The component $h_\perp$ of h orthogonal to the set $\mathbf{g}$ is now given by the formula

$$h_\perp = h - \mathbf{ga}, \tag{13}$$

and the condition $\langle\mathbf{g} | h_\perp\rangle = \langle\mathbf{g} | h\rangle - \langle\mathbf{g} | \mathbf{g}\rangle\mathbf{a} = 0$ gives immediately $\mathbf{a} = \langle\mathbf{g} | \mathbf{g}\rangle^{-1}\langle\mathbf{g} | h\rangle$, i.e.,

$$h_\perp = h - \mathbf{g}\langle\mathbf{g} | \mathbf{g}\rangle^{-1}\langle\mathbf{g} | h\rangle = (1 - Q)h, \tag{14}$$

where $Q = |\mathbf{g}\rangle\langle\mathbf{g} | \mathbf{g}\rangle^{-1}\langle\mathbf{g}|$ is a projection operator associated with the subspace of $\mathbf{g}$ satisfying the relations $Q^2 = Q$ and $Q^\dagger = Q$. For the normalization integral, one obtains again

$$\begin{aligned}\langle h_\perp | h_\perp\rangle &= \langle(1 - Q)h | (1 - Q)h\rangle = \langle h | 1 - Q | h\rangle \\ &= \langle h | h\rangle - \langle h | \mathbf{g}\rangle\langle\mathbf{g} | \mathbf{g}\rangle^{-1}\langle\mathbf{g} | h\rangle.\end{aligned} \tag{15}$$

In order to carry out the successive orthonormalization of the basis $\boldsymbol{\Phi} = \{\Phi_1, \Phi_2, \ldots, \Phi_n\}$ having the metric matrix $\boldsymbol{\Delta} = \langle\boldsymbol{\Phi} | \boldsymbol{\Phi}\rangle$, it is now convenient to study the *successive inversion* of this matrix through a step-by-step procedure. If $\mathbf{A}$ is an arbitrary matrix which may be partitioned in the following submatrices:

$$\mathbf{A} = \begin{pmatrix} \mathbf{A}_{11} & \mathbf{A}_{12} \\ \mathbf{A}_{21} & \mathbf{A}_{22} \end{pmatrix}, \tag{16}$$

one can easily derive the formula

$$\mathbf{A}^{-1} = \begin{pmatrix} \mathbf{A}_{11}^{-1} + \mathbf{A}_{11}^{-1}\mathbf{A}_{12}\mathbf{D}_{22}^{-1}\mathbf{A}_{21}\mathbf{A}_{11}^{-1}, & -\mathbf{A}_{11}^{-1}\mathbf{A}_{12}\mathbf{D}_{22}^{-1} \\ -\mathbf{D}_{22}^{-1}\mathbf{A}_{21}\mathbf{A}_{11}^{-1}, & \mathbf{D}_{22}^{-1} \end{pmatrix}, \tag{17}$$

where $\mathbf{D}_{22} = \mathbf{A}_{22} - \mathbf{A}_{21}\mathbf{A}_{11}^{-1}\mathbf{A}_{12}$; the validity of this formula may be proven by direct multiplication of (16) and (17) giving $\mathbf{A} \cdot \mathbf{A}^{-1} = \mathbf{1}$. The procedure becomes particularly simple, if $\mathbf{A}_{22}$ is a one-dimensional matrix, since $\mathbf{A}_{12}$ is a column vector, $\mathbf{A}_{21}$ is a row vector, and $\mathbf{D}_{22}$ is a number. In the "successive inversion" of the matrix $\mathbf{A}$, one starts from the element in the upper left corner, adds one row and column at a time, and applies formula (17) until the matrix is fully inverted.

If the method of successive inversion is now applied to the metric matrix of the combined set $(\mathbf{g}, h)$, one obtains according to (17) for the last column:

$$\begin{pmatrix} \langle \mathbf{g} | \mathbf{g} \rangle \langle \mathbf{g} | h \rangle \\ \langle h | \mathbf{g} \rangle \langle h | h \rangle \end{pmatrix}^{-1} = \begin{pmatrix} \ldots, & -\langle \mathbf{g} | \mathbf{g} \rangle^{-1} \langle \mathbf{g} | h \rangle D_{22}^{-1} \\ \ldots, & D_{22}^{-1} \end{pmatrix}, \tag{18}$$

where $D_{22} = \langle h | h \rangle - \langle h | \mathbf{g} \rangle \langle \mathbf{g} | \mathbf{g} \rangle^{-1} \langle \mathbf{g} | h \rangle$. A comparison with (14) shows that the numbers in the last column vector are proportional to the coefficients for the functions $(\mathbf{g}, h)$ in (14), and that one obtains a normalized function if one multiplies all these numbers by the normalization factor $D_{22}^{+1/2}$.

These results imply that it is possible to carry out the Schmidt procedure in terms of the original set $\mathbf{\Phi}$, if one carries out a successive inversion of the metric matrix $\Delta = \langle \mathbf{\Phi} | \mathbf{\Phi} \rangle$; the coefficients in the expansion of the successive functions φ are then given by the *last column vector in each step*, and the normalization may be performed by multiplying these numbers by the square root of the diagonal element involved.

For a solid, it may be very difficult to try to apply the Schmidt procedure to the atomic orbitals of the system, since one may never reach the end. It is even more disturbing, however, that the successive orthonormalization seems to destroy the natural symmetry of such a system, and it seems hence desirable to look for another approach.

B. Symmetric Orthonormalization

In solid-state theory, it had become clear through the work by Landshoff (1936) and by Wannier (1937) that one could probably construct orthonormal combinations of the atomic orbitals of the system which would still preserve the natural symmetry. In such an approach, it would be necessary to treat the given functions $\mathbf{\Phi} = \{\Phi_1, \Phi_2, \ldots, \Phi_n\}$ simultaneously on an equivalent basis instead of successively as in the Schmidt procedure.

In order to solve this problem, it is convenient to return to formula (9). Introducing the positive square root $\mathbf{\Delta}^{-1/2}$ and the substitution

$$\mathbf{A} = \mathbf{\Delta}^{-1/2}\mathbf{B}, \qquad \mathbf{A}^\dagger = \mathbf{B}^\dagger\mathbf{\Delta}^{-1/2}, \tag{19}$$

one obtains $\mathbf{A}^\dagger\mathbf{\Delta}\mathbf{A} = \mathbf{B}^\dagger\mathbf{B} = \mathbf{1}$, i.e., the problem has a solution if $\mathbf{B}$ is an arbitrary *unitary* matrix. The general solution of the orthonormality problem has hence the form (Löwdin, 1947)

$$\boldsymbol{\varphi} = \mathbf{\Phi}\mathbf{\Delta}^{-1/2}\mathbf{B}. \tag{20}$$

The special choice $\mathbf{B} = \mathbf{1}$ leads to the *symmetric orthonormalization*:

$$\boldsymbol{\varphi} = \mathbf{\Phi}\mathbf{\Delta}^{-1/2} = \mathbf{\Phi}(\mathbf{1} + \mathbf{S})^{-1/2}. \tag{21}$$

If the overlap matrix $\mathbf{S}$ fulfills the matrix inequality $-\mathbf{1} < \mathbf{S} < +\mathbf{1}$, one has the power series expansion

$$(\mathbf{1} + \mathbf{S})^{-1/2} = \mathbf{1} - \tfrac{1}{2}\mathbf{S} + \tfrac{3}{8}\mathbf{S}^2 - \tfrac{5}{16}\mathbf{S}^3 + \cdots, \tag{22}$$

and obtains

$$\varphi_\mu = \Phi_\mu - \tfrac{1}{2}\sum_\alpha \Phi_\alpha S_{\alpha\mu} + \tfrac{3}{8}\sum_{\alpha,\beta} \Phi_\alpha S_{\alpha\beta} S_{\beta\mu} - \tfrac{5}{16}\sum_{\alpha,\beta,\gamma} \Phi_\alpha S_{\alpha\beta} S_{\beta\gamma} S_{\gamma\mu} + \cdots. \tag{23}$$

This formula contains the previous results by Wannier and by Landshoff in a way which is now correct to all orders in the overlap S.

The series (22) is convergent only for a comparatively small class of molecules and solids, and it is then necessary that one evaluates $\mathbf{\Delta}^{-1/2}$ in some other way. Since $\mathbf{\Delta}$ is a self-adjoint matrix, $\mathbf{\Delta}^\dagger = \mathbf{\Delta}$, it may be brought to diagonal form $\mathbf{d}$ by a unitary transformation $\mathbf{U}$:

$$\mathbf{U}^\dagger\mathbf{\Delta}\mathbf{U} = \mathbf{d}. \tag{24}$$

One has also the formula $\mathbf{\Delta} = \mathbf{U}\mathbf{d}\mathbf{U}^\dagger$ corresponding to "the spectral resolution" of $\mathbf{\Delta}$, and an arbitrary function f of $\mathbf{\Delta}$ is then defined through the relation

$$f(\mathbf{\Delta}) = \mathbf{U}f(\mathbf{d})\mathbf{U}^\dagger; \tag{25}$$

for the matrix $\boldsymbol{\Delta}^{-1/2}$, one has particularly

$$\boldsymbol{\Delta}^{-1/2} = \mathbf{U}\mathbf{d}^{-1/2}\mathbf{U}^{\dagger}. \tag{26}$$

The practical evaluation of this quantity is by no means trivial, but, for cyclic systems, there exist closed formulas (Löwdin, 1950; Löwdin *et al.*, 1960; Calais and Appel, 1964).

The functions $\boldsymbol{\varphi}$ obtained by symmetric orthonormalization according to (21) have some important properties. In 1954, it was shown by Slater and Koster that, if the basis $\boldsymbol{\Phi}$ undergoes a unitary transformation $\mathbf{R}$, then the set $\boldsymbol{\varphi}$ undergoes the same transformation.

The proof is simple. One has $\boldsymbol{\Phi}' = \boldsymbol{\Phi}\mathbf{R}$ and $\boldsymbol{\Delta}' = \langle \boldsymbol{\Phi}' \,|\, \boldsymbol{\Phi}' \rangle = \mathbf{R}^{\dagger}\boldsymbol{\Delta}\mathbf{R}$. The matrix $\boldsymbol{\Delta}'$ is brought to diagonal form $\mathbf{d}$ by the unitary transformation $\mathbf{U}' = \mathbf{R}^{\dagger}\mathbf{U}$, and one obtains particularly

$$\begin{aligned}(\boldsymbol{\Delta}')^{-1/2} &= \mathbf{U}'\mathbf{d}^{-1/2}(\mathbf{U}')^{\dagger} = \mathbf{R}^{\dagger}\mathbf{U}\mathbf{d}^{-1/2}\mathbf{U}^{\dagger}\mathbf{R} \\ &= \mathbf{R}^{\dagger}\boldsymbol{\Delta}^{-1/2}\mathbf{R},\end{aligned} \tag{27}$$

which gives $\boldsymbol{\varphi}' = \boldsymbol{\Phi}'(\boldsymbol{\Delta}')^{-1/2} = \boldsymbol{\Phi}\mathbf{R} \cdot \mathbf{R}^{\dagger}\boldsymbol{\Delta}^{-1/2}\mathbf{R} = \boldsymbol{\Phi}\boldsymbol{\Delta}^{-1/2}\mathbf{R}$ i.e.,

$$\boldsymbol{\varphi}' = \boldsymbol{\varphi}\mathbf{R}. \tag{28}$$

The result implies that, if the functions $\boldsymbol{\Phi}$ are adapted to a particular symmetry group, the same applies also to the orthonormalized functions $\boldsymbol{\varphi} = \boldsymbol{\Phi}\boldsymbol{\Delta}^{-1/2}$.

Another feature of the functions $\boldsymbol{\varphi}$ given by (21) is that they resemble the initial functions $\boldsymbol{\Phi}$ as closely as possible (Pratt and Neustadter, 1956; Carlson and Keller, 1957; Lykos and Schmeising, 1961). In order to study this property in greater detail, it is convenient to study the metric matrix associated with the difference $(\boldsymbol{\Phi} - \boldsymbol{\varphi})$ when $\boldsymbol{\varphi} = \boldsymbol{\Phi}\mathbf{A}$ is an arbitrary linear combination of the original orbitals satisfying (9). One has

$$\begin{aligned}\langle \boldsymbol{\Phi} - \boldsymbol{\varphi} \,|\, \boldsymbol{\Phi} - \boldsymbol{\varphi} \rangle &= (\mathbf{1} - \mathbf{A})^{\dagger}\langle \boldsymbol{\Phi} \,|\, \boldsymbol{\Phi} \rangle(\mathbf{1} - \mathbf{A}) \\ &= (\mathbf{1} - \mathbf{A}^{\dagger})\boldsymbol{\Delta}(\mathbf{1} - \mathbf{A}) = \boldsymbol{\Delta} - \mathbf{A}^{\dagger}\boldsymbol{\Delta} - \boldsymbol{\Delta}\mathbf{A} + \mathbf{A}^{\dagger}\boldsymbol{\Delta}\mathbf{A} \\ &= \mathbf{1} + \boldsymbol{\Delta} - \mathbf{A}^{\dagger}\boldsymbol{\Delta} - \boldsymbol{\Delta}\mathbf{A}.\end{aligned} \tag{29}$$

Introducing the substitution (19), one obtains further

$$\begin{aligned}\langle \boldsymbol{\Phi} - \boldsymbol{\varphi} \,|\, \boldsymbol{\Phi} - \boldsymbol{\varphi} \rangle &= \mathbf{1} + \boldsymbol{\Delta} - \mathbf{B}^{\dagger}\boldsymbol{\Delta}^{1/2} - \boldsymbol{\Delta}^{1/2}\mathbf{B} \\ &= (\mathbf{1} - \boldsymbol{\Delta}^{1/2})^2 + 2\boldsymbol{\Delta}^{1/2} - \mathbf{B}^{\dagger}\boldsymbol{\Delta}^{1/2} - \boldsymbol{\Delta}^{1/2}\mathbf{B} \\ &= (\mathbf{1} - \boldsymbol{\Delta}^{1/2})^2 + \boldsymbol{\Delta}^{1/4}(\mathbf{1} - \mathbf{B})^{\dagger}(\mathbf{1} - \mathbf{B})\boldsymbol{\Delta}^{1/4} \\ &\quad + (\boldsymbol{\Delta}^{1/4}\mathbf{B}^{\dagger}\boldsymbol{\Delta}^{1/4} - \mathbf{B}^{\dagger}\boldsymbol{\Delta}^{1/2}) + (\boldsymbol{\Delta}^{1/4}\mathbf{B}\boldsymbol{\Delta}^{1/4} - \boldsymbol{\Delta}^{1/2}\mathbf{B}).\end{aligned} \tag{30}$$

In forming the trace of this matrix, the contributions from the last two terms vanish identically. Putting $\mathbf{C} = (\mathbf{1} - \mathbf{B})\mathbf{\Delta}^{1/4}$, where $\mathbf{\Delta}^{1/4}$ is the square root out of the *positive* square root $\mathbf{\Delta}^{1/2}$, one gets

$$\begin{aligned}\sum_{k=1}^{n} \|\Phi_k - \varphi_k\|^2 &= \operatorname{Tr}\langle \mathbf{\Phi} - \boldsymbol{\varphi} \mid \mathbf{\Phi} - \boldsymbol{\varphi}\rangle \\ &= \operatorname{Tr}(\mathbf{1} - \mathbf{\Delta}^{1/2})^2 + \operatorname{Tr}(\mathbf{C}^\dagger\mathbf{C}) \qquad (31) \\ &= \operatorname{Tr}(\mathbf{1} - \mathbf{\Delta}^{1/2})^2 + \sum_{k,l=1}^{n} |C_{kl}|^2.\end{aligned}$$

This quantity has a minimum for $\mathbf{C} = 0$, i.e., for $\mathbf{B} = \mathbf{1}$, which proves the "resemblance theorem" for the symmetric orthonormalization.

C. Canonical Orthonormalization

In molecular and solid-state theory, there are cases when also the symmetric orthonormalization procedure will break down, depending on the fact that, even if the basis $\mathbf{\Phi} = \{\Phi_1, \Phi_2, \ldots, \Phi_n\}$ is linearly independent from the mathematical point of view, it may be *approximately linearly dependent* from the computational point of view. This phenomenon causes a great many complications and may lead to very misleading results, since the associated secular equations may be almost identically vanishing (Parmenter, 1952). Unfortunately, it seems as if many of the conventionally used basic systems are strongly affected by approximate linear dependencies (Löwdin, 1960, 1962).

In order to systematize this problem, it is convenient to study the metric matrix $\mathbf{\Delta}$ in greater detail. It is hermitean and positive definite:

$$\mathbf{\Delta} > \mathbf{0}, \qquad (32)$$

which follows from the fact that, for any column vector $\mathbf{a} = \{a_k\}$ of complex number, one has

$$\mathbf{a}^\dagger\mathbf{\Delta}\mathbf{a} = \mathbf{a}^\dagger\langle \mathbf{\Phi} \mid \mathbf{\Phi}\rangle\mathbf{a} = \langle \mathbf{\Phi}\mathbf{a} \mid \mathbf{\Phi}\mathbf{a}\rangle > 0, \qquad (33)$$

according to the fourth axiom in (2). We note, that the relation $\mathbf{a}^\dagger\mathbf{\Delta}\mathbf{a} = 0$ necessarily implies $\mathbf{\Phi}\mathbf{a} = 0$, i.e., a linear dependency, and vice versa. The minimum value of the quantity $\mathbf{a}^\dagger\mathbf{\Delta}\mathbf{a}$, subject to the condition $\mathbf{a}^\dagger\mathbf{a} = 1$, is called the *measure of linear independence* μ of the set $\mathbf{\Phi} = \{\Phi_k\}$. One has

$$\mu = \min(\mathbf{a}^\dagger\mathbf{\Delta}\mathbf{a}/\mathbf{a}^\dagger\mathbf{a}), \qquad (34)$$

for arbitrary $\mathbf{a}$, and it is clear that μ is identical to the lowest eigenvalue of $\mathbf{\Delta}$. If an eigenvalue of $\mathbf{\Delta}$ is exactly or approximately vanishing, one is faced with an exact or approximate linear dependency, respectively, in the set $\mathbf{\Phi}$. In such a case, it may be necessary to refine the basis and to exclude certain functions.

In order to approach this problem, we will start by considering the general solution (20). Using (26) and choosing $\mathbf{B} = \mathbf{U}$, one obtains

$$\boldsymbol{\chi} = \mathbf{\Phi}\mathbf{\Delta}^{-1/2}\mathbf{U} = \mathbf{\Phi}\mathbf{U}\mathbf{d}^{-1/2}, \tag{35}$$

where we have used the notation $\boldsymbol{\chi}$ for the new functions; one has the simple connection $\boldsymbol{\chi} = \boldsymbol{\varphi}\mathbf{U}$. The transformation (35) is now often referred to as the "canonical orthonormalization"; it was introduced in 1956 by the author (Löwdin, 1956).

It should be observed that there are considerable differences in character between the orthonormal sets $\boldsymbol{\varphi} = \mathbf{\Phi}\mathbf{\Delta}^{-1/2}$ and $\boldsymbol{\chi} = \mathbf{\Phi}\mathbf{U}\mathbf{d}^{-1/2}$. If $\mathbf{\Phi}$ is a set of atomic orbitals of a molecular or solid-state system, the set $\boldsymbol{\varphi}$ is still rather strongly localized, whereas the set $\boldsymbol{\chi}$ consists of functions which are delocalized over the entire system in the same way as molecular orbitals or Bloch functions.

Relation (35) may now be written in the form

$$\chi_k = \frac{1}{d_k^{1/2}} \sum_\alpha \Phi_\alpha U_{\alpha k}, \tag{36}$$

and, for the sum of the absolute squares of the coefficients for Φ_α, one obtains

$$\sum_\alpha \left| \frac{U_{\alpha k}}{d_k^{1/2}} \right|^2 = \frac{1}{d_k}, \tag{37}$$

i.e., if an eigenvalue d_k is vanishing, the associated function χ_k blows up. One may hence arrange the functions $\boldsymbol{\chi} = \{\chi_1, \chi_2, \ldots, \chi_n\}$ after decreasing values of $d_1 \geq d_2 \geq d_3 \geq \cdots \geq d_n$, and the lowest eigenvalues will always reveal the existence of exact or approximate linear dependencies. In the case when an eigenvalue d_k is too small, the associated function χ_k may be deleted from the theory.

In this connection, one should observe that the canonical orthonormalization has a characteristic optimal property. Let us again consider the general transformation $\boldsymbol{\varphi} = \mathbf{\Phi}\mathbf{A}$ and the relation $\langle\boldsymbol{\varphi} \mid \boldsymbol{\varphi}\rangle = \mathbf{A}^\dagger\mathbf{\Delta}\mathbf{A} = \mathbf{1}$. Introducing the substitution (19), one obtains for the sum of the absolute square of the coefficients in the expansion $\varphi_k = \sum_\alpha \Phi_\alpha A_{\alpha k}$,

$$\sum_\alpha |A_{\alpha k}|^2 = \sum_\alpha A_{\alpha k}^* A_{\alpha k} = (\mathbf{A}^\dagger\mathbf{A})_{kk} = (\mathbf{B}^\dagger\mathbf{\Delta}^{-1}\mathbf{B})_{kk}, \tag{38}$$

and the smallest value is hence d_1^{-1} associated with the function χ_1. If one considers the same problem for all functions orthogonal to χ_1, one finds that the sum $\sum_\alpha |A_{\alpha k}|^2$ has the smallest value d_2^{-1}, etc., which is the characteristic optimum feature.

III. Further Aspects on the Nonorthogonality Problem

In the alkali halides consisting of ions with complete shells, a Slater determinant built up from the atomic orbitals involved is invariant under linear transformations, so one may just as well introduce Bloch functions or orthonormalized atomic orbitals (OAO's)—all expectation values will anyway be the same. The nonorthogonality catastrophe associated with the expression (1) is now resolved, and the solution depends on the fact that the denominator and numerator of the quotient (1) contain the same diverging factor.

One could also hope that the nonorthogonality problem in the valence-bond method in general would be solved by introducing OAO's, since they would explain some of the underlying assumptions (Rumer, 1932; Pauling, 1933). However, Slater (1951) showed by means of the simple example of the hydrogen molecule that a valence bond structure based on OAO's instead of ordinary AO's does not lead to chemical bonding, and that, in addition to the canonical structures, it would be necessary to introduce a large number of "polar structures." These ideas have been carried further by McWeeny (1954, 1960) and others, but the inclusion of the polar states offers about the same amount of complication as the nonorthogonality problem itself.

The matrix element of the Hamiltonian with respect to two Slater determinants built up from nonorthogonal functions is now easily constructed (Löwdin, 1955), but, so far, it has not been possible to give a simple expression for the same quantity with respect to two general valence-bond structures taking the overlap integrals into full account.* For a four-electron problem, one can still handle all the terms occurring by means of brute-force methods (Slater, 1953) but, for a six-electron problem, the complications seem insurmountable without a deeper analysis of the valence-bond structures themselves. In a study of the spin-degeneracy problem, the author (Löwdin, 1958) has expressed the valence-bond functions as sums of spin-projected Slater-determinants, and, by using this approach, it should now be possible to evaluate the matrix element of H with respect to two general valence bond structures, taking the overlap into full account.

In the molecular-orbital method for treating molecules and solids, the introduction of the OAO's has rendered considerable simplifications. In the Hückel theory (1930) of the mobile electrons of the conjugated systems, one could now easily include the overlap integrals (Löwdin, 1950). In the calculation of the cohesive energy of molecules and crystals in the

---

* *Note added in proof:* For an explicit solution, see Shull (1969).

Hartree–Fock scheme, based on the MO-LCAO-method and Mulliken's approximation for evaluating the molecular integrals, one could now reduce the expectation value of the electronic repulsion term to essentially so-called Coulomb integrals $(aa \mid bb)$ and overlap integrals (Löwdin, 1953, 1956).

In connection with the Pariser–Parr (1953; Parr, 1952) model for treating conjugated systems, the author (Löwdin, 1952) pointed out that one could rather well understand the assumption of "zero-differential-overlap," if one started from OAO's instead of ordinary AO's. An excellent survey of the development in this field has been given by Fischer-Hjalmars (1965) and Roos (1968) studied the basis for the "zero differential overlap method" in great detail in his thesis.

Even today, the nonorthogonality problem has not lost its actuality, and there are apparently still many problems to be solved in quantum chemistry and solid-state physics in connection with the valence-bond method, the Dirac–Van Vleck vector-coupling model, and the theory of magnetic properties and spin degeneracy in general. For a more detailed discussion, the reader is referred to a recent review by Herring (1966).

IV. Calculation of Cohesive and Elastic Properties of the Alkali Halides

A characteristic feature of Professor Waller's thesis suggestion in 1946 was that, even if the solution of the nonorthogonality problem would be a convenient starting point, the main emphasis would be on the calculation of the cohesive energy and the elastic constants of some of the alkali halides and on the comparison between the theoretical results and the experimental experience. For Professor Waller, theoretical physics was an integral part of physics itself, and he also tried to convey this fundamental philosophy to his students.

The starting point for this *ab initio* calculation (Löwdin, 1948) was the Hartree–Fock functions for the orbitals of the free ions, and the only empirical data used were the atomic numbers Z for the ions involved and the values of the fundamental constants e, m, h, ... As expected, the cohesive energies came out quite well, whereas the lattice constants showed somewhat larger errors. The study of the properties of the alkali halides under very high pressure including lattice transitions gave results within the error limits of Bridgman's measurements, whereas the values of the individual elastic constants showed rather large deviations from the corresponding experimental results.

It was perhaps somewhat surprising that, depending on the overlap between neighboring ions, the expectation value (1) of the energy showed energy terms depending simultaneously on the positions of several ions and hence corresponding to "many-body" forces. In the derivation of the Cauchy relations, one assumes that the particles of the solid interact with central forces of a two-body type having a potential of the form

$$\sum_{i<j} V_{ij}(r_{ij}), \tag{39}$$

whereas there are here also three-body potentials,

$$\sum_{i<j<k} V_{ijk}(r_{ij}, r_{jk}, r_{ki}), \tag{40}$$

four-body potentials, etc. Even the many-body potentials are apparently translationally and rotationally invariant, and a closer study reveals that these terms cause deviations from the Cauchy relations for the elastic constants. The calculations gave theoretical results in fairly good agreement with the experimental values.

All calculations were performed on ordinary desk computers of the type " Facit ESA" by a team of ten student computers with support of a grant from the Swedish Natural Science Research Council. All molecular integrals of two-, three-, and four-center type were evaluated by expanding all atomic orbitals occurring in terms of spherical harmonics around a single center following a technique introduced by Coolidge (1932) and Landshoff (1936) which was further refined (Löwdin, 1948, 1956; Lundqvist and Löwdin, 1951; Barnett and Coulson, 1951). This expansion technique in terms of so-called α-functions is even today of a certain value, and it is still under further development (Sharma, 1968).

The work on the calculation of the cohesive and elastic properties of the alkali halides was continued at the Institute for Theoretical Physics by Lundqvist (1954a,b, 1955; Lundqvist and Fröman, 1950; Lundqvist and Löwdin, 1951), who also studied the properties of the lattice vibrations. The numerical calculations were still carried out on desk computers.

In 1962, there was a renewed interest in this field in the Uppsala Quantum Chemistry Group connected with a previous study of the virial theorem and the scaling procedure (Fröman and Löwdin, 1962). The sodium chloride crystal has a cohesive energy of -184.4 kcal/mole, and according to the virial theorem, the kinetic energy contribution is $+184.4$ kcal/mole and the potential energy contribution -368.8 kcal/mole, of which -208.0 is the Madelung energy whereas -160.8 kcal/mole is the contribution depending on the "extension" of the ions and their electronic structure. The virial theorem unfortunately destroys the simplicity of the Born–Mayer model of the cohesive properties of the alkali halides, but the theorem is nevertheless true and its consequences should be studied.

Large-scale electronic computers were now available in Uppsala, and one started investigating the effect of scaling the atomic orbitals involved. All the previous desk calculations could now be repeated with higher accuracy, the effect of the interaction between next-nearest neighbors and those more remote could be included, and several other improvements could be performed in the theoretical work. Highly accurate numerical computations could be carried out at the Uppsala Data Center. In addition, precision measurements of the elastic constants could be carried out by members of the Solid-State Group at the Institute of Physics leading to a deepening of the experimental side of the problem.

In this way, Professor Waller's suggestion in 1946 has twenty years later developed into fruitful team work by quantum chemists, solid-state physicists, and numerical experts, and into an interesting exchange of ideas between theorists and experimenters (Mansikka and Bystrand, 1966; Vallin *et al.*, 1967; Calais *et al.*, 1967; Pettersson *et al.*, 1967, 1968).

ACKNOWLEDGMENT

With this paper, I would like to congratulate Professor Ivar Waller on his 70th birthday on June 11, 1968 and to wish him many years of happiness and continued scientific work. I would also like to take the opportunity to express my sincere gratitude to him for suggesting a very interesting thesis problem in 1946 and for his continued interest and encouragement during the work. As the leader of the Institute of Theoretical Physics at Uppsala University for many years, Professor Ivar Waller had the outstanding feature of setting very high standards for himself and his students for their scientific work. Even if these standards could seldom or never be met by his students—particularly not by myself—they were something to aim for, and they have certainly been essential for the quality of the rich production coming from the Institute of Theoretical Physics under Professor Ivar Waller's leadership.

REFERENCES

BARNETT, M. P., and COULSON, C. A. (1951). *Phil Trans*, **A243**, 221.
BLOCH, F. (1929). *Z. Physik* **52**, 555; **57**, 545.
CALAIS, J. L., and APPEL, K. (1964). *J. Math. Phys.* **5**, 1001.
CALAIS, J. L., MANSIKKA, K., PETTERSSON, G., and VALLIN, J. (1967). *Arkiv Fysik* **34**, 361.
CARLSON, D. C., and KELLER, J. M. (1957). *Phys. Rev.* **105**, 102.
COOLIDGE, A. S. (1932). *Phys. Rev.* **42**, 189.
COURANT, R., and HILBERT, D. (1931). "Methoden d. Math. Physik." Springer, Berlin.
FISCHER-HJALMARS, I. (1965). *Advan. Quantum Chem.* **2**, 25.
FRÖMAN, A., and LÖWDIN, P. O. (1962). *J. Phys. Chem. Solids* **23**, 75.
HEITLER, W., and LONDON, F. (1927). *Z. Physik* **44**, 455.
HERRING, C. (1966) *In* "Magnetism" Vol. 2B (G. T. Rado and H. Suhl, eds.), Chap. 1. Academic Press, New York.
HÜCKEL, E. (1930). *Z. Physik* **60**, 423; (1931) **70**, 204; (1931) **72**, 310.
HYLLERAAS, E. A. (1930). *Z. Physik* **63**, 771.
INGLIS, D. R. (1934). *Phys. Rev.* **46**, 135.

LANDSHOFF, R. (1936). *Z. Physik* **102**, 201.

LÖWDIN, P. O. (1947) *Arkiv Mat. Astr. Fysik* **35A**, 9.

LÖWDIN, P. O. (1948). A Theoretical Investigation into some Properties of Ionic Crystals. Thesis, Uppsala, Almqvist and Wiksells.

LÖWDIN, P. O. (1950). *J. Chem. Phys.* **18**, 365.

LÖWDIN, P. O. 1952. Letter to Dr. R. G. Parr of December 3; published in (1955) *Sv. Kem. Tidskr.* **67**, 381.

LÖWDIN, P. O. (1953). *Proc. Intern. Congr. Theort. Phys. Japan*, 599.

LÖWDIN, P. O. (1955). *Phys. Rev.* **97**, 1474, 1490.

LÖWDIN, P. O. (1956). *Advan. Phys.* **5**, 1, particularly p. 111–114.

LÖWDIN, P. O. (1958). *Colloq. Intern. Centre Natl. Recherche Sci. (Paris)* **82**, 23.

LÖWDIN, P. O. (1960). *Ann. Rev. Phys. Chem.* **11**, 107.

LÖWDIN, P. O., PAUNCZ, R., and DE HEER, J. (1960). *J. Math. Phys.* **1**, 461.

LÖWDIN, P. O. (1962). *J. Appl. Phys. Suppl.* **33**, S 251.

LUNDQVIST, S. O. (1954a). *Arkiv Fysik* **6**, 25.

LUNDQVIST, S. O. (1954b). *Arkiv Fysik* **8**, 177.

LUNDQVIST, S. O. (1955). *Arkiv Fysik* **9**, 435.

LUNDQVIST, S. O., and FRÖMAN, P. O. (1950). *Arkiv Fysik* **2**, 431.

LUNDQVIST, S. O., and LÖWDIN, P. O. (1951). *Arkiv Fysik* **3**, 147.

LYKOS, P. G., and SCHMEISING, H. N. (1961). *J. Chem. Phys.* **35**, 288.

MANSIKKA, K., and BYSTRAND, F. (1966). *J. Phys. Chem. Solids* **27**, 1073.

MCWEENY, R. (1954). *Proc. Roy. Soc. London* **A223**, 63, 306.

MCWEENY, R. (1960). *Rev. Mod. Phys.* **32**, 335.

PARMENTER, R. H. (1952). *Phys. Rev.* **86**, 552.

PARR, R. G. (1952). *J. Chem. Phys.* **20**, 1499.

PAULING, L. (1931). *J. Am. Chem. Soc.* **53**, 1367.

PAULING, L. (1933). *J. Chem. Phys.* **1**, 280.

PARISER, R., and PARR, R. G. (1953). *J. Chem. Phys.* **21**, 466.

PETTERSSON, G., VALLIN, J., CALAIS, J. L., and MANSIKKA, K. (1967). *Arkiv Fysik* **34** 371.

PETTERSSON, G., VALLIN, J., CALAIS, J. L., and MANSIKKA, K. (1968). *Arkiv Fysik* **37**, 267.

PRATT, G. W., JR., and NEUSTADTER, S. F. (1956). *Phys. Rev.* **101**, 1248.

ROOS, B. (1968). Application of the Zero Differential Overlap Approximation in Theoretical Studies of Organic and Organometallic Molecules. Thesis, Stockholm.

RUMER, G. (1932). *Nachr. Akad. Wiss. Goettingen, Mat.-Phys.-Chem.*, 372. "Göttinger Nachrichten."

SHARMA, R. R. (1968). *J. Math. Phys.* **9**, 505.

SHULL, H. (1969), *Intern. J. Quantum Chem.* **3**, 523.

SLATER, J. C. (1930a). *Phys. Rev.* **35**, 210.

SLATER, J. C. (1930b). *Phys. Rev.* **35**, 509.

SLATER, J. C. (1931). *Phys. Rev.* **37**, 481.

SLATER, J. C. (1931a). *Phys. Rev.* **37**, 481.

SLATER, J. C. (1951). *J. Chem. Phys.* **19**, 220.

SLATER, J. C. (1953). Quart. Progr. Rept. of Solid-State and Mol. Theory Group. M.I.T., p. 3, October 15, 1953 (unpublished).

SLATER, J. C., and KOSTER, G. F. *Phys. Rev.* **94**, 1498 (1954).

VALLIN, J., PETTERSSON, G., CALAIS, J. L., and MANSIKKA, K. (1967). *Arkiv Fysik* **34**, 199.

WANNIER, G. H. (1937). *Phys. Rev.* **52**, 191.

Symmetry Properties of Reduced Density Matrices and Natural *p*-States

W. A. BINGEL
and W. KUTZELNIGG
Theoretical Chemistry Group
University of Göttingen
Göttingen, Germany

I. Introduction

In the last few years, reduced density matrices have received increasing interest in quantum-chemical investigations. On the one hand, numerical first- and second-order density matrices (one- and two-particle density matrices) for certain states of simple atomic and molecular systems have been calculated starting from rather good approximate wave functions (Barnett *et al.*, 1965; Davidson, 1963; Davidson and Jones 1962; Smith, 1967). These matrices are particularly useful for testing the validity of different wave functions of the same system. Different approximations are most conveniently compared in terms of the eigenstates of these matrices, i.e., the natural spin-orbitals (NSO's) and natural spin-geminals (NSG's) as well as the corresponding eigenvalues, the occupation numbers (Kutzelnigg, 1965; Staemmler and Kutzelnigg, 1967).

On the other hand, the *general* properties of these matrices and their eigenstates, i.e., those properties which are independent of the nature of the wave functions used in their construction, are especially interesting and some effort has been spent on studying them (Bingel, 1960, 1961, 1962; Coleman, 1963; Kutzelnigg, 1965b; Löwdin, 1955; McWeeny, 1959, 1960, 1965; McWeeny and Mizuno, 1961; McWeeney and Kutzelnigg, 1968). The present paper attempts a review of such studies with special emphasis on the symmetry properties of both the density matrices and the natural p-states resulting from a given symmetry behavior of the wave functions from which the density matrices are constructed.

II. Symmetry Properties of Transition Density Matrices

The pth order transition density matrices are defined (Löwdin, 1955) (with the normalization of Coleman, 1963) as

$$D^p_{\alpha i,\beta j}(x, x') = \int \Psi_{\alpha i}(x, y)\Phi^*_{\beta j}(x', y)\, dy, \tag{1}$$

where x stands for the space- and spin-variables of the first p particles and y for the remaining $N-p$ ones, and the wave functions $\Psi_{\alpha i}$ $(i = 1, 2, \ldots, d_\alpha)$ and $\Phi_{\beta j}$ $(j = 1, 2, \ldots, d_\beta)$ are supposed to belong to irreducible representations (irr. rep.) $\Gamma^{(\alpha)}$ and $\Gamma^{(\beta)}$ of the symmetry group $\mathcal{G}$ of the system under consideration. It is then easy to show (Bingel, 1960; Coleman, 1962; Kutzelnigg, 1963a, 1965a), that the $d_\alpha \cdot d_\beta$ transition density matrices $D^p_{\alpha i,\beta j}(x, x')$ transform under simultaneous application of the symmetry operation R of $\mathcal{G}$ to *both* sets of arguments x and x' as the direct product representation $\Gamma^{(\alpha)} \times \Gamma^{(\beta)*}$ since R leaves the volume element dy invariant. This representation can be reduced in the usual way

$$\Gamma^{(\alpha)} \times \Gamma^{(\beta)*} = \sum_\gamma n_\gamma \Gamma^{(\gamma)}, \qquad \sum_\gamma n_\gamma d_\gamma = d_\alpha \cdot d_\beta, \tag{2}$$

and all $D^p_{\alpha j,\beta j}$ can be decomposed into their irreducible components

$$D^p_{\alpha i,\beta j}(x, x') = \sum_{\gamma, k} \sum_{r=1}^{n_\gamma} D^p_{\gamma k,r}(x, x')C(\alpha i\beta j \mid \gamma k r). \tag{3}$$

The vector-coupling coefficients C in (3) are unambiguously defined only if the group $\mathscr{G}$ is simply reducible, i.e., if all n_γ are either zero or one. It should be noted that the $D^p_{\alpha i,\beta j}$ (for $p < N$) are not necessarily orthogonal and the $D^p_{\gamma k,r}$—although orthogonal—are not normalized to unity.[1] Nevertheless, since the coefficients C are the unitary Clebsch–Gordan coefficients for the group $\mathscr{G}$ (Koster *et al.*, 1963), Eq. (3) can be inverted to give

$$D^p_{\gamma k,r}(x, x') = \sum_{i,j} C^*(\alpha i \beta j \,|\, \gamma k r) \cdot D^p_{\alpha i,\beta j}(x, x'). \tag{4}$$

The decomposition given by Eqs. (3) and (4) holds also for $\beta = \alpha$ and is correct even if $\Phi_{\alpha i} \equiv \Psi_{\alpha i}$ (all i) as long as the arguments x and x' are defined in different carrier spaces.

Any $D^p_{\gamma k,r}$ can be obtained from the corresponding $D^N_{\gamma k,r}$ by reduction, i.e., by integration over $N - p$ variables. Some of the components $D^p_{\gamma k,r}$ can vanish although their counterparts $D^N_{\gamma k,r}$ are nonzero. This occurs generally if $\Psi_{\alpha i}$ is a *single configuration function.*

Example 1: The ${}^1D$ state of the configuration p^2.

In this case, 25 different and orthonormal $D^2_{\gamma k,r}$ exist and correspond to the irreducible representations ${}^1S$, ${}^1P$, ${}^1D$, ${}^1F$, ${}^1G$. Any of the $D^1_{\alpha i,\alpha j}$ must, however, have the form

$$D^1_{\alpha i,\alpha j}(x_1, x_1') = \sum_{k,l} v_k^{\alpha i j} p_k(x_1) p_l(x_1')$$

where $p_k = p\sigma$, $p\pi$, or $p\bar{\pi}$ with α- or β-spin. The only possible irreducible components are now ${}^1S$, ${}^3P$, and ${}^1D$, of which ${}^3P$ is forbidden because it cannot be derived from any of the $D^2_{\gamma k,r}$. So only 6 different $D^1_{\gamma k,r}$ are present, which means that of the $25 D^1_{\alpha i \alpha j}$ only 6 are linearly independent. For an exact wave function of the same state ${}^1D$, the components ${}^1P$, ${}^1F$, and ${}^1G$ will not exactly vanish, but we can expect that they are small (i.e., have small trace), as compared to ${}^1S$ and ${}^1D$.

III. Symmetry Properties of p-Densities

These quantities are defined as the *diagonal* elements ($x' = x$) of the corresponding density matrices

$$D^p_{\alpha i,\beta j}(x) = D^p_{\alpha i,\beta j}(x, x). \tag{5}$$

---

[1] Note that orthogonality and normalization in this context refer to a Frobenius-type metric, i.e., $(D_1, D_2) = \int D_1^*(x, x') D_2(x, x')\, dx \cdot dx'$ whereas what is usually defined as the norm of a density matrix is the trace $\int D(x, x)\, dx$.

These p-densities can also be decomposed into their irreducible components (Bingel, 1960) in a manner formally equivalent to Eqs. (2) to (4):

$$(\Gamma^{(\alpha)} \times \Gamma^{(\beta)*}) = \sum_{\gamma} n_{\gamma}' \Gamma^{(\gamma)}, \tag{2'}$$

$$D^{p}_{\alpha i,\beta j}(x) = \sum_{\gamma k} \sum_{r=1}^{n_{\gamma}'} C(\alpha i \beta j \mid \gamma k r) D^{p}_{\gamma k,r}(x), \tag{3'}$$

$$D^{p}_{\gamma k,r}(x) = \sum_{i,j} C^{*}(\alpha i \beta j \mid \gamma k r) D^{p}_{\alpha i,\beta j}(x), \tag{4'}$$

but with one or more irreducible components of (2) missing[2] ($n_{\gamma}' \leq n_{\gamma}$). This follows from a theorem given by Van der Waerden (1932, p. 14). The missing components in Eqs. (2′) and (3′) are just those terms in Eq. (3) which vanish identically when we put $x' = x$. We therefore can distinguish the following different cases.

Case 1

If *all* products $\Psi_{\alpha i}(x, y) \cdot \Phi_{\beta j}(x, y)^{*}$ are linearly independent, then the parentheses in Eq. (2′) can be dropped, $n_{\gamma}' = n_{\gamma}$, and Eqs. (2′) to (4′) become identical to Eqs. (2) to (4) for $x' = x$. In this case, the p-densities transform just like the corresponding density matrices, i.e., according to the direct product representation.

Example 2

$$\Phi_1 = (x^2 - y^2) g(r) \qquad \Phi_2 = -2xy \cdot f(r)$$
$$\Psi_1 = x \cdot f(r) \qquad \Psi_2 = y \cdot f(r)$$

Both sets of functions are defined in the same carrier space R_3 and both transform according to the two-fold degenerate representation E of the group D_3. Nevertheless, all four products $\Psi_1 \cdot \Phi_1, \ldots$ are linearly independent and therefore transform like $E \times E = A_1 + A_2 + E$. The linear combinations of the four products in Table I transform according to the irreducible components A_1, A_2, and E. They have already been chosen in such a way that the numerical coefficients form a unitary matrix, i.e., they are identical with the Clebsch–Gordan coefficients for this group (Koster *et al.*, 1963). If we identify the functions on the right of this scheme with the (unnormalized) irreducible components $D^{1}_{\gamma k}(x)$, then

---

[2] Such a reduction can occur only if both irr. rep. $\Gamma^{(\alpha)}$ and $\Gamma^{(\beta)}$ are multidimensional.

TABLE I

Γ	$\Psi_1 \cdot \Phi_1$	$\Psi_1 \cdot \Phi_2$	$\Psi_2 \cdot \Phi_1$	$\Psi_2 \cdot \Phi_2$	$D^1_{\gamma k}$
A_1	$\frac{1}{\sqrt{2}}$			$\frac{1}{\sqrt{2}}$	$2^{-1/2}x(x^2-3y^2)fg$
A_2		$\frac{1}{\sqrt{2}}$	$-\frac{1}{\sqrt{2}}$		$2^{-1/2}y(3x^2-y^2)fg$
E,1	$\frac{1}{\sqrt{2}}$			$-\frac{1}{\sqrt{2}}$	$2^{-1/2}x(x^2+y^2)fg$
E,2		$\frac{1}{\sqrt{2}}$	$\frac{1}{\sqrt{2}}$		$-2^{-1/2}y(x^2+y^2)fg$

Eq. (4′) immediately gives the desired decomposition of the first-order transition-density for this example.

$$\begin{aligned} D^1_{1,1} &= \frac{1}{\sqrt{2}}(D_{A_1} + D_{E,1}), & D^1_{1,2} &= +\frac{1}{\sqrt{2}}(D_{A_2} + D_{E,2}), \\ D_{2,2} &= \frac{1}{\sqrt{2}}(D_{A_1} - D_{E,1}), & D^1_{2,1} &= -\frac{1}{\sqrt{2}}(D_{A_2} - D_{E,2}), \end{aligned} \tag{6}$$

where the subscripts $\alpha = \beta = E$ and the argument $x = (x, y, z)$ have been omitted. For simplicity's sake, we have chosen wave functions in 1-particle space and have calculated the unreduced density D^1. However, the same results would have been obtained if we had calculated the p-density for N-particle wave functions which transform in the same way as the simple 1-particle functions used here. Since in this example $n_\gamma{}' = n_\gamma$, Eq. (6) with the argument (x, x') also give the decomposition (3) of the density *matrix*.

Case 2

A quite different situation arises if the two sets of functions are *identical*: $\Phi_{\alpha i} = \Psi_{\alpha i}$ (all i). Instead of $d_\alpha{}^2$ we now have only $\frac{1}{2}d_\alpha \cdot (d_\alpha + 1)$ independent products, which span the symmetric direct product representation $[\Gamma^{(\alpha)} \times \Gamma^{(\alpha)*}]$, see Bingel (1960). Equation (2′)—with square brackets instead of parentheses—and Eq. (3′) still hold, but $n_\gamma{}' \leq n_\gamma$.

Example 3

$\Psi_1 = \Phi_1 = xf(r)$, $\Psi_2 = \Phi_2 = yf(r)$, again for the irr. rep. $\alpha = \beta = E$ of the group D_3. Now we have only 3 independent products, which span the rep. $[E^2] = A_1 + E$. The irr. rep. A_2 is now missing, as compared to Ex. 2. We can again find the irreducible components by inspection

$$\begin{aligned} D_{A_1} &= \tfrac{1}{2}({\Phi_1}^2 + {\Phi_2}^2) = \tfrac{1}{2}(x^2 + y^2)f^2, \\ D_{E,1} &= \tfrac{1}{2}({\Phi_1}^2 - {\Phi_2}^2) = \tfrac{1}{2}(x^2 - y^2)f^2, \\ D_{E,2} &= \Phi_1\Phi_2 = x \cdot y \cdot f^2. \end{aligned}$$

Inverting these equations gives the decomposition

$$\begin{aligned} D^1_{1,1} &= (D^1_{A_1} + D^1_{E,1}), \\ D^1_{2,2} &= (D^1_{A_1} - D^1_{E,1}), \\ D^1_{1,2} &= D^1_{2,1} = D^1_{E,2}\,. \end{aligned} \tag{7}$$

Case 3

A somewhat less trivial case occurs if $\beta = \alpha$ and $\Psi_{\alpha_i} = h_\alpha \Phi_{\alpha_i}$ where the common factor h_α is invariant with respect to $\mathscr{G}$. Otherwise everything is as in Case 2.

Example 4

Φ_1, Φ_2 as in Example 2, $h = z^2$. The three linearly independent transition densities transform again according to $[E^2]$ of D_3 and their decomposition into irreducible components is again given by Eq. (7), but with different expressions for these irreducible components.

Case 4

The *general* case of linearly dependent products has not been completely explored. If $\mathscr{G}$ is the 3-dimensional rotation inversion group K_h, the answer is of course well known. For the density matrices Eq. (2) becomes

$$\Gamma_l \times \Gamma^*_{l'} = \Gamma_{l+l'} + \Gamma_{l+l'-1} + \cdots + \Gamma_{|l-l'|} \tag{8a}$$

and the coefficients in Eq. (3) are the Clebsch–Gordan coefficients of the group K_h. For the p-densities, Eq. (2′) becomes

$$(\Gamma_l \times \Gamma^*_{l'}) = \Gamma_{l+l'} + \Gamma_{l+l'-2} + \cdots + \Gamma_{|l-l'|} \tag{8b}$$

with every other irreducible component missing. The coefficients in Eq. (3′) are now the Condon–Shortley coefficients.

Example 5

$$\begin{aligned} \Phi_1 &= 2yz \cdot g(r) \qquad & \Phi_2 &= -2xz \cdot g(r) \\ \Psi_1 &= x \cdot f(r) \qquad & \Psi_2 &= y \cdot g(r) \end{aligned}$$

This is just like Example 2, but with two other d-type functions for Φ_1 and Φ_2. We can therefore use the coupling coefficients of Table I to get the irreducible components according to Eq. (4′):

$$\begin{aligned} D_{A_1} &\equiv 0, \\ D_{A_2} &= -\sqrt{2}z(x^2+y^2)\cdot fg, \\ D_{E,1} &= 2\sqrt{2}xyz\cdot fg, \\ D_{E,2} &= -\sqrt{2}z(x^2-y^2)\cdot fg. \end{aligned}$$

The decomposition (6) still holds for the densities, but with the totally symmetric part D_{A_1} vanishing identically. A comparison of Examples 2 and 5 suggests that the missing irreducible components cannot be determined with group-theoretical arguments alone, but depend on the specific form of the functions Φ_i and Ψ_i. For example, one can consider all 12 transition-density matrices between the 3 p-functions and the 5 d-functions and obtain for the decomposition (2) from Eq. (8a)

$$P \times D = F + D + P$$

and for the decomposition (2′) from Eq. (8b)

$$(P \times D) = F + P.$$

On reducing the symmetry from K_h to D_3, the missing component D gives $A_1 + 2E$. However, this group-theoretical argument does not tell us why the missing component A_1 occurs with the subset of the functions of Example 5 (p_x, p_y and d_{yz}, $-d_{xz}$), but not with the functions (p_x, p_y and $d_{x^2-y^2}$, $-d_{xy}$) of Example 2.

IV. The First-Order Transition Density Matrices

A. Spin Symmetry

If the wave functions in Eq. (1) describe pure spin states (S and M_S are good quantum numbers), then the spin dependence of $D^{(1)}_{\alpha i,\beta j}(x_1, x_1')$ can be separated off (Bingel, 1960, 1961; McWeeny and Mizuno, 1961). All M_a, M_b-components of $D^{(1)}$ can be expressed in terms of two spinless quantities $P_1(r_1, r_1')$ and $Q_S^{st}(r_1, r_1')$ (in the notation of McWeeny, 1965), where

$$P_1(r_1, r_1') = N \int \Psi_a(r_1 s_1, x_2 \cdots x_N)\Phi_b{}^*(r_1' s_1, x_2 \cdots x_N)\, ds_1\, dx_2 \cdots dx_N \tag{9a}$$

$$\begin{aligned} Q_S^{st}(r_1, r\quad) = N \int &\Psi_a^{st}(r_1, s_1, x_2 \cdots x_N) \\ &\cdot S_{\bar{m}}^{(1)}(s_1)\Phi_b^{st}(r_1' s_1, x_2 \cdots x_N)\, ds_1\, dx_2 \cdots dx_N. \end{aligned} \tag{9b}$$

Here $\bar{m} = S_a - S_b$ and $S_{\bar{m}}^{(1)}$ is the spherical tensor of order 1 in the spin space of particle 1. The superscript "st" refers to certain "standard states" with respect to M_a, M_b (McWeeny, 1965).

B. Spatial Symmetry

For a spatial symmetry group $\mathscr{G}$, the behavior of $D^1(x \mid x')$ is now reduced to that of the two spinless quantities P_1 and Q_S^{st}. Since a purely spatial symmetry operation R does not act on $S_{\bar{m}}^{(1)}$ and leaves the volume element in Eq. (9) invariant, the argument used in Section II leads to the conclusion that both $P_1(r_1 r_1')$ and $Q_S^{\text{st}}(r_1 r_1')$ can be decomposed into irreducible components in a way completely analogous to Eqs. (2) to (4). For the diagonal elements $P_1(r) = P_1(r, r)$ (the electron density) and $Q_S^{\text{st}}(r) = Q_S^{\text{st}}(r, r)$ (the spin density), Eqs. (2′) to (4′) hold with the same changes as for the nondiagonal elements. The behavior of $P_1(r)$ and $Q_S^{\text{st}}(r)$ under the rotation-inversion group K_h has been investigated by one of the present authors (Bingel, 1960, 1962).

V. The Second-order Transition Density Matrices

A. Spin Symmetry

For wave functions in pure spin states, the second-order transition-density-matrix $D_{\alpha i,\beta j}^{(2)}(x_1 x_2, x_1' x_2')$ can be expressed in terms of the *three* spinless quantities (McWeeny, 1965; McWeeny *et al.*, 1961, 1968).

$$P_2(r_1 r_2\,;\, r_1' r_2') = N(N-1) \int \Psi_a \Psi_b^* \, ds_1\, ds_2\, dx_3 \cdots dx_N, \tag{10a}$$

$$Q_{\text{SL}}^{\text{st}}(r_1 r_2\,;\, r_1' r_2') = N(N-1) \int \Psi_a^{\text{st}} S_{\bar{m}}^{(1)}(s_1) \Psi_b^{\text{st}} \, ds_1\, ds_2\, dx_3 \cdots dx_N, \tag{10b}$$

$$Q_{\text{SS}}^{\text{st}}(r_1 r_2,\, r_1' r_2') = N(N-1) \int \Psi_a^{\text{st}} S_{\bar{m}}^{(2)}(s_1 s_2) \Psi_b^{\text{st}} \, ds_1\, ds_2\, dx_3 \cdots dx_N, \tag{10c}$$

with $\Psi_a = \Psi_a(r_1 s_1,\, r_2 s_2,\, x_3 \cdots x_N)$; $\Psi_b = \Psi_b(r_1' s_1,\, r_2' s_2,\, x_3 \cdots x_N)$. The definition of the spherical tensors $S^{(1)}$ and $S^{(2)}$ in spin space is given in the papers cited.

B. Spatial Symmetry

For a spatial symmetry group, the behavior of $D^2(x_1 x_2,\, x_1' x_2')$ is now reduced to that of the three spin-free quantities P_2, $Q_{\text{SL}}^{\text{st}}$, and $Q_{\text{SS}}^{\text{st}}$ as defined in Eq. (10). Just as in the case of the 1-particle quantities P_1 and

Q_S^{st} (see Section IV, B), P_2, Q_{SL}^{st}, and Q_{SS}^{st} can be decomposed into irreducible components along the lines of Eqs. (2) to (4). Furthermore, the *kind* of irreducible components which actually occur in a given case must be the same for all three quantities as well as for P_1 and Q_S. In the special case where $\Psi = \Phi$ of Eq. (1) belongs to a 1-dimensional irr. rep. of $\mathscr{G}$, all 5 spin-free quantities are *invariant* with respect to $\mathscr{G}$, i.e., belong to its identity representation. For the diagonal elements $P_2(r_1r_2)$, $P_2(r_1r_2, r_1r_2)$, etc., equations similar to Eqs. (2′) to (4′) hold.

C. Permutation Symmetry

As is well known (Löwdin, 1955), any $D^p(x, x')$ is antisymmetric with respect to permutation of either the unprimed coordinates x or the primed ones x'—provided that one permutes space and spin coordinates simultaneously. For D^2 this means that

$$\begin{aligned} D^2(x_1x_2; x_1'x_2') &= -D^2(x_2x_1; x_1'x_2') = -D^2(x_1x_2; x_2'x_1') \\ &= D^2(x_2x_1; x_2'x_1'). \end{aligned} \tag{11}$$

The behavior of spin-free matrices P_2, Q_{SL}^{st}, and Q_{SS}^{st} is less trivial (McWeeny and Kutzelnigg, 1968):

$$P_2(r_1r_2; r_1'r_2') = P_2(r_2r_1; r_2'r_1'), \tag{12a}$$

$$\begin{aligned} Q_{SL}^{st}(r_1r_2; r_1'r_2') + Q_{SL}^{st}(r_2r_1; r_2'r_1') = &-Q_{SL}^{st}(r_2r_1; r_1'r_2') \\ &-Q_{SL}^{st}(r_1r_2; r_2'r_1') \end{aligned} \tag{12b}$$

$$Q_{SS}^{st}(r_2r_1; r_2'r_1') = Q_{SS}^{st}(r_1r_2; r_1'r_2'). \tag{12c}$$

Note that none of these matrices is symmetric or antisymmetric with respect to exchange of either r_1 and r_2 *or* r_1' and r_2' and that Q_{SL} is not even symmetric or antisymmetric with respect to exchange of both sets simultaneously.

VI. Symmetry Properties of the Natural p-States

Natural spin orbitals (NSO's) and natural spin geminals (NSG's) are defined (Löwdin, 1955) as eigenfunctions of D^1 and D^2 respectively (cf., Eq. (1)).

$$N\int D^1(x_1, x_1')\chi_i(x_1')\,dx_1' = \nu_i\chi_i(x_1), \tag{13a}$$

$$\frac{N(N+1)}{2}\int D^2(x_1, x_2; x_1'x_2')\omega_i(x_1'x_2')\,dx_1'\,dx_2' = \mu_i\omega_i(x_1, x_2). \tag{13b}$$

They have been considered so far for *density matrices in the proper sense only* (i.e., for $\Psi = \Phi$), not for general transition-density matrices. The eigenvalues ν_i of $N \cdot D^1$ and μ_i of $[N(N+1)/2]. D^2$ are called the "occupation numbers" of the NSO's and NSG's, respectively. The eigenfunctions of the spinless density matrices P_1 and P_2 (Eqs. (9a) and (10a)) are referred to as the natural orbitals (NO's) and natural geminals (NG's). A quite general discussion of their symmetry properties, especially with respect to spin symmetry can be found in Kutzelnigg (1963a, 1965a), (see also McWeeny and Kutzelnigg, 1968). We limit ourselves here to indicating the results and refer the reader for the proofs to the original papers.

VII. Symmetry Properties of the NSO's and the NO's

A. Spin Symmetry of the NSO's

(1) If Ψ is an eigenstate of S_z (with arbitrary eigenvalue M_S and independently of whether or not Ψ is an eigenfunction of S^2), then D^1 is always of the factorized form[3] (Bingel, 1960; Löwdin, 1955; McWeeny, 1959, 1960).

$$ND^1 = P_1^{\alpha\alpha}\alpha(1)\alpha^*(1') + P_1^{\beta\beta}\beta(1)\beta^*(1') \tag{14}$$

and the NSO's are consequently pure spin-state functions (Bingel, 1960; Kutzelnigg, 1963a, 1965a), i.e., equal to a space function times α or β spin factor. If certain eigenvalues of $P^{\alpha\alpha}$ and $P^{\beta\beta}$ happen to coincide, then the corresponding NSO's can always be chosen as pure spin state functions. The space factors of α and β spin NSO's (i.e., the eigenstates of $P_1^{\alpha\alpha}$ and $P_1^{\beta\beta}$, respectively) are, for $M_S \neq 0$, generally different from each other and different from the NO's (i.e., the eigenstates of P_1), although some of them may coincide, in particular for approximate wave functions.

(2) If Ψ is also an eigenfunction of S^2 (with arbitrary quantum number S), then the matrices $P_1^{\alpha\alpha}$ and $P_1^{\beta\beta}$ can—for all states with the same S but different M_S—be expressed (Bingel, 1961; McWeeny, 1965; McWeeny and Mizuno, 1961) in terms of P_1 and Q_S^{st}.

$$\begin{aligned} P_1^{\alpha\alpha} &= \frac{1}{2} P_1 + \frac{M}{S} Q_S^{\text{st}}, \\ P_1^{\beta\beta} &= \frac{1}{2} P_1 - \frac{M}{S} Q_S^{\text{st}}. \end{aligned} \tag{15}$$

---

[3] This can easily be seen by noting that any wave function that is an eigenfunction of S_z can be written as a linear combination of Slater determinants in all of which the number N_α of particles with α spin is the same, namely $N_\alpha = M_S + (N/2)$.

This has, however (except for $M_S = 0$), no influence on the spin symmetry of the NSO's. Note that for $S = 0$, $M = 0$, M/S has to be interpreted as being equal to 0.

(3) If Ψ is an eigenstate of S_z with eigenvalue $M_S = 0$ and[4] eigenstate of S^2 with arbitrary quantum number S, then, as can be seen immediately from Eq. (15),

$$P_1^{\alpha\alpha} = P_1^{\beta\beta} = \tfrac{1}{2}P_1.$$

From this relation it follows that the NSO's are equal[5] to NO's times α or β spin factor, where both occur with the same occupation number.

B. Spatial Symmetry of the NSO's and the NO's

(1) The spatial parts of the NSO's and the NO's transform as irr. rep. of the spatial symmetry group $\mathscr{G}$ of the system *if* the wave function belongs to a *one-dimensional* irr. rep. of $\mathscr{G}$, since then P_1 and Q_S are totally symmetric (see Section IV, B). In this case, those NO's (NSO's) that together form a basis of the same irr. rep. have the same occupation numbers (Kutzelnigg, 1963a, 1965a). The general case has first been treated by one of the authors (Kutzelnigg, 1963a, 1965a), the special case of systems with Abelian groups independently by Löwdin (1963). That the rather trivial result for Abelian groups is probably not generalizable to arbitrary groups has probably first been recognized by Jörgensen (1962). As for an example which demonstrates that for degenerate states the NSO's and NO's are *not* symmetry adapted, see McWeeny and Kutzelnigg (1968).

(2) If Ψ belongs to a multidimensional irr. rep., then one can always choose (though not always uniquely) a subgroup of highest possible order, with respect to which a given function of the degenerate set belongs to a *one-dimensional* irr. rep. The NSO's and NO's are then adapted to this subgroup (Kutzelnigg, 1963a, 1965a; Kutzelnigg and Smith, 1968), which may be called the "*effective symmetry group.*"

Example 6

Let us consider a Π-state of a linear molecule of symmetry $C_{\infty v}$. From the two degenerate wave functions

$$\Psi_\pm = \exp(\pm i\phi_1)\chi(\cdots \pm(\phi_i - \phi_1), \ldots),$$

---

[4] That the second condition is necessary can be seen from the example of a wave function $\Psi = |a(1)\alpha(1)b(2)\beta(2)|$ which is eigenfunction of S_z with $M_S = 0$ but not eigenfunction of S^2 and for which $P_1^{\alpha\alpha} = a(1)a^*(1')$, $P_1^{\beta\beta} = b(1)b^*(1')$.

[5] The NSO's (etc.) are—except for a physically irrelevant phase factor—uniquely defined only for nondegenerate eigenvalues. Otherwise unitary transformations among any degenerate set are possible. If we state, e.g., that the NSO's of a state are identical with the NO's times spin factors, this can only mean that the spaces spanned by respectively degenerate sets are the same.

four first-order transition-density matrices can be constructed. Their dependence on the angles ϕ_1 and ϕ_1' is given by Bingel (1970):

$$\begin{aligned}
D^{(1)}_{++}(1, 1') &= \exp[i(\phi_1 - \phi_1')]f(\phi_1 - \phi_1' \ldots),\\
D^{(1)}_{--}(1, 1') &= \exp[-i(\phi_1 - \phi_1')]f(-(\phi_1 - \phi_1'), \ldots),\\
D^{(1)}_{+-}(1, 1') &= \exp[i(\phi_1 + \phi_1')]g(\phi_1 - \phi_1', \ldots),\\
D^{(1)}_{-+}(1, 1') &= \exp[-i(\phi_1 + \phi_1')]g(-(\phi_1 - \phi_1'), \ldots);
\end{aligned}$$

the remaining cylindrical coordinates ρ_1, z_1, ρ_1', z_1' are indicated by dots. Under the operations of $C_{\infty v}$ as applied to *both* ϕ_1 and ϕ_1', D_{+-} and D_{-+} transform like a Δ-type function. D_{++} and D_{--} remain invariant with respect to rotations but transform into each other for the reflections σ_v. Therefore the decomposition (3) takes the form

$$D^{(1)}_{++} = \frac{1}{\sqrt{2}}(D^{(1)}_{\Sigma^+} + D^{(1)}_{\Sigma^-}), \qquad D^{(1)}_{--} = \frac{1}{\sqrt{2}}(D_{\Sigma^+} - D_{\Sigma^-}),$$

$$D^{(1)}_{+-} = D^{(1)}_{\Delta}, \qquad D^{(1)}_{-+} = D^{(1)}_{\Delta}.$$

For the densities ($x_1' = x_1$), the Σ^--component vanishes identically.

Although neither D_{++} nor D_{--} are invariant under $C_{\infty v}$, they are of Σ-type and therefore invariant under the subgroup C_∞. Their NO's are therefore of $\sigma -$, $\pi^+ -$, $\pi^- -$, ... type, i.e., they are symmetry-adapted to the "effective" symmetry group C_∞. From the eigenvalue equation (13a) for D_{++} and D_{--}, the following relation between their NO's and occupation numbers can be derived (Bingel, 1970):

If $\chi(\phi, \rho, z)$ is an NO of D_{++} with occupation number ν, then $\chi(-\phi, \rho, z)$ is a NO of D_{--} with the same occupation number and vice versa. The σ-NO's are simultaneously eigenfunctions of D_{++} and D_{--}, and therefore also of D_{Σ^+}. These relations are illustrated schematically in Fig. 1.

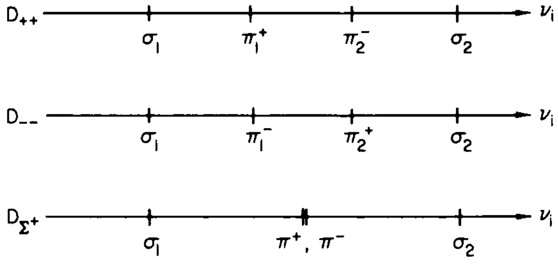

Fig. 1. Relation between the occupation numbers ν_i of D_{++}, D_{--}, and D_{Σ^+} for a Π-state of a linear molecule.

These results also hold for $\Lambda > 1$, i.e., for $\Delta-, \Phi-, \ldots$ states. D_{+-} and D_{-+} now span the irr. rep. 2Λ of $C_{\infty v}$.

Alternatively one can define symmetry adapted natural orbitals (SANO'S) (Kutzelnigg, 1963a, 1965a; McWeeny and Kutzelnigg, 1968) as eigenfunctions of the *totally symmetric part* ${D_0}^1$ of D^1. They are the best approximations of symmetry adapted type to the NO's. Since ${D_0}^1$ is (similar to D^1) a completely continuous operator, its eigenfunctions (including those with occupation number 0) form a complete set in the one-particle Hilbert space.

Theorems that connect the occupation numbers of the SANO's with other properties of the wave functions have been used (Kutzelnigg and Smith, 1968) to define in a rigorous way open and closed shell states in few-particle quantum mechanics, to classify further these states, and to study their properties.

(3) In the presence of spin-orbit interaction, Ψ may only be chosen to belong to an irr. rep. of the respective *double group*. If this representation is one-dimensional, statements (1) and (2) hold *mutatis mutandis*.

VIII. Symmetry Properties of the NSG's and the NG's

A. Spin- and Permutation-Symmetry of the NSG's

(1) The D^2 of a Ψ that is an eigenstate of S^2 and of S_z (with arbitrary S and M) can always be written in the following way (Kutzelnigg, 1963a, 1965a):

$$\begin{aligned} N(N-1)\cdot D^2 = {} & P_2^{aa}a(1,2)a^*(1',2') + P_2^{bb}b(1,2)b^*(1',2') \\ & + P_2^{cc}c(1,2)c^*(1',2') + P_2^{dd}d(1,2)d^*(1',2') \\ & + P_2^{cd}c(1,2)d^*(1',2') + P_2^{dc}d(1,2)c^*(1',2'), \end{aligned} \tag{16}$$

where P_2^{aa}, etc., are space functions that depend on r_1, r_2; ${r_1}'$, ${r_2}'$ and which can be expressed (McWeeny and Kutzelnigg, 1968) in terms of P_2, $Q_{\mathrm{SS}}^{\mathrm{st}}$, and $Q_{\mathrm{SL}}^{\mathrm{st}}$. The four possible spin functions are abbreviated as a, b, c, d:

$$\begin{aligned} & a = \alpha(1)\alpha(2); \quad b = \beta(1)\beta(2); \quad c = \frac{1}{\sqrt{2}}(\alpha(1)\beta(2) + \beta(1)d(2)); \\ & d = \frac{1}{\sqrt{2}}(\alpha(1)\beta(2) - \beta(1)\beta(2)). \end{aligned} \tag{17}$$

Consequently the NSG's are not necessarily eigenstates of S^2 (c and d mix), but they are eigenstates of S_z (a has $M_S = +1$, b has $M_S = -1$, c and *d* have $Ms = 0$). This last statement holds also for a Ψ which is only an eigenfunction of S_z, but not of S^2 (Weinhold and Wilson, 1967).

(2) If Ψ is an eigenfunction of S^2 and S_z with arbitrary S and with $M_S = 0$ then P_2^{cd} and P_2^{dc} in Eq. (16) vanish (Kutzelnigg, 1963a, 1965a) and the NSG's are pure spin-state functions, i.e., they are equal to spatial functions times one of the four spin functions (Löwdin, 1955).

In this case the spin functions *a* and *b* (but not *c*) have the same space factor and the corresponding NSG's the same occupation number. The space factors of the NSG's are not, in general, identical with the NG's.[6]

The factorization of D^2 for states with $M_S = 0$ (and *a fortiori* for $S = 0$) was first carried out by one of the present authors (Kutzelnigg 1963a, 1965a). An interesting application of this theorem can be found in a recent paper by Weinhold and Wilson (1967).

(3) If Ψ is an eigenstate of S^2 with $S = 0$, then (Kutzelnigg, 1963a, 1965a)

$$P_2^{aa} = P_2^{bb} = P_2^{cc},$$

and the NSG's are equal to the NG's times one of the four spin functions of Eq. (17).

The three triplet functions *a*, *b*, *c* occur with the same space factor and the corresponding eigenvalues (occupation numbers) have degeneracy divisible by 3. The NG's (eigenfunctions of P_2) are either symmetric with respect to a permutation of the space coordinates of the electrons (then they are simultaneously eigenfunctions of $P^t = P_2^{aa} = P_2^{bb} = P_2^{cc}$) or they are antisymmetric (then they are also eigenfunctions of $P^s = P_2^{dd}$). They have then to be multiplied by the spin functions *d* or *a*, *b*, *c*, respectively, to yield NSG's (which are necessarily antisymmetric with respect to space and spin exchange).

(4) That the NG's are either symmetric or antisymmetric with respect to particle exchange holds even in the general case of arbitrary spin quantum number S of the state. If we label the eigenvalues of $[N(N-1)/2] \cdot D^2$ for symmetric NG's as $\mu_i{}^s$ and those antisymmetric ones as $\mu_i{}^t$, the following sum rules hold (Kutzelnigg, 1963a, 1965a):

$$\begin{aligned}
&\sum_i \mu_i{}^{\mathrm{s}} = \tfrac{1}{8}N \cdot (N+2) - \tfrac{1}{2}S \cdot (S+1), \\
&\sum_i \mu_i{}^{\mathrm{t}} = \tfrac{3}{8}N(N-2) - \tfrac{1}{2}S \cdot (S+1), \qquad (18) \\
&\sum_i \mu_i{}^{\mathrm{s}} + \sum_i \mu_i{}^{\mathrm{t}} = N(N-1)/2.
\end{aligned}$$

[6] See Footnote 5.

In the special case $S = 0$, the μ_i^s and $\frac{1}{3}\mu_i^t$ can be identified with the occupation numbers of singlet and triplet NSG's, respectively. This theorem was first proven by one of the present authors (Kutzelnigg, 1963a, 1965a,b) and later rederived independently by Grimley and Peat (1965) and Weinhold and Wilson (1967). It should be noted that it also holds for other than pure spin states, if we replace $S(S + 1)$ by $\langle S^2 \rangle$.

(5) "Spin adapted NSG's" are defined (McWeeny and Kutzelnigg, 1968) as NG's times the appropriate spin factors.

B. Spatial Symmetry of the NG's and NSG's

Theorems analogous to those of Section II hold (see Kutzelnigg, 1963a, 1965a; McWeeny and Kutzelnigg, 1968). The symmetry properties of the natural p-states with $p > 2$ have not been investigated in detail, but the generalization of the above statements is trivial.

IX. Symmetry of the NO's and "Natural Expansion" of the Wave Functions

By "natural expansion" of a wave function, we understand its expansion in terms of Slater determinants built up from its NSO's. The question of how such an expansion differs from a conventional CI expansion is rather interesting, but has so far only been answered for *two-electron* systems (Kutzelnigg, 1963b). The answer is closely connected to the symmetry behavior of the NSO's.

We consider pure spin state two-electron functions, where we can separate off the spin and discuss only spatial functions $\Psi(r_1, r_2)$, which are symmetric with respect to particle exchange for singlets and antisymmetric for triplets.

As Hurley *et al.* (1953) have shown and as Löwdin and Shull (1956) have discussed in detail (see also Kutzelnigg, 1963b), a spin-free two-electron singlet function can always be brought to diagonal form

$$\Psi(1, 2) = \sum_i c_i \phi_i(1) \phi_i^*(2). \tag{19}$$

The ϕ_i of Eq. (19) diagonalize P_1; in fact (if the ϕ_i form an orthonormal set)

$$P_1(1, 1') = 2 \sum_i c_i^2 \phi_i(1) \phi_i^*(1') \tag{20}$$

and can therefore be referred to as NO's. On the other hand, a set of functions that diagonalizes P_1 does not necessarily diagonalize Ψ as well, because pairs of coefficients in (19) may differ just in their sign, which leads to pairwise degeneracies of the eigenvalues c_i^2 of P_1 and to a freedom of unitary transformations in P_1, but not in Ψ. The indetermination of the NO's can then be *either* removed by requiring that they be symmetry-adapted (to the effective symmetry group) *or* that they diagonalize (19) as well. These two requirements are compatible only if Ψ is *totally symmetric* with respect to the effective symmetry group, but not if Ψ is antisymmetric with respect to some operation R of this group, because a wave function of type (19) with symmetry-adapted ϕ_i is always *symmetric* with respect to R.

Following Carlson and Keller (1961) (see also Coleman, 1963), any spinfree Ψ (Barnett *et al.*, 1965; Bingel, 1960) can be expanded in terms of its NO's,

$$\Psi(1, 2) = \sum_i c_i \cdot u_i(1)v_i^*(2), \tag{21}$$

where both the u_i and v_i are NO's in the sense that they diagonalize P_1, but where in general $u_i \neq v_i$. This expansion is compatible with the choice of symmetry-adapted NO's even for a Ψ that is antisymmetric with respect to R. In fact, of any pair u_i, v_i, one orbital must be symmetric, the other antisymmetric with respect to R. Since Ψ should be a singlet, i.e., $\Psi(1, 2) = \Psi(2, 1)$, the coefficient of $u_i(1)v_i^*(2)$ and $v_i^*(1)u_i(2)$ must be the same; therefore (Kutzelnigg, 1963b)

$$\Psi(1, 2) = \sum_i c_i[u_i(1)v_i^*(2) + v_i^*(1)u_i(2)] \tag{22}$$

and we can label the NO's such that, for example, the u_i are symmetric and the v_i antisymmetric with respect to R.

Triplet wave functions must satisfy $\Psi(1, 2) = -\Psi(2, 1)$. Expansion (19) is therefore not possible, at least not with real ϕ_i's, but one has even for totally symmetric triplets to use the expansion (23), first introduced by Löwdin and Shull (1956):

$$\Psi(1, 2) = \sum_i c_i[u_i(1)v_i^*(2) - v_i^*(1)u_i(2)], \tag{23}$$

For totally symmetric Ψ (with respect to the effective symmetry group), any pair u_i, v_i must belong to the same symmetry species,[7] whereas for a Ψ that is antisymmetric with respect to R, they must belong to different species.

[7] For degenerate species of dimension d, u_i and v_i belong to the same subspecies. Altogether there are then $2d$ orbital products, all of which have the same coefficient, up to sign.

X. Degeneracies of the Eigenvalues of D^p due to Symmetry

We have encountered several kinds of degeneracies of the occupation numbers of the p states that are due to symmetry. We summarize them now.

(1) If Ψ belongs to a one-dimensional irr. rep. of $\mathscr{G}$, then those natural p-states that together span the same d-dimensional irr. rep. of $\mathscr{G}$ have the same occupation number. The corresponding p-states are d-fold degenerate (Kutzelnigg, 1963a, 1965a).

(2) If $M_S = 0$, the NSO's are equal to NO's times α- or β-spin factors. Any NSO is evenly degenerate (Bingel, 1960; McWeeny, 1959).

(3) A closely related even degeneracy of the eigenstates of D^1 has been shown by Micha (1964) (see also Smith, 1965). It occurs if Ψ is invariant under time reversal. A state can however be both time reversal invariant and symmetry-adapted only if it belongs to the totally symmetric irr. rep. of the respective double group, or—in the absence of spin-orbit interaction —if $S = 0$.

(4) For $(4n + 2)$-electron antisymmetric wave functions, the natural $(2n + 1)$ states are evenly degenerate (Coleman, 1963). Particularly interesting is the case $n = 0$, i.e., all the NSO's of any two-electron state are evenly degenerate.

(5) For a nontotally symmetric two-electron singlet state, pairs of NO's belonging to different symmetry species have the same occupation number.

Note that, e.g., the degeneracies (2) and (5) are independent, so that NSO occupation numbers of a non-totally-symmetric two-electron singlet state actually have degeneracies divisible by four (corresponding to $u_i\alpha$, $u_i\beta$; $v_i\alpha$, $v_i\beta$). Similarly the NSO's of a two-electron triplet state with $M_S = 0$ have occupation numbers with a degeneracy divisible by four.

ACKNOWLEDGMENT

We gratefully acknowledge financial support by the Deutsche Forschungsgemeinschaft and by a NATO grant for research and collaboration. An exchange of visits with several quantum chemistry groups has stimulated this work very much. In this context, we appreciate in particular discussions with R. McWeeny. Finally we thank A. J. Coleman who organized the meeting on density matrix theory for which a preliminary version of this review article has been prepared.

REFERENCES

BARNETT, G., LINDERBERG, J., and SHULL, H. (1965). *J. Chem. Phys.* **43**, 580.

BINGEL, W. A. (1960). *J. Chem. Phys.* **32**, 1522.

BINGEL, W. A. (1961). *J. Chem. Phys.* **34**, 1066.

BINGEL, W. A. (1962). *J. Chem. Phys.* **36**, 2842.

BINGEL, W. A. (1970). To appear in *Theor. Chim. Acta.*

CARLSON, D. C., and KELLER, J. M. (1961). *Phys. Rev.* **121**, 659.

COLEMAN, A. J. (1962). Preprint 23, Quantum Theory Project, Gainesville (unpublished).

COLEMAN, A. J. (1963). *Rev. Mod. Phys.* **35**, 668.

DAVIDSON, E. R. (1963). *J. Chem. Phys.* **39**, 875.

DAVIDSON, E. R., and JONES, L. L. (1962). *J. Chem. Phys.* **37**, 2966.

GRIMLEY, T. B., and PEAT, F. D. (1965). *Proc. Phys. Soc.* **86**, 247.

HURLEY, A. C., LENNARD JONES, J., and POPLE, J. A. (1953). *Proc. Roy. Soc.* **A220**, 446.

JÖRGENSEN, C. K. (1962). "Orbitals in Atoms and Molecules." Academic Press, London.

KOSTER, G. F., DIMMOK, J. O., WHEELER, R. G., and STATZ, H. (1963). "Properties of the Thirty-Two Point Groups." M.I.T. Press, Cambridge, Massachusetts.

KUTZELNIGG, W. (1963a). *Z. Naturforsch.* **18a**, 1058.

KUTZELNIGG, W. (1963b). *Theoret. Chim. Acta* **1**, 327.

KUTZELNIGG, W. (1965a). *Z. Naturforsch.* **20a**, 168.

KUTZELNIGG, W. (1965b). *Theoret. Chim. Acta* **3**, 241.

KUTZELNIGG, W., and SMITH, V. H., JR. (1968). *Intern. J. Quant. Chem.* **II**, 531.

LÖWDIN, P. O. (1955). *Phys. Rev.* **97**, 1474.

LÖWDIN, P. O. (1963). *Rev. Mod. Phys.* **35**, 629.

LÖWDIN, P. O., and SHULL, H. (1956). *Phys. Rev.* **101**, 1730.

MCWEENY, R. (1959). *Proc. Roy. Soc.* **A253**, 242.

MCWEENY, R. (1960). *Rev. Mod. Phys.* **32**, 335.

MCWEENY, R. (1965). *J. Chem. Phys.* **42**, 1717.

MCWEENY, R., and MIZUNO, Y. (1961). *Proc. Roy. Soc.* **A259**, 554.

MCWEENY, R., and KUTZELNIGG, W. (1968). *Intern. J. Quant. Chem.* **II**, 187.

MICHA, D. (1964). *J. Chem. Phys.* **41**, 3648.

SMITH, D. (1965). *J. Chem. Phys.* **43**, S258.

SMITH, V. H., Jr. (1967). *Theoret. Chim. Acta* **7**, 245.

STAEMMLER, V., and KUTZELNIGG, W. (1967). *Theoret. Chim. Acta* **9**, 67.

VAN DER WAERDEN, B. L. (1932). Die gruppentheoretische Methode in der Quantenmechanik.

WEINHOLD, F., and WILSON, E. B., JR. *J. Chem. Phys.* **46**, 2752.

Symmetry Adaptation to Sequences of Finite Groups

D. J. KLEIN, C. H. CARLISLE,
and F. A. MATSEN

Molecular Physics Group
Department of Chemistry
The University of Texas
Austin, Texas

I. General Introduction

Symmetry adaptation of a vector space with respect to a group of a Hamiltonian factors the representation of the Hamiltonian and provides an *a priori* assignment of group theoretical quantum numbers to its states.

For certain systems, symmetry adaptation of the basis with respect to a group sequence approximately factors the representation and provides approximate group theoretical quantum numbers.

In this paper, we restrict ourselves to symmetry adaptation with respect to sequences of finite groups. We treat three types of sequences:

A. The descent in symmetry sequence; e.g., point group sequences:

$$\mathscr{R}(3) \supset \mathscr{O}_h \supset \mathscr{D}_3 . \tag{1}$$

The method of descent in symmetry has been widely employed (see, for example, Matsen and Plummer, 1968, or Watanabe, 1966).

B. The ascent in symmetry sequences; e.g., symmetric group sequences:

$$\mathscr{S}_A \otimes \mathscr{S}_B \otimes \mathscr{S}_C \otimes \cdots \subset \mathscr{S}_N \tag{2}$$

where $\mathscr{S}_N$ is the symmetric group on $N = N_A + N_B + N_C + \cdots$ objects. Specific examples of these types are the following:

1. p-mal theory (a 2-mal is called a geminal),
2. intermolecular forces,
3. functional group interaction,
4. atomic and nuclear shell theory,
5. exchange coupling, and
6. superexchange coupling.

Although the sequence (2) is widely applicable, it has been explicitly employed only infrequently in chemical problems; it has been extensively used in nuclear shell theory by Jahn (1954), Elliott *et al.* (1953), and others.

C. Mixed sequences; e.g., systems with descending point group symmetry and ascending symmetric group symmetry.

Section II contains an introduction to symmetry adaptation and the assignment of group theoretical quantum numbers. For symmetry adaptation with respect to a finite group, the matric basis of the Frobenius (group) algebra may be employed; Section III reviews Wedderburn's construction of a matric basis. For symmetry adaptation with respect to a group sequence, a special matric basis called the *sequence adapted* matric basis may be employed; Section IV contains our modification of Wedderburn's method to yield a constructive proof of the existence of a sequence adapted matric basis. Section V develops some of the properties of the sequence adapted matric basis. Sections VI and VIII consider the sequence adapted matric basis for special types of group sequences; formulas for the corresponding sequence adapted irreducible representation matrix elements are given. Section VII relates the present development to other treatments concerning induced representations. Section IX gives two methods for obtaining a sequence adapted irreducible representation from one that is not sequence adapted, and Section X describes their application to the symmetric group. Section XI briefly mentions the application to longer sequences than studied in the preceding sections. Section XII presents examples from the symmetric group applying formulas and methods from the preceding Section V–XI. Finally, Sections XIII–XV return to a discussion of the applications of the kets projected out using sequence adapted matric bases.

II. Theoretical Introduction

Let $V(\nu)$ be an f^ν dimensional vector space with a basis

$$\{|\nu i\rangle; \qquad i = 1 \quad \text{to} \quad f^\nu\}. \tag{3}$$

If $V(\nu)$ is invariant to a group $\mathscr{G}$, it may be decomposed into minimally invariant vector spaces $V(\nu;\alpha)$,

$$V(\nu) = \dot{\sum_{\alpha}} V(\nu;\alpha), \tag{4}$$

where α labels an irreducible representation Γ^α of $\mathscr{G}$. The subspaces $V(\nu;\alpha)$ have bases

$$\{|\nu\sigma;\alpha r\rangle; \qquad \sigma = 1 \quad \text{to} \quad f^{\nu\alpha}, \quad r = 1 \quad \text{to} \quad f^\alpha\}. \tag{5}$$

Here the ket $|\nu\sigma;\alpha r\rangle$ transforms as the rth column of the f^α-dimensional irreducible representation $\Gamma^\alpha(\mathscr{G})$:

$$G|\nu\sigma;\alpha r\rangle = \sum_{s=1}^{f^\alpha} [G]^\alpha_{sr} |\nu\sigma;\alpha s\rangle, \qquad G \in \mathscr{G}. \tag{6}$$

σ distinguishes among kets with the same α and r quantum numbers, and $[G]^\alpha_{sr}$ is the (sr)th element of the representation of G in Γ^α.

If $\mathscr{G}$ is the symmetry group of the Hamiltonian H,

$$[H, G] = 0, \qquad G \in \mathscr{G}, \tag{7}$$

then the special Wigner–Eckart theorem holds:

$$\langle \nu\sigma;\alpha r|H|\nu\sigma';\alpha' r'\rangle = \delta_{\alpha\alpha'}\,\delta_{rr'}\langle \nu\sigma;\alpha\|H\|\nu\sigma';\alpha\rangle. \tag{8}$$

It follows that the representation of H on the symmetry adapted basis (5) is factored into blocks, each labeled by an index α, and that the αth block is factored into f^{α} identical blocks each $f^{\nu\alpha} \times f^{\nu\alpha}$.

The eigenvalues of H in $V(\nu)$ are denoted $E(\nu K; \alpha)$ and the eigenkets are

$$|\nu K; \alpha r\rangle = \sum_{\sigma=1}^{f^{\nu\alpha}} |\nu\sigma; \alpha r\rangle\langle \nu\sigma; \alpha r \,|\, K\rangle, \tag{9}$$

where K distinguishes among the $f^{\nu\alpha}$ different eigenkets with the same α and r. The indices α and r are called the *group theoretical quantum numbers* of H with respect to $\mathscr{G}$.

If $f^{\nu\alpha} \geq 2$, the group theoretical quantum numbers α and r do not uniquely characterize a state. An additional (though approximate) group theoretical quantum number may be obtained on decomposing the Hamiltonian into the sum of zero-order and perturbation terms:

$$H = H^0 + H'. \tag{10}$$

The symmetry group $\mathscr{G}^0$ of the zero-order Hamiltonian H^0 is defined by

$$[G^0, H^0] = 0, \qquad G^0 \in \mathscr{G}^0. \tag{11}$$

Let V^0 be a vector space spanned by the eigenkets of H^0. The vector space can be decomposed into eigenspaces $V^0(K^0; \alpha^0)$,

$$V^0 = \dot{\sum_{K^0}} \dot{\sum_{\alpha^0}} V^0(K^0; \alpha^0), \tag{12}$$

where $V^0(K^0; \alpha^0)$ has a basis

$$\{\, |K^0; \alpha^0 r^0\rangle; \qquad r^0 = 1 \quad \text{to} \quad f^{\alpha^0} \}. \tag{13}$$

Here α^0 is the group theoretical quantum number supplied by $\mathscr{G}^0$, r^0 is the degeneracy index labeling the (r^0)th column of $\Gamma^{\alpha^0}(\mathscr{G}^0)$, and K^0 represents all the other quantum numbers. We have

$$\langle K^0; \alpha^0 r^0 |\, H^0 \,| K^{0\prime}; \alpha^{0\prime} r^{0\prime}\rangle = \delta_{K^0 K^{0\prime}}\, \delta_{\alpha^0 \alpha^{0\prime}}\, \delta_{r^0 r^{0\prime}} \langle K^0; \alpha^0 \|\, H^0 \,\| K^0; \alpha^0\rangle. \tag{14}$$

If $\mathscr{G}$ is a subgroup of $\mathscr{G}^0$, $\mathscr{G} \subset \mathscr{G}^0$, then $V^0(K^0; \alpha^0)$ is invariant to $\mathscr{G}$. If $\mathscr{G} \not\subset \mathscr{G}^0$, then $V^0(K^0; \alpha^0)$ is not (barring accidental degeneracy) invariant to $\mathscr{G}$.

A vector space which is invariant to $\mathscr{G}$ can be *induced* from $V^0(K^0; \alpha^0)$. We define $\mathscr{G}^{\vee}$ to be the smallest group containing both $\mathscr{G}^0$ and $\mathscr{G}$,

$$\mathscr{G}^{\vee} \equiv \mathscr{G} \vee \mathscr{G}^0, \tag{15}$$

that is, $\mathscr{G}^\vee$ is the *join* of $\mathscr{G}$ and $\mathscr{G}^0$. The *induced* space $V(K^0; \alpha^0\uparrow)$ is defined as the space generated by the elements of $\mathscr{G}^\vee$ acting on the kets of $V^0(K^0; \alpha^0)$. If the space $V^0(K^0; \alpha^0)$ has no symmetry with respect to $\mathscr{G}^\vee$ beyond that specified by α^0, then one basis for the induced space $V(K^0;\alpha^0\uparrow)$ is

$$\{C_j\,|K^0; \alpha^0 r^0\rangle; \qquad r^0 = 1 \text{ to } f^{\alpha^0}, \quad j = 1 \text{ to } g^\vee/g^0\}. \tag{16}$$

where $g^\vee$ and g^0 are the orders of $\mathscr{G}^\vee$ and $\mathscr{G}^0$, and C_j is the jth left coset multiplier of $\mathscr{G}^0$ in $\mathscr{G}^\vee$. The dimension of $V(K^0; \alpha^0\uparrow)$ is

$$f^{\alpha^0\uparrow} = f^{\alpha^0} g^\vee/g^0. \tag{17}$$

We call $V(K^0; \alpha^0\uparrow)$ a *configuration* space for the Hamiltonian H with respect to the zero-order Hamiltonian H^0.

If the Hamiltonian matrix elements between different configurations are much smaller than the difference between the corresponding diagonal elements,

$$\begin{aligned}&\langle K^0; \alpha^0 \uparrow k\,|H|\,K^{0\prime}; \alpha^{0\prime} \uparrow k'\rangle \\ &\qquad \ll |\langle K^0; \alpha^0 \uparrow k\,|H|\,K^0; \alpha^0 \uparrow k\rangle - \langle K^{0\prime}; \alpha^{0\prime} \uparrow k'\,|H|\,K^{0\prime}; \alpha^{0\prime} \uparrow k'\rangle|,\end{aligned} \tag{18}$$

then the mixing between different configurations (also called *configuration interaction*) is expected to be small. The perturbed eigenkets will be dominated by a single zero-order configuration, say the $(K^0; \alpha^0)$th. Such a perturbed eigenket transforming as the rth column of the αth irreducible representation Γ^α of $\mathscr{G}$ is of the form

$$|K^0, \tau\alpha^0; \alpha r\rangle = \sum_{K^{0\prime}} \sum_{\alpha^{0\prime}} \sum_{k=1}^{f^{\alpha^0\uparrow}} |K^{0\prime}; \alpha^{0\prime} \uparrow k\rangle\langle K^{0\prime}; \alpha^{0\prime} \uparrow k\,|\,K^0, \tau\alpha^0; \alpha r\rangle. \tag{19}$$

Here τ distinguishes among kets with the same K^0, α^0, α, and r. The significance of the approximate quantum numbers K^0 and α^0 is reflected in the fact that the coefficients $\langle K^{0\prime}; \alpha^{0\prime} \uparrow k\,|\,K^0, \tau\alpha^0; \alpha r\rangle$ are small or zero if $K^0; \alpha^0 \neq K^{0\prime}; \alpha^{0\prime}$.

Since (18) holds, configuration interaction may be neglected. The total Hamiltonian is then separately diagonalized within each configuration to obtain approximate eigenkets of the form

$$|K^0, \tau; \alpha^0, \alpha r\rangle = \sum_{k=1}^{f^{\alpha^0\uparrow}} |K^0; \alpha^0 \uparrow k\rangle\langle K^0; \alpha^0 \uparrow k\,|\,\tau; \alpha r\rangle. \tag{20}$$

We now consider symmetry adaptation with regard to the three types of sequences listed in Section I.

A. Descent in Symmetry

The group $\mathscr{G}$ of the perturbed Hamiltonian is a subgroup of $\mathscr{G}^0$,

$$\mathscr{G} \subseteq \mathscr{G}^0. \tag{21}$$

In this case, $\mathscr{G}^\vee = \mathscr{G}^0$, so that $\alpha^0\uparrow = \alpha^0$ and $V(K^0; \alpha^0\uparrow) = V(K^0; \alpha^0)$. The neglect of configuration interaction, as in (20), is equivalent to Rayleigh–Schroedinger perturbation theory for a zero-order degenerate state.

The method of descent in symmetry using (21) has found wide application in atomic, ligand field, and nuclear theory. Molecular problems are often treated proceeding from an outer direct-product point group $\mathscr{G}^0$, as in the Hartree–Fock theory, to the inner direct product point group $\mathscr{G}$. Longer sequences than (21) are treated by iteration of the method. An example of a longer sequence arising in ligand field problems is

$$\begin{aligned}(\mathscr{R}(3))^N \otimes (SU(2)^\sigma)^N &\supset [\mathscr{R}(3)]^N \otimes [SU(2)^\sigma]^N \\ &\supset [\mathscr{O}]^N \otimes [SU(2)^\sigma]^N \supset [\mathscr{D}_3]^N \otimes [SU(2)^\sigma]^N \supset [{}^d\mathscr{D}_3]^N \\ &\supset [{}^{Zd}\mathscr{D}_3]^N.\end{aligned} \tag{22}$$

Here $(\cdots)^N$ and $[\cdots]^N$ denote Nth rank outer and inner direct products, respectively; the superscript σ refers to a group on the spin space; and superscripts d and Zd refer to double and Zeeman double groups, respectively. The coupling of electronic and vibrational motion in semirigid molecules (see Longuet-Higgins, 1963, and Altmann, 1967) yields another example of descent in symmetry.

B. Ascent in Symmetry

The zero-order group $\mathscr{G}^0$ is a subgroup of $\mathscr{G}$,

$$\mathscr{G} \supseteq \mathscr{G}^0 \tag{23}$$

In this case $\mathscr{G}^\vee = \mathscr{G}$. The terminology of referring to $V(K^0; \alpha^0\uparrow)$ is common in the case when $\mathscr{G}^0 = \{\mathscr{I}\}$ and $\mathscr{G}$ is the symmetric group $\mathscr{S}_N$. For instance, a 3-electron molecule might have a zero-order Hamiltonian of only 1-electron operators so that a suitable zero-order wave function might consist of a simple product of orbitals as $|aab\rangle$; here we would have $K^0 = aab$, $\mathscr{S}_3 \supseteq \{\mathscr{I}\}$, $V^0(K^0; \alpha^0)$: $\{|aab\rangle\}$, and $V(K^0; \alpha^0\uparrow)$: $\{|aab\rangle, |aba\rangle, |baa\rangle\}$.

The method of ascent in symmetry may be employed in the description of systems which consist of a number of localized subsystems. Such systems are expected to have approximate local permutational symmetries arising from the symmetric groups permuting electron indices within the individual subsystems. Approximately localized chemical systems might include Rydberg states, biradicals, organic excimers, polynuclear transition metal complexes, exchange-coupled molecules in crystals, and molecules near the separated atom limit. Such sequences of symmetric groups as (2) may be used in fractional parentage techniques (Jahn, 1954; Elliott *et al.*, 1953; and Kaplan, 1961), in symmetry adapted perturbation techniques (Hirschfelder and Silbey, 1966; Amos and Musher, 1967, 1969; Murrell and Shaw, 1967; and Hirschfelder, 1967), and in certain configuration interaction treatments (Kaplan, 1965; and Klein, 1969b).

C. Mixed Descent and Ascent in Symmetry

In some cases neither $\mathscr{G}^0$ nor $\mathscr{G}$ is a subgroup of the other. The development preceding Cases A and B still holds. An example of the present case can occur for a system consisting of localized subsystems each with approximate local permutational symmetries and point group symmetries:

$$\mathscr{G}^0 = (\mathscr{S}_A \otimes \mathscr{S}_B) \otimes ([\mathscr{G}_A]^{N_A} \otimes [\mathscr{G}_B]^{N_B}) \tag{24}$$

$$\mathscr{G} = \mathscr{S}_N \otimes [\mathscr{G}_{AB}]^N, \tag{25}$$

$$\mathscr{G}^\vee = \mathscr{S}_N \otimes ([\mathscr{G}_A]^{N_A} \otimes [\mathscr{G}_B]^{N_B}). \tag{26}$$

Here $\mathscr{G}_A$, $\mathscr{G}_B$, and $\mathscr{G}_{AB}$ are point groups; $[\cdots]^{N_A}$, $[\cdots]^{N_B}$, and $[\cdots]^N$ indicate inner direct products; and $N = N_A + N_B$.

Thus in many cases a basis of kets symmetry adapted to a group $\mathscr{G}^\vee$ and a subgroup $\mathscr{G}$ is useful in providing additional symmetry characterization. Such symmetry adapted kets may be "projected" from a set of primitive kets using sequence adapted matric basis elements of the group algebra.

III. Review of Wedderburn's Construction of a Matric Basis

A finite group $\mathscr{G}$ is a basis for the corresponding group algebra $A(\mathscr{G})$. (See Löwdin, 1967, for a recent treatment.) We outline the steps in the proof of the existence of a matric basis given by Wedderburn in 1907.

Since $A(\mathscr{G})$ is semisimple, it is the direct sum of invariant simple subalgebraas $A^\alpha(\mathscr{G})$,

$$A(\mathscr{G}) = \sum_\alpha A^\alpha(\mathscr{G}), \tag{27}$$

where

$$A^{\alpha}(\mathscr{G})A^{\beta}(\mathscr{G}) = \delta_{\alpha\beta} A^{\alpha}(\mathscr{G}). \tag{28}$$

The identity $\mathscr{I} \in A(\mathscr{G})$ has a unique resolution

$$\mathscr{I} = \sum_{\alpha} e^{\alpha} \tag{29}$$

into the sum of pairwise orthogonal principle idempotents e^{α}. That is,

$$e^{\alpha} e^{\beta} = \delta_{\alpha\beta} e^{\alpha}, \qquad e^{\alpha} \in A^{\alpha}(\mathscr{G}). \tag{30}$$

Each principal idempotent e^{α} is the sum of pairwise orthogonal primitive idempotents

$$e^{\alpha} = \sum_{r=1}^{f^{\alpha}} e^{\alpha}_{rr}, \tag{31}$$

$$e^{\alpha}_{rr} e^{\alpha}_{ss} = \delta_{rs} e^{\alpha}_{rr}. \tag{32}$$

This decomposition of e^{α} is not unique. For a given decomposition of e^{α}, the simple subalgebra $A^{\alpha}(\mathscr{G})$ is decomposed in a particular way into a direct sum of one-dimensional linear sets,

$$\begin{aligned} A^{\alpha}_{rs}(\mathscr{G}) &= e^{\alpha}_{rr} A^{\alpha}(\mathscr{G}) e^{\alpha}_{ss}, \\ A^{\alpha}(\mathscr{G}) &= \dot{\sum_{r,s}} A^{\alpha}_{rs}(\mathscr{G}). \end{aligned} \tag{33}$$

These linear sets satisfy the multiplication rule

$$A^{\alpha}_{rs}(\mathscr{G}) A^{\beta}_{tu}(\mathscr{G}) = \delta_{\alpha\beta}\, \delta_{st}\, A^{\alpha}_{ru}(\mathscr{G}). \tag{34}$$

One element is selected from each of the sets $A^{\alpha}_{1s}(\mathscr{G})$, $s = 2$ to f^{α}; the selected element being denoted by e^{α}_{1s}. This selection is not unique.

Because of the multiplication rule for the sets $A^{\alpha}_{rs}(\mathscr{G})$, and because $e^{\alpha}_{rr} \in A^{\alpha}_{rr}(\mathscr{G})$, there exist elements $e^{\alpha}_{s1} \in A^{\alpha}_{s1}(\mathscr{G})$, $s = 2$ to f^{α}, such that

$$e^{\alpha}_{s1} e^{\alpha}_{1s} = e^{\alpha}_{ss} \qquad \text{and} \qquad e^{\alpha}_{1s} e^{\alpha}_{s1} = e^{\alpha}_{11}. \tag{35}$$

Once the elements e^{α}_{s1}, $s = 2$ to f^{α}, are determined, the matric basis elements e^{α}_{rs} may be defined by the equation

$$e^{\alpha}_{rs} = e^{\alpha}_{r1} e^{\alpha}_{1s}, \qquad r, s = 1 \quad \text{to} \quad f^{\alpha}. \tag{36}$$

The matric basis elements then satisfy the multiplication rule

$$e^{\alpha}_{rs} e^{\beta}_{tu} = \delta_{\alpha\beta}\, \delta_{st}\, e^{\alpha}_{ru}. \tag{37}$$

Symmetry adaptation of a primitive ket $|Q\rangle$ is accomplished by applying an e^{α}_{rs} to $|Q\rangle$,

$$|Qs;\alpha r\rangle = N^{\alpha}_{Qs} e^{\alpha}_{rs} |Q\rangle, \tag{38}$$

where N^{α}_{Qs} is a normalization constant. Such symmetry adapted kets obey the special Wigner–Eckart theorem

$$\begin{aligned}\langle Qs;\alpha r|\,\mathscr{O}\,|Q'u;\beta t\rangle &= N^{\alpha}_{Qs} N^{\beta}_{Q'u} \langle Q|\, e^{\alpha}_{sr}\mathscr{O}e^{\beta}_{ut}\,|Q'\rangle \\ &= \delta_{\alpha\beta}\,\delta_{ru}\langle Qs;\alpha\|\,\mathscr{O}\,\|Q't;\alpha\rangle,\end{aligned} \tag{39}$$

where we have chosen e^{α}_{rs} such that ${e^{\alpha}_{rs}}^{\dagger} = e^{\alpha}_{sr}$ and assumed $\mathscr{O}$ commutes with $\mathscr{G}$. Further, such kets obey the more general Wigner–Eckart theorem[1]

$$\langle Qs;\alpha r|\,\mathscr{O}_t{}^{\beta}|Q'v;\gamma u\rangle = \langle \alpha r|\,\beta t,\gamma u\rangle\langle Qs;\alpha\|\,\mathscr{O}^{\beta}\,\|\,Q'v;\gamma\rangle \tag{40}$$

where $\mathscr{O}_t{}^{\beta}$ is an irreducible tensorial operator transforming as the tth column of the βth irreducible representation Γ^{β} of $\mathscr{G}$, and $\langle\alpha r\,|\,\beta t,\gamma u\rangle$ is a Clebsch–Gordan coefficient.

IV. Construction of the Sequence Adapted Matric Basis

In this section, we outline a method for the selection of a matric basis of a group algebra $A(\mathscr{G}^{\vee})$ sequence adapted to the algebra $A(\mathscr{G})$ of one of its subgroups $\mathscr{G} \subseteq \mathscr{G}^{\vee}$. The method is an extension of Wedderburn's proof.

The algebra $A(\mathscr{G})$ for the subgroup has a matric basis with elements e^{α}_{rs}. Then the identity is resolvable into the sum of pairwise orthogonal primitive idempotents in $A(\mathscr{G})$,

$$\mathscr{I} = \sum_{\alpha}\sum_{r=1}^{f^{\alpha}} e^{\alpha}_{rr}. \tag{41}$$

The idempotents e^{α}_{rr} are not necessarily primitive in $A(\mathscr{G}^{\vee})$ but each is the sum of pairwise orthogonal primitive idempotents in $A(\mathscr{G}^{\vee})$,

$$e^{\alpha}_{rr} = \sum_{\alpha^{\vee}}\sum_{\rho=1}^{f^{\alpha^{\vee}\alpha}} e^{\alpha^{\vee}}_{(\rho\alpha r)(\rho\alpha r)}. \tag{42}$$

The primitive idempotent $e^{\alpha^{\vee}}_{(\rho\alpha r)(\rho\alpha r)}$ belongs to $A^{\alpha^{\vee}}(\mathscr{G}^{\vee})$, and ρ indexes the $f^{\alpha^{\vee}\alpha}$ distinct primitive idempotents in $A^{\alpha^{\vee}}(\mathscr{G}^{\vee})$. The number $f^{\alpha^{\vee}\alpha}$ is called the frequency.

---

[1] The form given here applies to simply reducible groups (Wigner, 1965).

Further, each of the elements

$$e^{\alpha^\vee}_{(\rho\alpha r)(\rho\alpha r)}\,;\ \alpha^\vee,\ \alpha \text{ ranging};\quad \rho = 1 \text{ to } f^{\alpha^\vee\alpha};\quad r = 1 \text{ to } f^{\alpha} \tag{43}$$

is distinct and orthogonal to every other. This is shown on considering the product of two of these elements

$$e^{\alpha^\vee}_{(\rho\alpha r)(\rho\alpha r)}\, e^{\beta^\vee}_{(\sigma\beta s)(\sigma\beta s)} = e^{\alpha^\vee}_{(\rho\alpha r)(\rho\alpha r)}\, e^{\beta}_{rr}\, e^{\beta}_{ss}\, e^{\beta^\vee}_{(\sigma\beta s)(\sigma\beta s)}, \tag{44}$$

where we have used the relations

$$e^{\alpha^\vee}_{(\rho\alpha r)(\rho\alpha r)}\, e^{\alpha}_{rr} = e^{\alpha^\vee}_{(\rho\alpha r)(\rho\alpha r)}, \tag{45}$$

$$e^{\beta}_{ss}\, e^{\beta^\vee}_{(\sigma\beta s)(\sigma\beta s)} = e^{\beta^\vee}_{(\sigma\beta s)(\sigma\beta s)}, \tag{46}$$

which follow from the fact that the decomposition (42) is in terms of primitive idempotents. Since the e^{α}_{rr} and e^{α}_{ss} are matric basis elements for $A(\mathscr{G})$, we already know that

$$e^{\alpha}_{rr}\, e^{\beta}_{ss} = \delta_{\alpha\beta}\, \delta_{rs}\, e^{\alpha}_{rr}. \tag{47}$$

Thus the product (44) is zero unless $\alpha = \beta$ and $r = s$. If $\alpha = \beta$ and $r = s$, then

$$e^{\alpha^\vee}_{(\rho\alpha r)(\rho\alpha r)}\, e^{\beta^\vee}_{(\sigma\alpha r)(\sigma\alpha r)} = \delta_{\alpha^\vee\beta^\vee}\, \delta_{\rho\sigma}\, e^{\alpha^\vee}_{(\rho\alpha r)(\rho\alpha r)}, \tag{48}$$

the $\delta_{\rho\sigma}$ following from the fact that the decomposition (42) is in terms of primitive idempotents. Thus

$$e^{\alpha^\vee}_{(\rho\alpha r)(\rho\alpha r)}\, e^{\beta^\vee}_{(\sigma\beta s)(\sigma\beta s)} = \delta_{\alpha^\vee\beta^\vee}\, \delta_{\rho\sigma}\, \delta_{\alpha\beta}\, \delta_{rs}\, e^{\alpha^\vee}_{(\rho\alpha r)(\rho\alpha r)}. \tag{49}$$

Using (41) and (42),

$$\mathscr{I} = \sum_{\alpha^\vee} \sum_{\alpha} \sum_{\rho=1}^{f^{\alpha^\vee\alpha}} \sum_{r=1}^{f^{\alpha}} e^{\alpha^\vee}_{(\rho\alpha r)(\rho\alpha r)}. \tag{50}$$

From the preceding paragraph we see that this (50) is a resolution of $\mathscr{I}$ into primitive idempotents, each of which is contained in one of the simple subalgebras $A^{\alpha^\vee}(\mathscr{G}^\vee)$. This then has accomplished a specific choice of the general nonunique decomposition in (31) and (29). The proof then follows that of Wedderburn (1907), to yield

$$e^{\alpha^\vee}_{(\rho\alpha r)(\sigma\beta s)}\, e^{\beta^\vee}_{(\rho'\alpha' r')(\sigma'\beta' s')} = \delta_{\alpha^\vee\beta^\vee}\, \delta_{\sigma\rho'}\, \delta_{\beta\alpha'}\, \delta_{sr'}\, e^{\alpha^\vee}_{(\rho\alpha r)(\sigma'\beta' s')}, \tag{51}$$

this being the result we have sought.

Kets symmetry adapted to both $\mathscr{G}^\vee$ and the subgroup $\mathscr{G}$ are obtained by applying a sequence adapted matric basis element to a primitive ket $|Q\rangle$. For instance, a ket which transforms as the $(\rho\alpha r)$th column of the $(\alpha^\vee)$th irreducible representation of $\mathscr{G}^\vee$ is

$$|Q(\sigma\beta s);\, \alpha^\vee(\rho\alpha r)\rangle = N^{\alpha^\vee}_{Q(\sigma\beta s)}\, e^{\alpha^\vee}_{(\rho\alpha r)(\sigma\beta s)}\, |Q\rangle. \tag{52}$$

Such kets obey the Wigner–Eckart theorem[2]

$$\langle\alpha^\vee(\rho\alpha r)|\, \mathscr{O}^{\beta^\vee}_{(\sigma\beta s)}\, |\gamma^\vee(\tau\gamma t)\rangle = \langle\alpha^\vee(\rho\alpha r)|\, \beta^\vee(\sigma\beta s)\gamma^\vee(\tau\gamma t)\rangle\langle\alpha^\vee \,\|\, \mathscr{O}^{\beta^\vee} \,\|\gamma^\vee\rangle, \tag{53}$$

where $\langle\alpha^\vee \,\|\mathscr{O}^{\beta^\vee}\|\, \gamma^\vee\rangle$ is a reduced matrix element, $\mathscr{O}^{\beta^\vee}_{(\sigma\beta s)}$ is an irreducible tensorial operator transforming as the $(\sigma\beta s)$the column of the $(\beta^\vee)$th irreducible representation of $\mathscr{G}^\vee$, and we have suppressed the symbols to the left of the semicolon in (52). The Clebsch–Gordan coefficient for $\mathscr{G}^\vee$ appearing in (53) has symmetry properties not only with respect to $\mathscr{G}^\vee$ but with respect to the subgroup $\mathscr{G}$ also; for instance,

$$\langle\alpha^\vee(\rho\alpha r)\,|\, \beta^\vee(\sigma\beta s)\gamma^\vee(\tau\gamma t)\rangle = 0 \qquad \begin{cases}\text{if} \quad f^{\beta^\vee \boxtimes \gamma^\vee;\, \alpha^\vee} = 0 \\ \text{if} \quad f^{\beta\boxtimes\gamma;\,\alpha} = 0\end{cases}. \tag{54}$$

Here $f^{\beta^\vee \boxtimes \gamma^\vee;\, \alpha^\vee}$ is the frequency of $\Gamma^{\alpha^\vee}$ in the Kronecker product of $\Gamma^{\beta^\vee}$ and $\Gamma^{\gamma^\vee}$; $f^{\beta\boxtimes\gamma;\,\alpha}$ is the frequency of Γ^α in the Kronecker product of Γ^β and Γ^γ. The kets (52) symmetry adapted to both $\mathscr{G}$ and $\mathscr{G}^\vee$ also obey a second Wigner–Eckart theorem:

$$\langle\alpha^\vee(\rho\alpha r)\,|\mathscr{O}_s{}^\beta|\, \gamma^\vee(\tau\gamma t)\rangle = \langle\alpha r\,|\, \beta s, \gamma t\rangle\langle\alpha^\vee(\rho\alpha)\,\|\mathscr{O}^\beta\|\, \gamma^\vee(\tau\gamma)\rangle, \tag{55}$$

where $\mathscr{O}_s{}^\beta$ is an irreducible tensorial operator with respect to $\mathscr{G}$ and $\langle\alpha r\,|\, \beta s, \gamma t\rangle$ is a Clebsch–Gordan coefficient for $\mathscr{G}$.

V. Properties of the Sequence Adapted Matric Basis

From the preceding section, we see that the matric basis elements of $A(\mathscr{G})$ are simply expressed in terms of the adapted matric basis elements of $A(\mathscr{G}^\vee)$ by the formula

$$e^\alpha_{rs} = \sum_{\alpha^\vee} \sum_{\rho=1}^{f^{\alpha^\vee \alpha}} e^{\alpha^\vee}_{(\rho\alpha r)(\rho\alpha s)}. \tag{56}$$

With the orthogonality relations and this equation, it follows that

$$e^\alpha_{rs}\, e^{\alpha^\vee}_{(\rho\beta t)(\sigma\gamma u)} = \delta_{\alpha\beta}\, \delta_{st}\, s^{\alpha^\vee}_{(\rho\alpha r)(\sigma\gamma u)}. \tag{57}$$

---

[2] The form given here applies to simply reducible groups (Wigner, 1965).

Further, it follows that

$$e^{\alpha}_{rs}\, e^{\alpha^\vee} = \sum_{\rho=1}^{f^{\alpha^\vee \alpha}} e^{\alpha^\vee}_{(\rho\alpha r)(\rho\alpha s)}. \tag{58}$$

These operators in (58) may be used to symmetry adapt a ket to both the groups $\mathscr{G}^\vee$ and $\mathscr{G}$ simultaneously.

The sequence adapted matric basis elements may be expanded in terms of the group elements of $\mathscr{G}^\vee$,

$$e^{\alpha^\vee}_{(\rho\alpha r)(\sigma\beta s)} = \frac{f^{\alpha^\vee}}{g^\vee} \sum_{G^\vee \in \mathscr{G}^\vee} [(G^\vee)^{-1}]^{\alpha^\vee}_{(\sigma\beta s)(\rho\alpha r)}\, G^\vee. \tag{59}$$

The numbers $[(G^\vee)^{-1}]^{\alpha^\vee}_{(\sigma\beta s)(\rho\alpha r)}$ are matrix elements of the sequence adapted $(\alpha^\vee)$the irreducible representation $\Gamma^{\alpha^\vee}$ of $\mathscr{G}^\vee$. Here $f^{\alpha^\vee}$ is the dimension of $\Gamma^{\alpha^\vee}(\mathscr{G}^\vee)$, and $g^\vee$ is the order of $\mathscr{G}^\vee$. Alternately, the group elements may be expressed in terms of the sequence adapted matric basis

$$G^\vee = \sum_{\alpha^\vee} \sum_{\rho\alpha r} \sum_{\sigma\beta s} [G^\vee]^{\alpha^\vee}_{(\rho\alpha r)(\sigma\beta s)}\, e^{\alpha^\vee}_{(\rho\alpha r)(\sigma\beta s)}. \tag{60}$$

For an element G of the subgroup $\mathscr{G}$, an alternate expression is possible:

$$\begin{aligned} G &= \sum_{\alpha} \sum_{r} \sum_{s} [G]^{\alpha}_{rs}\, e^{\alpha}_{rs} \\ &= \sum_{\alpha} \sum_{\rho\alpha r} \sum_{s} [G]^{\alpha}_{rs}\, e^{\alpha^\vee}_{(\rho\alpha r)(\rho\alpha s)}, \end{aligned} \tag{61}$$

where we have substituted (56). Comparing (60) and (61), it follows that the sequence adapted representation $\Gamma^{\alpha^\vee}(\mathscr{G}^\vee)$ is such that the matrix representations of $G \in \mathscr{G}$ are block-diagonalized with each block corresponding to an irreducible representation of $\mathscr{G}$:

$$[G]^{\alpha^\vee}_{(\rho\alpha r)(\sigma\beta s)} = \delta_{\alpha\beta}\, \delta_{\rho\sigma} [G]^{\alpha}_{rs}. \tag{62}$$

This is, in fact, an alternate criterion for $\Gamma^{\alpha^\vee}(\mathscr{G}^\vee)$ to be sequence adapted and will be applied in later sections.

The property (62) of the sequence adapted irreducible representation elements may be employed to express a sequence adapted matric basis element $e^{\alpha^\vee}_{(\rho\alpha r)(\sigma\beta s)}$ in terms of the left coset multipliers C_p of $\mathscr{G}$ in $\mathscr{G}^\vee$,

$$\begin{aligned} e^{\alpha^\vee}_{(\rho\alpha r)(\sigma\beta s)} &= \frac{f^{\alpha^\vee}}{g^\vee} \sum_{p} \sum_{G \in \mathscr{G}} [G^{-1} C_p^{-1}]^{\alpha^\vee}_{(\sigma\beta s)(\rho\alpha r)}\, C_p G \\ &= \frac{f^{\alpha^\vee}}{g^\vee} \sum_{p} \sum_{G \in \mathscr{G}} \sum_{t=1}^{f^{\beta}} [G^{-1}]^{\beta}_{st} [C_p^{-1}]^{\alpha^\vee}_{(\sigma\beta t)(\rho\alpha r)}\, C_p G \\ &= \frac{f^{\alpha^\vee} g}{g^\vee f^{\beta}} \sum_{p} \sum_{t=1}^{f^{\beta}} [C_p{}^{-1}]^{\alpha^\vee}_{(\sigma\beta t)(\rho\alpha r)}\, C_p\, e^{\beta}_{ts}. \end{aligned} \tag{63}$$

In the case, $\mathscr{G}$ is a product of two disjoint symmetric groups, $\mathscr{S}_A$ and $\mathscr{S}_B$, contained in a larger symmetric group $\mathscr{G}^\vee = \mathscr{S}_N$ as studied by Jahn (1954) and Kaplan (1961), the coefficients of $C_p e^\beta_{ts}$ in (63) may be called *spin-free fractional parentage coefficients.*

Employing a double coset decomposition of $\mathscr{G}^\vee$ of the form

$$\mathscr{G}^\vee = \mathscr{G}C_1\mathscr{G} \oplus \mathscr{G}C_2\mathscr{G} \oplus \cdots \oplus \mathscr{G}C_M\mathscr{G}, \tag{64}$$

the sequence adapted matric basis elements may be decomposed:

$$\begin{aligned} e^{\alpha^\vee}_{(\rho\alpha r)(\sigma\beta s)} & \\ &= \frac{f^{\alpha^\vee}}{g^\vee} \sum_{p=1}^{M} \sum_{G\in\mathscr{G}} \sum_{G'\in\mathscr{G}} d_p^{-1}[G^{-1}C_p^{-1}(G')^{-1}]^{\alpha^\vee}_{(\sigma\beta s)(\rho\alpha r)} G'C_pG \\ &= \frac{f^{\alpha^\vee}}{g^\vee} \sum_{p=1}^{M} \sum_{G\in\mathscr{G}} \sum_{G'\in\mathscr{G}} \sum_{t=1}^{f^\beta} \sum_{u=1}^{f^\alpha} d_p^{-1}[G^{-1}]^\beta_{st}[C_p^{-1}]^{\alpha^\vee}_{(\sigma\beta t)(\rho\alpha u)}[G'^{-1}]^\alpha_{ur} G'C_pG \\ &= \frac{f^{\alpha^\vee} g^2}{g^\vee f^\alpha f^\beta} \sum_{p=1}^{M} d_p^{-1} \sum_{t=1}^{f^\beta} \sum_{u=1}^{f^\alpha} [C_p^{-1}]^{\alpha^\vee}_{(\sigma\beta t)(\rho\alpha u)} e^\alpha_{ru} C_p e^\beta_{ts}. \end{aligned} \tag{65}$$

Here d_p is the number of times an element of the double coset $\mathscr{G}C_p\mathscr{G}$ will be obtained on multiplying out all g^2 possible products; d_p is equal to the order of the intersection $C_p\mathscr{G}C_p^{-1} \wedge \mathscr{G}$. In the case, $\mathscr{G}$ is a product of two disjoint symmetric groups, $\mathscr{S}_A$ and $\mathscr{S}_B$, contained in a larger symmetric group $\mathscr{G}^\vee = \mathscr{S}_N$, simple formulas for the double coset multipliers C_p and the numbers d_p are known (see Sasaki, 1965; Coleman, 1963; or Matsen and Klein, 1970).

The formula (63) is useful in constructing kets symmetry adapted to $\mathscr{G}^\vee$ from primitive kets already symmetry adapted to $\mathscr{G}$. Formula (65) is equally useful in evaluating matrix elements over primitive kets symmetry adapted to the subgroup $\mathscr{G}$. Physical applications of such formulas will be discussed in Sections XIII–XV.

VI. Canonical Subgroups

If all the frequencies $f^{\alpha^\vee\alpha}$ are one or zero, $\mathscr{G}$ is said to be a canonical subgroup of $\mathscr{G}^\vee$. When $\mathscr{G}$ is canonical, we may suppress the indices, ρ and σ. We may rewrite (56)–(58) as

$$e^\alpha_{rs} = \sum_{\alpha^\vee} e^{\alpha^\vee}_{(\alpha r)(\alpha s)}, \tag{66}$$

$$e^\alpha_{rs}\, e^{\alpha^\vee}_{(\beta t)(\gamma u)} = \delta_{\alpha\beta}\, \delta_{st}\, e^{\alpha^\vee}_{(\alpha r)(\gamma u)}, \tag{67}$$

$$e^{\alpha^\vee} e^\alpha_{rs} = e^{\alpha^\vee}_{(\alpha r)(\alpha s)}. \tag{68}$$

Equation (68) is of particular interest since it supplies an explicit formula for a sequence adapted matric basis element of $A(\mathscr{G}^\vee)$. This equation may be used to construct $e^{\alpha^\vee}_{(\alpha r)(\alpha s)}$ whenever one is dealing with a canonical subgroup, as is often the case in systems of physical interest.

We may rewrite equation (68) expanding the left-hand side in terms of the group elements of $\mathscr{G}^\vee$ and $\mathscr{G}$,

$$\begin{aligned} e^{\alpha^\vee} e^{\alpha}_{rs} &= \frac{f^{\alpha^\vee} f^{\alpha}}{g^\vee g} \sum_{G^\vee \in \mathscr{G}^\vee} \sum_{G \in \mathscr{G}} \chi^{\alpha^\vee}((G^\vee)^{-1})[G^{-1}]^{\alpha}_{sr} G^\vee G \\ &= \frac{f^{\alpha^\vee}}{g^\vee} \sum_{G^\vee \in \mathscr{G}^\vee} \left\{ \frac{f^{\alpha}}{g} \sum_{G \in \mathscr{G}} \chi^{\alpha^\vee}(G(G^\vee)^{-1})[G^{-1}]^{\alpha}_{sr} \right\} G^\vee, \end{aligned} \tag{69}$$

where $\chi^{\alpha}((G^\vee)^{-1})$ is an irreducible character. On expanding the right-hand side of (68),

$$e^{\alpha^\vee}_{(\alpha r)(\alpha s)} = \frac{f^{\alpha^\vee}}{g^\vee} \sum_{G^\vee \in \mathscr{G}^\vee} [(G^\vee)^{-1}]^{\alpha^\vee}_{(\alpha s)(\alpha r)} G^\vee, \tag{70}$$

and comparing (69) and (70), we obtain

$$[(G^\vee)^{-1}]^{\alpha^\vee}_{(\alpha s)(\alpha r)} = \frac{f^{\alpha}}{g} \sum_{G \in \mathscr{G}} \chi^{\alpha^\vee}(G(G^\vee)^{-1})[G^{-1}]^{\alpha}_{sr}. \tag{71}$$

This is an explicit formula for the sequence adapted irreducible representation matrix elements $[(G^\vee)^{-1}]^{\alpha^\vee}_{(\alpha s)(\alpha r)}$.

To obtain a formula for the more general matrix elements $[G^\vee]^{\alpha^\vee}_{(\alpha r)(\beta s)}$ when $\alpha \neq \beta$, we may use a relation of the form

$$e^{\alpha^\vee}_{(\alpha r)(\alpha r)} G^\vee e^{\alpha^\vee}_{(\beta s)(\beta s)} = [G^\vee]^{\alpha^\vee}_{(\alpha r)(\beta s)} e^{\alpha^\vee}_{(\alpha r)(\beta s)}. \tag{72}$$

Expanding the left- and right-hand sides of (72) in terms of group elements and comparing the coefficients yields

$$\begin{aligned} &[G^\vee]^{\alpha^\vee}_{(\alpha r)(\beta s)}[(G_1{}^\vee)^{-1}]^{\alpha^\vee}_{(\beta s)(\alpha r)} \\ &= \frac{f^{\alpha^\vee}}{g^\vee} \sum_{G_2{}^\vee \in \mathscr{G}^\vee} [(G_2{}^\vee)^{-1}]^{\alpha^\vee}_{(\alpha r)(\alpha r)} [(G_1{}^\vee)^{-1} G_2{}^\vee G^\vee]^{\alpha^\vee}_{(\beta s)(\beta s)}\,; \qquad G^\vee, G_1{}^\vee \in \mathscr{G}^\vee \end{aligned} \tag{73}$$

Choosing $G_1{}^\vee = G^\vee$ yields an explicit expression for the magnitude of $[G^\vee]^{\alpha^\vee}_{(\alpha r)(\beta s)}$ (so long as we are using a unitary matric basis for $\mathscr{G}^\vee$); any phase for $[G^\vee]^{\alpha^\vee}_{(\alpha r)(\beta s)}$ can yield a symmetry adapted representation. After choosing a phase for a particular $[G^\vee]^{\alpha^\vee}_{(\alpha r)(\beta s)}$, consistent phases for other elements $G_1{}^\vee \neq G^\vee$ may be obtained from (73).

The results of this section apply in complete generality only to canonical subgroups. Such groups occur often in systems of physical significance. Wigner (1968), has given conditions that a subgroup be canonical. In addition, we will be able to apply the relations of this section in some instances in which the subgroup is not canonical.

VII. Induction, Subduction, and the Frobenius Reciprocity Theorem

The sequence adapted matric basis is intimately related to the theory of induced and subduced representations and the Frobenius reciprocity theorem. Such relations indicate the correspondence of the present work to a wide literature concerning induced representations; see, for example, Coleman, 1968b, Mackey, 1968, or Robinson, 1961. To show this relation, we construct induced and subduced representations in terms of the symmetry adapted matric basis. Such a construction yields the Frobenius reciprocity theorem as an immediate consequence.

The space $A(\mathscr{G}^\vee)e^\alpha$ is left-invariant to $\mathscr{G}^\vee$ and generates a representation which is, in general, reducible; thus,

$$\Gamma^{\alpha\uparrow}(\mathscr{G}^\vee) = \dot{\sum_{\alpha^\vee}} f^{\alpha\uparrow\alpha^\vee}\Gamma^{\alpha^\vee}(\mathscr{G}^\vee). \tag{74}$$

$\Gamma^{\alpha\uparrow}(\mathscr{G}^\vee)$ is said to be induced on $\mathscr{G}^\vee$ from $\Gamma^\alpha(\mathscr{G})$. Using such relations as (57), we see that the sequence adapted basis of $A(\mathscr{G}^\vee)e^\alpha$ is

$$\left\{e^{\alpha^\vee}_{(\sigma\beta s)(\rho\alpha r)}\,;\ \alpha^\vee,\ \beta \text{ ranging,}\qquad \begin{matrix}\rho = 1 \text{ to } f^{\alpha^\vee\alpha}, & r = 1 \text{ to } f^\alpha\\ \sigma = 1 \text{ to } f^{\alpha^\vee\beta}; & s = 1 \text{ to } f^\beta\end{matrix}\right\}. \tag{75}$$

The space $A(\mathscr{G})e^{\alpha^\vee}$ is left invariant to $\mathscr{G}$ and generates a representation which is, in general, reducible; thus

$$\Gamma^{\alpha^\vee\downarrow}(\mathscr{G}) = \dot{\sum_{\alpha}} f^{\alpha^\vee\downarrow\alpha}\Gamma^\alpha(\mathscr{G}). \tag{76}$$

$\Gamma^{\alpha^\vee\downarrow}(\mathscr{G})$ is said to be subduced on $\mathscr{G}$ from $\Gamma^{\alpha^\vee}(\mathscr{G}^\vee)$. Using relations such as (58), we see that the symmetry adapted basis of $A(\mathscr{G})e^{\alpha^\vee}$ is

$$\{e^{\alpha^\vee}_{(\rho\alpha r)(\rho\alpha s)}\,;\ \alpha \text{ ranging,}\qquad \rho = 1 \text{ to } f^{\alpha^\vee\alpha},\quad r, s = 1 \text{ to } f^\alpha\}. \tag{77}$$

Comparing the two sequence adapted bases, (75) and (76), we see that

$$f^{\alpha^\vee\downarrow\alpha} = f^{\alpha^\vee\alpha} = f^{\alpha\uparrow\alpha^\vee}. \tag{78}$$

This result is the Frobenius reciprocity theorem.

We note that in Section II, the space $V^0(K^0; \alpha^0)$ invariant to $\mathscr{G}^0$ was induced to a space $V(K^0; \alpha^0\uparrow)$ invariant under $\mathscr{G}^\vee$. The representation of $\mathscr{G}^\vee$ on $V^0(K^0; \alpha^0\uparrow)$ is just $\Gamma^{\alpha^0\uparrow}(\mathscr{G}^\vee)$.

VIII. Semidirect Products

In the particular case when the group $\mathscr{G}^\vee$ is a product of a normal subgroup $\mathscr{G}$ and a second group $\mathscr{C}$,

$$\mathscr{G}^\vee = \mathscr{G}\mathscr{C}, \tag{79}$$

$$C\mathscr{G}C^{-1} = \mathscr{G}, \qquad C \in \mathscr{C}, \tag{80}$$

such that the only element $\mathscr{G}$ and $\mathscr{C}$ have in common is the identity

$$\mathscr{G} \wedge \mathscr{C} = \{\mathscr{I}\}, \tag{81}$$

$\mathscr{G}^\vee$ is said to be the *semidirect* product of $\mathscr{G}$ and $\mathscr{C}$. In such a case, many of the formulas of the preceding sections for sequence adaptation to the sequence $\mathscr{G} \subseteq \mathscr{G}^\vee$ appear in especially simple forms. The theory of sequence adaptation to a semidirect product sequence of point groups has been discussed by Altmann (1963) and McIntosh (1960); the theory in the case of space groups has been discussed by Seitz (1936) and Bouckaert *et al.* (1936). An excellent general treatment is given in Section 7 of Coleman (1966).

Here we present a brief treatment of the theory illustrating the simplification of some of the formulas of the preceding sections. The theory is based on the fact that if Γ^α is an irreducible representation of $\mathscr{G}$, then $\Gamma^{C\alpha}(\mathscr{G})$ defined for any $C \in \mathscr{C}$ such that

$$[G]^{C\alpha} \equiv [CGC^{-1}]^\alpha, \qquad G \in \mathscr{G}, \quad C \in \mathscr{C} \tag{82}$$

is also an irreducible representation of $\mathscr{G}$.

Case A

In the case that each $C\alpha$ is not equivalent to any other $C'\alpha$, $C' \neq C \in \mathscr{C}$ and $C' \in \mathscr{C}$, we have

$$\Gamma^{\alpha\uparrow}(\mathscr{G}) \text{ is irreducible}, \tag{83}$$

$$e^{\alpha\uparrow}_{(\alpha r)(\alpha r)} = e^{\alpha}_{rr}. \tag{84}$$

Equations (83) and (84) are special examples of Eqs. (74) and (56), respectively. Equation (83) is obtained on considering the induced representation $\Gamma^{\alpha\uparrow}(\mathscr{G}^\vee)$ on the coset basis of $A(\mathscr{G}^\vee)e^\alpha$,

$$\{Ce^\alpha_{rs}; \qquad C \in \mathscr{C}, \quad r, s = 1 \text{ to } f^\alpha\}. \tag{85}$$

On this coset basis, the representation $[G]^{\alpha\uparrow}$ of $G \in \mathscr{G}$ is seen to be the direct sum of the different $[G]^{C\alpha}$. Further on this basis (85) for $A(\mathscr{G}^{\vee})e^{\alpha}$, the representation $[C]^{\alpha\uparrow}$ of $C \in \mathscr{C}$ is seen to be

$$[C]^{\alpha\uparrow}_{C_1 rs,\, C_2 tu} = \begin{cases} \delta_{rt}\,\delta_{su}, & C_1 = CC_2 \\ 0, & \text{otherwise.} \end{cases} \tag{86}$$

The matrix representation $[C]^{\alpha\uparrow}$, $C \in \mathscr{C}$, is seen to have no diagonal elements unless $C = \mathscr{I}$. The character $\chi^{\alpha\uparrow}(C) = 0$, $C \in \mathscr{C}$, unless $C = \mathscr{I}$, and

$$\chi^{\alpha\uparrow}(G^{\vee}) = \sum_{C_1 rs} \sum_{C_2 rs} [G]^{\alpha\uparrow}_{C_1 rs,\, C_2 tu} [C]^{\alpha\uparrow}_{C_2 tu,\, C_1 rs} = \begin{matrix} c\chi^{\alpha}(G^{\vee}), & G^{\vee} \in \mathscr{G} \\ 0, & G^{\vee} \notin \mathscr{G}, \end{matrix} \tag{87}$$

where $G^{\vee} = GC$ is the right coset decomposition of $G^{\vee}$, and c is the order of $\mathscr{C}$. Since the character (87) is normalized

$$\frac{1}{g^{\vee}} \sum_{G^{\vee} \in \mathscr{G}^{\vee}} \chi^{\alpha\uparrow}(G^{\vee}) \chi^{\alpha\uparrow}((G^{\vee})^{-1}) = 1, \tag{88}$$

It must be irreducible and (83) is established. Since (83) holds, $e^{\alpha}_{rr} \in A^{\alpha\uparrow}(\mathscr{G}^{\vee})$, so that

$$e^{\alpha\uparrow} e^{\alpha}_{rr} = e^{\alpha}_{rr}, \tag{89}$$

and using (68), (84) is established. The sequence adapted irreducible representation $\Gamma^{\alpha\uparrow}(\mathscr{G}^{\vee})$ and the corresponding sequence adapted matric basis elements are thus completely determined by the present treatment for the case when all the $C\alpha$, $C \in \mathscr{C}$, are not equivalent.

Case B

In this case each $C\alpha$, $C \in \mathscr{C}$, is equivalent to α. Thus the αth irreducible representation of CGC^{-1}, $C \in \mathscr{C}$ and $G \in \mathscr{G}$, is equal up to a unitary transformation $[U_C]^{\alpha}$ to the αth representation of G:

$$[CGC^{-1}]^{\alpha} = [U_C]^{\alpha}[G]^{\alpha}[U_C^{-1}]^{\alpha}. \tag{90}$$

(We note that the symbol $[C]^{\alpha}$ is undefined since α labels an irreducible representation Γ^{α} of $\mathscr{G}$ and $C \notin \mathscr{G}$, unless $C = \mathscr{I}$.) The matrices $[U_C]^{\alpha}$, $C \in \mathscr{C}$, form a projective representation of $\mathscr{C}$; this is seen on considering the representation of $C_1 C_2 G (C_1 C_2)^{-1}$ for $C_1, C_2 \in \mathscr{C}$,

$$\begin{aligned} [U_{C_1 C_2}]^{\alpha}[G]^{\alpha}[U^{-1}_{C_1 C_2}]^{\alpha} &= [C_1 C_2 G C_2^{-1} C_1^{-1}]^{\alpha} \\ &= [U_{C_1}]^{\alpha}[U_{C_2}]^{\alpha}[G]^{\alpha}[U_{C_2}^{-1}]^{\alpha}[U_{C_1}^{-1}]^{\alpha} \end{aligned} \tag{91}$$

or

$$[G]^\alpha = ([U^{-1}_{C_1C_2}]^\alpha[U_{C_1}]^\alpha[U_{C_2}]^\alpha)[G]^\alpha([U^{-1}_{C_1C_2}]^\alpha[U_{C_1}]^\alpha[U_{C_2}]^\alpha)^{-1} \tag{92}$$

By Schur's lemma, the unitary matrix $[U^{-1}{}_{C_1C_2}]^\alpha[U_{C_1}]^\alpha[U_{C_2}]^\alpha$ must be scalar:

$$[U^{-1}_{C_1C_2}]^\alpha[U_{C_1}]^\alpha[U_{C_2}]^\alpha = e^{i\theta_{C_1C_2}}[\mathscr{I}]^\alpha, \tag{93}$$

$$[U_{C_1}]^\alpha[U_{C_2}]^\alpha = e^{i\theta_{C_1C_2}}[U_{C_1C_2}]^\alpha. \tag{94}$$

We consider the case in which $\theta_{C_1C_2}$ may be chosen to be zero:

$$[U_{C_1}]^\alpha[U_{C_2}]^\alpha = [U_{C_1C_2}]^\alpha. \tag{95}$$

When (95) holds, the irreducible representation matrices of $\Gamma^{\alpha^\vee}(\mathscr{G}^\vee)$ are Kronecker products:

$$[GC]^{(\alpha,\xi)} = ([G]^\alpha[U_C]^\alpha) \otimes [C]^\xi, \tag{96}$$

where the irreducible representations $\Gamma^{\alpha^\vee}(\mathscr{G}^\vee)$ in the induced representation $\Gamma^{\alpha\uparrow}(\mathscr{G}^\vee)$ are in one-to-one correspondence with the irreducible representations Γ^ξ of $\mathscr{C}$ and are labeled

$$\alpha^\vee \Bumpeq (\alpha, \xi). \tag{97}$$

To establish that (96) is an irreducible representation matrix for $\mathscr{G}^\vee$, we first show that it is a representation. For arbitrary G, $G' \in \mathscr{G}$, and C, $C' \in \mathscr{C}$:

$$[GC]^{(\alpha,\xi)}[G'C']^{(\alpha,\xi)} = ([G]^\alpha[U_C]^\alpha[G']^\alpha[U_{C'}]^\alpha) \otimes ([C]^\xi[C']^\xi), \tag{98}$$

where we have used the general relation $([A] \otimes [B])([C] \otimes [D]) = ([A][C]) \otimes ([B][D])$ which holds for arbitrary matrices $[A]$, $[B]$, $[C]$, and $[D]$ such that the indicated multiplications are compatible. We proceed, using (90), then (96),

$$\begin{aligned} [GC]^{(\alpha,\xi)}[G'C']^{(\alpha,\xi)} &= ([G]^\alpha[CG'C^{-1}]^\alpha[U_C]^\alpha[U_{C'}]^\alpha) \otimes ([C]^\xi[C']^\xi) \\ &= ([GCG'C^{-1}]^\alpha[U_{CC'}]^\alpha) \otimes [CC']^\xi \\ &= [GCG'C']^{(\alpha,\xi)}. \end{aligned} \tag{99}$$

Thus we see that (96) does define a representation of $\mathscr{G}^\vee$ with the character

$$\chi^{(\alpha,\xi)}(GC) = \chi^\alpha(G)\chi^\xi(C). \tag{100}$$

Since the character (100) is normalized

$$\frac{1}{g^\vee}\sum_{G\in\mathscr{G}}\sum_{C\in\mathscr{C}}\chi^{(\alpha,\xi)}(GC)\chi^{(\alpha,\xi)}(C^{-1}G^{-1}) = 1, \tag{101}$$

the representation (96) is irreducible and the notation (97) is justified.

The irreducible representation matrix elements of $[GC]^{(\alpha,\,\xi)}$ are

$$[GC]^{(\alpha,\,\xi)}_{(r,\,i)(s,\,j)} = \sum_{t=1}^{f^\alpha} [G]^\alpha_{rt}[U_C]^\alpha_{ts}[C]^\xi_{ij} \tag{102}$$

and the sequence adapted matric basis elements are

$$e^{(\alpha,\,\xi)}_{(r,\,i)(s,\,j)} = \frac{f^\alpha f^\xi}{g^\vee} \sum_{G\in\mathscr{G}} \sum_{C\in\mathscr{C}} \sum_{t=1}^{f^\alpha} [G^{-1}]^\alpha_{st}[U_{C^{-1}}]^\alpha_{tr}[C^{-1}]^\xi_{ji}GC. \tag{103}$$

In the case $\Gamma^\alpha(\mathscr{G}^\vee)$ is one-dimensional, (103) simplifies further.

Case C

In this case, some but not all the $C\alpha$, $C\in\mathscr{C}$, are equivalent to α. The subset $\bar{\mathscr{K}} \subseteq \mathscr{C}$ for which all $\bar{K}\in\bar{\mathscr{K}}$ are such that $\bar{K}\alpha$ is equivalent to α forms a group called the *little co-group* of $\Gamma^\alpha(\mathscr{G})$ in $\mathscr{G}^\vee = \mathscr{G}\mathscr{C}$. One may induce $\Gamma^\alpha(\mathscr{G})$ into the *little* group $\mathscr{K} \equiv \mathscr{G}\bar{\mathscr{K}}$ by the procedure of Case B; each of these resulting irreducible representations of $\mathscr{K}$ may be induced into $\mathscr{G}^\vee$ by the procedure of Case A.

There are many point group sequences which are expressible as semidirect products. A few examples are (in the Schoenflies notation):

$$\begin{array}{rcl}
\mathscr{D}_{nh} \supseteq \mathscr{D}_n & : & \mathscr{D}_{nh} = \mathscr{D}_n\mathscr{C}_\sigma \\
\mathscr{D}_{2nh} \supseteq \mathscr{C}_{2n} & : & \mathscr{D}_{2nh} = \mathscr{C}_{2n}\mathscr{C}_i \\
\mathscr{C}_{nv} \supseteq \mathscr{C}_n & : & \mathscr{C}_{nv} = \mathscr{C}_n\mathscr{C}_\sigma \\
\mathscr{D}_{2nd} \supseteq \mathscr{D}_{2n} & : & \mathscr{D}_{2nd} = \mathscr{D}_{2n}\mathscr{C}_\sigma \\
\mathscr{O} \supseteq \mathscr{D}_2 & : & \mathscr{O} = \mathscr{D}_2\mathscr{D}_3{}' \\
\mathscr{O} \supseteq \mathscr{T} & : & \mathscr{O} = \mathscr{T}C_2''
\end{array} \tag{104}$$

Another frequent example is the sequence consisting of the single and double point groups. Yet other examples are found in the groups for semirigid molecules (see Altmann, 1967; and Serre, 1968). The semidirect product theory is thus widely applicable when working with point group sequences. Sequences of symmetric groups are, however, very seldom expressible in terms of semidirect products.

IX. Unitary Transformation of an Irreducible Representation

In Section V, we obtained formulas by which a sequence adapted matric basis of $\mathscr{G}^\vee$, or equivalently a sequence adapted irreducible representation of $\mathscr{G}^\vee$, could be obtained knowing only the characters of $\mathscr{G}^\vee$ and the matric basis, or irreducible representations, of $\mathscr{G}$. Another method for obtaining a sequence adapted irreducible representation would be to start with one that is not sequence adapted and transform to the sequence adapted one by means of a unitary matrix $[U]^{\alpha^\vee}$. Letting $[G^\vee]^{\alpha^\vee}$ be a matrix element of an irreducible representation of $G^\vee$ which is *not* sequence adapted, we know that there is a unitary matrix $[U]^{\alpha^\vee}$ such that

$$[G^\vee]^{\alpha}_{(\rho\alpha r)(\sigma\beta s)} = \sum_{i,\,j=1}^{f^{\alpha^\vee}} [U]^{\alpha^\vee}_{(\rho\alpha r)i}[G^\vee]^{\alpha^\vee}_{ij}[U^\dagger]^{\alpha^\vee}_{j(\sigma\beta s)} \tag{105}$$

and

$$[G^\vee]^{\alpha^\vee}_{ij} = \sum_{\rho\alpha r}\sum_{\sigma\beta s}[U^\dagger]^{\alpha^\vee}_{i(\rho\alpha r)}[G^\vee]^{\alpha^\vee}_{(\rho\alpha r)(\sigma\beta s)}[U]^{\alpha^\vee}_{(\sigma\beta s)j}. \tag{106}$$

The matrix $[U]^{\alpha^\vee}$ may also be used to transform between the sequence adapted and nonsequence adapted matric bases,

$$e^{\alpha^\vee}_{(\rho\alpha r)(\sigma\beta s)} = \sum_{i,\,j=1}^{f^{\alpha^\vee}} [U]^{\alpha^\vee}_{(\rho\alpha r)i}[U^\dagger]^{\alpha^\vee}_{j(\sigma\beta s)}\, e^{\alpha}_{ij}, \tag{107}$$

$$e^{\alpha^\vee}_{ij} = \sum_{\rho\alpha r}\sum_{\sigma\beta s}[U^\dagger]^{\alpha^\vee}_{i(\rho\alpha r)}[U]^{\alpha^\vee}_{(\sigma\beta s)j}\, e^{\vee}_{(\rho\alpha r)(\sigma\beta s)}. \tag{108}$$

We consider two methods to obtain $[U]^{\alpha^\vee}$.

Method A

We choose $G^\vee = G \in \mathscr{G}$ in (106) and use (72),

$$[G]^{\alpha^\vee}_{ij} = \sum_{\rho\alpha r}\sum_{s}[U^\dagger]^{\alpha^\vee}_{i(\rho\alpha r)}[G]^{\alpha}_{rs}[U]^{\alpha^\vee}_{(\rho\alpha s)j}. \tag{109}$$

Next, multiplying by $[G^{-1}]^{\alpha}_{tu}$, summing over all $G \in \mathscr{G}$, and using the orthogonality theorem for irreducible representations,

$$\sum_{G\in\mathscr{G}}[G^{-1}]^{\alpha}_{tu}[G]^{\alpha}_{ij} = \frac{g}{f^\alpha}\sum_{\rho=1}^{f^{\alpha^\vee\alpha}}[U\dagger]^{\alpha^\vee}_{i(\rho\alpha u)}[U]^{\alpha^\vee}_{(\rho\alpha t)j}. \tag{110}$$

If $\mathscr{G}$ is canonical in $\mathscr{G}^\vee$,

$$[U^\dagger]^{\alpha^\vee}_{i(\alpha u)}[U]^{\alpha^\vee}_{(\alpha t)j} = \frac{f^\alpha}{g}\sum_{G\in\mathscr{G}}[G^{-1}]^{\alpha}_{tu}[G]^{\alpha^\vee}_{ij}. \tag{111}$$

Choosing $t = u$, $i = j$ yields an explicit expression for $|[U]^{\alpha^\vee}_{(\alpha t)i}|^2$; any phase for $[U]^{\alpha^\vee}_{(\alpha t)i}$ can yield a sequence adapted basis. After choosing a phase for a particular $[U]^{\alpha^\vee}_{(\alpha t)i}$, consistent phases for other elements

$[U^\dagger]^{\alpha^\vee}_{j(\alpha u)}$ may be obtained from (111). Once $[U]^{\alpha^\vee}$ is thus determined, (66) may be employed to obtain the sequence adapted matric basis. This procedure has been previously described by Matsen and Ellzey (1967) and a procedure of some similarity has been described by Kaplan (1961) to obtain kets symmetry adapted to $\mathscr{G}$ and $\mathscr{G}^\vee$.

Method B

The matrix $[U]^{\alpha^\vee}$ may also be determined by a second method. We define the class operator for the subgroup $\mathscr{G}$

$$K_\tau \equiv \sum_{G \in \mathscr{C}_\tau} G, \tag{112}$$

where $\mathscr{C}_\tau$ is the τth class of $\mathscr{G}$. The αth irreducible representation of K_τ in $\mathscr{G}$ is

$$[K_\tau]^\alpha = K_\tau^\alpha [\mathscr{I}]^\alpha \tag{113}$$

where $[\mathscr{I}]^\alpha$ is the unit matrix and K_τ^α is the class eigenvalue

$$K_\tau^\alpha = \chi_\tau^\alpha \, n_\tau / f^\alpha. \tag{114}$$

Recalling Eq. (62), we see that $[K_\tau]^{\alpha^\vee}$ will be diagonal if $\Gamma^{\alpha^\vee}(\mathscr{G}^\vee)$ is symmetry adapted to $\mathscr{G}$. If $\mathscr{G}$ is canonical in $\mathscr{G}^\vee$, and if all the K_τ^α for α such that $f^{\alpha^\vee\alpha} \neq 0$ are all different, then $[K_\tau]^{\alpha^\vee}$ will be diagonal if, and only if, $\Gamma^{\alpha^\vee}(\mathscr{G}^\vee)$ is symmetry adapted to $\mathscr{G}$. Thus, if in such a case we are given a nondiagonal $[K_\tau]^{\alpha^\vee}$, a unitary matrix $[U]^{\alpha^\vee}$ such that (105) holds may be found by diagonalization of $[K_\tau]^{\alpha^\vee}$.

X. Application to the Symmetric Group

We consider the symmetric group $\mathscr{S}_N$ of permutations on the integers $1, 2, 3, \ldots, N$ and the subgroup $\mathscr{S}_A \otimes \mathscr{S}_B$ consisting of the product of two disjoint symmetric groups, $\mathscr{S}_A$ and $\mathscr{S}_B$, of permutations on the integers $1, 2, \ldots, N_A$ and $N_A + 1, N_A + 2, \ldots, N$. The subgroup $\mathscr{S}_A \otimes \mathscr{S}_B$ is of particular interest when an N-particle system may be described in terms of two localized subsystems A and B consisting of N_A and $N_B = N - N_A$ particles. Although $\mathscr{S}_A \otimes \mathscr{S}_B$ is not necessarily canonical in $\mathscr{S}_N$, the frequencies $f^{\alpha^\vee\alpha} = f^{[\lambda_A]\otimes[\lambda_B];[\lambda]}$ (with $\alpha^\vee \Leftrightarrow [\lambda]$, $\alpha \Leftrightarrow [\lambda_A] \otimes [\lambda_B]$) are one or zero (Matsen and Klein, 1969) so long as $[\lambda]$ corresponds to a two-columned Young tableau. (We note that it is just precisely these Young tableaux which arise in the description of the spin-free symmetry of electronic systems.) Thus, working only with $[\lambda]$ corresponding to two-columned tableau, we may treat $\mathscr{S}_A \otimes \mathscr{S}_B$ as canonical in $\mathscr{S}_N$.

Irreducible representations for a two-columned $[\lambda]$ of $\mathscr{S}_N$ may be obtained sequence adapted to $\mathscr{S}_A \otimes \mathscr{S}_B$ by use of formulas (71) and (73); the irreducible characters needed in these formulas may be readily calculated by a method described by Coleman, 1968a. Alternately we might construct (Rutherford, 1948, or Robinson, 1961) the Young–Yamanouchi orthogonal representation and transform to the desired representation by one of the methods of Section IX. The Young–Yamanouchi orthogonal representation is already adapted to the sequence of groups

$$\mathscr{S}_N \supseteq \mathscr{S}_{N-1} \supseteq \mathscr{S}_{N-2} \supseteq \cdots \supseteq \mathscr{S}_1. \tag{115}$$

Thus the initial irreducible representation is adapted to $\mathscr{S}_A$ though not necessarily to $\mathscr{S}_B$. In application of the methods of Section IX, we then need only consider a unitary transformation which effects a sequence adaptation to $\mathscr{S}_B$. Working with the portion of the Young–Yamanouchi orthogonal representation $\Gamma^{[\lambda]}(\mathscr{S}_N)$ adapted to a $[\lambda_A]r_A$ of $\mathscr{S}_A$, the subgroup $\mathscr{S}_B$ may in effect be treated as canonical, i.e., the formulas for canonical subgroups obtained previously may be applied.

The class $\mathscr{C}_{(2)}$ of all transpositions in $\mathscr{S}_B$ has class eigenvalues (Corson, 1948)

$$K_{(2)}^{[\lambda_B]} = -\tfrac{1}{2}N_B(N_B - 1) + p_B(N_B - p_B + 1). \tag{116}$$

Here $[\lambda_B]$ is given by the partition $[2^{p_B}, 1^{N_B - 2p_B}]$, the only type of partition which may arise as long as $[\lambda]$ is two-columned. These class eigenvalues are all different in value, so that the class $\mathscr{C}_{(2)}$ of $\mathscr{S}_B$ may be used in conjunction with Method B of Section IX. We note that Method B of Section IX for calculating a unitary transformation to effect a symmetry adaptation may be more efficient than Method A, since Method A requires $N_B!$ Young–Yamanouchi matrices and Method B requires only $\tfrac{1}{2}N_B(N_B - 1)$ matrices using the class $\mathscr{C}_{(2)}$ of $\mathscr{S}_B$.

The case $N_B = 2$ and $\mathscr{S}_B = \{\mathscr{I}, (N, N-1)\}$ may be treated especially simply. Using what is essentially Method B of Section IX restricted to $N_B = 2$, Jahn (1954) has found an explicit formula for the unitary transformation. The present discussion applies to more general cases.

XI. Chains of Subgroups

A matric basis, or equivalently an irreducible representation, may be successively adapted to a sequence of subgroups of a finite group $\mathscr{G}_1$,

$$\mathscr{G}_1 \supseteq \mathscr{G}_2 \supseteq \cdots \supseteq \mathscr{G}_n. \tag{117}$$

Such a subgroup sequence is called a *chain*. An element of a matric basis adapted to such a chain may be denoted

$$e^{\alpha_1}_{(\rho_1\alpha_2;\, \rho_2\alpha_3;\, \ldots;\, \rho_{n-1}\alpha_n r_n)(\sigma_1\beta_2;\, \sigma_2\beta_3\, \ldots;\, \sigma_{n-1}\beta_n s_n)}. \tag{118}$$

If the frequency indices $f^{\alpha_i\alpha_{i+1}}$ are all zero or one, the chain is said to be *canonical*. In this case the ρ_i and σ_i indices in (118) may be suppressed. If $\mathscr{G}_n$ is Abelian, the indices r_n and s_n may be suppressed. Recently, conditions that a canonical chain exist ending with an Abelian group have been given (Janusz, 1966).

XII. Examples from the Symmetric Group

In this section we consider explicit examples of three types of symmetric group chains. Some of the formulas and methods of the previous sections are displayed or applied. The first type of symmetric group chain is the *Young–Yamanouchi* chain, obtained by sequentially removing one particle index at a time,

$$\mathscr{S}_N \supseteq \mathscr{S}_{N-1} \supseteq \mathscr{S}_{N-2} \supseteq \cdots \supseteq \mathscr{S}_2 \supseteq \mathscr{S}_1. \tag{119}$$

The second type of symmetric group chain is the *Jahn–Serber* chain obtained by sequentially removing two particle indices at a time,

$$\begin{aligned}\mathscr{S}_N &\supseteq \mathscr{S}_{N-2} \otimes \{\mathscr{I}, (N, N-1)\}\\ &\supseteq \mathscr{S}_{N-4} \otimes \{\mathscr{I}, (N-2, N-3)\} \supseteq \mathscr{S}_{N-6} \otimes \{\mathscr{I}, (N-4, N-5)\} \supseteq \ldots\end{aligned} \tag{120}$$

The final Abelian group in this chain is either $\mathscr{S}_2$ or $\mathscr{S}_1 \otimes \{\mathscr{I}, (23)\}$ as N is even or odd. There are other symmetric group chains which we discuss later.

A. A Young–Yamanouchi Chain: $\mathscr{S}_4 \supseteq \mathscr{S}_3 \supseteq \mathscr{S}_2 \supseteq \mathscr{S}_1$

The procedure for constructing the Young–Yamanouchi orthogonal representation sequence adapted to (119) has been described by Rutherford (1948) and Robinson (1961). The superscript α_1 plus the subscripts $\alpha_2\alpha_3 \cdots \alpha_N$ on the matric basis elements (118) correspond in the present case to Yamanouchi symbols $(u_N u_{N-1} u_{N-2} \ldots u_1)$, where u_j is the row of the corresponding Young tableau in which the integer j occurs. Each Yamanouchi symbol is in one-to-one correspondence with a standard Young tableau. The sequence $(u_{N-1}u_{N-2} \cdots u_1)$, $(u_{N-2}u_{N-3} \cdots u_1)$, $(u_{N-3} \ldots u_1), \ldots, (u_1)$ is thus seen to be in correspondence with a sequence of Young tableaux for $\mathscr{S}_{N-1}$, $\mathscr{S}_{N-2}$, $\mathscr{S}_{N-3}$, $\ldots$, $\mathscr{S}_1$; this sequence of Young tableaux yields the sequence $\alpha_2\alpha_3\alpha_4 \cdots \alpha_N$. As a specific example, we consider the $\alpha_1 = [2, 1, 1] = [2, 1^2]$ irreducible representation of $\mathscr{S}_4$. One sequence adapted matric basis element is

$$\begin{aligned} e^{[2,1,1]}_{(3121)(3211)} = {} & \\ & (\sqrt{3}/48)\{-3(13) - (14) + 3(23) + (24) + 3(123) - (124) - 3(132) \\ & \quad + (134) + (142) + 3(143) - (234) - 3(243) \\ & \quad + (1234) + 3(1243) - 2(1324) - (1342) \\ & \quad + 2(1423) - 3(1432) + 2(13)(24) - 2(14)(23)\}. \end{aligned} \tag{121}$$

In this chain we may illustrate Eq. (56) as

$$e^{[2,1]}_{(121)(211)} = e^{[2,1^2]}_{(3121)(3211)} + e^{[3,1]}_{(1121)(1211)} + e^{[2,2]}_{(2121)(2211)}, \tag{122}$$

and Eq. (67) as

$$e^{[2,1]}_{(121)(211)} e^{[2,1^2]}_{(3211)(3121)} = e^{[2,1^2]}_{(3121)(3121)}, \tag{123}$$

and Eq. (63) as

$$\begin{aligned} e^{[2,1^2]}_{(3121)(3211)} = {} & \tfrac{3}{8}\{\mathscr{I} - \tfrac{5}{6}(14) - \tfrac{5}{6}(24) - \tfrac{1}{3}(34)\}e^{[2,1]}_{(121)(211)} \\ & + \sqrt{13}/16\{-(14) + (24)\}e^{[2,1]}_{(211)(211)}. \end{aligned} \tag{124}$$

In (124) we have chosen the coset multipliers of $\mathscr{S}_3$ in $\mathscr{S}_4$ to be $\mathscr{I}$, (14), (24), and (34).

B. A Jahn–Serber Chain: $\mathscr{S}_4 \supseteq \mathscr{S}_2 \otimes \mathscr{S}_{(2)}$

The unitary representation transforming from the Young–Yamanouchi orthogonal representation to the Jahn–Serber representation has been given by Elliot *et al.* (1953) and Jahn (1954). One may use modified Yamanouchi symbols though we will use the notation of Section XI for the present example with $\alpha_1 = [2, 1^2]$. For this chain $\mathscr{S}_4 \supseteq \mathscr{S}_2 \otimes \mathscr{S}_{(2)}$ we illustrate Eq. (67) as

$$e^{[2,1^2]}_{([1^2]\otimes[1^2])([1^2]\otimes[1^2])} = e^{[2,1^2]}(e^{[1^2]} \otimes e^{[1^2]}) \tag{125}$$

and Eq. (65) as

$$e^{[2,1^2]}_{([1^2]\otimes[1^2])([1^2]\otimes[1^2])} = \tfrac{1}{8}e^{[1^2]} \otimes e^{[1^2]} - \tfrac{1}{4}(e^{[1^2]} \otimes e^{[1^2]})(23)(e^{[1^2]} \otimes e^{[1^2]}), \tag{126}$$

where we have chosen the double coset multipliers as $\mathscr{I}$ and (23). We illustrate Eq. (71) for an irreducible representation matrix element

$$\begin{aligned} [(23)]^{[2,1^2]}_{([1^2]\otimes[1^2])([1^2]\otimes[1^2])} &= \tfrac{1}{4} \sum_{G \in \mathscr{S}_2 \otimes \mathscr{S}_{(2)}} \chi^{[2,1^2]}((23)G)[G^{-1}]^{[1^2]\otimes[1^2]} \\ &= \tfrac{1}{4}\{-1 \cdot 1 + 0 + 0 - 1 \cdot 1\} = -\tfrac{1}{2}. \end{aligned} \tag{127}$$

Equations (71) and (73) may be conveniently employed to generate the matrix representations for the present case.

C. $\mathcal{S}_6 \supseteq \mathcal{S}_3 \otimes \mathcal{S}_{(3)} \supseteq \mathcal{S}_2 \otimes \mathcal{S}_{(2)}$

Here $\mathcal{S}_3$, $\mathcal{S}_{(3)}$, $\mathcal{S}_2$, and $\mathcal{S}_{(2)}$ are the symmetric groups of permutations on the sets of integers $\{1, 2, 3\}$, $\{4, 5, 6\}$, $\{1, 2\}$, and $\{5, 6\}$. For $\alpha_1 = [2, 1^4]$, the Young–Yamanouchi representation has the rth row and column corresponding to the rth standard Young tableau when they are listed in lexigraphical order. Constructing the unitary matrix $[U]^{[2,1^4]}$ by the Method B of Section IX yields

$$[U]^{[2,1^4]} = \begin{bmatrix} 1 & \cdot & \cdot & \cdot & \cdot \\ \cdot & 1 & \cdot & \cdot & \cdot \\ \cdot & \cdot & \sqrt{\frac{1}{2}} & \sqrt{\frac{1}{2}} & \cdot \\ \cdot & \cdot & -\sqrt{\frac{3}{10}} & \sqrt{\frac{3}{10}} & \sqrt{\frac{2}{5}} \\ \cdot & \cdot & \sqrt{\frac{1}{5}} & -\sqrt{\frac{1}{5}} & \sqrt{\frac{3}{5}} \end{bmatrix}, \tag{128}$$

with zeros in all the blank positions and where we have chosen the five different rows of the sequence adapted representation to be associated with subgroup symmetries as follows

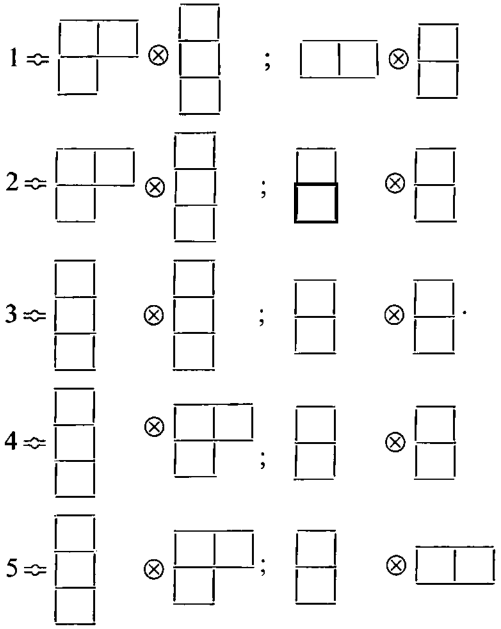

(129)

Since $\mathscr{S}_6$ is generated by the set $\{(12), (23), (34), (45), (56)\}$, the sequence adapted representation will be completely determined if we specify their five matrices. Applying the unitary transformation (105) to the Young–Yamanouchi representation of $[(34)]^{[2,1^4]}$ yields the sequence adapted representation

$$[(34)]^{[2,1^4]} = \begin{bmatrix} -1 & \cdot & \cdot & \cdot & \cdot \\ \cdot & -\frac{1}{3} & \frac{2}{3} & \frac{2}{3} & \cdot \\ \cdot & \frac{2}{3} & -\frac{1}{3} & \frac{2}{3} & \cdot \\ \cdot & \frac{2}{3} & \frac{2}{3} & -\frac{1}{3} & \cdot \\ \cdot & \cdot & \cdot & \cdot & -1 \end{bmatrix} \tag{130}$$

The sequence adapted representations of $(12), (23), (45), (56) \in \mathscr{S}_3 \otimes \mathscr{S}_{(3)}$ are readily given by (62) in terms of the irreducible representations of $\mathscr{S}_3$ sequence adapted to $\mathscr{S}_2$.

A similar application of Method B of Section IX to the $\alpha_1 = [2^2, 1^2]$ irreducible representation of $\mathscr{S}_6$ yields a unitary transformation matrix

$$[U]^{[2^2,1^2]} = \begin{bmatrix} \sqrt{\frac{2}{3}} & \sqrt{\frac{1}{3}} & \cdot & \cdot & \cdot & \cdot & \cdot & \cdot & \cdot \\ -\sqrt{\frac{2}{9}} & \frac{2}{3} & \sqrt{\frac{1}{3}} & \cdot & \cdot & \cdot & \cdot & \cdot & \cdot \\ \frac{1}{3} & -\sqrt{\frac{2}{9}} & \sqrt{\frac{2}{3}} & \cdot & \cdot & \cdot & \cdot & \cdot & \cdot \\ \cdot & \cdot & \cdot & \sqrt{\frac{2}{3}} & \sqrt{\frac{1}{3}} & & \cdot & \cdot & \cdot \\ \cdot & \cdot & \cdot & -\sqrt{\frac{2}{9}} & \frac{2}{3} & \sqrt{\frac{1}{3}} & \cdot & \cdot & \cdot \\ \cdot & \cdot & \cdot & \frac{1}{3} & -\sqrt{\frac{2}{9}} & \sqrt{\frac{2}{3}} & \cdot & \cdot & \cdot \\ \cdot & \cdot & \cdot & \cdot & \cdot & \cdot & \sqrt{\frac{5}{9}} & -\frac{1}{3} & \sqrt{\frac{1}{3}} \\ \cdot & \cdot & \cdot & \cdot & \cdot & \cdot & -\sqrt{\frac{5}{18}} & \sqrt{\frac{1}{18}} & \sqrt{\frac{2}{3}} \\ \cdot & \cdot & \cdot & \cdot & \cdot & \cdot & \sqrt{\frac{1}{6}} & \sqrt{\frac{5}{6}} & \cdot \end{bmatrix} \tag{131}$$

where we have chosen the 9 rows of the sequence adapted representation as follows:

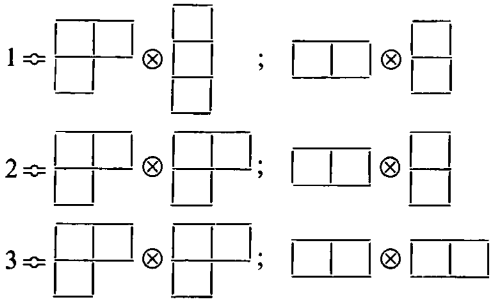

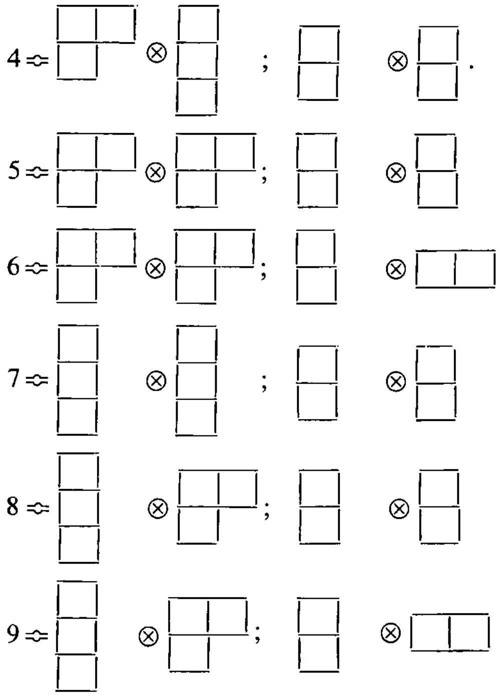

(132)

The sequence adapted representation of (34) is

$$[(34)]^{[2^2,1^2]}=\begin{bmatrix} \frac{1}{3} & \sqrt{\frac{8}{9}} & \cdot & \cdot & \cdot & \cdot & \cdot & \cdot & \cdot \\ \sqrt{\frac{8}{9}} & -\frac{1}{3} & \cdot & \cdot & \cdot & \cdot & \cdot & \cdot & \cdot \\ \cdot & \cdot & -1 & \cdot & \cdot & \cdot & \cdot & \cdot & \cdot \\ \cdot & \cdot & \cdot & -\frac{7}{9} & -\sqrt{\frac{8}{81}} & \cdot & -\sqrt{\frac{20}{81}} & \frac{2}{9} & \cdot \\ \cdot & \cdot & \cdot & -\sqrt{\frac{8}{81}} & -\frac{5}{9} & \cdot & \sqrt{\frac{40}{81}} & -\sqrt{\frac{8}{81}} & \cdot \\ \cdot & \cdot & \cdot & \cdot & \cdot & -\frac{1}{3} & \cdot & \cdot & \sqrt{\frac{8}{9}} \\ \cdot & \cdot & \cdot & -\sqrt{\frac{20}{81}} & \sqrt{\frac{40}{81}} & \cdot & \frac{1}{9} & -\sqrt{\frac{20}{81}} & \\ \cdot & \cdot & \cdot & \frac{2}{9} & -\sqrt{\frac{8}{81}} & \cdot & -\sqrt{\frac{20}{81}} & -\frac{7}{9} & \cdot \\ \cdot & \cdot & \cdot & \cdot & \cdot & \sqrt{\frac{8}{9}} & \cdot & \cdot & \frac{1}{3} \end{bmatrix} \tag{133}$$

The sequence adapted representations of (12), (23), (45), and (56) are again readily given in block diagonal form in terms of the representations of $\mathscr{S}_3$.

Finally, we note the Young–Yamanouchi representation for $\alpha_1 = [2^3]$ is already sequence adapted to the desired chain. This may be easily seen on noting that given $\alpha_1 = [2^3]$ and a $[\lambda_A]$ of $\mathscr{S}_3$, there is at most only one $[\lambda_B]$ of $\mathscr{S}_B$ such that $f^{[\lambda_A]\otimes[\lambda_B];\alpha_1} = 1$. Similar occurrences happen for general $\mathscr{S}_N$ with N even whenever $\alpha_1 = [2^{N/2}]$.

XIII. Local Permutational Symmetry and Chemical Structure

Many properties of N-electron systems are predicted with a spin-free Hamiltonian. Since a spin-free Hamiltonian commutes with the group of permutations on the spin-free coordinates of the electrons, the spin-free states of an N-electron system are labeled by partitions $[\lambda]$ of N. The Pauli-allowed states are

$$[\lambda] = [2^p, 1^{N-2p}], \tag{134}$$

where the correspondence with spin S is given by

$$S = \tfrac{1}{2}N - p. \tag{135}$$

There is no need to introduce spin into such a spin-free problem (see Matsen, 1964; and Kaplan, 1965). Even in the spin formulation, spin-free permutational symmetry still arises and the theory of the symmetric group still applies (see Wigner, 1959; Serber, 1934a,b; Yamanouchi, 1936, 1938; Kotani, 1961; Pauncz, 1967; Harris, 1967; and many others). Here we will employ the spin-free formulation. In the first part of this section, we discuss the theory of localized subsystems, deriving a Wigner–Eckart theorem for local permutational symmetries which holds in the limit of complete localization. In the last part of this section, we discuss the bearing of local permutational symmetry on chemical structure.

Many polyelectronic systems may be treated to a good approximation as a collection of subsystems, each subsystem retaining some features of the isolated subsystem. Let us consider an aggregate system composed of localized subsystems A, B, C, ... Let the vector spaces $V_A([\lambda_A]r_A)$, $V_B([\lambda_B]r_B)$, ... be associated with the electrons for subsystems A, B, ... Here $[\lambda_A]r_A$, $[\lambda_B]r_B$, ... denote *local permutational symmetries* for the localized subsystems A, B, C, ... The product space

$$\mathbf{V}([\boldsymbol{\lambda}]\mathbf{r}) = V_A([\lambda_A]r_A) \otimes V_B([\lambda_B]r_B) \otimes \cdots \tag{136}$$

for the total system has a basis of product kets

$$|\mathbf{K}; [\boldsymbol{\lambda}]\mathbf{r}\rangle = |K_A; [\lambda_A]r_A\rangle \otimes |K_B; [\lambda_B]r_B\rangle \otimes \cdots. \tag{137}$$

Here

$$[\boldsymbol{\lambda}] = [\lambda_A] \otimes [\lambda_B] \otimes \cdots \tag{138}$$

and

$$\mathbf{r} = r_A \otimes r_B \otimes \cdots \tag{139}$$

identify a column of an irreducible representation of the product of symmetric groups

$$\mathscr{S} = \mathscr{S}_A \otimes \mathscr{S}_B \otimes \cdots. \tag{140}$$

From such a product ket (137) we may project kets of different total permutational symmetries,

$$|\mathbf{K}; \sigma[\boldsymbol{\lambda}], [\lambda](\rho[\boldsymbol{\lambda}']\mathbf{s})\rangle = N(\mathbf{K}[\boldsymbol{\lambda}]\sigma) e^{[\lambda]}_{(\rho[\boldsymbol{\lambda}']\mathbf{s})(\sigma[\boldsymbol{\lambda}]r)} |\mathbf{K}; [\boldsymbol{\lambda}]\mathbf{r}\rangle, \tag{141}$$

where $N(\mathbf{K}[\boldsymbol{\lambda}]\sigma)$ is a normalization factor and where $[\lambda]$ labels any $\Gamma^{[\lambda]}$ of $\mathscr{S}_N$ contained in the representation $\Gamma^{[\boldsymbol{\lambda}]\uparrow}$ of $\mathscr{S}_N$ induced from the irreducible representation $\boldsymbol{\Gamma}^{[\boldsymbol{\lambda}]}$ of $\mathscr{S}$.

In the limit of zero differential overlap between localized subsystems, local permutational symmetries can be exact quantum numbers. This may be shown if the Hamiltonian is a *local* operator $\mathscr{O}$ such that it commutes with $\mathscr{S}_N$ and such that in the limit of zero differential overlap (ZDO) between kets $|K_I; [\lambda_I]r_I\rangle$ and $|K_J; [\lambda_J]r_J\rangle$, $I \neq J = A, B, C, \ldots$

$$\lim_{\text{ZDO}} \langle \mathbf{K}; [\boldsymbol{\lambda}]\mathbf{r} | G\mathscr{O} | \mathbf{K}'; [\boldsymbol{\lambda}'']\mathbf{r}'\rangle = 0, \qquad G \notin \mathscr{S}, \quad G \in \mathscr{S}_N, \tag{142}$$

We have

$$\begin{aligned} &\lim_{\text{ZDO}} \langle \mathbf{K}; (\rho[\boldsymbol{\lambda}]), [\lambda](\sigma[\boldsymbol{\lambda}']\mathbf{s}) | \mathscr{O} | \mathbf{K}'; (\rho'[\boldsymbol{\lambda}''])[\lambda'](\sigma'[\boldsymbol{\lambda}''']\mathbf{s}')\rangle \\ &\qquad = \delta_{[\lambda][\lambda']}\, \delta_{\sigma\sigma'}\, \delta_{[\boldsymbol{\lambda}'][\boldsymbol{\lambda}''']}\, \delta_{\mathbf{ss}'} \lim_{\text{ZDO}} \langle \mathbf{K}; [\boldsymbol{\lambda}]\mathbf{r} | e^{[\lambda]}_{(\rho[\boldsymbol{\lambda}]\mathbf{r})(\rho'[\boldsymbol{\lambda}'']\mathbf{r}')} \mathscr{O} | \mathbf{K}'; [\boldsymbol{\lambda}'']\mathbf{r}'\rangle, \end{aligned} \tag{143}$$

where we have noted the normalization factors are 1 in this limit. Now expanding the matric basis element $e^{[\lambda]}_{(\rho[\boldsymbol{\lambda}]\mathbf{r})(\rho'[\boldsymbol{\lambda}'']\mathbf{r}')}$ and employing (142) and (62),

$$\begin{aligned} &\lim_{\text{ZDO}} \langle \mathbf{K}; (\rho[\boldsymbol{\lambda}]), [\lambda](\sigma[\boldsymbol{\lambda}']\mathbf{s}) | \mathscr{O} | \mathbf{K}'; (\rho'[\boldsymbol{\lambda}''])[\lambda'](\sigma'[\boldsymbol{\lambda}''']\mathbf{s}')\rangle \\ &\qquad = \delta_{[\boldsymbol{\lambda}][\boldsymbol{\lambda}'']}\, \delta_{\rho\rho'}\, \delta_{[\lambda][\lambda']}\, \delta_{\sigma\sigma'}\, \delta_{[\boldsymbol{\lambda}'][\boldsymbol{\lambda}''']}\, \delta_{\mathbf{ss}'} \lim_{\text{ZDO}} \langle \mathbf{K}; [\boldsymbol{\lambda}]\mathbf{r} | \mathscr{O} | \mathbf{K}'; [\boldsymbol{\lambda}]\mathbf{r}\rangle. \end{aligned} \tag{144}$$

It is seen that if the Hamiltonian is a local operator (as is the usual case), kets of different local permutational symmetries, $[\boldsymbol{\lambda}] \neq [\boldsymbol{\lambda}'']$ will not mix in the ZDO limit; in this case $[\boldsymbol{\lambda}]\mathbf{r}$ is an exact quantum number.

Approximate local permutational symmetries arise when the subsystems have small but nonzero differential overlap. In general, the differential overlap between subsystems decreases exponentially as their separation increases (see, for example, Herring, 1962), so that local permutational quantum numbers increase exponentially in accuracy with increasing separation. This behavior is in contrast to that for local point group symmetry for which the accuracy of the local point group quantum numbers increases, with increasing separation, no faster than the inverse cube of the separation between subsystems, due to the so-called Van der Waals interaction.

A ket of a desired local permutational symmetry $[\boldsymbol{\lambda}]$ may be obtained by applying an operator $\kappa_{[\boldsymbol{\lambda}]}^{[\lambda]} \in A^{[\lambda]}(\mathscr{S}_N)$ which is sequence adapted (on the right) to $\boldsymbol{\Gamma}^{[\boldsymbol{\lambda}]}$ of $\mathscr{S}$ to a primitive ket. One choice for $\kappa_{[\boldsymbol{\lambda}]}^{[\lambda]}$ is the sequence adapted matric basis element $e_{(\sigma[\boldsymbol{\lambda}']\mathbf{s})(\rho[\boldsymbol{\lambda}]\mathbf{r})}^{[\lambda]}$. A more general choice is

$$\kappa_{[\boldsymbol{\lambda}]}^{[\lambda]} = \sum_{\rho r} \sum_{\sigma[\boldsymbol{\lambda}']\mathbf{s}} [\kappa]_{(\sigma[\boldsymbol{\lambda}']\mathbf{s})(\rho[\boldsymbol{\lambda}]\boldsymbol{r})}^{[\lambda]} \, e_{(\sigma[\boldsymbol{\lambda}']\mathbf{s})(\sigma[\boldsymbol{\lambda}]\boldsymbol{r})}^{[\lambda]} . \tag{145}$$

One type of operator of this form may be easily constructed from an appropriate Young tableau $T_\kappa^{[\lambda]}$. If each $[\lambda_J]$ is Pauli-allowed

$$[\lambda_J] = [2^{p_J}, 1^{N_J - 2p_J}], \qquad J = A, B, C, \ldots, \tag{146}$$

then an appropriate $T_\kappa^{[\lambda]}$ is such that only $2p_A$ of the N_A indices associated with A are paired among themselves in $T_\kappa^{[\lambda]}$; only $2p_B$ of the N_B indices associated with B are paired among themselves; .... We say that there are $p_A + p_B + \cdots$ pairs in the separated subsystem limit, and if the total permutational symmetry is

$$[\lambda] = [2^p, 1^{N-2p}], \tag{147}$$

we relate local permutational symmetry to chemical structure by defining

$$M = p - p_A - p_B - p_C - \cdots, \tag{148}$$

as the number of chemical *bonds*. One might further identify bonds between particular subsystems from the structure of $T_\kappa^{[\lambda]}$. The *generalized structure projector*

$$\kappa_{[\boldsymbol{\lambda}]}^{[\lambda]} = N_I^{[\lambda]} P_I^{[\lambda]} Q_I^{[\lambda]} \sigma_{I\kappa} = \sigma_{I\kappa} N_\kappa^{[\lambda]} P_\kappa^{[\lambda]} Q_\kappa^{[\lambda]} \tag{149}$$

constructed from $T_\kappa^{[\lambda]}$ is (Klein, 1969a) sequence adapted (on the right) to $\boldsymbol{\Gamma}^{[\boldsymbol{\lambda}]}$ of $\mathscr{S}$. Here $N_\kappa^{[\lambda]}$ is the antisymmetric sum of permutations down columns of $T_\kappa^{[\lambda]}$, $P_\kappa^{[\lambda]}$ is the symmetric sum of permutations along rows of $T_\kappa^{[\lambda]}$, and

$$Q_\kappa^{[\lambda]} = Q_A^{[\lambda_A]} Q_B^{[\lambda_B]} Q_C^{[\lambda_C]} \ldots, \tag{150}$$

where $Q_J^{[\lambda_J]}$ is the antisymmetric sum over the $N_J - 2p_J$ electron indices which are not paired in the Jth subsystem in the separated subsystem limit, $J = A, B, C, \ldots$. Alternately one might define a generalized structure projector

$$\kappa_{[\lambda]}^{[\lambda]} = P_I^{[\lambda]} N_I^{[\lambda]} R_I^{[\lambda]} \sigma_{I\kappa} = \sigma_{I\kappa} P_\kappa^{[\lambda]} N_\kappa^{[\lambda]} R_\kappa^{[\lambda]}, \tag{151}$$

where

$$R_\kappa^{[\lambda]} = R_A^{[\lambda_A]} R_B^{[\lambda_B]} \cdots \tag{152}$$

and $R_J^{[\lambda_J]}$ is the symmetric sum along the p_J rows of $T_\kappa^{[\lambda]}$ for the $2p_J$ electron indices of the Jth subsystem which are paired among themselves. Any of the choices (145), (149), or (151) for $\kappa_{[\lambda]}^{[\lambda]}$ are such that

$$\kappa_{[\lambda]}^{[\lambda]} e^{[\lambda]} = \kappa_{[\lambda]}^{[\lambda]} \tag{153}$$

and thus may be used to project out kets of local permutational symmetry $[\lambda]$.

In the case (Klein, 1969a) that each subsystem $J = A, B, \ldots$ either involves no bonds (i.e., all the electrons in J not paired in the separated subsystem limit are not paired in $T_\kappa^{[\lambda]}$) or involves only one bond and is a doublet, $[\lambda_J] = [2^{p_J}, 1]$, the generalized structure projector (149) reduces to the ordinary structure projector

$$\kappa^{[\lambda]} = N_I^{[\lambda]} P_I^{[\lambda]} \sigma_{I\kappa}. \tag{154}$$

The ordinary spin-free structure projector is (see Matsen, 1964, Matsen *et al.*, 1966; or Matsen and Cantu, 1969) in one-to-one correspondence with the Slater bond-function projector in the spin formulation. It thus follows that the ordinary structure projector and Slater bond-function projector are sequence adapted to $\Gamma^{[\lambda]}(\mathscr{S})$ in this particular case. Their Their correspondence with chemical structure is due to the approximate local permutational symmetry.

One particular local permutational symmetry that the ordinary structure projector (154) always has is

$$[\lambda] = [2] \otimes [2] \otimes \cdots \otimes [2] = [2]^p, \tag{155}$$

where $\mathscr{S}$ is chosen to be the group which permutes along the rows of $T_\kappa^{[\lambda]}$. Such a structure projector is then expected to be useful in quantum mechanical calculations if the local permutational symmetry (155) is a good approximate quantum number. Pauling's (see Pauling, 1933; or Matsen, 1964) correspondence between chemical structure and the $\kappa^{[\lambda]}$ was obtained through a study of the signs of exchange integrals which arise in an orthogonal orbital treatment. In the present treatment, the correspondence between chemical structure and the $\kappa^{[\lambda]}$ could be obtained if the Wigner–Eckart theorem (144) held approximately for $[\boldsymbol{\lambda}]$ as in (155). The assignment of approximate local permutational symmetries is very important in quantum mechanical calculations involving large numbers of electrons, since the total number of local permutational symmetries $[\boldsymbol{\lambda}]$ which may yield a given total permutational symmetry $[\lambda]$ increase precipitously with the total number of electrons.

Sequence adapted operators are expected to be of use in theories of molecular or atomic structure where local permutational symmetries may arise. Treatments of atoms or molecules involving localized electron pairs (see Miller and Rudenberg, 1968, and references therein), atoms in molecules approximations (see Hurley, 1963, or Ellison, 1963), localized group functions (see McWeeny, 1960), etc. should involve local permutational symmetries; the techniques developed here should be applicable in these treatments.

XIV. Local Permutational Symmetry in Perturbation Theories for "Exchange" Energies

A formal perturbation approach is one way in which a collection of approximately localized subsystems may be treated. If the localized subsystems are only weakly interacting, it is hoped that application of low orders of the perturbation treatment yield a reliable result. In such a case the zero-order Hamiltonian H^0 may be composed of a sum of subsystem Hamiltonians for each individual localized subsystem. If spin interactions are neglected we have

$$[H^0, \mathbf{G}] = 0, \qquad \mathbf{G} \in \boldsymbol{\mathscr{S}}. \tag{156}$$

The total perturbed Hamiltonian

$$H = H^0 + V \tag{157}$$

commutes with the N-particle symmetric group $\mathscr{S}_N$,

$$[H, G] = 0, \qquad G \in \mathscr{S}_N. \tag{158}$$

If we neglect point group symmetry considerations for the time being, we see that we are dealing with a case of ascent in symmetry, which offers some complication in conventional perturbation treatments (see Löwdin, 1969). Recently there have been a number of perturbation formalisms developed to calculate "exchange" energies starting from a zero-order Hamiltonian commuting only with $\mathscr{S}$ (see Eisenschitz and London, 1930; Murrell *et al.*, 1965; Salem, 1965; Hirschfelder and Silbey, 1966; Murrell and Shaw, 1967; Hirschfelder, 1967; Micha, 1968; Musher and Amos, 1968; Amos and Musher, 1969; and others). In some of these previous treatments the local permutational symmetry is essentially ignored by choosing $\mathscr{S} = \{\mathscr{I}\}$. One may expect that for more general choices of $\mathscr{S}$, local permutational symmetry will play a critical role simplifying the computational aspects and that the techniques of the preceding sections should be applicable. Here we present a generalization of the Hirschfelder–Silbey theory which employs the tools developed in previous sections.

We consider the different states arising from the same separated subsystem limit. The zero-order ket $|(0)[\boldsymbol{\lambda}]\mathbf{r}\rangle$ is a product of kets for each of the subsystems and formally we have

$$H^0\,|(0)[\boldsymbol{\lambda}]\mathbf{r}\rangle = E^0([\boldsymbol{\lambda}])\,|(0)[\boldsymbol{\lambda}]\mathbf{r}\rangle. \tag{159}$$

From $|(0)[\boldsymbol{\lambda}]\mathbf{r}\rangle$ we may project kets of different total permutational symmetries,

$$|(0)\rho[\boldsymbol{\lambda}];\,[\lambda](\sigma[\boldsymbol{\lambda}']\mathbf{s})\rangle = e^{[\lambda]}_{(\sigma[\boldsymbol{\lambda}']\mathbf{s})(\rho[\boldsymbol{\lambda}]\mathbf{r})}\,|(0)[\boldsymbol{\lambda}]\mathbf{r}\rangle, \tag{160}$$

where we have employed a sequence adapted matric basis element to accomplish this projection. We have

$$|(0)[\boldsymbol{\lambda}]\mathbf{r}\rangle = \sum_{\rho[\lambda]} |(0)\rho[\boldsymbol{\lambda}];\,[\lambda](\rho[\boldsymbol{\lambda}]\mathbf{r})\rangle. \tag{161}$$

Under the gradual increase of the perturbation, the zero-order projected ket $|(0)\rho[\boldsymbol{\lambda}];\,[\lambda](\sigma\boldsymbol{\lambda}']\mathbf{s})\rangle$ will change *smoothly* into the perturbed ket $|\rho[\boldsymbol{\lambda}];\,[\lambda](\sigma[\boldsymbol{\lambda}']\mathbf{s})\rangle$ if the zero-order projected kets are *stablized.* This stabilized basis is the eigenket basis to the Hamiltonian H on the vector space with the basis

$$\{|(0)\rho[\boldsymbol{\lambda}];\,[\lambda](\sigma[\boldsymbol{\lambda}']\mathbf{s})\rangle;\qquad \rho = 1 \quad \text{to} \quad f^{[\boldsymbol{\lambda}][\lambda]}\}. \tag{162}$$

(This corresponds to finding the stabilized zero-order kets in the conventional Rayleigh–Schroedinger perturbation theory of an energy level whose zero-order degeneracy is split up by the perturbation.) The sequence adapted matric basis which projects out the stabilized zero-order projected kets is called the *stabilized* sequence adapted matric basis. We now assume that our sequence adapted matric basis is stabilized, so that the kets (160) are stabilized, and we may proceed without a new notation for the stabilized kets.

We have formally

$$H|\rho[\boldsymbol{\lambda}];[\lambda](\sigma[\boldsymbol{\lambda}']\mathbf{s})\rangle = E(\rho[\boldsymbol{\lambda}];[\lambda])|\rho[\boldsymbol{\lambda}];[\lambda](\sigma[\boldsymbol{\lambda}']\mathbf{s})\rangle, \tag{163}$$

and in analogy to (161), we define

$$|[\boldsymbol{\lambda}]\mathbf{r}\rangle = \sum_{[\lambda]\rho} |\rho[\boldsymbol{\lambda}];[\lambda](\rho[\boldsymbol{\lambda}]\mathbf{r})\rangle. \tag{164}$$

Next, letting C_j be a left coset multiplier of $\mathscr{S}$ in $\mathscr{S}_N$, we see that the kets in the sets

$$\{C_j|[\boldsymbol{\lambda}]\mathbf{r}\rangle; \quad \mathbf{r}=1 \ \text{to} \ f^{[\boldsymbol{\lambda}]}, \ j=1 \ \text{to} \ N!/\mathbf{g}\} \tag{165}$$

and

$$\begin{aligned}\{|\rho[\boldsymbol{\lambda}];[\lambda](\sigma[\boldsymbol{\lambda}']\mathbf{s})\rangle; \quad & \rho=1 \ \text{to} \ f^{[\boldsymbol{\lambda}][\lambda]}, \ \sigma=1 \ \text{to} \ f^{[\boldsymbol{\lambda}'][\lambda]};\\ [\lambda],[\boldsymbol{\lambda}'] \ \text{ranging}; \quad & \mathbf{s}=1 \ \text{to} \ f^{[\boldsymbol{\lambda}]}\}\end{aligned} \tag{166}$$

are equal in number. Further, the sets (165) and (166) are each invariant to $\mathscr{S}_N$ and each generate the representation $\Gamma^{[\boldsymbol{\lambda}]\uparrow}$ of $\mathscr{S}_N$ induced by $\Gamma^{[\boldsymbol{\lambda}]}$ of $\mathscr{S}$. We proceed to find a set of coupled equaiions for the kets of (165) which may replace the Schroedinger equation (163) for the kets of the set (166):

$$\begin{aligned}HC_j|[\boldsymbol{\lambda}]\mathbf{r}\rangle &= \sum_{[\lambda]\rho} E(\rho[\boldsymbol{\lambda}];[\lambda])C_j|\rho[\boldsymbol{\lambda}];[\lambda](\rho[\boldsymbol{\lambda}]\mathbf{r})\rangle\\ &= \sum_{[\lambda]\rho} E(\rho[\boldsymbol{\lambda}];[\lambda])C_j e^{[\lambda]}_{(\rho[\boldsymbol{\lambda}]\mathbf{r})(\rho[\boldsymbol{\lambda}]\mathbf{r})}|[\boldsymbol{\lambda}]\mathbf{r}\rangle.\end{aligned} \tag{167}$$

Now applying C_j to the sequence adapted matric basis element, then using the coset decomposition (63), we obtain

$$\begin{aligned}&C_j e^{[\lambda]}_{(\rho[\boldsymbol{\lambda}]\mathbf{r})(\rho[\boldsymbol{\lambda}]\mathbf{r})}\\ &\quad= \sum_{\sigma[\boldsymbol{\lambda}']\mathbf{s}} [C_j]^{[\lambda]}_{(\sigma[\boldsymbol{\lambda}']\mathbf{s})(\rho[\boldsymbol{\lambda}]\mathbf{r})} e^{[\lambda]}_{(\sigma[\boldsymbol{\lambda}']\mathbf{s})(\rho[\boldsymbol{\lambda}]\mathbf{r})}\\ &\quad= \frac{\mathbf{g}f^{[\lambda]}}{N!\,f^{[\boldsymbol{\lambda}]}} \sum_{\sigma[\boldsymbol{\lambda}']\mathbf{s}} [C_j]^{[\lambda]}_{(\sigma[\boldsymbol{\lambda}']\mathbf{s})(\rho[\boldsymbol{\lambda}]\mathbf{r})} \sum_{l} \sum_{\mathbf{t}=1}^{f^{[\boldsymbol{\lambda}]}} [C_l^{-1}]^{[\lambda]}_{(\rho[\boldsymbol{\lambda}]\mathbf{t})(\sigma[\boldsymbol{\lambda}']\mathbf{s})} C_l e^{[\boldsymbol{\lambda}]}_{\mathbf{tr}}\\ &\quad= \frac{\mathbf{g}f^{[\lambda]}}{N!\,f^{[\boldsymbol{\lambda}]}} \sum_{l} \sum_{\mathbf{t}=1}^{f^{[\boldsymbol{\lambda}]}} [C_l^{-1}C_j]^{[\lambda]}_{(\rho[\boldsymbol{\lambda}]\mathbf{t})(\rho[\boldsymbol{\lambda}]\mathbf{r})} C_l e^{[\boldsymbol{\lambda}]}_{\mathbf{tr}}.\end{aligned} \tag{168}$$

Substituting back in (167) gives

$$HC_j\,|[\boldsymbol{\lambda}]\mathbf{r}\rangle = \sum_{[\lambda]\rho}\sum_{l,\mathbf{t}} E(\rho[\boldsymbol{\lambda}];[\lambda])\,\frac{f^{[\lambda]}\mathbf{g}}{N!\,f^{[\boldsymbol{\lambda}]}}\,[C_l^{-1}C_j]^{[\lambda]}_{(\rho[\boldsymbol{\lambda}]\mathbf{t})(\rho[\boldsymbol{\lambda}]\mathbf{r})}\,C_l\,|[\boldsymbol{\lambda}]\mathbf{t}\rangle, \tag{169}$$

or defining

$$A_{l\mathbf{t},j\mathbf{r}} = \frac{\mathbf{g}}{N!\,f^{[\boldsymbol{\lambda}]}}\sum_{[\lambda]\rho} f^{[\lambda]}E(\rho[\boldsymbol{\lambda}];[\lambda])[C_l^{-1}C_j]^{[\lambda]}_{(\rho[\boldsymbol{\lambda}]\mathbf{t})(\rho[\boldsymbol{\lambda}]\mathbf{r})}, \tag{170}$$

we obtain the desired set of coupled equations

$$HC_j\,|[\boldsymbol{\lambda}]\mathbf{r}\rangle = \sum_{l}\sum_{\mathbf{t}=1}^{f^{[\boldsymbol{\lambda}]}} A_{l\mathbf{t},j\mathbf{r}}\,C_l\,|[\boldsymbol{\lambda}]\mathbf{t}\rangle. \tag{171}$$

We expand $E(\rho[\boldsymbol{\lambda}];[\lambda])$ and $|[\boldsymbol{\lambda}]\mathbf{t}\rangle$ in perturbation series

$$E(\rho[\boldsymbol{\lambda}];[\lambda]) = \sum_{n=0}^{\infty} E^{(n)}(\rho[\boldsymbol{\lambda}];[\lambda]), \tag{172}$$

$$|[\boldsymbol{\lambda}]\mathbf{t}\rangle = \sum_{n=0}^{\infty} |(n)[\boldsymbol{\lambda}]\mathbf{t}\rangle. \tag{173}$$

Similarly,

$$A_{l\mathbf{t},j\mathbf{r}} = \sum_{n=0}^{\infty} A^{(n)}_{l\mathbf{t},j\mathbf{r}}, \tag{174}$$

where

$$A^{(n)}_{l\mathbf{t},j\mathbf{r}} = \frac{\mathbf{g}}{N!\,f^{[\boldsymbol{\lambda}]}}\sum_{[\lambda]\rho} f^{[\lambda]}E^{(n)}(\rho[\boldsymbol{\lambda}];[\lambda])[C_l^{-1}C_j]^{[\lambda]}_{(\rho[\boldsymbol{\lambda}]\mathbf{t})(\rho[\boldsymbol{\lambda}]\mathbf{r})}. \tag{175}$$

We also define the unitarily transformed zero-order Hamiltonian and corresponding perturbation,

$$H_j^{0} = C_j H^0 C_j^{-1}, \tag{176}$$

$$V_j = C_j V C_j^{-1}. \tag{177}$$

Noting that

$$A^{(0)}_{l\mathbf{t},j\mathbf{r}} = \delta_{lj}\,\delta_{\mathbf{tr}}\,E^0([\boldsymbol{\lambda}]), \tag{178}$$

we substitute the perturbation expansions (173) and (174) in (171) to obtain the perturbation equations:

$$0\text{-}order: \quad \{H_j{}^0 - E^0([\boldsymbol{\lambda}])\}C_j\,|(0)[\boldsymbol{\lambda}]\mathbf{r}\rangle = 0, \tag{179}$$

$$\begin{aligned} 1st\text{-}order: \quad & \{H_j{}^0 - E^0([\boldsymbol{\lambda}])\}C_j\,|(1)[\boldsymbol{\lambda}]\mathbf{r}\rangle + V_jC_j|(0)[\boldsymbol{\lambda}]\mathbf{r}\rangle \\ & = \sum_{l,\mathbf{t}} A^{(1)}_{l\mathbf{t},j\mathbf{r}}\, C_l\,|(0)[\boldsymbol{\lambda}]\mathbf{t}\rangle, \end{aligned} \tag{180}$$

$$\begin{aligned} n\text{th-}order: \quad & \{H_j{}^0 - E^0([\boldsymbol{\lambda}])\}C_j\,|(n)[\boldsymbol{\lambda}]\mathbf{r}\rangle + V_jC_j|(n-1)[\boldsymbol{\lambda}]\mathbf{r}\rangle \\ & = \sum_{m=1}^{n} \sum_{l,\mathbf{t}} A^{(m)}_{l\mathbf{t},j\mathbf{r}}\, C_l\,|(n-m)[\boldsymbol{\lambda}]\mathbf{t}\rangle \end{aligned} \tag{181}$$

Given the $A^{(m)}_{l\mathbf{t},j\mathbf{r}}$, $m = 0, 1, 2, \ldots, n$, one may in principle then determine the nth-order kets $C_j\,|(n)[\boldsymbol{\lambda}]\mathbf{r}\rangle$ from the Eqs. (181).

We next consider the determination of the nth-order perturbation energies $E^{(n)}(\rho[\boldsymbol{\lambda}]; [\lambda])$, and thus the $A^{(n)}_{l\mathbf{t},j\mathbf{r}}$, given the $(n-1)$th order and lower-order perturbation kets. From the Schrődinger equation (163), we have

$$\{H^0 - E^0([\boldsymbol{\lambda}]) + V - (E(\rho[\boldsymbol{\lambda}]; [\lambda]) - E^0([\boldsymbol{\lambda}]))\}\,|\rho[\boldsymbol{\lambda}]; [\lambda](\rho[\boldsymbol{\lambda}]\mathbf{r})\rangle = 0. \tag{182}$$

Taking the bracket with the zero-order ket $|(0)[\boldsymbol{\lambda}]\mathbf{r}\rangle$, we obtain

$$\begin{aligned} & \{E(\rho[\boldsymbol{\lambda}]; [\lambda]) - E^0([\boldsymbol{\lambda}])\}\langle(0)[\boldsymbol{\lambda}]\mathbf{r}|\, e^{[\lambda]}_{(\rho[\boldsymbol{\lambda}]\mathbf{r})(\rho[\boldsymbol{\lambda}]\mathbf{r})}\,|[\boldsymbol{\lambda}]\mathbf{r}\rangle \\ & \quad = \langle(0)[\boldsymbol{\lambda}]\mathbf{r}|\, V e^{[\lambda]}_{(\rho[\boldsymbol{\lambda}]\mathbf{r})(\rho[\boldsymbol{\lambda}]\mathbf{r})}\,|[\boldsymbol{\lambda}]\mathbf{r}\rangle. \end{aligned} \tag{183}$$

Substituting in the perturbation expansions (172) and (173) and collecting together terms of a given total order, we obtain

$$1st\text{-}order: \quad E^{(1)}(\rho[\boldsymbol{\lambda}]; [\lambda])\mathscr{I}^{(0)}_{[\lambda]\rho} = V^{(0)}_{[\lambda]\rho}, \tag{184}$$

$$2nd\text{-}order: \quad E^{(2)}(\rho[\boldsymbol{\lambda}]; [\lambda])\mathscr{I}^{(0)}_{[\lambda]\rho} + E^{(1)}(\rho[\boldsymbol{\lambda}]; [\lambda])\mathscr{I}^{(1)}_{[\lambda]\rho} = V^{(1)}_{[\lambda]\rho}, \tag{185}$$

$$nth\text{-}order: \quad \sum_{m=1}^{n} E^{(m)}(\rho[\boldsymbol{\lambda}]; [\lambda])\mathscr{I}^{(n-m)}_{[\lambda]\rho} = V^{(n-1)}_{[\lambda]\rho}, \tag{186}$$

where we have defined

$$\mathscr{I}^{(m)}_{[\lambda]\rho} = \langle(0)[\boldsymbol{\lambda}]\mathbf{r}|\, e^{[\lambda]}_{(\rho[\boldsymbol{\lambda}]\mathbf{r})(\rho[\boldsymbol{\lambda}]\mathbf{r})}\,|(m)[\boldsymbol{\lambda}]\mathbf{r}\rangle, \tag{187}$$

$$V^{(m)}_{[\lambda]\rho} = \langle(0)[\boldsymbol{\lambda}]\mathbf{r}|\, V e^{[\lambda]}_{(\rho[\boldsymbol{\lambda}]\mathbf{r})(\rho[\boldsymbol{\lambda}]\mathbf{r})}\,|(m)[\boldsymbol{\lambda}]\mathbf{r}\rangle. \tag{188}$$

The equations (184)–(186) are the desired equations giving $E^{(n)}(\rho[\boldsymbol{\lambda}];[\lambda)])$ in terms of the lower-order perturbed kets.

The sets of equations (179)–(181) and (184)–(186) then constitute a general perturbation formalism in which local permutational symmetry plays a major role. The derivation for this generalization of the Hirschfelder–Silbey theory follows their development closely (Hirschfelder and Silbey, 1966; and Hirschfelder, 1967), their development being obtained on taking $\mathscr{S} = \{\mathscr{I}\}$ and discarding the symbols $[\boldsymbol{\lambda}]$ and $\mathbf{r}$. The present formulation is advantageous over that of Hirschfelder and Silbey in the case that $\mathscr{S} \neq \{\mathscr{I}\}$. For example, the number of energy equations (184)–(186) for an N-electron case is smaller in the present treatment. Such a simplification does not apply in the calculations on H_2 which have been carried out (Certain *et al.*, 1968; and Hirschfelder and Certain, 1968). Of all the perturbation techniques studied in these two articles "the Hirschfelder–Silbey procedure gives the most uniformly good results."

We can also develop a more general perturbation formalism which not only applies to the case of ascent in symmetry, but also applies to cases of mixed ascent and descent in symmetry (Case C of Section II). In this more general case, the group $\mathscr{G}^0$ commuting with the zero-order Hamiltonian H^0 is not necessarily related in any special way to the group $\mathscr{G}$ commuting with the perturbed Hamiltonian. However, defining $\mathscr{G}^\wedge$ as the intersection of $\mathscr{G}^0$ and $\mathscr{G}$,

$$\mathscr{G}^\wedge = \mathscr{G}^0 \wedge \mathscr{G}, \tag{189}$$

we note that the zero-order kets may be sequence adapted to $\mathscr{G}^0$, $\mathscr{G}^\wedge$

$$H^0\,|(0)\alpha^0(\rho^0\alpha^\wedge r^\wedge)\rangle = E^0(\alpha^0)\,|(0)\alpha^0(\rho^0\alpha^\wedge r^\wedge)\rangle. \tag{190}$$

The zero-order projected kets are obtained by application of a sequence adapted matric basis element $e^{\alpha}_{(\sigma\beta^\vee s^\vee)(\rho\alpha^\vee r^\vee)}$ of $\mathscr{G}$ to the zero-order kets of (190),

$$|(0)\rho^0\alpha^\wedge\rho;\alpha(\sigma\beta^\wedge s^\wedge)\rangle = e^{\alpha}_{(\sigma\beta^\vee s^\vee)(\rho\alpha^\vee r^\vee)}|(0)\alpha^0(\rho^0\alpha^\wedge r^\wedge)\rangle. \tag{191}$$

The stabilized zero-order projected kets are in this case obtained by diagonalizing H on the basis

$$\{|(0)\rho^0\alpha^\wedge\rho;\alpha(\sigma\beta^\wedge s^\wedge)\rangle;\qquad \rho^0 = 1 \quad\text{to}\quad f^{\alpha^0\alpha^\vee},\quad \rho = 1 \text{ to } \quad f^{\alpha\alpha^\vee}\}. \tag{192}$$

Once the stabilized zero-order projected kets are obtained, the development proceeds much as before. Choosing $\mathscr{G}^0 = \mathscr{S} \subseteq \mathscr{S}_N = \mathscr{G}$ yields the formalism first discussed. Choosing $\mathscr{G} \subseteq \mathscr{G}^0$ yields the conventional

Rayleigh–Schroedinger perturbation theory for degenerate zero-order states.

We thus see that the concept of sequence adaptation can play a major role in the Hirschfelder–Silbey perturbation formalism. It should be expected to play a role in other formalisms as well.

XV. Magnetism and Local Permutational Symmetry

A collection of approximately localized paramagnetic subsystems, A, B, ..., each associated with a particular local permutational symmetry, can interact with one another via a spin-free Hamiltonian to yield a number of states of different total permutational symmetry. In conventional treatments, the local permutational symmetries are identified with local spins, and in the conventional terminology, these local spins are said to "interact" with one another, giving rise to a "magnetically ordered" system. In actuality, the interaction between these localized paramagnetic subsystems is not[3] due to interacting spins, but rather it is due to spin-free electrostatic interaction. The splitting of the different total permutational symmetries $[\lambda]$ arising from the same set $[\boldsymbol{\lambda}]$ of local permutational symmetries is due to some slight differential overlap of the different subsystems.

The interaction between such approximately localized paramagnetic subsystems has long (Heisenberg, 1928; Dirac, 1929; Van Vleck, 1934) been described in terms of the effective Heisenberg spin Hamiltonian,

$$H = \mathscr{J}_0 + \sum_{I,J} \mathscr{J}_{IJ} \vec{S}_I \cdot \vec{S}_J, \tag{193}$$

acting on a spin space

$$V^\sigma([\boldsymbol{\lambda}]) = V_A{}^\sigma([\lambda_A]) \otimes V_B{}^\sigma([\lambda_B)] \otimes \cdots \tag{194}$$

associated with the local permutational symmetry $[\boldsymbol{\lambda}]$. Such an effective Hamiltonian describes spin-free interactions in terms of spin operators. The general form (194) may be derived (Herring, 1962, 1966; Matsen and Klein, 1970) starting from a spin-free Hamiltonian. In such a derivation, one uses an antisymmetrized space-spin ket of a given local permutational symmetry $[\boldsymbol{\lambda}]$; a double coset decomposition somewhat analogous to (65) is used; only the identity and transposition double coset multipliers are retained; the Dirac identity is used to convert the transposition double

---

[3] There may be a small contribution to the interaction due to the small spin interaction terms in the Breit–Pauli Hamiltonian.

coset multipliers on the spin space to spin operators; and the Wigner–Eckart theorem is employed to obtain the desired form for the spin operators.

The sequence adapted matric basis elements can (Matsen and Klein, 1970) play an important role in such derivations, since the primitive ket from which the states of different total permutational symmetry $[\lambda]$ are projected are of a particular local permutational symmetry $[\boldsymbol{\lambda}]$. Sequence adapted irreducible representation matrix elements arise in formulas for the so-called exchange integrals $\mathscr{J}_{IJ}$ of (193) or in formulas for the energy levels of (193). Similarly, local permutational symmetry and the mathematical tools described in the earlier sections may be applied in the derivation of Hamiltonians more general than the effective Heisenberg spin Hamiltonian (194). Such more general Hamiltonians might take into account superexchange interactions, in addition to the exchange interactions, or a limited amount of configuration interaction, or effects due to point group degeneracy.

XVI. Summary and Conclusion

A sequence of symmetry groups corresponding to a sequence of Hamiltonians of increasing accuracy gives a sequence of quantum numbers of increasing accuracy. In particular, we treated the sequence of a zero-order and perturbed Hamiltonian, H^0 and H, with corresponding symmetry groups $\mathscr{G}^0$ and $\mathscr{G}$; longer sequences may be treated by iteration of such two-fold sequences. The employment of H^0 and H and the properties of the corresponding symmetry groups $\mathscr{G}^0$ and $\mathscr{G}$ in computational schemes was discussed. Although in many previous treatments the case of descent in symmetry, $\mathscr{G} \subseteq \mathscr{G}^0$, has been discussed and applied, the present treatment assumes no such relation between $\mathscr{G}^0$ and $\mathscr{G}$. The present discussion then applies to the ascent in symmetry case, $\mathscr{G}^0 \subseteq \mathscr{G}$, and the mixed descent and ascent symmetry case, $\mathscr{G}^0 \nsupseteq \mathscr{G}$ and $\mathscr{G} \nsupseteq \mathscr{G}^0$, as well as to the descent in symmetry case, $\mathscr{G} \subseteq \mathscr{G}^0$. General group theoretical techniques applicable in such general cases were discussed. Finally, the application of these group theoretical techniques in particular problems in quantum chemistry was described.

To symmetry adapt a ket to both a group and a subgroup, the sequence adapted matric basis elements of the group algebra were introduced. The existence and properties of these sequence adapted matric basis elements were established through a constructive generalization of Wedderburn's proof. Explicit formulas for the sequence adapted matric basis element of a canonical group were given, (68) and (72); related formulas for the corresponding sequence adapted irreducible representation matrix elements were given, (71) and (73). Other methods (Sections VIII and IX) of obtaining the sequence adapted irreducible representations were discussed. Finally, the application to symmetric group sequences was outlined (Section X) and illustrated (Section XII).

The application of the symmetric group sequences was discussed in Sections XIII–XV. Local permutational symmetry was found to be an approximate quantum number near the limit of zero differential overlap between subsystems. Approximately localized subsystems such as occur in theories of chemical structure involving atomic shells, atoms-in-molecules, diatomics-in-polyatomics, group functions, pair correlated wave functions, etc., may use the group theoretical technique described here for symmetric group sequences. A generalization of the Hirschfelder-Silbey perturbation theory was presented. The use of similar concepts in the derivation of effective Heisenberg spin Hamiltonians was indicated. In addition to these quantum mechanical applications described here, the mathematical techniques may be employed in spin-free density matrix treatments, the spin-free evaluation of Pauling numbers, the development of spin-free geminal theory, a general aggregate theory of electronic systems, etc. These techniques should thus find use in future developments in quantum chemistry.

REFERENCES

ALTMANN, S. L. (1963). *Phil. Trans. Roy. Soc.* **A255**, 216.

ALTMANN, S. L. (1967). *Phil. Trans. Roy. Soc.* **A298**, 184.

AMOS, A. T., and MUSHER, J. I. (1967). *Chem. Phys. Letters* **1**, 149.

AMOS, A. T., and MUSHER, J. I. (1969). *Chem. Phys. Letters* (submitted).

BOUCKAERT, L. P., SMOLUCHOWSKI, R., and WIGNER, E. P. (1936). *Phys. Rev.* **50**, 58.

CERTAIN, P. R., HIRSCHFELDER, J.O., KOLOS, W., and WOLNIEWICZ, L. (1968) *J. Chem. Phys.* **49**, 24.

COLEMAN, A. J. (1963). *Rev. Mod. Phys.* **35**, 645.

COLEMAN, A. J. (1966). Induced Representations With Applications to S_n and GL(n). Queen's Univ., Kingston, Ontario.

COLEMAN, A. J. (1968a). "Advances in Quantum Chemistry," P. O. Lōwdin, ed.), Vol. 4, p. 83. Academic Press, New York.

COLEMAN, A. J. (1968b). "Group Theory and Its Applications" (E. M. Loebl, ed.), p. 57. Academic Press, New York.

CORSON, E. M. (1948). *Phys. Rev.* **73**, 57.

DIRAC, P. A. M. (1929). *Proc. Roy. Soc.* **A123**, 714.

EISENSCHITZ, R., and LONDON, F. (1930). *Z. Physik* **60**, 491.

ELLIOT, J. P., HOPE, J., and JAHN, H. A. (1953). *Phil. Trans. Roy. Soc.* **A246**, 241.

ELLISON, F. O. (1963). *J. Am. Chem. Soc.* **85**, 3540.

Flodmark, S. (1962). *Phys. Rev.* **132**, 1343.

Harris, F. E. (1967). "Advances in Quantum Chemistry" (P.-O. Löwdin, ed.), Vol. **3** p. 61. Academic Press, New York.

Heisenberg, W. (1928). *Z. Physik* **39**, 619.

Heisenberg, W. (1927). *Z. Physik* **41**, 239.

Herring, C. (1962). *Rev. Mod. Phys.* **34**, 631.

Herring, C. (1966). *In* "Magnetism" Vol. 2B (G. T. Rado and H. Suhl, eds.), Chap. 1. Academic Press, New York.

Hirschfelder, J. O. (1967). *J. Chem. Phys. Letters* **1**, 325, 363.

Hirschfelder, J. O., and Certain, P. R., (1968) *Intern. J. Quantum Chem.* **25**, 125.

Hirschfelder, J. O., and Silbey, R. (1966). *J. Chem. Phys.* **45**, 2188.

Hurley, A. C. (1963). *Rev. Mod. Phys.* **40**, 448.

Jahn, H. A. (1954). *Phys. Rev.* **96**, 989.

Janusz, G. J. (1966). *Proc. Am. Math. Soc.* **17**, 520.

Kaplan, I. G. (1961). *Zh. E. T. E.* **41**, 560, 790.

Kaplan, I. G. (1965). *T. E. Kh.* **1**, 608, 619.

Klein, D. J. (1969a). *J. Chem. Phys.* **50**, 5140.

Klein, D. J. (1969b). *J. Chem. Phys.* **50**, 5151.

Kotani, M. (1961). "Handbuch der Physik," (S. Flugge, ed.), Vol. 37, Part II. Springer-Verlag, Berlin.

Longuet-Higgins, H. L. (1963). *Mol. Phys.* **6**, 445.

Löwdin, P.-O. (1967). *Rev. Mod. Phys.* **39**, 259.

Löwdin, P.-O. (1969). Univ. of Florida Quantum Theory Project Preprint No. 131.

McIntosh, H. V. (1960). *J. Mol. Spectry.* **5**, 269.

McWeeny, R. (1960). *Rev. Mod. Phys.* **32**, 335.

Mackey, G. W. (1968). "Induced Representations." Benjamin, New York.

Matsen, F. A. (1964). "Advances in Quantum Chemistry," (P.-O. Löwdin, ed.), Vol. 1, p. 59. Academic Press, New York.

Matsen, F. A., and Ellzey, M. L. (1967). Finite Associative Algebras. Univ. of Texas Tech. Rept.

Matsen, F. A., and Plummer, O. R. (1968). "Group Theory and Its Applications" (E. M. Loebl, ed.), p. 221. Academic Press, New York.

Matsen, F. A., and Cantu, A. A. (1969). *J. Phys. Chem.* **73**, 2489.

Matsen, F. A., and Klein, D. J. (1969). *J. Phys. Chem.* **73**, 2477.

Matsen, F. A., and Klein, D. J. (1970). *J. Phys. Chem.* (to be submitted).

Matsen, F. A., Cantu, A. A., and Poshusta, R. D. (1966). *J. Phys. Chem.* **70**, 1558.

Micha, D. (1968). *J. Chem. Phys.* **48**, 3639.

Miller, K. J., and Ruedenberg, K. (1968). *J. Chem. Phys.* **48**, 3414.

Murrell, J. N., and Shaw, G. (1967). *J. Chem. Phys.* **46**, 1768.

Murrell, J. N., Randic, M., and Williams, D. R. (1965). *Proc. Roy. Soc.* **A284**, 566.

Musher, J. I., and Amos, A. T. (1968). *Phys. Rev.* **174**, 94.

Pauling, L. (1933). *J. Chem. Phys.* **1**, 280.

Pauncz, R. (1967). "Alternant Molecules Orbital Method." Saunders, Philadelphia, Pennsylvania.

Poshusta, R. D., and Kramling, R. W. (1968). *Phys. Rev.* **167**, 139.

Robinson, G. de B. (1961). "The Symmetric Group." Univ. of Toronto Press, Toronto.

Rutherford, D. E. (1948). "Substitutional Analysis." Edinburgh Univ. Press, Edinburgh, Scotland.

SALEM, L. (1965). *Disc. Faraday Soc.* **40**, 150.
SASAKI, F. (1965). *Phys. Rev.* **138**, B1338.
SEITZ, F. (1936). *Ann. Math.* **37**, 17.
SERRE, J. (1968). *Intern. J. Quantum Chem.* **2S**, 107.
SERBER, R. (1934a). *Phys. Rev.* **45**, 461.
SERBER, R. (1934b). *J. Chem. Phys.* **2**, 697.
VAN VLECK, J. H. (1934). *Phys. Rev.* **45**, 405.
WATANABE, H. (1966). "Operator Methods in Ligand Field Theory." Prentice-Hall, Englewood Cliffs, New Jersey.
WEDDERBURN, J. H. M. (1907). *Proc. London Math. Soc.* **2**, 99.
WIGNER, E. P. (1959). "Group Theory." Academic Press, New York.
WIGNER, E. P. (1965). "Quantum Theory of Angular Momentum" (L. C. Biedenharn and H. Van Dam, eds.), p. 89. Academic Press, New York.
WIGNER, E. P. (1968). "Spectroscopic and Group Theoretical Methods in Physics" (F. Bloch, et al., eds.), p. 131. Wiley (Interscience), New York.
YAMANOUCHI, T. (1936). *Proc. Phys.-Math. Soc. Japan* **18**, 623.
YAMANOUCHI, T. (1938). *Proc. Phys.-Math. Soc. Japan* **20**, 547.

The Method of Optimized Valence Configurations: A Reasonable Application of the Multiconfiguration Self-Consistent-Field Technique to the Quantitative Description of Chemical Bonding*

ARNOLD C. WAHL
and G. DAS
Argonne National Laboratory
Argonne, Illinois

I. Introduction

As the Hartree–Fock wave functions have been achieved for larger and larger molecules over the past decade (see Krauss, 1967; Yoshimine and McLean, 1967; Nesbet, 1967a; Wahl *et al.*, 1967),[1] it has become quite obvious that chemically useful energy curves and surfaces will not be generally obtainable for nontrivial molecules until a satisfactory solution of the correlation problem can be found and developed computationally. Any method which claims to have solved the correlation problem in a relevant way needs, however, to meet several rather stringent and sometimes conflicting requirements.

(1) Yield reliably an accuracy of ~0.1 eV in interaction potentials between atoms and molecules from about 0.5 bohrs inside the equilibrium position to dissociation.

---

* Work performed under the auspices of the U.S. Atomic Energy Commission.

[1] Nesbet (1967a) and Wahl *et al.* (1967) present some discussion of the Hartree–Fock model.

(2) Be computationally and economically feasible for obtaining continuous energy curves and surfaces, namely be capable of characterizing molecular formation and dissociation.
(3) Be extendable to many electron systems.

Many approaches have been taken over the years and most of them fall into six broad categories.

(A) Direct correlation—explicit inclusion of r_{12}.
(B) *Straight* configuration interaction: Brute force inclusion of many arbitrary configurations permitted by the basis set.
(C) *Pensive* configuration interaction with selection and optimization to achieve most effective configurations.
(D) Perturbation theory.
(E) Pair theory.
(F) Nonvariational methods.

In order to put the method of Optimized Valence Configurations,[2] which is one application of approach (C), in perspective, we have made an attempt to assess progress made by a variety of methods[3] as displayed in Table I. This assessment is based on the following criterion: the largest *molecular* system reported for which an energy lower than the Hartree–Fock one has been obtained. For such systems the percentage of bonding energy and the percentage of correlation energy achieved are tabulated.

In perusing this table, it is apparent that essentially all methods are capable of meeting requirements (1) and (2). It is mainly in regard to requirement (3) that difficulties are encountered.

The method of Optimized Valence Configurations[3] has avoided some of these difficulties in extension by concentrating only upon the changes in

---

[2] The following articles on the OVC method have appeared since 1966: Bertoncini *et al.* (1970), Das (1967), Das and Wahl (1966, 1967, 1970), Sutton *et al.* (1970), Wahl *et al.* (1967), Zemke *et al.* (1969).

[3] Other methods and approaches are discussed by the following: Ahlrichs and Kutzelnigg (1968); Bender and Davidson (1966, 1967, 1969); Brändas (1968); Brown and Shull (1968); Browne and Matsen (1964); Conroy (1964), Ebbing and Henderson (1965); Edmiston and Krauss (1966); Goddard *et al.* (1969, private communication); Grimaldi (1965); Handy and Boys (1969); Harris and Michels (1967); Kolos (1968); Kolos and Wolniewicz (1968); Kutzelnigg (private communication); Matcha and Brown (1968); Pauncz (1967); Rothenberg (1967); Tuan and Sinanoglu (1964). The technique of Handy and Boys is so new that it is somewhat difficult to comment upon until more results are obtained.

TABLE I

SUMMARY OF TYPICAL METHODS USED FOR CORRELATING MOLECULAR WAVE FUNCTIONS[a]

Method	Advantages	Disadvantages	Representative systems[b]
Direct Correlation: (By variational method): Linear combination of elliptic functions with explicit inclusion of r_{12}	Accuracy Completeness	Complexity of function Difficulty of interpretation Limited to 2 electrons	H_2: 100% of correlation energy and 100% of binding energy[c]
Straight Configuration Interaction: Superposition of configurations based on orbitals which have not been optimized	Simplicity Ease o fprograming	Problem of basis functions Complexity of function Difficulty of interpretation Size of matrix to be diagonlized Data management Sophisticated programing	LiH: 83% of correlation energy and 93% of binding energy[d] N_2: 43% of correlation energy[e] F_2: 4% of correlation energy, 30% of binding energy[f]
Geminals constructed from SCF-MO's and iterated to reach NO expansion	Interpretability Possible to develop correlation rules		LiH: 38% of correlation energy[g]
Iterative Natural Orbitals: Alternate CI and NO analysis until wave function and orbitals converge	Final wave function interpretable Possible to develop correlation rules	Sophisticated programing Initial size of matrix to be diagonalized and data management	LiH: 89% of correlation energy and 89% of binding energy[h] HF: 70% of correlation energy[i]
Naturally Correlated Pairs: Introduce geminals from localized MO's with explicit r_{12} dependence into interative NO framework	Compact wave function Possible to interpret and develop correlation rules. Easy selection of configurations	Sophisticated programing required Ambiguous choice of proper correlation factor	LiH: 40% of correlation energy[j] BH NH

TABLE I (continued)

Method	Advantages	Disadvantages	Representative systems^b
Direct Calculation of Natural Orbitals: Solve decoupled equations in the antisymmetrized product of strongly orthogonal geminal approximation	Interpretability Possible to develop correlation rules	Sophisticated programing	LiH: 78% of correlation energy^k BeH_2: 50% of correlation energy and 90% binding energy (estimated not calculated)^l
Spin generated SCF (GI Method)	Interpretability Ease of programing	Difficult to extend to many more electrons	BH: 22% correlation energy and 91% binding energy H_2O. 9% correlation energy and 67% binding energy^t
Pseudo Natural Orbitals: Natural orbitals determined for selected electron pairs, then used in *n* electron problem	Interpretability Possible to develop correlation rules	Sophisticated programing	He_2^+, H_3, H_3^{+m}
MCSCF Optimized Valence Configurations: Best orbitals determined by solving Fock type equations in CI framework Configurations chosen to evaluate only the extra molecular correlation energy	Compact wave function Possible to interpret and develop correlation rules	Sophisticated programing Difficulty of choosing initial configurations Possible convergence difficulties	Li_2: 30% correlation energy, 95% binding energy^n NaLi: 95% binding energy F_2: 8% of correlation energy, 90% of binding energy
Transcorrelated Pairs: Extension of James-Collidge type function to a many electron system (Nonvariational method)	Compact wave function High accuracy attainable	Possible difficulty of interpretations Sophisticated programing Difficulty of choice of correlation function No lower bound	LiH: 90% correlation energy^r

TABLE I (continued)

Method	Advantages	Disadvantages	Representative systems[b]
Alternate Molecular orbitals			H_2: 85% correlation energy, 96% binding energy[o]
Correlation and Shape Function			H_3^+ H_2: 99% correlation energy, 99% binding energy[q]
Perturbation Theory: Fifth order			H_2: 99% correlation energy 99% binding energy[p]
Pair Theory Approach[s]	Great simplification	Not variational	HF[u], CO[u]

[a] The references provided with each method contain further relevant references. Since we have restricted entries in this table to systems for which the computed energy is lower than the Hartree Fock level (if not, correlation energy is, of course, difficult to define), primarily diatomic systems are represented, The only polyatomic. calculations which satisfy this condition are on H_3, BeH_2, and H_2O.

[b] Percentage of binding energy is only given when a potential curve has been computed.

[c] See Kolos (1968) and Kolos and Wolniewicz (1968).

[d] See Browne and Matsen (1964) and Brown and Shull (1968).

[e] See Grimaldi (1965).

[f] See Harris and Michels (1967).

[g] See Ebbing and Henderson (1965).

[h] See Bender and Davidson (1966).

[i] See Bender and Davidson (1967).

[j] See Rothenberg (1967).

[k] See Ahlrichs and Kutzelnigg (1968).

[l] See Kutzelnigg (1969).

[m] See Edmiston and Krauss (1966).

[n] See Wahl *et al.* (1967) and Das and Wahl (1970).

[o] See Pauncz (1967) and Brandas (1968).

[p] See Matcha and Brown (1968).

[q] See Conroy (1964).

[r] See Handy and Boys (1969).

[s] See Taun and Sinanoglu (1964) and Nesbet (1967b).

[t] See Goddard *et al.* (1969; private communication).

[u] Siu and Davidson, preprint (1970), and Bender and Davidson (1969).

the correlation energy taking place as a molecule forms. Thus, for larger systems, that part of the molecular correlation energy which varies insignificantly with internuclear distance is not pursued. In this paper we would like to review the essential features and spirit of the OVC method, tracing its formal and computational development along with a presentation of results obtained by the method.

II The OVC Method

The OVC method attempts to retain the good points of the Hartree-Fock (H–F) orbital picture, namely the conceptual appeal, many good one electron properties, and its dominant position in any expansion of the exact wave function. It recognizes, however, the serious shortcomings of the Hartree–Fock model of most molecules, namely that there is no flexibility built into the wavefunction which can be expected to adequately describe molecular formation and dissociation. The two main sources of this error which distort the calculated H–F potential-energy curve are, of course, the increase in correlation energy as the molecule forms and the constrained form of the molecular orbital picture which forces the improper description of the molecular dissociation.

The OVC method consists of *building* molecules *from Hartree–Fock* atoms or ions *at infinite separation* and only rigorously pursuing the *changes* occurring as the *molecule forms.* These changes, occurring primarily in the valence orbitals, are accounted for by the introduction of Optimized Valence Configurations, which are constructed by promoting a valence electron pair from the Hartree–Fock ground state into allowed excited orbitals. Readjustments in the core and most of the added correlation in the valence orbitals are automatically achieved through the complete multiconfigurational self-consistent-field (MCSCF) optimization[4] process, but added correlation in the core is neglected. In this way, our calculated potential curves can be expected to be approximately parallel to the experimental one. These methods were proposed as a practical means of describing the difference between a molecule and its constituent atoms as a continuous function of the internuclear distances rather than as a procedure to determine the absolute extremum of the energy surface for the total system (i.e., the exact wave function).

---

[4] The approach is discussed in the articles cited in footnote 2. See also Clementi (1967), Clementi and Veillard (1967), Frenkel (1950), Gilbert (1965), Hartree *et al.* (1939), Hinze and Roothaan (1967), Kibartas *et al.* (1955), Kutzelnigg (1964), Löwdin (1955a b; 1959), McWeeny (1955), McWeeny and Steiner (1965), Shull and Löwdin (1959), Slater (1953), Veillard (1966), Watson (1961), Yutsis *et al.* (1954), Yutsis (1952).

We consider the formulation of the method of optimized valence configurations in three steps of increasing complexity, namely, (1) that applicable to only σ-bonded molecules as discussed by Das and Wahl (1966), Das (1967), and Bertoncini *et al.* (1970); (2) that applicable to multiple bonds with excited configurations formed by double excitation from one shell to another as discussed by Das and Wahl (1967), Wahl *et al.* (1967), and Sutton *et al.* (1970); and (3) that applicable to multiple bonds with excitated configurations formed both by the "diagonal" excitations of the above sort and by split-shell excitations, discussed by Das and Wahl (1970), and Zemke *et al.* (1969). Each step will be illustrated with results of computations on representative molecules. (We restrict ourselves to the closed-shell case throughout the discussion, except for reference to ODC calculations on π states of H_2.)

In what follows, we adopt the following notation. The set $\{i\}$ will refer to the shells belonging to both the H–F as well as the excited configurations with $i \leq n$ reserved for the former; ϕ_i will refer to the variational part of the functions belonging to shell i, the corresponding orbitals being

$$\phi_{im_i} = \phi_i \exp(im_i \phi), \tag{1}$$

where m_i can be either $|m_i|$ or $-|m_i|$. Owing to the central role of the Hartree–Fock function, we shall invariably separate it out from other configurations and give it the special symbol Φ_0.

A. A Single σ-Bond

The general form of the Molecular Orbital Hartree–Fock (MOHF) wave function with one σ-bond[5] is of the form

$$\Phi_0 \equiv [\text{core}]\sigma^2.$$

As will be illustrated below by numerical results, consideration of correlation in only the σ-bond is enough to secure a good quantitative description of the bonding where the σ^2 orbital is one quantum number higher than the core. Thus we need consider a wave function as the superposition of configurations of the kind

$$\Psi = A_0 \Phi_0 + \sum_{i > n_{\text{HF}}} A_{i\sigma} \Phi_{i\sigma} \tag{2}$$

where $\Phi_{i\sigma}$ is the configuration obtained by replacing σ in Φ_0 by an excited shell i and

$$A_0{}^2 + \sum_i A_{i\sigma}^2 = 1.$$

---

[5] This scheme is treated in Das (1967), Das and Wahl (1966), and Bertoncini *et al.* (1970).

It is easy to see that the general analytical form of $\Phi_{i\sigma}$ is

$$\Phi_{i\sigma} = \tilde{A}[\phi_i(1{,}2)\Phi_{\text{core}}(3{,}4, \ldots N)], \tag{3}$$

where N is the total number of electrons, $\tilde{A}$ is the antisymmetrizer defined as

$$\tilde{A} = (N!)^{-1/2} \sum_P (-1)^P, \tag{4}$$

Φ_{core} is the closed shell orbital product representing the core electrons,

$$\phi_i(1, 2) = (d_i)^{-1/2} \sum_{m_i} \phi_{im_i}(1)\alpha(1)\phi_{i\bar{m}_i}(2)\beta(2). \tag{5}$$

With respect to Ψ of Eq. (2) as the wave function, the total energy defined as expectation value of the Hamiltonian is given by

$$\begin{aligned} E = & \sum_{i < n_{\text{core}}} n_i\left(h_i + \frac{1}{2} \sum_{d \leq n_{\text{core}}} n_j P_{ij}\right) \\ & + \sum_{i > n_{\text{core}}} 2A_{i\sigma}^2\left(h_i + \sum_{j < n_{\text{core}}} n_j P_{ij}\right) \\ & + \sum_{i,\, j > n_{\text{core}}} (d_i\, d_j)^{1/2} A_{i\sigma} A_{j\sigma} K_{ij}, \end{aligned} \tag{6}$$

where n_{core} is the number of core shells,

$$\begin{aligned} \Phi_{\sigma\sigma} &\equiv \Phi_0, \\ A_{\sigma\sigma} &= A_0, \\ h_i &= \int \phi_{im_i}(1)h(1)\phi_{im_i}(1)\, dV, \end{aligned} \tag{7}$$

with h representing the one-electron bare nuclear field and,

$$\begin{aligned} J_{ij} &= (d_i\, d_j)^{-1} \sum_{m_i,\, m_j} \iint \phi_{im_i}^*(1)\phi_{jm_j}^*(2)r_{12}^{-1}\phi_{im_i}(1)\phi_{im_j}(2), \\ K_{ij} &= (d_i\, d_j)^{-1} \sum_{m_i,\, m_j} \iint \phi_{im_i}(2)\phi_{jm_j}(1)r_{12}^{-1}\phi_{im_i}(1)\phi_{jm_j}(2), \\ P_{ij} &= J_{ij} - \tfrac{1}{2}K_{ij}. \end{aligned} \tag{7a}$$

The minimum in E is achieved if A's satisfy the secular equation

$$\sum_j A_{j\sigma} H_{i\sigma j\sigma} = EA_{i\sigma}, \tag{8}$$

where $H_{i\sigma j\sigma}$ is the matrix element between $\Phi_{i\sigma}$ and $\Phi_{j\sigma}$, $\Phi_{\sigma\sigma}$ being Φ_0, and, concurrently, the orbitals satisfy

$$\begin{aligned} F_{\text{core}}\phi_i &= \varepsilon_i \phi_i + \sum_{j>n_{\text{core}}} \varepsilon_{ij}\phi_j, \qquad i \leq n_{\text{core}}, \\ F_i\phi_i &= \varepsilon_i \phi_i + \sum_{j \neq i} \varepsilon_{ij}\phi_j, \qquad i > n_{\text{core}} \end{aligned} \tag{9}$$

with

$$\varepsilon_{ij} = \varepsilon_{ji}. \tag{10}$$

The operators F_{core} and F_i are given by

$$\begin{aligned} F_{\text{core}} &= h + \sum_{j \leq n_{\text{core}}} n_j P_j + \sum_{j > n_{\text{core}}} 2A_{j\sigma}^2 P_j, \\ F_i &= A_{i\sigma}^2\left(h + \sum_{j \leq n_{\text{core}}} n_j P_j\right) \\ &\quad + \sum_j (d_i\, d_j)^{1/2} A_{i\sigma} A_{j\sigma} K_j, \end{aligned} \tag{11}$$

where the operators P_j, K_j are defined as

$$\begin{aligned} P_j &= \mathrm{J}_j - \tfrac{1}{2}K_j, \\ J_j(1)\phi_i(1) &= \left[\int r_{12}^{-1}\phi_j{}^2(2)\, dT_2\right]\phi_i(1), \\ K_j(1)\phi_i(1) &= \left\{(d_i\, d_j)^{-1} \sum_{n_i,\, m_j} \int r_{12}^{-1}\phi_i(2)\phi_j(2)\right. \\ &\qquad \left. \exp[-i(m_i - m_j)(\phi_1 - \phi_2)]\, dT_2\right\}\phi_j(1). \end{aligned} \tag{12}$$

We present in Table II and Figs 1–5 results of calculations on several molecules based on the above analysis.[6] Looking at the results shown for H_2 and Li_2 from Das and Wahl (1966) and Das (1967), it is clear that information of chemical accuracy can be obtained on systems in which the chemical bond consists of two isolated electrons. Accordingly a predictive

---

[6] In Figs. 1(b), (c), and 2(b), (c) the outermost contour in all cases corresponds to a density of 6.1×10^{-5} e$^-$/bohr^3. Each successive inner contour then increases by a factor of 2.

TABLE II

COMPARISON OF COMPUTED H–F, ODC AND OVC SPECTROSCOPIC CONSTANTS WITH EXPERIMENTS FOR H_2, Li_2, NALI, F_2,[a] NAF

	ω_e (cm^{-1}(	R_e (bohrs)	D_e (eV)
		$H_2\ {}^1\Sigma_g$	
H–F[b]	4561	1.39	3.64
ODC[b]	4214	1.42	4.13
OVC[b]	4398	1.40	4.63
Experimental	4400	1.40	4.75
		$Li_2\ {}^1\Sigma_g$	
H–F[c]	326	5.26	0.17
ODC[b]	344	5.43	0.46
OVC[b]	345	5.09	0.93
OVC[c]	345	5.09	0.99
Experimental	351	5.05	1.05
		NaLi $^1\Sigma_g$	
H–F[b]	264	5.56	0.05
OVC[d]	256	5.48	.85
Experimental	—	—	—
		$F_2\ {}^1\Sigma_g$	
H–F[d]	1257	2.50	−1.37
ODC[b] (ϵ_{ij} not matched)	678	2.74	0.54
ODC[e] (ϵ_{ij} matched)			0.67
OVC ($3\sigma_g$ only)[f]	704	2.72	0.81
OVC (all promotions into $3\sigma_u$)[f]	N.C	2.70	0.95
OVC (split shell)[e]			1.71
OVC (split shell with atomic correction)[e]	1010	2.59	1.57
Experimental	892	2.68	1.68
		NaF $^1\ \Sigma_g$	
H–F[f]	570	3.65	3.08
OVC[f]	570	3.66	3.70
Experimental	536	3.64	4.94

[a] Only diagonal excitations are considered except for F_2.

[b] See Das and Wahl (1966).

[c] See Das (1967).

[d] See Bertoncini *et al.* (1970).

[e] See Das and Wahl (1970).

[f] See Wahl *et al.* (1967).

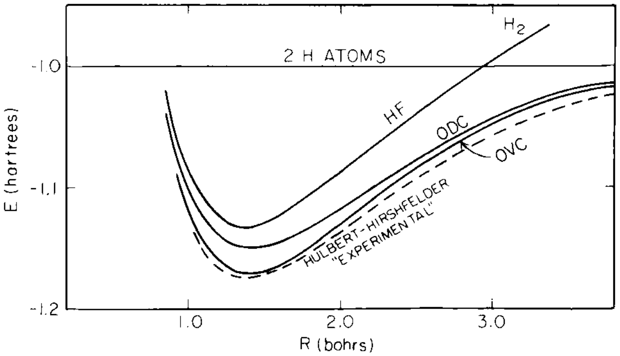

Fig. 1 a. Comparison of Hartree-Fock (HF); optimal double configuration (ODC), and optimal valence configuration, (OVC) potential curves with experimental one for H_2 (Das and Wahl, 1966).

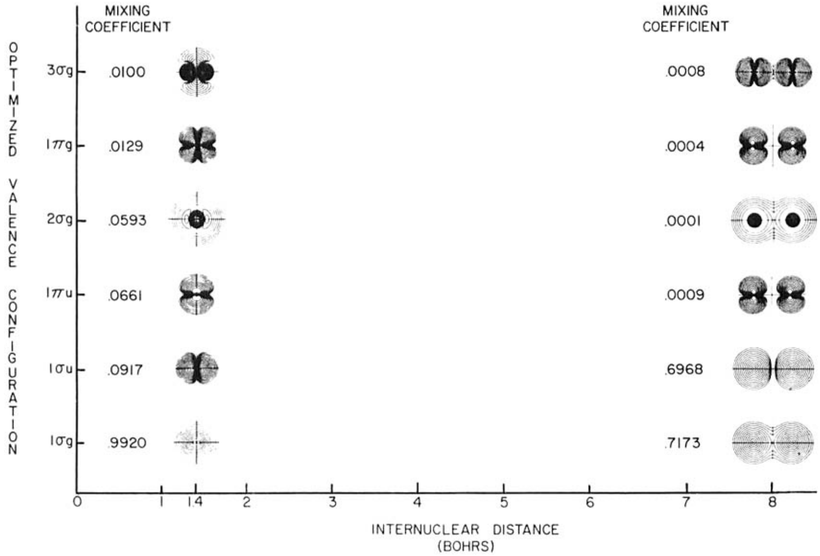

Fig. 1 b. Hydrogen molecule formation contours for EHF wave functions and the orbitals making up the H_2 OVC wave function at R_e and near dissociation. (Orbital density is displayed.) Note that these best configuration orbitals occupy the same space as the Hartree-Fock orbital being correlated. A very strong feature of the MCSCF process (as used in this work) is its ability to properly form and place such correlating orbitals and to orchestrate their changing shape, role, and importance as a molecule forms (see Fig. 2b, also).

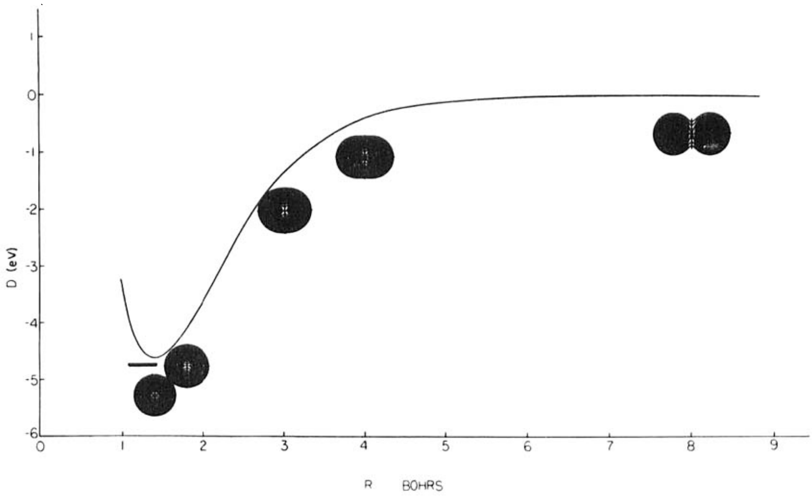

Fig. 1 c. Extended Hartree-Fock H_2 wave functions; total charge-density contours of the H_2 OVC wave function as the molecule forms (Das and Wahl, 1966, 1967). The horizontal line is the level of the H_2 experimental energy.

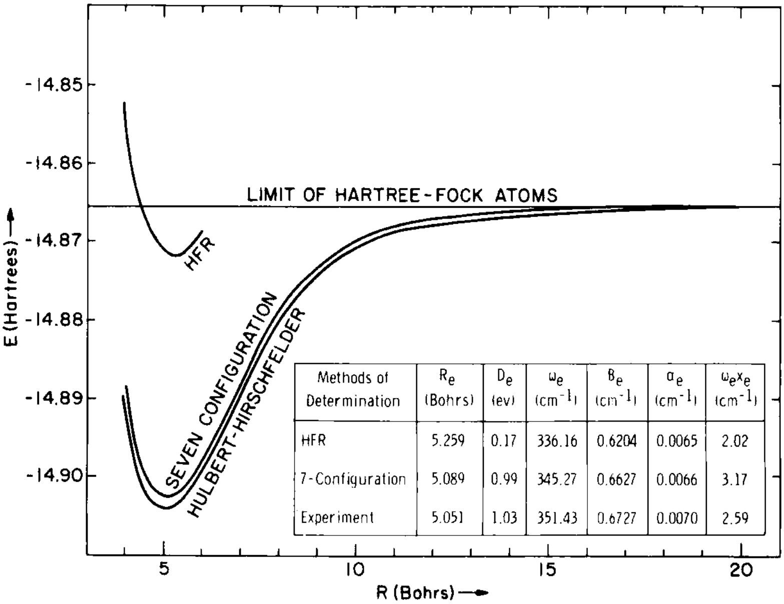

Methods of Determination	R_e (Bohrs)	D_e (ev)	ω_e (cm^{-1})	B_e (cm^{-1})	α_e (cm^{-1})	$\omega_e x_e$ (cm^{-1})
HFR	5.259	0.17	336.16	0.6204	0.0065	2.02
7-Configuration	5.089	0.99	345.27	0.6627	0.0066	3.17
Experiment	5.051	1.03	351.43	0.6727	0.0070	2.59

Fig. 2 a. Comparison of Hartree-Fock and optimal valence configuration potential curves with experimental one for Li_2 (Das and Wahl, 1966), Das (1967).

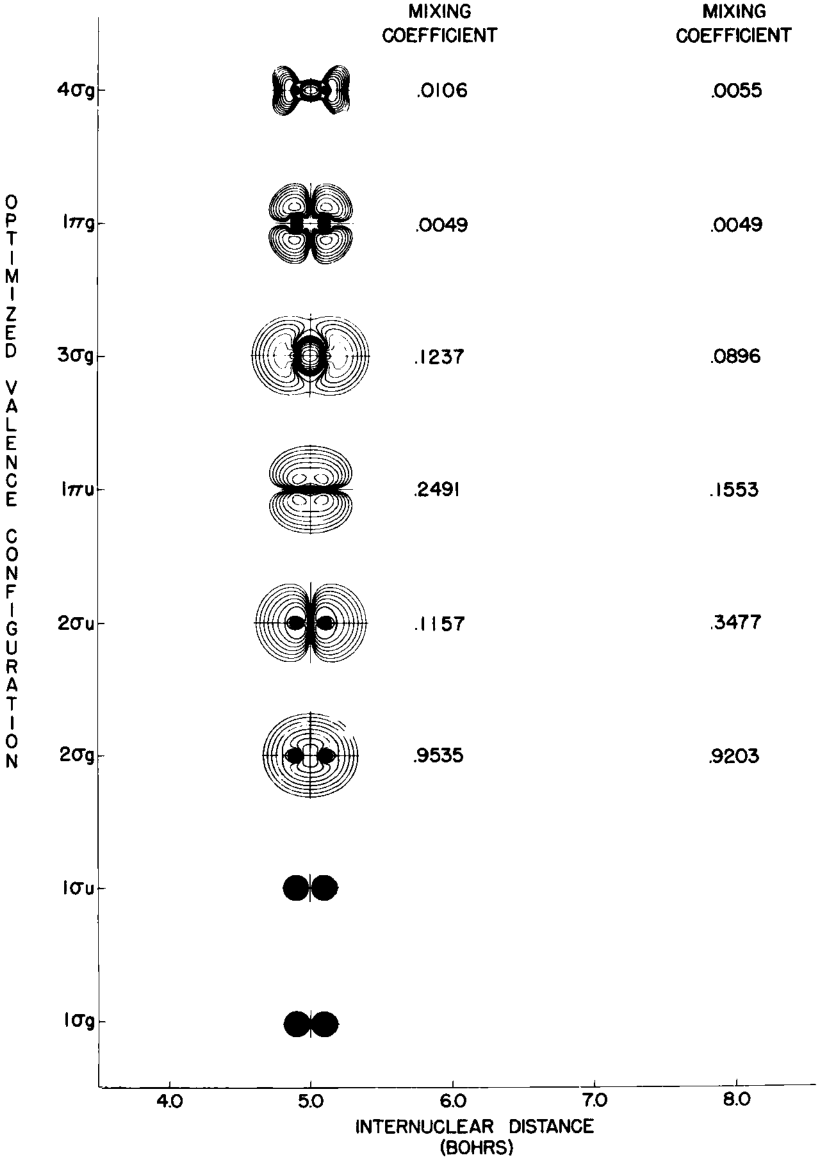

Fig. 2 b . Lithium molecule formation contours for EHF wave functions; the orbitals making up the Li_2 OVC wave function at R_e (Das and Wahl, 1966, 1967).

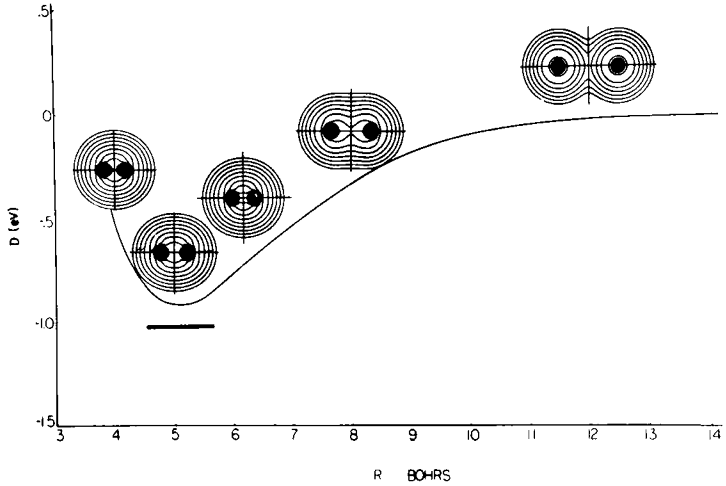

Fig. 2 c . Extended Hartree–Fock Li_2 wave functions; total charge density contours of the Li_2 OVC wave function as the molecule forms. The horizontal line is the level of the Li_2 experimental binding energy (Das and Wahl, 1966, 1967).

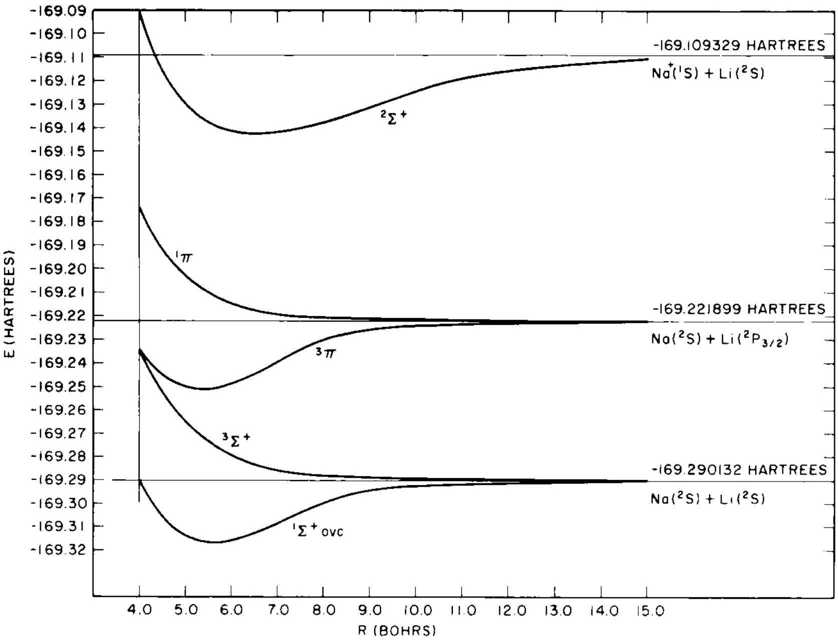

Fig. 3 a . Calculated potential curves for NaLi (Bertoncini *et al.*, 1970).

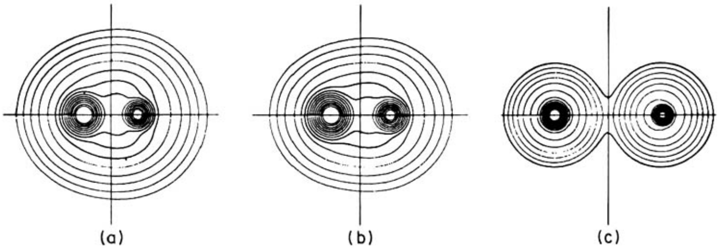

Fig. 3 b . OVC $^1\Sigma$ and Hartree–Fock total charge density contours for the $^1\Sigma^+$ state of NaLi at (a) R = 5.0 bohrs, (b) $R = 5.5$ and (c) $R = 15.0$ bohrs. Picture at 15 bohrs is two-thirds, the scale of other two pictures. Highest contour value = 1 electron/bohr^3; each successive outer contour decreased in value by a factor of 2.

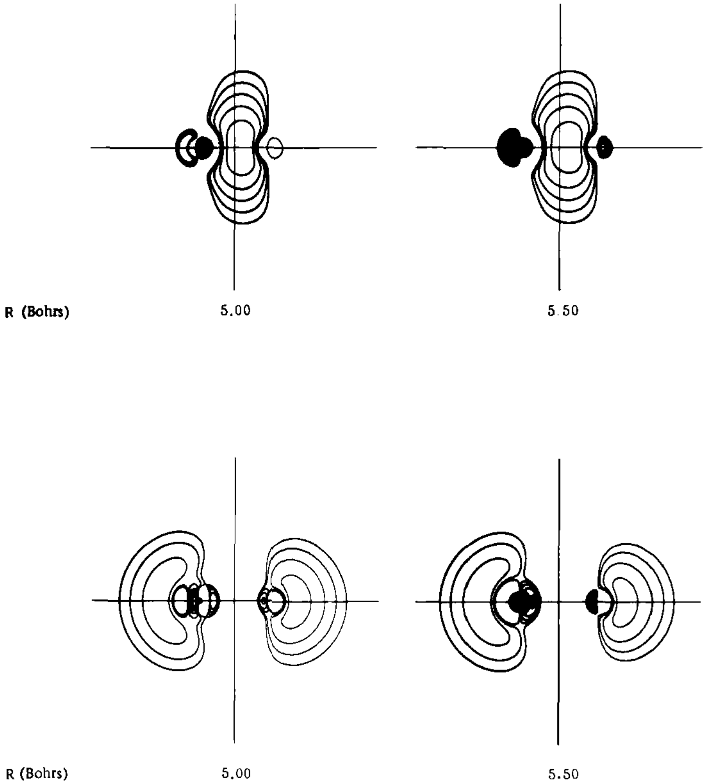

Fig. 3 c . Contours of charge density differences associated with the formation of the chemical bond in the $^1\Sigma$ state of NaLi. Upper diagram shows the region where charge has increased relative to dissociated atoms. Lower diagram shows where charge density has decreased relative to dissociated atoms, for both upper and lower diagrams, largest contour value plotted = 0.1 electron/bohr^3; contour ratio = 0.5. (Bertoncini *et al.*, 1970). Based on OVC wave function which dissociates properly into a Na^{1}S and Li^{1}S atom.

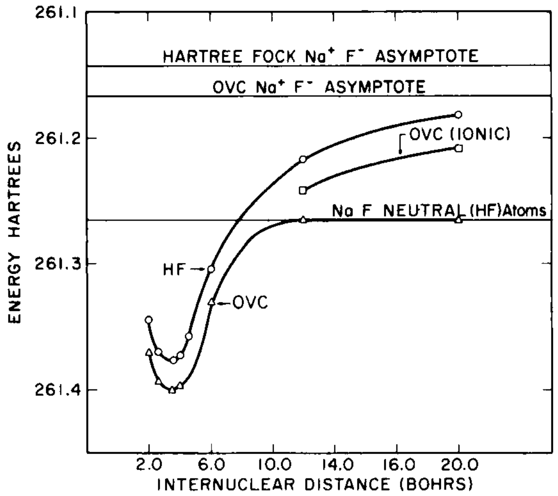

Fig. 4. Comparison of Hartree–Fock and Optimized Valence Configuration potential curves for NaF (Wahl *et al.* 1967). (Diagonal excitations only.)

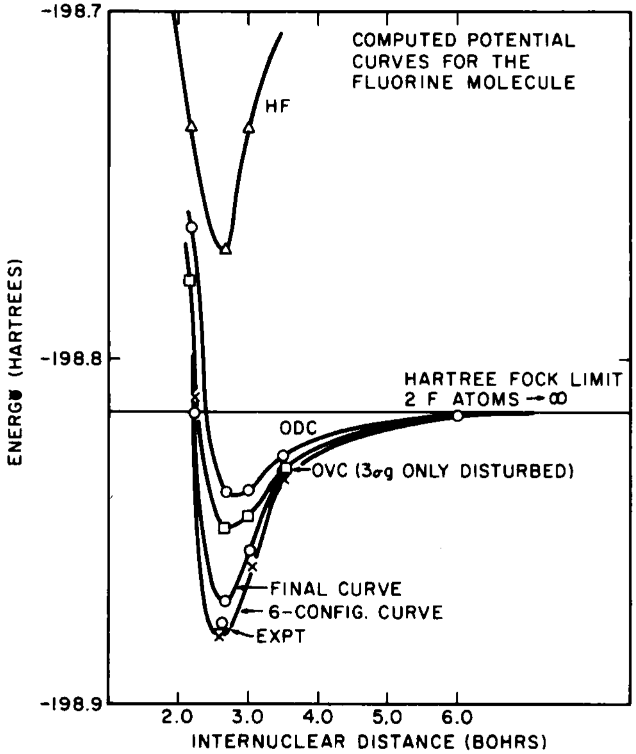

Fig. 5. Comparison of Hartree–Fock ODC and OVC potential curves for F_2 (Das and Wahl, 1966, Wahl *et al.*, 1967). Final and 6 configuration curves include split shell correlation (Das and Wahl, 1970).

calculation was performed by Bertoncini *et al.* (1970) on NaLi, a system not observed experimentally. The results shown in Table III correspond

TABLE III

PREDICTED PROPERTIES[a] OF THE MOLECULE NALI ($^1\Sigma$)

Optimized Valence Configuration Calculations	
Equilibrium internuclear separation, R_e (bohrs)	5.56
Dissociation energy, D_e (eV)	0.847
Vibrational frequency, ω_e (cm^{-1})	249.88
$\omega_e X_e$ (cm^{-1})	0.673
Rotational constant, B_e (cm^{-1})	0.361
α_e	.0036
Dipole moment, μ (debyes)	1.1
Ionization potential, IP (eV)	4.23

[b] The NaLi system, to our knowledge, has not yet been observed experimentally. It is an ideal case for the OVC model and thus a precision of a few percent is attached to R_e, D_e, ω_e, B_e, and IP.

to rigorously converged OVC-wave functions of the above form. The cases of F_2 and NaF, however, obviously indicate that correlation involving orbitals in addition to the single bonding orbital in the molecule is important for a proper description of the chemical bond. As a next step in the method, a model was investigated in which the cross-shell correlation between π and σ is assumed to be negligible with respect to the molecular bonding. Accordingly we consider excited configurations that correspond to double excitations from any of the "molecular" shells that result from the compounding of the atomic-valence shells which are multiply occupied. To a good approximation, it is sufficient to restrict ourselves only to double occupied excited shells rather than include configurations with pairs of singly occupied excited shells. This type of shell-to-shell double excitation will be termed diagonal excitation.

B. Several Bonds: Diagonal Excitations

The configuration-mixed wave function[7] is of the form

$$\begin{aligned}\Psi = A_0\Phi_0 &+ \sum_{\substack{\theta;\, i \leq n_{\mathrm{HF}} \\ u > n_{\mathrm{HF}}}} A_{\theta iu}\Phi_{\theta iu} \\ &+ \sum_{\substack{\theta;\, i,\, j \leq n_{\mathrm{HF}} \theta\, i \neq j, \\ u,\, v > n_{\mathrm{HF},\, u \neq v}}} A_{\theta ijuv}\Phi_{\theta;\, ij;\, uv} + \cdots,\end{aligned} \tag{13}$$

---

[7] Wahl *et al.* (1967) and Das and Wahl (1967) consider the problem of diagonal excitations.

where $\Phi_{\theta;\, ij\ldots;\, uv\ldots}$ refers to configurations with the Hartree–Fock shells $i, j, \ldots$ diagonally excited to $u, v, \ldots$. The index θ refers to the pairing of the open shells thus generated. For the examples to be given below, truncation of the series up to the terms shown was found sufficient and corresponds to permitting only up to quadrupole excitations.

In order to write down the expression for the total energy we notice that the matrix-elements are non zero only between ϕ_0 and $\phi_{\theta;\, i,\, u}$ and $\phi_{\theta;\, i,\, u}$ and $\phi_{\theta;\, ij;\, uv}$. These will be of the forms

(i) Diagonal Matrix-Elements:

$$\langle 0|H|0\rangle = \sum_{k<n_{\mathrm{HF}}} n_{ok} h_k + \frac{1}{2} \sum_{k,\, l<n_{\mathrm{HF}}} n_{ok} n_{ol} P_{kl},$$

$$\begin{aligned}\langle \theta; i; u|H|\theta; i; u\rangle = \sum n_{iu;\, k} h_k &+ \frac{1}{2} \sum_{k,\, l} n_{iu;\, k} n_{iu;\, l} \\ &\times (J_{\theta iu;\, kl} J_{kl} - k^{+}_{\theta iu;\, kl} K^{+}_{kl} - k^{-}_{\theta iu;\, kl} K^{-}_{kl}),\end{aligned}$$

where $n_{0;\, k}$, $n_{iu;\, k}$ are occupation numbers in Φ_0, $\phi_{\theta;\, iu} \ldots$ and $J_{\theta iu;\, kl}$, $k^{+}_{\theta iu;\, kl}$, $k^{-}_{\theta iu;\, kl}$ are the vector coupling coefficients; K^{+}_{kl}, K^{-}_{kl} are defined as

$$K^{+}_{kl} = \int \phi_k(1)\phi_k(2) r_{12}^{-1} \phi_l(1)\phi_l(2) \exp[i(|m_k| - |m_l|)(\phi_1 \phi_2)]\, dT_1\, dT_2,$$

$$K^{-}_{kl} = \int \phi_k(1)\phi_k(2) r_{12}^{-1} \phi_l(1)\phi_k(2) \exp[i(|m_k| + |m_l|)(\phi_1 - \phi_2)]\, dT_1\, dT_2.$$

The diagonal matrix element for the quadruply excited configurations can similarly be written down.

(ii) Off-Diagonal Matrix Elements[8]:

$$\langle 0|H|\Phi_{\theta;\, i,\, u}\rangle = k_\theta{}^{+} K^{+}_{iu} + k_\theta{}^{-} K^{-}_{uv},$$

$$\begin{aligned}\langle \Phi_{\theta';\, i';\, u'}|H|\Phi_{\theta;\, i;\, u}\rangle &= \delta_{uv'}(k^{+}_{\theta\theta'} K^{+}_{ii'} + k^{-}_{\theta\theta'} K^{-}_{\theta\theta'}) \\ &\quad + \delta_{ii'}(l^{+}_{\theta\theta'} k^{+}_{uv'} + l^{-}_{\theta\theta'} K^{-}_{uv'}),\end{aligned}$$

$$\langle \Phi_{\theta';\, ij;\, uv}|H|\Phi_{\theta;\, i;\, u}\rangle = k^{+}_{\theta\theta'} K^{+}_{jv} + k^{-}_{\theta\theta'} K^{-}_{jv},$$

and $k_\theta{}^{\pm}$, $k^{\pm}_{\theta\theta'}$, $l^{\pm}_{\theta\theta}$ are vector coupling constants. We can then proceed to obtain the Fock equations corresponding to the above wave function; however, since this is straightforward and introduces no new element in our discussion, we do not write them explicitly. This formalism was applied to F_2 and to a variety of molecular systems to gain some insight into the nature of molecular correlation and its change with bond polarity; the molecules studied are tabulated in Tables II, IV, and V. The wave functions, which provide a set of properly formed excited orbitals (Figs. 7–12) particularly useful in configuration interaction calculations, are available from the authors on request (see Fig. 5 for F_2 potential curve).

---

[8] For some cases a fourth type of integral is encountered, namely; $J^{(2)}_{kl} = \int \phi_k{}^2(1) r_{12}^{-1} \phi_l^2(2) \exp[i(|m_k| + |M_l|)(\phi_1 - \phi_2)]\, dT_1\, dT_2$.

TABLE IV

FORM OF OVC WAVE FUNCTIONS[a]

	Li_2	Be_2	B_2	C_2	BN	BeO	LiF	HeNe	N_2	CO	BF	F_2
Core orbitals	$1\sigma_g{}^2 1\sigma_u{}^2$	$1\sigma_g{}^2 1\sigma_u{}^2$	$1\sigma_g{}^2 1\sigma_u{}^2$	$1\sigma_g{}^2 1\sigma_u{}^2$	$1\sigma^2 2\sigma^2$	$1\sigma^2 2\sigma^2$	$1\sigma^2 2\sigma^2$	$1\sigma^2 2\sigma^2$	$1\sigma_g 1\sigma_u{}^2$	$1\sigma^2 2\sigma^2$	$1\sigma^2 2\sigma^2$	$1\sigma_g{}^2 1\sigma_u{}^2$
Valence orbitals in Φ_u	$2\sigma_g{}^2$	$2\sigma_g{}^2$	$2\sigma_g{}^2$	$2\sigma_g{}^2$	$3\sigma^2$	$3\sigma^2$	$3\sigma^2$	$3\sigma^2$	$2\sigma_g{}^2$	$3\sigma^2$	$3\sigma^2$	$2\sigma_g{}^2$
		$2\sigma_u{}^2$	$2\sigma_u{}^2$	$2\sigma_u{}^2$	$4\sigma^2$	$4\sigma^2$	$4\sigma^2$	$4\sigma^2$	$2\sigma_u{}^2$	$4\sigma^2$	$4\sigma^2$	$2\sigma_u{}^2$
			$3\sigma_g{}^2$	$1\pi_u{}^4$	$1\pi^4$	$1\pi^4$	$1\pi^4$	$1\pi^4$	$3\sigma_g{}^2$	$5\sigma^2$	$5\sigma^2$	$3\sigma_g{}^2$
									$1\pi_u{}^4$	$1\pi^4$	$1\pi^4$	$1\pi_u{}^4$
												$1\pi_g{}^4$
New orbitals	$2\sigma_u$											
	$3\sigma_g$	$3\sigma_g$		$3\sigma_g$	5σ	5σ	5σ	5σ				
	$3\sigma_u$	$3\sigma_u$	$3\sigma_u$	$3\sigma_u$	6σ	6σ	6σ	6σ	$3\sigma_u$	6σ	6σ	$3\sigma_v$
	$1\pi_u$	$1\pi_u$	$1\pi_u$									
	$1\pi_g$	$1\pi_g$	$1\pi_g$	$1\pi_g$	2π	2π	2π		$1\pi_g$	2π	2π	

[a] Configurations considered were generated by a double excitation from all valence orbitals in Φ_0 to new orbitals for a given system. All wave functions were thus of the form $\Psi = \Phi_0 + \sum_a \sum_i C_{ai}\, \Phi_{ai}$ where a labels only valence orbitals in Φ_0 and i labels only new orbitals. $\pi \rightarrow \pi'$ excitation. Results are only presented for N_2.

TABLE V

Configuration Interaction Energies and Partial

	Li_2	Be_2	$B_2\,{}^1\Sigma_g{}^+$	C_2	BN	BeO
Number of promoted configurations	5	8	9	8	8	8
Homonuclear pair energy contributions						
$2\sigma_g \rightarrow 2\sigma_u$	−0.00441					
$2\sigma_g \rightarrow 3\sigma_g$	−0.00577	−0.00159		−.00179	−.00033	−.00028
$2\sigma_g \rightarrow 3\sigma_u$	−0.00047	−0.00231	−0.00414	−.00359	−.00445	−.00398
$2\sigma_g \rightarrow 1\pi_u$	−0.01734	−0.01746	−0.01814			
$2\sigma_g \rightarrow 1\pi_g$	−0.00048	−0.00038	−0.00017	−.00193	−.00167	−.00174
$\epsilon_{2\sigma_g}$	−0.02847	−0.02174	−0.02244	−.00731	−.00645	−.00600
$2\sigma_u \rightarrow 3\sigma_g$		−0.03450		−.06268	−.02875	−.01142
$2\sigma_u \rightarrow 3\sigma_u$		−0.00003	−0.00018	+.00004	−.00020	−.00070
$2\sigma_u \rightarrow 1\pi_u$		−0.00010	−0.00066			
$2\sigma_u \rightarrow 1\pi_g$		−0.00741	−0.00807	−.00906	−.00469	−.00091
$\epsilon_{2\sigma_u}$		−0.04204	−0.00891	−.07178	−.03364	−.01303
$3\sigma_g \rightarrow 3\sigma_u$			−0.00165			
$3\sigma_g \rightarrow 1\pi_u$			+0.00008			
$3\sigma_g \rightarrow 1\pi_g$			−0.00305			
$\epsilon_{3\sigma_g}$			−0.00462			
$1\pi_u \rightarrow 3\sigma_g$				−.00008	−.00029	−.00011
$1\pi_u \rightarrow 3\sigma_u$				−.00030	−.00048	−.00133
$1\pi_u \rightarrow 1\pi_g(4)^b$						
$1\pi_u \rightarrow 1\pi_g(5)^b$						
$1\pi_u \rightarrow 1\pi_g(6)^b$						
$\epsilon_{1\pi_u}$				−.00038	−.00077	−.00144
$1\pi_g \rightarrow 3\sigma_u$						
$\epsilon_{1\pi_g}$						
E_{OVC}	−14.89962	−29.16821	−49.08893	−75.47378	−78.94764	−89.46712
$E_{HF}{}^c$	−14.87116	−29.10444	−49.05296	−75.39402	−78.90600	−89.44652
$E_{OVC} - E_{HF}$	−0.02847	−0.06378	−0.03597	−.07976	−.04164	−.02060

---

[a] ϵ_i = Partial pair energy for orbital i. The $\pi \rightarrow \pi'$ contributions reported in Table III of Sutton *et al.* (1970) were incorrect. This table is a corrected one in which the $\pi \rightarrow \pi'$ excitations have been omitted from the CI calculations except for the system N_2 for which these contributions have now been included correctly. A complete errata of Table III of Sutton *et al.* (1970) is forthcoming. We are extremely grateful to Professor Fritz Schaeffer for originally pointing out the error in N_2.

PAIR ENERGIES FOR OVC WAVE FUNCTIONS

LiF	HeNe	N_2[a]	CO	BF	F_2	
8	8	8	7	7	5	
						Hetero-nuclear pair energy contributions
−.00043	−.00140					$3\sigma \to 5\sigma$
−.00334	−.00035	−.00443	−.00043	−.00060	−0.00218	$3\sigma \to 6\sigma$
−.00111	−.00002	−.00083	−.00118	−.00100		$3\sigma \to 2\pi$
−.00488	−.00177	−.00526	−.00161	−.00160	−0.00218	$\epsilon_{3\sigma}$
−.01043	−.00575					$4\sigma \to 5\sigma$
−.00092	−.00253	−.00054	−.00815	−.01140	−0.00218	$4\sigma \to 6\sigma$
−.00025	−.00011	−.00744	−.00320	−.00054		$4\sigma \to 2\pi$
−.01160	−.00839	−.00798	−.01135	−.01194	−0.00218	$\epsilon_{4\sigma}$
		−.00297	−.00019	−.00010	−0.06525	$5\sigma \to 6\sigma$
		−.00151	−.00030	−.00026		$5\sigma \to 2\pi$
		−.00448	−.00049	−.00036	−0.06525	$\epsilon_{5\sigma}$
−.00011	−.00008					$1\pi \to 5\sigma$
−.00065	−.00039	−.00029	−.00019	−.00019	−0.00025	$1\pi \to 6\sigma$
		−.01332				$1\pi \to 2\pi(4)^b$
		−.01081				$1\pi \to 2\pi(5)^b$
		−.01761				$1\pi \to 2\pi(6)^b$
−.00076	−.00047	−.04203	−.00019	−.00019	−0.00025	$\epsilon_{1\pi}^{a}$
					−0.00093	
					−0.00093	
−107.00575	−131.39853	−109.08101	−112.79724	−124.17321	−198.83291	
−106.98775	−131.38743	−108.97922	−112.78074	−124.15891	−198.76059	
−.01800	−.01110	−.10179	−.01650	−.01430	−0.07196	

[b] The notations (4), (5), and (6) refer respectively to the $^1\sum$, $^3\sum$, and $^1\Delta$ symmetry of the two electrons which have been removed from a filled π shell and promoted to an empty π' shell.

[c] The energy E_{HF} for these matrix SCF calculations is estimated to be within ~0.01 a.u. of the Hartree–Fock limit.

In Table V we present an energy analysis of OVC wave functions for a variety of molecules (Sutton *et al.* 1970). The wave functions are available from the authors on request (request First Row Correlation Study Functions: Nondynamical Intrashell).

Some interesting features contained in this table are the unique character of molecular correlation energy, the difficulty of associating it with the dissociated atom correlation energy [9] and perhaps the utility of associating it with united atom correlation energy which seems much more relevant to the molecular case near the equilibrium internuclear distance of the molecule.[10]

Partial pair energies are given (Eq. (13) in Sutton *et al.* 1970), associated with excitation from the $n = 2$ level of a variety of molecules into the "holes" of $n = 2$ level in these same systems. This corresponds to a part of the nondynamical contribution to the total pair correlation energy. In our OVC process, these calculations were performed in a frozen Φ_0 framework (Φ_0 was frozen to be the Hartree–Fock orbitals) for economic reason, but the energies are considered to be representative. In all the above OVC calculations, a basis set consisting of $4s$-type, $3p$-type, and $2d$-type Slater orbitals in sigma molecular symmetry, and $3p$-type and $2d$-type in π molecular symmetry were used. Where the ground state atom did not have a filled $2p$ orbital, the $2p$ orbital exponent was obtained from an excited state atomic calculation. The orbital exponents of the d functions were obtained by maximizing the overlap of the absolute value of the d function and the molecular orbital being correlated.[11] This technique is based on the observation that effective correlation orbitals span the same

---

[9] It is also clear that an excitation which is important in one molecule is not necessarily important in another, even when it appears that it accomplishes the same purpose. For example, the $3\sigma_g{}^2 \rightarrow 3\sigma_v{}^2$ excitation is very important for F_2 but unimportant for B_2 even though it formally leads to proper dissociation of the molecule in both cases. This evidently means that it is not very important to remove the ionic contributions in the simple MO picture in the case of B_2.

[10] This viewpoint was suggested in conversation with M. Krauss and A. Weiss. These gentlemen are currently analyzing these energy contributions in terms of their united atom counterparts. For example, the molecular excitation $2\sigma_u^2 \rightarrow 3\sigma_g{}^2$ is very important; it corresponds in united atom terminology to a $3p^2 \rightarrow 3d^2$ excitation, which is well known to be important.

[11] In order to economically obtain orbital exponents for effective correlating basis functions, we approximately maximized the exchange integral $K_{ij} = < \varphi_i(1)\varphi_i{}^*(2)$ $1|2_{12}\varphi_i(2)\varphi_j{}^*(1) >$ between the orbital to be correlated (i) and the correlating orbital (j) by maximizing the overlap of the *absolute* value of these two orbitals $< |\varphi_i||\varphi_j| >$. This procedure tested on NaF has yielded orbital exponents within less than 5% of those obtained by brute force orbital exponent variation within the OVC calculation. In later work we rigorously maximize the exchange integral to achieve starting orbitals.

space as the orbital being correlated or, stated differently, that effective correlation is dominated by the exchange integral between the primary and the correlating orbital.

C. Several Bonds: Diagonal and Split-Shell Excitations

From the results shown and our experience as discussed in Sutton *et al.* (1970), Das and Wahl (1967), and Wahl *et al.* (1967) regarding the computations performed to obtain them, we can make several important observations. First, the types of excitations so far used, *viz.* the diagonal excitations, to construct the excited configurations are not in general adequate to represent the changes taking place in the valence shell where more than two electrons are involved in the bonding process. It is necessary, therefore, to include split-shell excitations. Second, only the correlation in the highest lying occupied shells in the molecule which correspond to unpaired electrons in the atoms is strongly R-dependent, that *within* (and, by extrapolation between) other shells being rather weakly dependent on R. Third, the number of configurations to adequately represent intrashell correlation of the latter shells is very large, so that the fact that this is weakly dependent on R is a great advantage in regard to the study of the chemical bond since it is already established that the correlation between the nonpaired electrons of the atoms as they form the molecule is adequately expressible in terms of a few configurations. In addition to its associated clumsiness, the MCSCF procedure for a large number of configurations is usually difficult to converge and is thus quite time-consuming. Since the excited configurations are *primarily determined* by their interaction with the *dominant configurations* and only *very weakly* by their *mutual interaction*, a fullblown MCSCF implies an extravagance, especially where a complete accuracy in the OVC function is not desired. With a view to simplifying the methodology, we thus proposed the following procedure for carrying out the OVC-computations:

(1) A basis set of functions is chosen by adequately augmenting the one used for the Roothaan–Hartree–Fock (RHF) wave function. The number of additional functions required is usually small (see Veillard, 1966).

(2) The RHF-orbitals are obtained by solving the usual SCF equations.

(3) The configurations that are necessary to insure that the molecule dissociates formally into Hartree–Fock atoms in their appropriate states are optimally mixed and all orbitals optimized for various internuclear distances using Multiconfiguration Self-Consistent Field (MCSCF) techniques.

(4) In addition to the obvious configurations of step (3), there are configurations whose contributions are small at large internuclear separation but increase sharply as the separation decreases. These are constructed and optimized one by one along with the configurations of step (3). Because the terms representing their coupling with each other are small compared with those representing their coupling with the configurations from step (3), we have found the following procedure particularly useful and sufficiently accurate in obtaining these configurations. By *variationally maximizing* the *coupling integral between the major configurations and any of the excited ones, initial approximations to the excited orbitals are found.* This process, which is also used in step (5) below, is explained in detail later on. These starting orbitals are then used for carrying out a series of MCSCF calculations where the mutual interaction of the excitation is left out of consideration. This is followed by a final CI over all the configurations selected and optimized.

(5) The remaining configurations, whose contributions are mainly atomic and vary slowly with internuclear distance or are too small for inclusion in step (4), are then obtained using a perturbation treatment.

We report below the application of the above method to the molecule F_2 (see also, Das and Wahl, 1970). In doing so we present further clarifications and details of the different steps of the method outlined above.

TABLE VI

DOUBLE CONFIGURATION SCF RESULT ON THE $^1\pi_u$, $3\pi_u$, $^1\pi_g$, AND $\pi^3{}_g$ STATES OF H_2, (INVOLVE SPLIT SHELL EXCITATION)

	State			
	$^1\pi_u$	$^3\pi_u$	$^1\pi_g$	$^3\pi_g$
E (hartrees)	−0.71583	−0.73306	−0.64625	−0.64652
Expt.	−0.71859	−0.73813	−0.65926	
R (bohrs)	1.947	1.965	2.058	2.052
Expt.	1.952	1.961	2.002	
ω_e (cm^{-1})	2489	2474	2098	2123
Expt.	2443	2465	2265	2268
β_e (cm^{-1})	31.5	30.9	28.0	28.2
Expt.	31.4	31.1	29.8	
$\omega_e X_e$ (cm^{-1})	61.5	54.9	10.3	−9.51
Expt.	67.0	61.4	78.5	75
α_e (cm^{-1})	1.565	1.470	1.756	1.614
Expt.	1.626	1.425	1.515	

[a] These results indicate effectiveness of the simple Optimized Double Configuration model for these excited stages of H_2. The result for the $^3\pi_g$ and $^1\pi_g$ states were obtained using the basis set designed for the $^1\pi_u$ and $^3\pi_u$ states and thus are of poorer quality (see Zemke *et al.*, 1969).

We must emphasize, however, that the theory is applicable to any general diatomic molecule, F_2 serving merely as a good illustration of the different aspects of the method. (Results for the simple split-shell excitation case of H_2 π states are given in Table VI and Fig. 6.)

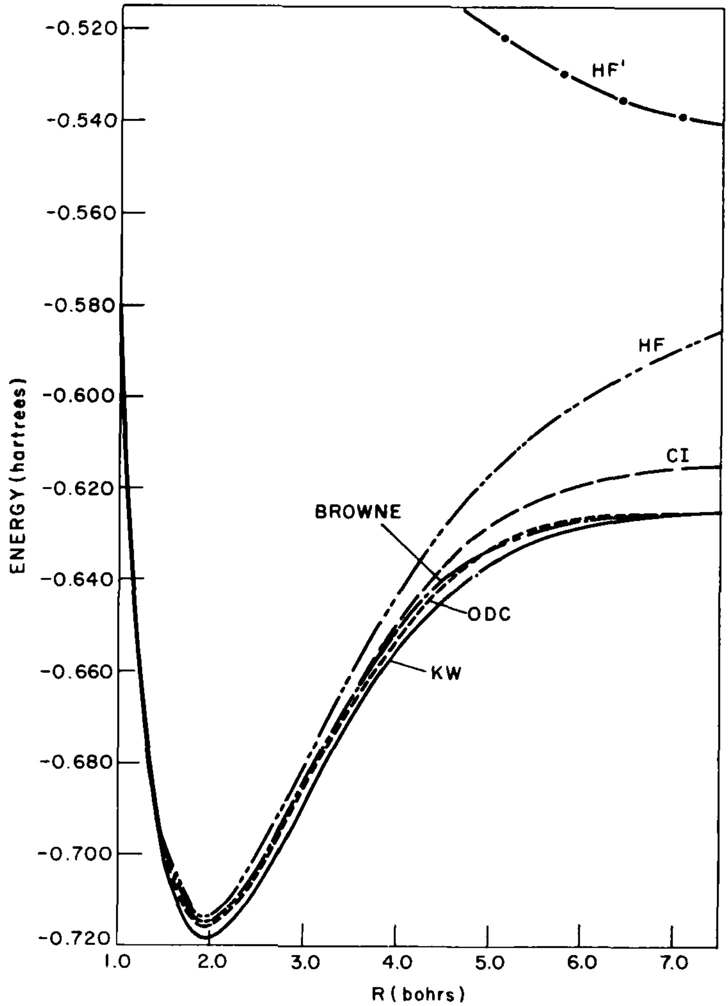

Fig. 6. Comparison of Hartree–Fock (H–F) straight double configuration interaction using the Hartree–Fock solution $1\sigma_g 1\pi_u$(H–F) and $1\sigma_u 1\pi_g$(H–F′) for each of the two configurations (CI), Large Configuration Interaction (Browne), explicity correlated wave function (Kolos and Wolniewicz), with optimized double configuration (ODC) model for $^1\pi_u$ state of H_2 (a split-shell case). Note the good quality of the ODC model in comparison with the much more complicated Browne and Kolos–Wolniewicz results.

The Heitler–London function for F_2 in MO-representation is

$$\Psi_{\mathrm{HL}} = 2^{-1/2}(1\sigma_g{}^2 1\sigma_u{}^2 2\sigma_g{}^2 2\sigma_u{}^2 1\pi_u{}^4 1\pi_g{}^4)[3\sigma_g{}^2 - 3\sigma_u{}^2]$$

in obvious notation. In the spirit of step (3) above, we optimally determine for various internuclear distances the function

$$\Psi(3) = (\mathrm{core})1\pi_u{}^4 1\pi_g{}^4 \cdot [a(3\sigma_g{}^2) + b(3\sigma_u{}^2)],$$

where we use the abbreviation

$$(\mathrm{core}) \equiv 1\sigma_g{}^2 1\sigma_u{}^2 2\sigma_g{}^2 2\sigma_u{}^2.$$

This wave function leads to a proper description of the dissociation of F_2 into two Hartree–Fock F atoms in their ground state. In step (4), we first consider the configurations obtained by replacing the $3\sigma_g$-, $3\sigma_u$-shells by excited shells such as $n\sigma_{g,u}$, $n = 4, 5, \ldots$ or $m\pi_{g,u}$, $m = 2, 3, \ldots$. However, the contributions from these excitations are too small to warrant their inclusion in the wave function at this stage. They are treated in step (5). The only remaining important configurations that contribute significantly to the molecular correlation are the following:

$$(\mathrm{core})2\pi_u{}^3 1\pi_g{}^4 3\sigma_g 3\sigma_u 2\pi_g({}^1\Sigma_u{}^+ \times {}^1\Sigma_u{}^+),$$

$$(\mathrm{core})1\pi_u{}^4 1\pi_g{}^3 3\sigma_g 3\sigma_u 2\pi_u({}^1\Sigma_u{}^+ \times {}^1\Sigma_u{}^+),$$

$$(\mathrm{core})1\pi_u{}^2 1\pi_g{}^4 3\sigma_g{}^2 3\sigma_u{}^2({}^1\Sigma_g{}^+),$$

$$(\mathrm{core})1\pi_g{}^4 1\pi_g{}^2 3\sigma_g{}^2 3\sigma_u{}^2({}^1\Sigma_g{}^+),$$

all of those contributors vanish at infinite internuclear separation. The symbols within brackets refer to the coupling scheme of the open shells. The other coupling scheme ${}^3\Sigma^+ \times {}^3\Sigma^+$ for the first two configurations in (3), contributes very little. Instead of doing a complete MCSCF with the six configurations—two in Eq. (2) and four represented by Eq. (3), we froze $3\sigma_g$, $3\sigma_u$ as obtained in step (3) and optimized only $2\pi_u$, $2\pi_g$ as indicated in step (4). This was found to lead to an optimization "error" $\lesssim -0.0010$ a.u. at all separations.

In step (5) we obtain the remainder of the correlation pertinent to the bonding. This consists of two kinds of excitations—one representing the remaining part of the correlation that is essentially molecular, the other that represents the correlations among the valence electrons on each center modified by the bonding. This latter needs a different treatment owing to the fact that these excitations are quite numerous even though optimized. Although their individual contributions are small, they add up to a significant effect. Before we describe our techniques to handle these terms, we consider the sort of excitations that we finally selected. The criterion for this selection, of course, depends on the accuracy at which we are aiming. In the present calculations, we set our limit of accuracy as 0.1 eV in the bonding. We verified that the correlation in the inner shells $1\sigma_g$, $1\sigma_u$, $2\sigma_g$, $2\sigma_u$ as well as their cross-shell correlation with valence shells does not take any significant part in the bonding to this accuracy. Certainly at internuclear distances smaller than the equilibrium value, these correlations show some appreciable changes; however, at such distances the nuclear repulsion overshadows such small changes. Thus we confine ourselves only to the correlation in and between the shells $3\sigma_g$, $3\sigma_u$, $1\pi_u$, $1\pi_g$. The configurations we selected in step (5) are of two types:

Type I:

(a) (core)$1\pi_{u,g}^3\, 1\pi_{g,u}^4\, 3\sigma_{g,u}\, m\sigma_{g,u}\, n\pi_{g,u}(^1\Sigma^+ \times {}^1\Sigma^+)$;
$m \geq 4, \quad n \geq 2,$

(b) (core)$1\pi_{u,g}^3\, 1\pi_{g,u}^4\, 3\sigma_{g,u}\, m\sigma_{g,u}\, n\pi_{g,u}(^1\Delta \times {}^1\Delta$ or ${}^3\Delta \times {}^3\Delta)$;
$\lambda \equiv \delta, \quad \phi, \ldots,$ etc., $m \geq 1, \quad n \geq 2.$

Type II:

(a) (core) $1\pi_u{}^4 1\pi_g{}^4 n\sigma_{g,u}^2$; $\quad n \geq 4,$

(b) (core)$1\pi_u{}^4 1\pi_g{}^4 (n\pi_{u,g})^2(^1\Sigma_g{}^+)$; $\quad n \geq 2.$

The symmetry indices g,u are permuted in all different ways subject to the symmetry requirements of the state ${}^1\Sigma_g{}^+$. We now describe the method we have followed to obtain these terms:

A second-order perturbation series for the energy

$$\Delta E^{(2)} = -\sum_i \frac{\langle 0|H|i\rangle^2}{E_i - E_0} \tag{14}$$

will involve two types of integrals $\langle 0|H|i\rangle$ corresponding to the two types of configurations shown above. For the type II functions we have, using Roothaan's expansion formalism and suppressing any constant factor,

$$\langle 0|H|i\rangle = \mathbf{D}_{\text{ex}}^{+}\mathbf{K}\mathbf{D}_{\text{val}} \tag{15}$$

where $\mathbf{K} \equiv \{K_{pq,rs}\}$ is the exchange supermatrix and $\mathbf{D}_{val}$, $\mathbf{D}_{ex}$ represent the "density matrices" for the valence and excited shells. For the type I functions, let 1, 2 represent valence shells and 3, 4 the excited shells. Then, again in expansion formalism and suppressing constant factors,

$$\langle 0|\,H\,|i\rangle = \mathbf{D}_{12}^{+}\mathscr{J}\mathbf{D}_{34}, \tag{16}$$

where D_{ij} is a cross-shell density matrix given by

$$D_{ij,\,pq} = C_{ip}\,C_{jq} \tag{17}$$

and $\mathscr{J}$ is some linear combination of the Coulomb and exchange supermatrices. A fast convergence of the series (4) can be secured if $|i\rangle$'s are obtained such that the corresponding term in the series is maximum under the constraints of orthogonality to all the orbitals obtained already. We prefer, however, to extremize just $\langle 0|\,H\,|i\rangle$ for getting these orbitals. We thereby avoid the lengthy iterative processes; further it is not necessary to obtain $|i\rangle$ for each term of the series. Only one extremization for each type will yield all the excited orbitals as eigenfunctions belonging to the respective type. Let us consider the equation to extremize the coupling represented by Eq. (5):

$$\mathbf{KD}_{\mathrm{val}}\,\mathbf{C}_{\mathrm{ex}} = \varepsilon\mathbf{SC}_{\mathrm{ex}} + \sum \varepsilon_j\mathbf{SC}_j \tag{18}$$

where $\mathbf{S}$ is the overlap matrix and ε's are the usual Lagrangian multipliers arising from the constraints of orthonormality. It is clear that since we do not propose to alter $\mathbf{D}_{\mathrm{val}}$, the solution of Eq. (18) is noniterative and can be performed immediately. Further, obviously,

$$\mathbf{C}_{\mathrm{ex}}^{(1)+}\mathbf{KD}_{\mathrm{val}}\mathbf{C}_{\mathrm{ex}}^{(2)} = 0,$$

where $\mathbf{C}_{\mathrm{ex}}^{(1)}$, $\mathbf{C}_{\mathrm{ex}}^{(2)}$ are two solutions of Eq. (8), ruling out the possibility of these solutions to mix and give rise to a new type of terms in Eq. (14). A similar situation holds in the type-II case. Let us first assume that $\mathbf{C}_3$, $\mathbf{C}_4$ belong to different symmetry species λ and λ'. Then the equations to maximize coupling (6) are given by

$$\begin{aligned} \mathbf{M}_{\lambda\lambda'}\mathbf{C}_4 &= \varepsilon\mathbf{S}_\lambda\mathbf{C}_3 + \sum_j^{(\lambda)} \varepsilon_{3j}\mathbf{S}_\lambda\mathbf{C}_j, \\ \mathbf{M}_{\lambda\lambda'}^{+}\mathbf{C}_3 &= \varepsilon\mathbf{S}_{\lambda'}'\mathbf{C}_4 + \sum_j^{(\lambda')} \varepsilon_{4j}\mathbf{S}_{\lambda'}\mathbf{C}_j, \end{aligned} \tag{19}$$

where the summations are over all orbitals belonging respectively to λ and λ' excluding $\mathbf{C}_3$ and $\mathbf{C}_4$. $\mathbf{M}_{\lambda\lambda'}$ is given by

$$\mathrm{M}_{\lambda p,\,\lambda' q} = \sum_{\mu r,\,\mu' s} \mathscr{J}_{\lambda p\lambda' q,\,\mu r,\,\mu' s}\,\mathrm{D}_{12\,rs},$$

with $_{\mu,\,\mu'}$ being the symmetry species of 1 and 2, respectively. After an easy manipulation, Eqs. (15) are uncoupled to yield

$$\begin{aligned}\mathbf{M}^{+}_{\lambda\lambda'}\left(\mathbf{S}_{\lambda}^{-1} \quad \sum_{j}^{(\lambda)} \mathbf{C}_j \mathbf{C}_j{}^{+}\right) M_{\lambda\lambda'} \mathbf{C}_4 &= \varepsilon^2 S_{\lambda'} \mathbf{C}_4 ,\\ \mathbf{M}_{\lambda\lambda'}\left(\mathbf{S}_{\lambda'}^{-1} - \sum_{j}^{(\lambda')} \mathbf{C}_j \mathbf{C}_j{}^{+}\right) M^{+}_{\lambda\lambda'} \mathbf{C}_3 &= \varepsilon^2 S_{\lambda} \mathbf{C}_3 ,\end{aligned} \tag{20}$$

which can be immediately solved. When $\mathbf{C}_3$, $\mathbf{C}^4$ are of the same symmetry species, it can be shown that their linear combinations

$$\begin{aligned}\mathbf{u} &= \mathbf{C}_3 + \mathbf{C}_4 ,\\ \mathbf{v} &= \mathbf{C}_3 - \mathbf{C}_4\end{aligned}$$

satisfy

$$\begin{aligned}\mathbf{M}\,\mathbf{u} &= \varepsilon\,\mathbf{S}\,\mathbf{u}\\ \mathbf{M}\,\mathbf{v} &= \varepsilon'\,\mathbf{S}\,\mathbf{v}\end{aligned}$$

provided the supermatrix in Eq. (16) is symmetric.

We report below the results of calculations on F_2, carried out along the above lines. The basis set used in these calculations is slightly inferior (0.001 a.u. in the H–F energy) to the one used in earlier reports. This choice of the basis set (namely a common basic set for *g*,*u* symmetries) was motivated primarily by economic considerations. The basis set, which consists of 18 σ-functions and 10 π-functions, rules out the type I(b) excitations automatically, although from independent evidence such excitations are not at all negligible. However, on the basis of atomic correlation energies and other numerical checks, we believe that individual contributions from the excitations considered cannot be off by more than 10% of their calculated values. A complete resolution of this uncertainty would require extensive experimentation with the basis set. This we refrain from since our purpose here is primarily illustrative.

In Table VII we list the mixing coefficients of the six dominant molecular configurations. In Table VIII we present the energetic contributions from different terms at different internuclear instances. The first row gives the double configuration (Eq. (2)) values with the present basis set. They differ slightly from the values of Wahl *et al.* (1967) owing to the difference in the basis sets. The second row gives eight-configuration values from the same source and the difference between the first and second rows given in the third row will be used to correct for the basis set as well as the fact that we do not include any Type II excitations in the present calculations. The fourth row gives the values for the six-configuration function. The fifth row gives the contributions from the "atomic" excitations. The sixth row gives the

TABLE VII

MIXING COEFFICIENTS FOR THE SIX- CONFIGURATION WAVE FUNCTION

Configurations	1.8	2.2	2.68	3.0	3.5	6.0
$1\pi_u^4 1\pi_g^4 3\sigma_g^2$	0.99350	0.98662	0.97048	0.94974	0.89700	0.72040
$1\pi_u^4 1\pi_g^4 3\sigma_u^2$	−0.05731	−0.10779	−0.20462	−0.29010	−0.43255	−0.69343
$1\pi_u^2 1\pi_g^4 3\sigma_g^2 3\sigma_u^2$	0.01296	0.01709	0.01614	0.01109	−0.00184	−0.00729
$1\pi_u^4 1\pi_g^2 3\sigma_g^2 3\sigma_u^2$	0.02083	0.03435	0.04659	0.05022	0.05004	0.01023
$1\pi_u^3 1\pi_g^4 3\sigma_g 3\sigma_u^2 \pi_g$	−0.04927	0.05570	0.05834	0.05460	−0.04294	0.00291
$1\pi_u^4 1\pi_g^3 3\sigma_g 3\sigma_u 2\pi_g$	0.08154	0.10194	−0.10226	0.09059	0.06273	0.00312

TABLE VIII

ENERGY ANALYSIS

Contributing terms	1.8	2.2	2.68	3.0	3.5	6.0
Two main configurations (i.e., $3\sigma_g^2$ and $3\sigma_u^2$)	−198.4324	−198.7679	−198.84287	−198.84193	−198.8296	−198.8178
Column 4 of Table IX Wahl *et al.* (1967)	−198.4454	−198.7772	−198.84853	−198.84551	−198.83094	−198.8180
Basis function and extra molecular correlation correction	−0.0130	−0.0093	−0.0056	−0.0036	−0.0013	−0.0002
Six-Configuration function of Table I	−198.4760	−198.8171	−198.8834	−198.8716	−198.8437	−198.8178
Atomic correlation terms from Table II	−0.0394	−0.0325	−0.0253	−0.0250	−0.0286	−0.0384
Total energy	−198.5284	−198.8589	−198.9143	−198.9002	−198.8736	−198.8564

energy values for our final potential curve (Fig. 5). The Dunham's analysis of this curve yields the spectroscopic values given in Table IX.

TABLE IX
SPECTROSCOPIC CONSTANTS

Source	R_e (a.u.)	D_e (eV)	ω_e (cm^{-1})
This calculation	2.59	1.57	1021
		1.39 ± 0.03[b]	892[g]
		1 49 ± 0 .07[c]	
Experimental	2.68[a]	1.68 ± 0.09[d]	
		1.65 ± 0.05[e]	
		1.65[f]	

[a] D. Andrychuk (1951).
[b] V. H. Dibeler *et al.* (1969).
[c] W. Stricker and L. Kraus (1968).
[d] R. Iczkowski and J. Margrave (1959).
[e] M. G. Evans (1950).
[f] J. Berkowitz (to be published)
[g] G. Herzberg, Diatomic Molecules (1955).

In considering the counterbalancing effects (Das and Wahl, 1970) not included in our calculations, we feel that the results support a binding energy for F_2 of 1.6 eV and do not support the recent value of 1.39 eV, (see Table IX).

III. Discussion

It has been the purpose of this paper to review and bring up to date the conceptual features, the analysis, and results obtained by the application of the method of Optimized Valence Configurations to diatomic molecules. We feel that several significant conclusions can be drawn from the experience obtained in developing this method and in assessing its relationship to other schemes.

1. It is possible to quantitatively separate the "molecular" aspects of the changing correlation energy of two approaching atoms from the remaining correlation which can be labeled as "atomic"; namely, that consideration of the correlation of only the so-called valence electrons is sufficient to yield an accurate description of the chemical bond and, in accordance with the basic assumption of the method, there exists a distinct separation in behavior between optimal configurations that represent the extra correlation resulting from molecular bonding and those that will ordinarily be associated with the correlation in separated atoms.

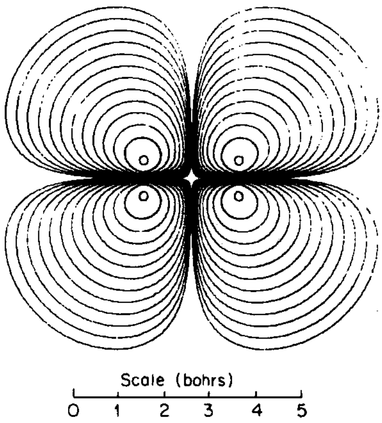

Fig. 7. 1-pi-*g* orbital for N_2

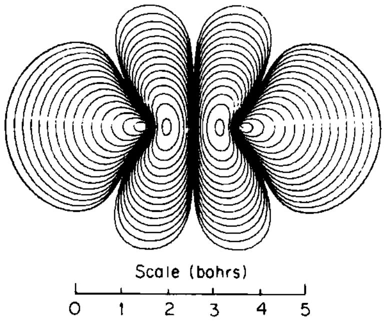

Fig. 8. 3 sigma-*u* orbital for N_2

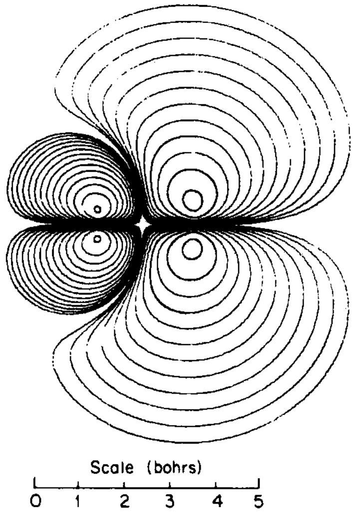

Fig. 9. 2 pi orbital for CO

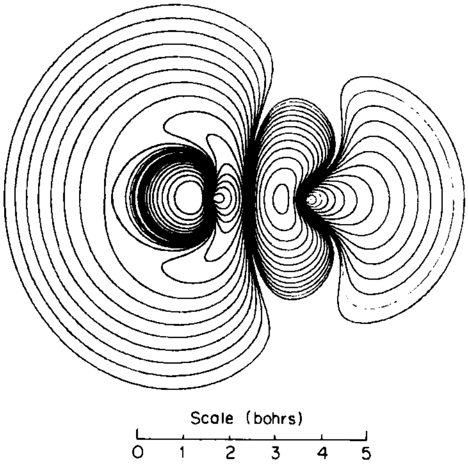

Fig. 10. 6 sigma orbital for CO

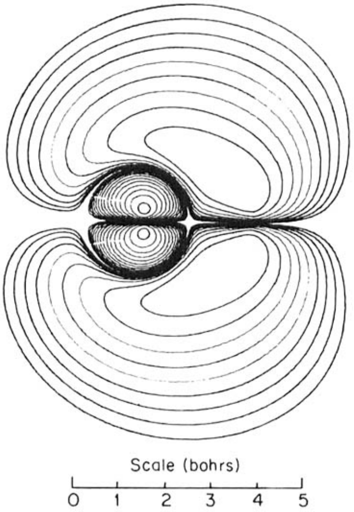

Fig. 11. 2 pi orbital for BF

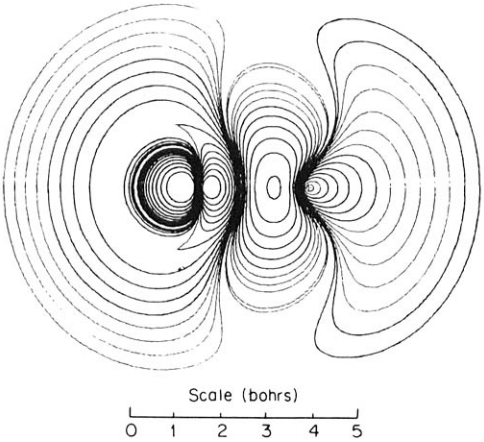

Fig. 12. 6 sigma orbital for BF

Figs. 7–12. Contour diagrams of electron charge density for some effective OVC correlation orbitals in the isoelectronic systems N_2, CO, and BF. The O atom in Figs. 9 and 10 and the F atom in Figs. 11 and 12 are at the left. Note how as bond polarity changes the character of the effective correlation orbital changes from $2p$ character in N_2 to essentially $3p$ character in BF. A similar trend is seen in the iso-electron series C_2, BN, BeO, LiF, HeNe where the effective correlation orbitals shift from essentially a $2p\sigma_g$, a $2p\sigma_u$, and a $2p\pi_g$, in the case of C_2, to a $3p\sigma$, a $3d\sigma$, and a $3p\pi$ centered on the F as the ionicity of the bond increases. The outermost contour in all diagrams corresponds to an electronic charge density of 6.1×10^{-5} electrons/bohr^3 and each successive inner contour rises by a factor of two. The highest contour value plotted is 1.0 electron/bohr. In the case of the 6σ orbital of CO and BF, there is an unobvious node in the leftmost lobe. It is interesting to note that even though the OVC process was begun with $n = 2$ molecular orbitals; namely, unfilled atomic valence orbitals of radial quantum number 2, the MCSCF procedure converged to a best orbital of higher quantum number in the cases of CO and BF since these proved to be variationally more effective in correlating these ionic systems at their equilibrium separation. A significant point which has emerged from the calculations presented in this paper is the effectiveness of the multiconfiguration SCF procedure in achieving the changing nature of the correlating orbital as a molecule forms (Fig. 1(b)) or as bond polarity changes. We see that the very nature of our best correlating orbitals shifts from a truly molecular orbital toward an atomic orbital as the nature and polarity of the chemical bond changes.

2. That the number of significant configurations representing extra molecular correlation is small and readily obtainable by a *sequence* of *limited MCSCF computations*, followed by a single CI involving all new orbitals thus obtained while those configurations representing atomic correlation are indeed numerous but are easily accounted for by a suitable perturbation technique. Such a separation is of paramount importance in making quantitative predictions about the chemical bond and energy surfaces, particularly as the arduous search for tractable methods of attacking the correlation problem is extended to longer molecules.
3. The MCSCF procedure, when applied to all configurations simultaneously, is cumbersome, expensive, and slowly convergent. A simplified approach which we have proposed and adopted, namely a series of *limited MCSCF calculations* involving new orbitals one at a time optimized along with only the *dominant* configurations to yield a set of properly formed orbitals for subsequent use in a larger CI calculation, yields accurate results with reasonable computational effort.
4. An excellent *initial guess* for excited *starting* orbitals can be obtained by maximization of the exchange integral between the orbital of the Hartree–Fock configuration being correlated and the excited orbital.

We are currently proceeding to apply the method in its current form to a variety of bonding situations including Van der Waals type and to the computation of a simple chemical reaction surface, and to develop it as a means of evaluating realistic excitation energies and molecular properties in addition to interaction potentials.

REFERENCES

AHLRICHS, R., and KUTZELNIGG, W., (1968). *J. Chem. Phys.* **48**, 1819.
ANDRYCHUK, D., (1951). *Can. J. Phys.* **29**, 151.
BENDER, C. F., and DAVIDSON, E. R. (1966). *J. Phys. Chem.* **70**, 2675.
BENDER, C. F., and DAVIDSON, E. R. (1967). *J. Chem. Phys.* **47**, 360.
BENDER, C. F., and DAVIDSON, E. R. (1969). *Phys Rev.* **183**, 23.
BERKOWITZ, J. to be published.
BERTONCINI, P. J., DAS, G., and WAHL, A. C., (1970). *J. Chem. Phys.* (April).
BRÄNDAS, E. (1968). *Intern. J. Quantum Chem.* **11**. 793.
BROWN, R. E., and SHULL, H. (1968). *Intern. J. Quantum Chem.* **11**, 663.
BROWNE, J. C., and MATSEN, F. A. (1964). *Phys. Rev.* **135**, A1227.
CLEMENTI, E. (1967). *J. Chem. Phys.* **46**, 3842.
CLEMENTI, E., and VEILLARD, A. (1966). *J. Chem. Phys.* **44**, 3050.
CLEMENTI, E., and VEILLARD, A. (1967). *Theoret. Chem. Acta.* **7**, 133.

CONROY, H. (1964). *J. Chem. Phys.* **41,** 1327, 1331, 1336, and 1341.
DAS, G. (1967). *J. Chem. Phys.* **46,** 1568.
DAS, G., and WAHL, A. C. (1966). *J. Chem. Phys.* **44,** 876.
DAS, G., and WAHL, A. C. (1967). *J. Chem. Phys.* **47,** 2934.
DAS, G., and WAHL, A. C. (1970). *Phys. Rev. Letters.* **24,** 440
DIBELER, V. H. *et al.* (1969). *J. Chem. Phys.* **50,** 4592.
EBBING, D. D., and HENDERSON, R. C. (1965). *J. Chem. Phys.* **42,** 2225.
EDMISTON, C., and KRAUSS, M. (1966). *J. Chem. Phys.* **45,** 1833.
EVANS, M. G. *et al.* (1950). *J. Chem. Soc.*, 1524.
FRENKEL, J. Advanced general theory, *in* " Wave Mechanics," Oxford Univ. Press (Clarendon). [Reprinted by Dover New York, 1950, pp. 460–462.]
GILBERT, T. L. (1965). *J. Chem. Phys.* **43,** S248.
GRIMALDI, F. (1965). *J. Chem. Phys.* **43,** S59.
HANDY, N. C., and BOYS S. F. (1960).
HARRIS, F. E., and MICHELS, H. H. (1967). *Intern. J. Quantum Chem.* **1S,** 329
HARTREE, D. R., HARTREE, W., and SWIRLES, B. (1939). *Phil. Trans. Roy. Soc. (London), Ser. A,* **238,** 292.
HERZBERG, G. (1955). " Diatomic Molecules," 2nd ed. Van Nostrand, Princeton, New Jersey
HINZE, J., and ROOTHAAN, C. C. J. (1967). *Prog. Theoret. Phys. (Kyoto)* **40,** 37.
ICZKOWSKI, R., and MARGRAVE, J. (1959) *J. Chem. Phys.* **30,** 403.
KIBARTAS, V. V., KAUETSKIS, V. I., and YUTSIS, A. P. (1955). *Soviet Phys.—J.E.T.P.* **2g,** G23.
KOLOS, W. (1968). *Intern. J. Quantum Chem.* **11,** 471.
KOLOS, W., and WOLNIEWICZ, L. (1968.) *Phys. Rev. Letters* **20,** 243.
KRAUSS, M. (1967). Compendium of *ab initio* calculations of molecular energies and properties. "Technical Note," No. 438. Natl. Bur. Std., Washington, D.C.
KUTZELNIGG, W. (1964). *J. Chem. Phys,* **40,** 3640.
KUTZELNIGG, W. (1969) Preprint.
LÖWDIN, P.-O. (1955a). *Phys. Rev.* **97,** 1497, Sec. 5.
LÖWDIN, P.-O. (1955b). *Phys. Rev.* **97,** 1509.
LÖWDIN, P.-O. (1959). *Advan. Chem. Phys.* **2,** 207
MATCHA, R. L., and BROWN, W. B. (1968). *J. Chem. Phys.* **48,** 74.
MCWEENY, R. (1965). *Proc. Roy. Soc. (London), Ser. A* **232,** 114.
MCWEENY, R., and STEINER, R. (1965). *Advan. Quantum Chem.* **2,** 93.
NESBET, R. K. (1967a). "Advances in Quantum Chemistry," Vol. 3.
NESBET, R. K. (1967b). *Phys. Rev.* **155,** 51.
PAUNCZ, R. "Alternate Molecular Orbital Method " (1967). Saunders, Philadelphia.
ROTHENBERG, S. (1967). *Intern. J. Quantum Chem.* **1S,** 475.
SHULL, H., and LÖWDIN, P.-O. (1959). *J. Chem. Phys.* **30,** 617.
SINANOGLU, O. (1964). *Advan. Chem. Phys.* **2,** 315.
SIU, A. K. Q., and DAVIDSON, E. R. Preprint (1970).
SLATER, J. C. (1953). *Phys. Rev.* **91,** 528.
STRICKER, W., and KRAUS, L. (1968). *Z. Naturforsch.* **23a,** 436.
SUTTON, P., BERTONCINI, P., DAS, G., GILBERT, T. L., WAHL, A. C., and SINANOGLU, O. (1970). *Intern. J. Quantum Chem.* **IIIS,** 479.
TUAN, D. F., and SINANOGLU, O. (1964). *J. Chem. Phys.* **41,** 2677.

VEILLARD, A. (1966). *Theoret. Chim. Acta* **4,** 22.

WAHL, C., BERTONCINI, P. J., DAS, G., and GILBERT, T. L. (1967). *Intern. J. Quantum Chem.* **1S,** 123.

WATSON, R. E. (1961). *Ann. Phys.* **13,** 250.

YOSHIMINE, M., and MCLEAN, A. D. (1967) *Intern. J. Quantum Chem.* **1S,** 313.

YUTSIS, A. P., KIBARTAS, V. V., and GLEMBOTSKIY, I. I. (1954). *Zh. Eksperim. i Theor. Fiz.* **34,** 425.

YUTSIS, A. P. (1952). *Zh. Eksperim. i Theor. Fiz.* **23,** 129.

ZEMKE, W., LYKOS, P., and WAHL, A. C. (1969). *J. Chem. Phys.* **51,** 5635.

Author Index

Numbers in italics refer to pages on which the complete references are listed.

Subject Index